Habitat classification using airborne and spaceborne remote sensing for biodiversity assessment in Wales

JOHANNA FRIEDERIKE BREYER

A thesis submitted in fulfilment of the requirements for the degree of Doctor of Philosophy

December, 2009

University of Wales, Aberystwyth

Supervisors: Dr Richard Lucas and Dr Aled Rowlands

Declaration and Statements

Declaration

This work has not previously been accepted in substance for any degree and is not being concurrently submitted in candidature for any degree.

Signed .... Date ....

Statement 1

This thesis is the result of my own investigations expect where otherwise stated. Where correction services have been used, the extent and nature of the correction is clearly marked in footnote(s). Other sources area acknowledged by footnotes and giving explicit references. A bibliography is appended.

Signed .... Date ....

Statement 2

I hereby give consent for my thesis, if accepted, to be available for photocopying and for inter-library loan, and for the title and summery to be made available to outside organizations.

Signed .... Date ....

Acknowledgements

I feel very fortunate to have been able to learn and benefit from the support of many different people during the course of this study:

Alan Gay at IBERS and formerly IGER is thanked for the opportunity to acquire CASI images over my field sites and for a lot of time and help especially in the early days.
At IGER I would also like to thank Carron James for support during image acquisition, Mike Hayes for detailed vegetation data and Mike Abberton for allowing me to use IGER's ovens to dry over a 1000 bags of grass.

Staff at ADAS in Devil's Bridge, as well at Trawscoed farm are thanked for generous access to the study sites at Pwllpeiran and Trawscoed respectively and the opportunity to take such an extensive number of vegetation samples.

I am grateful to Mike Walker from the RSPB at Lake Vyrnwy for his enthusiasm, support and patience in waiting for results, as well as the 2006 CBC data.

In grateful memory of the late Dr. Aileen Smith (1953-2009), who first encouraged me.

Abstract

Biodiversity and its conservation are an important subject as human pressure on natural resources increases continuously. Without accurate means of measuring biodiversity, however, monitoring is very difficult and conservation efforts might not be targeted effectively. There is a great demand for biodiversity assessment on a regional scale in order to support national conservation aims as stated, for example, in the UK Biodiversity Action Plan. Remote sensing lends itself to interpretation at the landscape scale and this study aims to assess a variety of optical and laser remote sensing data with regard to their usefulness for biodiversity assessment in Wales.

The study was divided into four distinct areas to evaluate different remote sensing data with regard to their utility for facilitating the measurement and assessment of distinct elements of biodiversity. These components are vegetation composition and condition, land cover on a regional scale, three-dimensional woodland structure and the interaction of flora and fauna within the landscape structure. Methodological advances include a novel land cover mapping approach from multispectral remote sensing data comparable to traditional manual habitat surveys as well as an analysis of forest vertical profile under consideration of bird habitat preferences.

Remote sensing data investigated included airborne hyperspectral data, multispectral satellite imagery and airborne LiDAR.
The potential of hyperspectral data for the differentiation of grasslands of varying levels of improvement was tested at two experimental grassland study sites and the results suggest a strong correlation between biomass and the red-edge region of the electromagnetic spectrum. A relationship between the presence of non-photosynthetic vegetation and the level of agricultural improvement was further

established and utilized in the formulation of rules for the classification of grass-land habitats.

The outcomes of this study were used to support the landscape-scale land cover mapping of the extent of 38 classes from a multi-temporal combination of two spaceborne multispectral sensors (SPOT 5 HRG and IRS LISS IV). The derived maps achieved a moderate accuracy of 64%, though individual classes, especially woodlands and bogs, exceeded this value.

The ability of Light Detection and Ranging (LiDAR) and terrestrial laser scanner data to capture the three-dimensional structure of forests was investigated. It was found that both sensor types were limited in their ability to accurately represent forest vertical profile due to respective downward and upward signal attenuation through the canopy. However, both provided an accurate digital terrain model and correlated well in their estimation of canopy height.

Despite the limitations of vertical forest structure assessment from airborne Li-DAR, observation of bird species could be linked to distinct forest vertical profiles. Specialist woodland species were found to have the strongest habitat preferences with regard to the vertical forest structure.

This project has achieved advancements in the mapping of agricultural land and habitats in Wales, using remote sensing data, specifically in the differentiation of grassland improvement levels and tree species discrimination from multispectral satellite imagery. Furthermore, a strong correspondence between airborne and terrestrial laser scanner outputs has been established and LiDAR forest profiles have been shown to relate well to known woodland bird habitat preferences.

The added value derived from examining these four research areas as part of a single study, consists of the knowledge gained in how best to harness the respective remote sensing methods for the evaluation of very different aspects of biodiversity. It has further been shown that it is possible to use optical remote sensing data at a high spatial and spectral resolution, but low availability to inform and improve the utilization of more widely accessible, but less detailed images. Furthermore, a method has been developed which allows the interpolation of avian diversity from the assessment vertical forest structure. As biodiversity consists of many different elements at a wide variety of scales it is crucial to be able to perform such integrated analyses of its various components. However, only a combined approach towards the utilization of remote sensing, as demonstrated in this study, is likely to gain the necessary data.

The outcomes of this research support Wales-wide assessment of biodiversity and facilitate the production of regional or national vegetation maps as well as structural attributes for input into models. Components of the study can be used to support, for example, climate change research, assessments of biodiversity and policy decisions. Optical and laser remote sensing data can be successfully utilized for Wales-wide biodiversity components analysis.

-

Table of Contents

List of Figures

List of Tables

'

Chapter 1

Introduction

1.1 Biodiversity

1.1.1 Definition of biodiversity

Biodiversity is the variation of all life forms at all levels of biological organization (e.g., molecular, organismal, populations, species or ecosystems (Wilcox, 1984)). This variation is a product of evolution and the constant specialization and speciation events occurring over time.

Biodiversity has generally been studied at three distinct levels; genetic, species and the ecosystem.. An increase in diversity is only possible through speciation events, which occur by way of natural selection and is expressed at the gene level (where the gene is the fundamental unit of natural selection). Genetic diversity is hence considered by some as the 'real' biodiversity.

The majority of studies on biodiversity are undertaken at the species or population

level because the scale and extent of the study can be easily defined. The species level also lends itself to the illustration of events and processes which influence diversity and reduce the intrinsic complexity of the natural environment to an easily comprehensible level.

Ecosystem studies of biodiversity are rarer, in part because of the difficulty in defining the limits of an ecosystem. The extent of ecosystems is generally larger, which restricts many empirical studies and hence many assessments and predictions of diversity are based on modeled data. Where levels of biodiversity are high, the ecosystem is generally more stable. The resilience to disturbance of any ecosystem is also determined by its inherent diversity, which determines the ability of the system to adapt to changing circumstances. A high number of species is an 'insurance policy' for extreme events (e.g., not all species will be susceptible to all diseases or require a certain temperature range). After an extinction event, empty functional niches (e.g., prey for a certain predator species) can be filled by a similar species.

To maintain diversity, the ability to adapt and change needs to be preserved.

Population and species extinctions are natural events and take place at all times for a number of reasons. They are opposed by speciation events and the respective rates of extinction and speciation occurrences, as well as species abundance and distributions, determine the level of biodiversity present on Earth at any time, which is not static. However, conservationists agree that the rate of extinction has risen in historic times to an unnatural level as a direct consequence of human activities (Chapin III et al., 2000). 40% of the 40.177 species assessed using the IUCN (International Union for the Conservation of Nature and Natural Resources) red list criteria in 2008 are now threatened with extinction and a large proportion

of species are currently vulnerable to extinction (Figure 1.1).

Habitat destruction, over-harvesting of resources, pollution, climate change and the introduction of invasive species have been identified as the most important causes of biodiversity loss, all of which can be attributed to human activity and population pressure.
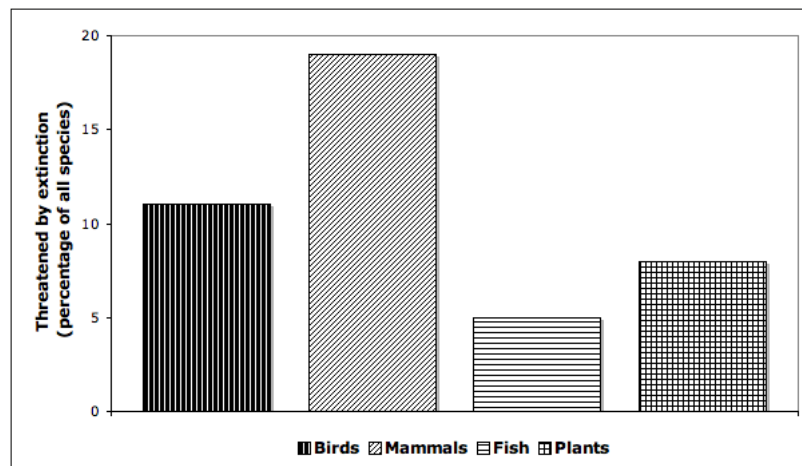
Figure 1.1: Proportion of the global number of bird, mammal, fish and plant species that are currently threatened with extinction. (Redrawn from Pimm et al. (1995))

1.1.2   Biodiversity in Wales

In Wales, a number of habitats are considered to be of special importance for biodiversity and therefore have received conservation status.

One of the main repositories of terrestrial biodiversity within Wales is contained in the large stretches of sparsely inhabited upland, located in the Cambrian Mountains and the Preseli and Brecon Beacon hill ranges, whose main human land use consists of extensive grazing by sheep and, to a lesser extent, cattle. The dominant

land cover types here are rough grasslands (e.g., consisting of *Molinia caerulea, Nardus stricta* and *Festuca ovina*), dry and wet moorlands (*Calluna vulgaris* and *Vaccinium myrtilus*) and climatically sensitive blanket bogs (*Sphagnum spp.* and *Eriophorum vaginatum*). 40% of the UK's land cover consists of uplands and these areas contain 75% of the world's heather moorlands. In the context of the UK, the northern Snowdonia mountain range also contains a UK-wide very rare alpine environment and endemic plant species such as the eyebright *Euphrasia cambrica.* Wales also has a large and varied coastline and several river estuaries with extensive associated areas of salt marshes and coastal wetlands (e.g., around the mouths of the Severn, Mawddach and Dyfi rivers) of international importance. Many sites are recognized as being important by the Convention on Wetlands of International Importance (RAMSAR convention).

The maintenance of a high level of biological diversity is one of the most important tasks of conservation in Wales. However, whilst conservation is important in Wales, there is also the need to house and feed a population increasing through natural growth and immigration. Hence, many of the diverse and biologically valuable areas are under increasing pressure and threat from anthropogenically-induced influences.

1.1.3   Biodiversity loss and human influence

Few areas of the global land and seascape have remained untouched by anthropogenic activity, either directly (e.g., through actual physical alterations such as building or agriculture) or indirectly (e.g, through air- or seaborne pollution or the

inadvertent introduction of alien species). As a result, the rapid loss of natural habitats has become one of the greatest threats to biodiversity.

The associated loss of faunal and floral species is a major concern, particularly for conservationist and politicians who are increasingly aware of the potential value of the natural environment for economy, health and quality of life and the risks of disturbance of often not yet fully understood natural patterns and processes. The environment, even if truly free from human influence, is in a constant state of flux. Changes do occur frequently, whether as a result of natural events and processes which can lead to extinction of populations, establishment of new populations or migration. Whilst the environment is highly variable, there is considerable resilience in the system to change and many ecosystems oscillate around a state of relative equilibrium.

However, the frequency and severity of change and change inducing events and processes have increased exponentially over the last century, largely because of changes in climate and human use of the landscape. There is increasing concern that the severity of extreme events might cause irreversible change in the environment, disturbing natural balances and shifting the original equilibrium to one that is less familiar. Land cover and land use change, as a result of the above events, have been identified as the most significant variable to affect biodiversity in terrestrial ecosystems over the next 100 years (Chapin III et al., 2000; Sala et al., 2000).

Conservation is, however, just one land use that competes with the need to house and feed ever increasing human populations on a finite land resource. Hence, many land areas that support a diversity of flora and fauna are often under considerable threat from anthropogenically-induced influences. Furthermore, whilst species

conservation efforts often concentrate on dedicated reserves, changes in land use, population pressure and, potentially, climate change will in future reduce the feasibility of such reserves. Efforts to integrate biodiversity and conservation concerns into land use decisions are hence increasingly undertaken. Reliable, spatially explicit information on land cover and habitat is an urgent requirement to enable policy makers and land managers to make informed decisions.

1.1.4 Biodiversity quantification

The true rate of biodiversity loss is impossible to identify, not least because of the difficulties of quantifying biodiversity, as explained below, but also because not all species on the planet are known or, if known, are described. Studies also have a distinct macroscopic bias towards the visible world. The majority of global biodiversity exists though on the microscopic level (e.g., amongst insects and microbes, the amount and trends in biodiversity here are mostly unknown due to the difficulty of monitoring). Because of the interconnected nature of ecosystems, where there is a large amount of interdependency amongst species at all scales, this microscopic biodiversity is just as important as that which can be observed by the naked eye.

Biodiversity is not equal across the globe. In terrestrial ecosystems, diversity is consistently higher in the tropics and fewer species occur towards the polar regions. 'Biodiversity hotspots' are defined as regions with a high level of endemic species and are found were very specialized habitats require a diverse range of adaptations (e.g., in the Amazon basin and other rainforest regions). As much attention has focused on these 'hotspots', biodiversity loss is sometimes perceived to be mainly

a problem in developing and/or tropical regions.

This misperception ignores the problem of biodiversity loss occurring at the same time within developed countries, including the UK, because of human population pressures and its associated problems, as described above. The UK is hence implementing Biodiversity Action Plans (BAP), which devolve some of the responsibility for the inventory of and action to conserve biodiversity to local authorities. However, to effectively preserve biodiversity, reliable regional assessment and monitoring methods need to be employed to detect trends and allow targeted use of available resources.

Definitive quantification of biodiversity is problematic, largely because of the different elements of diversity that are intricately interlinked (e.g., flora, fauna, climate and the physical environment) and the varying scales involved (e.g, microbes to large mammals and plants). The greatest diversity also tends to be found where studies/inventories have been targeted and hence the view of global biodiversity can be skewed.

As a general indication, biodiversity is often plotted as a function of the species richness of a geographic area and often with some reference to temporal scale (Whittaker, 1972). There are also a number of objective measures to empirically estimate biodiversity, as listed in Table 1.1, which are in widespread use (Krebs, 2008). They are, however, all limited for wider application and often relate to a particular use of the data. Most studies therefore calculate more than one measure to provide an estimate of diversity.

where

Relative measures of biodiversity (e.g., high or low) are often used as an indicator

Table 1.1: Biodiversity measures

Index name	Definition
Species richness	S
Simpson Index	$D = 1 - \frac{\sum_{i=1}^{S} n_i(n_i-1)}{N(N-1)}$
Shannon-Weaver Index	$H' = \sum_{i=1}^{S} p_i \ln p_i - [(S-1)/2N]$

Table 1.2: Diversity index symbol definitions

Symbol	Definition
S	Number of species (species richness)
N	Total number of all individuals
n_1	Number of individuals of species i (species abundance)
p_1	Relative abundance of each species ($\frac{n_i}{N}$)

of the health of the environment. However, such measurements are only meaningful if they are compared against a benchmark (e.g., for the ecosystem being considered). However, benchmarks and trends can only be reliably established through monitoring over time and, for this reason, there is an increasing need to monitor and, where possible, predict trends and changes and their likely consequences.

It is, however, very rare for biodiversity to be surveyed as a single measure. Much more frequently, elements of biodiversity, such as species abundance and habitat distribution or condition are recorded over a certain area as part of a larger framework. These records are subsequently combined in measures such as the above. Habitat availability, for example, is one of the most important facilitators for stable levels of biodiversity and data on the spatial distribution and condition of various habitats are hence of considerable value to all assessments of biodiversity. These data, however, are very difficult to obtain on a regional scale while at the same

retaining sufficient detail to allow meaningful interpretation.

For these reasons this study firstly focuses on the representation within remote sensing data of two main components of the Welsh landscape (grasslands and forests), as well as more general habitat mapping and finally attempts to illustrate how detailed knowledge of a habitat can be linked to the distribution of species which utilize these habitat elements (Section 1.3).

1.1.5   Landscape ecology and biodiversity

For the reasons mentioned above, there is an increasing and urgent need to create inventories of habitats and species to aid policy decisions and the responsible and sustainable management of land resources. By ensuring the conservation of existing habitats and utilizing the potential for habitat expansion and integration into the landscape, biological diversity can be maintained and the resilience of the systems maintained.

However, there is no consensus within the scientific community on the most meaningful way to measure biodiversity and the scales at which measurement should be taken. For this reason, mechanisms for providing standard measures of biodiversity at scales ranging from local to regional are needed.

Spatial quantification of biodiversity and its elements have first been undertaken by landscape ecologist. Turner et al. (2001) describes landscape ecology as the reciprocal effect of spatial pattern on ecological processes and as a consequence, this comparatively new discipline has developed an understanding of ecological phenomena, which is inextricably linked with the spatial distribution of landscape elements.

The term landscape ecology was first used by Troll (1939), a German biogeogra-

pher who recognized the potential of aerial photographs for the analysis of spatial patterns.

While traditionally, ecological studies assumed spatial homogeneity, landscape ecologists now routinely consider the implications of spatial patterns and variations as a function of ecological processes, regardless of the scale at which these occur (e.g., individual, population, communities or ecosystems). Landscape ecology can hence be defined as the ecology of spatial configuration and as the study of ecological causes and consequences on spatial patterns, processes and change in the landscape (Turner et al., 2001).

In this context, the landscape is defined by the visible features of an area of land, such as vegetation. These features can originate from variability in the physical environment (i.e., the topography determined by the underlying bedrock formations), natural interactions of living organisms (flora and fauna) with each other or the physical environment, natural disturbances, (e.g., floods or earthquakes) or anthropogenic influences (e.g., building activity and land use, such as agriculture or forestry). The classification and mapping of such features is one of the largest areas of research within the discipline of remote sensing.

Landscape ecologists frequently use maps of habitat extent, with these either generated from ground surveys, manual aerial photography interpretation or, increasingly, from the automated analysis of remotely sensed data. The improving capacity to observe landscapes remotely at fine spatial resolutions, and in three dimensions, from an ever greater range of optical and laser sensors facilitates the generation of such maps. Data analysis and interpretation methods are, however, also required to evolve constantly in order to deliver useful spatial information at

larger scales than is feasible to record manually.

This study hence aims to contribute to the effort to improve and expand such interpretation methods.

When assessing biodiversity, the issue of scale is an important consideration. A common mismatch between the requirements of science and those of policy makers or land managers occurs because of different approaches to scale. Most experimental designs are on a small scale with a comparatively short life span and an arrangement that allows sufficient repeats to obtain statistically valid results. Applied science, however, requires information on an appropriately larger scale to devise management regimes and inform policy decisions and direction.

There is further an increasing requirement for spatial information on biodiversity because of the importance of species distributions in determining diversity and the nature and consequences of change. The extinction of a species is often preceded by range contraction, an increasing rarity of the species or fragmentation of a species habitat. The area of a given habitat and the number of species it is able to support within this area are also directly related (Equation 1.1), with some variations (e.g., in the size of organisms). All of these are phenomena that can be quantified spatially.

$$S = cA^z \tag{1.1}$$

$$log(S) = log(c) + zlog(A) \tag{1.2}$$

The structure of a landscape is dependent on and determined by the size of the area, which is considered and specifically by the grain or resolution at which land-

scape features are defined. Hence, scale will strongly influence the specified hetero-
geneity of the studied landscape and identifying the optimal scale for quantifying
the relationship between spatial heterogeneity and the ecological process of interest
is a major challenge for landscape ecologists.

1.2 Remote sensing

1.2.1 Remote sensing in the landscape context

In many ways, landscape ecology as a science has arisen as a result of the need
to understand human impacts of the landscape. However, many landscape de-
scriptors, whilst providing a general overview of the distribution and geometry of
elements, do not consider the impacts of management (e.g., sheep grazing, heather
burning) on the landscape. Much of these changes are subtle and may occur over
long time periods (decades). Capturing such changes requires an understanding
of the impacts of management practices on the landscape. Given the dynamics
of many landscapes, remote sensing data acquired over over periods ranging from
weeks to years need to be used in order to adequately the variation that occurs.
However, most mapping exercises and particularly those at a regional level, focus
on the establishment of a static map for a particular year. An example are the
UK land cover maps for 1990, 2000 and 2007. However, such approaches do not
capture the temporal variability occurring within seasons and between years.

Troll (1939) was strongly influenced by the novel opportunities arising from the use
of aerial photography in regional vegetation studies. Since then, the potential of
remote sensing to provide information on the landscape has expanded enormously

and an increasing number of operating modes are being exploited (e.g., LiDAR, hyperspectral optical data, Radar). These data are typically used within the framework of Geographical Information Systems (GIS) and are widely exploited by landscape ecologist as a means to observe, visualize and analyze ecological patterns across a range of scales. With advances in these technologies and computer processing ability, the use of remote sensing data in landscape ecology studies has expanded rapidly in recent years (Turner et al., 2001).

Remote sensing data facilitate the observation of patterns in the landscape but also, through time series, processes leading to change. Understanding these changes and predicting future changes is an important requirement for conservation, particularly in relation to policy-driven decision making processes. In the past and even today, the observation and tracking of these processes has been largely neglected partly because of the means to compare between the present and the past have so far been limited. Long-term studies are also rare because of the lack of long-term funding and commitment to monitoring and very few are consistent over long time-periods. There is also limited comparability between independent surveys of various ages as they suffer from the inevitable bias of their original design purpose and the varying viewpoints and backgrounds of the scientists involved.

For monitoring, it is essential for processes occurring in the landscape under the current climate to be observed. As pointed out by Reichholf (2005), it is a fallacy to assume that one point in time as the optimal state of nature (i.e., that of the most diverse and healthy) because of the constant flux of natural balances. It is also not presumptuous to conclude from the observations of the landscape, its

connectivity and state in relation to the distribution of its faunal occupants.

In many early remote sensing studies, data from the Landsat series of sensors was largely utilized for land cover mapping. These data were however limited by coverage, because of the persistence of cloud cover in the UK, and also spatial resolution, which at 30 m, was relatively coarse for habitat mapping. In recent years, a wider range of optical sensors have been acquiring data over the United Kingdom and the greater repeat coverage has allowed more images to be obtained. These satellite sensors (e.g., SPOT 5 HRG, Terra-1 ASTER) have also provided data at a finer spatial resolution (typically < 20 m) which allows more detail in the landscape to be resolved. There is also increasing capacity to obtain longtime-series of these data and also to retrieve three-dimensional information with increased availability of LiDAR and SAR. Hence, the opportunities for characterizing, mapping and monitoring landscapes across a range of scales has increased significantly.

Scale is a further significant consideration during landscape mapping. For example, assessments of biodiversity may focus on a small patch (e.g., a pond) or a much larger region. The method of quantifying the landscape then varies and may be based on ground survey or utilize different forms of remote sensing data ranging from aerial photography to satellite sensor data. In each case, biophysical properties are retrieved or the landscape is classified, but the level of detail varies depending upon factors such as spatial resolution but also upon the classification scheme applied. Within the United Kingdom , for example, hedgerows are an important component of the landscape but are omitted from many classifications (e.g., the UK land cover map (Fuller et al., 2002, 2006) and most of the original Phase 1 survey). Therefore, linking the spatial maps of the landscape to mean-

ingful quantitative indicators of biodiversity (e.g., bird species distributions) is limited.

The capacity to be able to observe, map and monitor the landscape using remotely sensed data has come at a time where there is an urgent need for information on the environment. In particular, human-induced interference with the landscape has led to changes that reduced biodiversity. These included political and socio-historical pressures (particularly fluctuating policy and market forces) which are the underlying causes of change in agriculturally dominated landscapes (Baudry and Poggio, 2007). However, in addition, a more ominous threat of climate change is anticipated to lead to far more impacts and significant loses of species. For these reasons, there is a need to quantify and integrate information on the spatial and temporal components of the landscape to fully document and interpret the impacts of human-induced and climate change, including those leading to habitat fragmentation and loss of biodiversity. Establishing baselines of habitat condition and extent is also fundamental to the assessment of change but these need to be at an appropriate scale and level of detail.

1.2.2 Vegetation mapping

In all landscapes, the richness and abundance of both flora and fauna is dependent upon the vegetation present. Many plants (e.g., ground flora, epiphytes) occur as a consequence of the environmental conditions (e.g., sunlight, nutrients) imposed by other plants (e.g., trees) or competition within and between species. The majority of faunal species are dependent upon the type and condition of local flora. Hence, to quantify biodiversity within a landscape, spatial mapping of vegetation

extent and characteristics (i.e., species, structure, biomass and seasonal phenology) at appropriate spatial and also temporal scales is fundamental. However, many maps of the landscape have insufficient descriptors of plant species composition but also the state and condition of vegetation. As a consequence, the diversity of flora and fauna and their response to change (whether natural or anthropogenic) has proved difficult to quantify. Existing vegetation cover can also be a mitigating factor in the management of climate change effects. In particular, local microclimates are often dependent on the land cover present and this might therefore offer a certain amount of resilience to temperature and precipitation changes. However, existing mapping of vegetation often falls considerably below the detail which is required to inform and assist in the implementation of management strategies and accurate maps of, where possible, individual species, species communities and habitats are needed.

In the past, environmental protection of species has only proven effective if coupled with habitat protection. To observe processes and change and monitor its effects, it is necessary to establish a baseline against which to compare change. In the UK (and specifically Wales), such a baseline was established through the Phase 1 survey of the late 1980s and early 1990s. As the primary spatial dataset of semi-natural habitats and the extent of agriculture across Wales, this survey was based on a combination of field observations and aerial photography interpretation. The maps generated from the Survey are still widely used today in decision making and and as a baseline against which to measure change. However, a limitation of the Phase 1 Survey is that updates have not occurred and yet significant changes in the landscape have taken place as a consequence of changes in, for example, agricultural policy. Therefore, wide-ranging changes of land cover and land use have

taken place in the meantime, resulting in great inaccuracies between the survey and the actual up-to-date status of the landscape. Additionally, the Phase I survey was conducted over a long time period by a great range of surveyors of widely varying skill and aptitude, causing large inconsistencies from the outset (Wyatt, 1991). The classification system is also very open to interpretation and often does not deliver sufficient information for some ecological applications (e.g., biodiversity assessments). Therefore, to maximize utility, the Phase 1 Survey would require regular updates but this has not been possible because of the lack of financial and resource investment and political will.

Rodwell (1991) expressed the hope that the National Vegetation Classification (NVC) would fulfill the function of a national vegetation survey system for the UK. This Phase II Survey is far more detailed than the Phase 1 and was developed from the late 1970s. However, the cost and effort involved in this very detailed ground-based survey technique is prohibitive and hence it has not been undertaken at a national level. Currently, the Phase II Survey is only used to advise on the distribution of vegetation communities within small areas of high ecological interest that were identified within the coarser Phase I Survey.

This study therefore uses the example of grasslands to explore the potential of hyperspectral remote sensing imagery for the detailed analysis of the ecological diversity and interest of a defined vegetation community.

1.2.3 Land cover mapping in Wales

Several attempts to map land cover types across Wales (some of which equate to Phase 1 habitats) have utilized satellite sensor data as opportunities for routine mapping are provided. Using 30 m Landsat Thematic Mapper (TM) data, the first satellite-derived (pixel-based) map of land cover was generated in 1990 as part of the United Kingdom Land Cover Map (UK LCM) (Fuller et al., 1994). A follow-up map (based on segmented objects) was generated for 2000 (Fuller et al., 2002) and a further update was anticipated for 2007 (Fuller et al., 2006). For the 1990 and 2000 maps, Landsat sensor data from winter and summer were the primary data source and the classification was undertaken using a supervised algorithm trained with samples representing a range of land cover types.

These maps have so far been taken up very reluctantly by the ecological community, due to their low resolution and occasional large inaccuracies, but also due to a gross lack of understanding amongst the intended users of the possibilities and limitations of remote sensing, which has lead to a large discrepancy between expectations on the one hand and delivered map on the other. Nonetheless, the land cover map project has been one of the principal drivers in the development and application of object-based image analysis (OBIA; Lang et al. (2006); Hay et al. (2008)) in the environmental sector.

Land cover maps largely based on optical, satellite-borne remote sensing data and created through a standardized, automated classification system could offer a cost-effective, large-scale solution to obtain sufficient spatial and temporal detail on the distribution of habitats. In particular, the use of these data would:

1. potentially remove the bias associated with human collection and interpre-

tation of plant surveys.

2. facilitate better observations of changes in agricultural areas. Intensification of agriculture is one of the main drivers of biodiversity loss (Reichholf, 2005; Stevens et al., 2006) but can be readily mapped and monitoring using remote sensing data particularly if coupled with ancillary datasets such as the Land Parcel Information System (LPIS) and Mastermap data (Lucas et al., 2006b).

A system of mapping and spatial inventory, with capacity for generation of spatial metrics, is essential to establish conservation and research priorities and to obtain the elusive goal of sensitive conservation of the landscape and its resources (Rodwell, 1991). An integrative GIS-based system providing information on the spatial distribution of plant species, as well as associated information, such as soil and climatic conditions, is also necessary for identifying areas suitable for habitat restoration or expansion in the event of climate change (e.g., the best combination of climate and soils for particular types of broadleaf afforestation). Additionally, spatial information on, for example, the distance to the nearest patches of the same species or community would be helpful in the decision-making process. This would assist in the development of strategies for reinforcing existing networks and their connectivity or expanding networks and creating 'spearhead' patches as opposed to 'stepping stones'. The argument for improving the density of existing networks first is the multilateral, positive effect this could have on secondary species dependent on the connectivity between patches of the targeted restoration community and the natural expansion which will most likely follow an improvement of the network structure. In this context, Avery (2008) calls for the creation of a national map of habitat creation opportunities with regard to helping flora and fauna adapt to a changing climate.

Reliable tools are also required to identify range declines, as smaller, isolated populations are often a result of range collapses due to a decline in external conditions (climate, habitat, food) and are subsequently at greater risk of random extinction (Hanski, 1998). These populations also demonstrate a much lower resilience to sub-optimal conditions.

A particular advantage of using remote sensing for monitoring is that data can be acquired on a regular, repetitive basis and using the same wavelength regions, such that consistent comparisons within and between regions can be made. Furthermore, data can be acquired in different seasons, thereby allowing the temporal variations in reflectance to be exploited for mapping and monitoring purposes. The use of these data is particularly beneficial as the degree of spectral distinction between different vegetation types varies across the seasons (e.g., deciduous and coniferous forests are easier to distinguish in the leaf-off season).

This study therefore aims to demonstrate a land cover mapping approach from multi-spectral data which incorporates these elements.

1.2.4 Assessing vertical landscape structure

Biodiversity encompasses multiple biological elements and landscape structure and composition is one of the most fundamental of these elements. The term landscape structure implies a third dimension and vertical structure indices have been proposed as surrogate measure for biodiversity in forest ecosystems (Barbeito et al., 2009). The vertical configuration of vegetation in a forest, for example, is to many species, especially birds, as important as the area and location of the forest itself. Species utilize different layers within the vertical canopy profile for feeding, nest-

ing and courtship. Each canopy layer creates a unique niche composed of habitat features.

Most vegetation mapping from remote sensing data, however, has been conducted in two dimensions only, both manually (Wyatt, 1991) and from remotely sensed sources (Fuller et al., 1994, 2002, 2006; European and Commission, 1994). These maps have primarily focused on the two dimensional distribution and arrangement of habitats and have mostly disregarded vertical landscape elements, such as vegetation height.

The same applies to the majority of landscape descriptors, which focus on only two dimensional measures such as core area, area:perimeter ratios and distance between landscape features of the same type. This is demonstrated by the common use of FRAGSTATS (McGarigal and Marks, 2002), which provides tools for describing the structure of a landscape and linkages between elements but in two dimensions only.

All elements of the landscape (water, soil, vegetation, air), however, have a third dimension which is actively and wholly used by living organisms, but which is less well considered by landscape ecologists and during biodiversity components analysis. This has partly been a consequence of a lack of spatial information on the three-dimensional structure of systems.

With the advent of new technologies such as Light Detection and Ranging (LiDAR) and Radar this is now changing. The relative infancy of these technologies and their application to characterizing vegetation has so far resulted in a relative lack of information on the three dimensional structure of landscape elements and their contribution to biodiversity.

One of the aims of the present study is hence to further investigate the extraction of

three dimensional landscape information from laser remote sensing data of forests and the utilization of this structure by biodiversity indicators, i.e. birds.

1.3 Aims

The primary aim of this research is to establish the potential for utilizing a combination of airborne and spaceborne remotely sensed data to enhance the mapping and monitoring of biodiversity elements in Wales.

More specifically, the study aimed to:

1. Establish the potential of airborne hyperspectral data for the estimation of grassland biomass and differentiation of grassland improvement levels

2. Demonstrate the use of multi-temporal optical remote sensing data for large-scale habitat and land cover mapping, focusing specifically on forests, grasslands and moorlands

3. Evaluate and compare the potential and limitations of airborne LiDAR and terrestrial laser scanning data for the quantification of tree height, canopy openness and forest vertical profiles of different woodland types

4. Illustrate relationships between the vertical canopy structure of forests derived from airborne LiDAR and the distribution of woodland bird species

The research contributes to a better understanding of the use of remote sensing data for grassland differentiation, habitat mapping, as well as forest structure assessment in the UK from the individual field/stand to the landscape level (based on spaceborne optical data). Habitat maps provide opportunities to assess landscape

connectivity and fragmentation, as well as for interpolation of floral and faunal species distribution within the landscape, which are prerequisites for biodiversity assessment.

The project further contributes to scientific knowledge relating to the information content of airborne LiDAR data and also provides a unique insight into how the habitat suitability for woodland bird species might be assessed using remote sensing data without the need for extensive ground surveys.

1.3.1 Thesis outline by chapter

Chapter 1 has introduced the thesis and the context in which this study is expanding current knowledge. The particular aims of the research were outlined.

Chapter 2 provides a review of habitat and land cover observations from remote sensing and the subsequent opportunities for mapping habitats and detecting change.

Chapter 3 describes the location and main characteristics of three principal study sites (Trawscoed, Pwllpeiran and Lake Vyrnwy) and explains their suitability for this research. The significance of the study sites within the Welsh landscape will also be explained.

Chapter 4 outlines the data collection of all data used in the study, including field, airborne and spaceborne remote sensing data. All necessary pre-processing steps are explained.

Chapter 5 considers differences in the reflectance characteristics of grasslands at various levels of improvement using airborne hyperspectral data and identifies links

with their species composition and structure.

Chapter 6 demonstrates the concept of a rule-based approach to habitat classification (implemented within eCognition), with particular focus on grasslands and forests. The production of detailed habitat maps of the study areas from spaceborne optical remote sensing data is demonstrated and an assessment of the classification accuracy is provided.

Chapter 7 focuses on retrieving information about the vertical canopy profile of forests using airborne and terrestrial laser scanner data.

Chapter 8 focuses on the use of airborne laser scanner data for assessing the distribution of woodland bird species based on retrieved information on forest structure (e.g., height, openness and distribution of elements within the vertical profile).

Chapter 9 discusses the remote sensing of both faunal and floral biological diversity in the three-dimensional landscape, with an emphasis on biodiversity assessments and the implications for climate change adaptation and mitigation. The chapter also considers in how far the aims of the study have been obtained and evaluates the results of the research with regards to current knowledge in remote sensing of the environment.

Chapter 2

Review

2.1 Habitat and land cover manifestation within remote sensing data

As outlined in chapter 1, reliable and current information on land cover is important in the management of spatial resources and especially the monitoring and conservation of biodiversity. For this purpose, many field surveys are undertaken annually, with data collected by individuals and organizations under a wide variety of remits and survey designs. Once captured, these data become a snapshot in time and rarely can be retaken because of constant change in the environment. Variability and inconsistency in the data also occurs because of survey conditions and the bias associated with the differing experience, thoroughness and training of each surveyor.

As field data are collected to serve many different purposes, comparability both between different areas and over time is often low. Even if different questions from

the original study arise at a later point, it is often very difficult or even impossible to re-interpret the data. Furthermore the time required and cost involved in most manual surveys often are prohibitive or, at the very least, prevent repeat efforts at intervals that would allow continuous monitoring.

The Phase 1 Habitat Survey (Howe et al., 2005; JNCC, 2003) undertaken in Wales between 1987 and 1997 is an example. This Survey was aimed at obtaining a complete inventory of land cover and the distribution of approximately 80 semi-natural habitats and other land cover classes across Wales. Conducted over ten years at great expense, this survey is unlikely to be repeated in the foreseeable future (Stevens et al., 2004). Despite rapid changes in the environment, the Phase 1 Survey is still used today by a wide range of agencies to support planning and conservation policy, although local adjustments may be made from time to time and through local studies.

Wyatt (1991) and Cherrill and McClean (1999) investigated the qualitative variability of the survey as a function of individual bias and changing circumstance over the survey period and came to the conclusion that inconsistency through individual surveyor bias caused by differences in training and aptitude was a significant factor.

Whilst field survey techniques are extremely valuable, approaches that maximize the use of of the available remotely sensed data are desirable.

In general terms, remote sensing utilizes instruments mounted on satellites or aircrafts to acquire spectral or topographical information of the land surface. Sensors are divided between passive and active operational modes. Passive, or optical, remote sensing sensors capture the reflectance of the sunlight from the earth's surface while active sensors, such as LiDAR (Light Detection and Ranging) or Radar (Ra-

dio Detection and Ranging), emit a signal (e.g., a laser beam or microwaves) to the ground and obtain data via the proportion and strength of the returning signal. Remote sensing data from spaceborne sensors are particularly advantageous as they provide:

1. Coverage of a large spatial extent

2. Repeat (temporal) coverage, allowing rapid changes over large areas to be mapped

3. Consistency in observation in terms of spectral wavelength regions and spatial resolution

4. Long-term time series with which to detect change

Whilst remote sensing data of even finer spatial resolution (1-2m) have been provided for many years by airborne sensors (e.g., Compact Airborne Spectrographic Imager (CASI)), data of similar spatial resolution are increasingly being acquired by spaceborne sensors (e.g., IKONOS, Quickbird). Data from airborne sensors rarely provide complete coverage of regions, but they can be used to support the interpretation of data acquired by spaceborne sensors and validation of data providors.

Remote Sensing data acquired by spaceborne sensors are less affected by these problems and remain indefinitely available for re-processing once new procedures (e.g., atmospheric correction) are developed or for re-interpretation. Even so, technological progress occurs and data from some sensors may only be comparable for a restricted period of time (e.g., in the case of the Landsat MSS) and direct comparisons with data from other sensors may be problematic.

These limitations can, however, often be minimized through a range of image pro-

cessing techniques and data from satellite sensors are therefore relatively consistent within and between years.

Images are furthermore acquired on a repetitive basis in predictable cycles and large spatial and temporal coverage is therefore ensured although, in the case of optical sensors, cloud cover may limit the amount of usable imagery. Many optical remote sensing instruments record data at wavelengths that are not visible to the human eye or an ordinary camera (e.g., the near and shortwave infrared region (NIR and SWIR)) but which contain a wealth of information that can be utilized to discriminate between different land cover types.

For land cover mapping, data from satellite sensors are routinely exploited but their use is limited for the following reasons:

1. Only snapshots in time are provided and many studies have attempted to map areas for a specified year.

2. The ground surface is often obscured by cloud cover and often sub-optimal combinations of data have been used for mapping depending on availability

3. Mapping has typically relied on data acquired by a single sensor (typically Landsat) and has often only used one or two images per year

4. Data from both optical and active sensors such as Radar and LiDAR have rarely been integrated to aid land cover mapping

The following section provides an overview of previous approaches to mapping habitats from optical sensors.

2.1.1 Passive remote sensors

In Wales, the most well known mapping products which have utilized satellite imagery have been the Land Cover Maps of 1990, 2000 (Fuller et al., 1994, 2002) and 2007 (Fuller et al., 2006). These maps were generated primarily by using 30 m spatial resolution Landsat sensor data (see Section 1.2). Since the land cover maps were generated, a number of satellite sensors observing at finer spatial resolution (e.g., the 10 m SPOT 5 HRG) have become available and provide unique opportunities for refining land cover maps. A particular advantage of these sensors is that the detail contained allows objects (e.g., houses, clusters of trees) to be better resolved.

An alternative approach to discriminating and mapping habitats was suggested by Lucas et al. (2007) as part of a pilot study commissioned by the Countryside Council for Wales (CCW) and the British National Space Centre (BNSC). In this study, which focused on the Berwyn Mountains in mid north Wales, time-series of Landsat TM/Enhanced TM data from four dates (March, April, July and September) were used as input to a rule-based segmentation and classification procedure developed within the Definiens suite of software (Definiens Developer; (Definiens, 2008)). The approach differed from the traditional methods in that the landscape was first segmented into objects of sizes that varied from individual pixels to entire fields (as defined using land parcel boundaries). A series of numerical rules were then applied on the basis of known linkages between the distribution of habitats in the landscape and their manifestation within remote sensing data. The sequential application of these rules allowed a number of semi-natural habitats and agricultural land covers to be discriminated to a level comparable to that obtained previously using the Phase 1 Survey (see Section 1.2).

Based on the success of mapping semi-natural habitats and agricultural land in the Berwyn Mountains, a further project aimed to extend the mapping approach to first update and/or refine the Phase 1 Survey for a range of environments (lowlands, uplands, coastal) within Wales and then to apply the resulting rule-set to generate a revised and updated national map.

2.1.2 Active remote sensors

Active remote sensing utilizes energy generated by the sensor itself to emit a signal (e.g., laser beams or microwaves) towards the land surface The most commonly used types of active sensors are Radar and LiDAR.

The limitations of active sensors are that the data are difficult and complex to interpret, primarily because they still are a relatively new technology. They are also generally not acquired over wide areas, with the exception of spaceborne SAR, which has not been used extensively in Wales. However, an exception is the NextMap Britain data which was acquired using an airborne interferometric X-band SAR and provides wall-to-wall estimates of terrain height and vegetation surface height (above mean sea level).

Airborne LiDAR provides very accurate information on the three-dimensional structure of surfaces but they are spatially limited in extent. Satellite based sensors, such as ICESat and the X-, C- and L-band SAR (e.g., TerraSAR-X, ENVISAT ASAR and ALOS PALSAR) enable more or less wall-to-wall coverage of entire landscapes (Hyde et al., 2006a). However, these sensors do not have the high resolution required to make precise statements regarding the structure of

landscapes (e.g., forests).

2.1.3 Spectral reflectance of vegetation
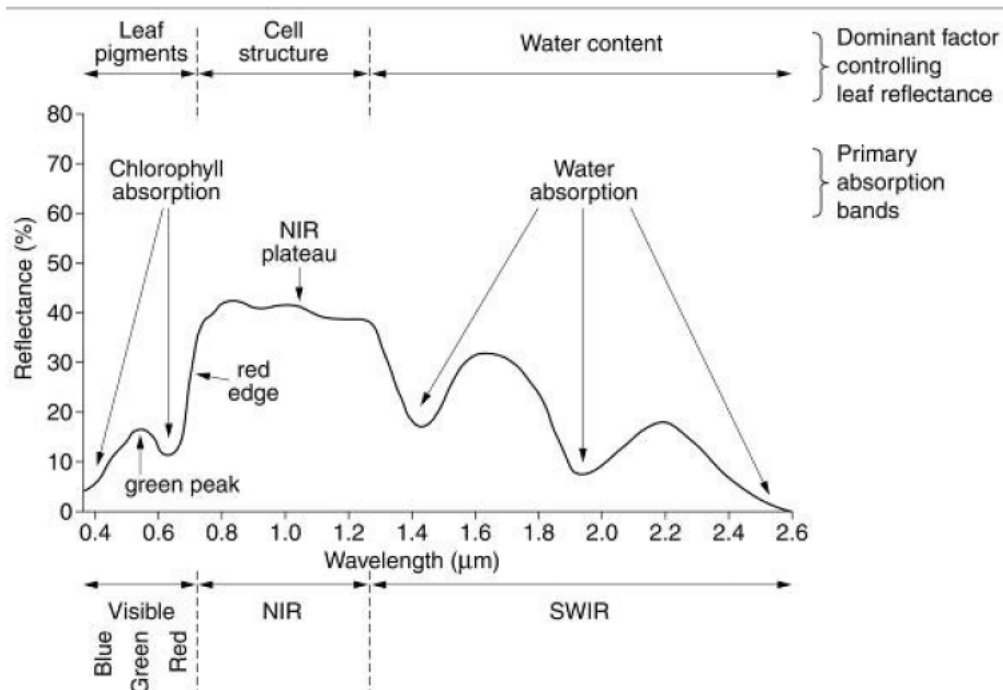
Figure 2.1: Vegetation Reflectance Curve (re-drawn from Elachi (1987))

Figure 2.1 illustrates a typical vegetation reflectance response across the light spectrum from the visible blue (400-500nm), green (500-600 nm) and red (600-700 nm) to to the near infrared (NIR: 700-1200 nm) and shortwave infrared wavelengths (SWIR; 1200-2500 nm). The intensity of the reflectance corresponds in turn to the sensitivity of the visible wavelengths to the amount of photosynthetic leaf pigments (chlorophyll a and b and carotenoids), the NIR wavelengths to the internal cell structure of leaves as a function air-water interfaces, and the SWIR to the

moisture content of vegetation (SWIR).

At the canopy scale the NIR and SWIR reflectances are also linked to the canopy structure, this applies to grasslands, as well as to forest and shrub.

Vegetation spectral reflectance is primarily a function of (Asner, 1998):

- optical properties of tissue, leaf, woody stems and litter

- canopy biophysical properties (leaf and stem area, orientation and foliage clumping)

- soil reflectance and hence vegetation density

- illumination conditions

- viewing geometry

While illumination conditions and viewing geometry can be mostly eliminated as factors due to standardization of atmospheric correction and rigorous nadir-looking data capture, the other factors are the variables which could hold the key to identifying the spectral signatures of grassland and forest communities, through their biophysical and biochemical characteristics. These factors are determined through measurable phenological phenomena in the vegetation canopy.

From spectral data, a wide range of indices can be developed with the Normalized Difference Vegetation Index (NDVI) being amongst the most frequently used. This index demonstrates sensitivity to the productivity of vegetation, with values

ranging from -1 to +1. Vegetation supports an NDVI > 0, with values derived from image data rarely exceeding 0.6. (Section 4.1.1).

Additional information on vegetation attributes can be obtained through spectral unmixing of the reflectance bands. Depending on spatial resolution and the homogeneity of the land surface captured in the image, the measured spectra of most pixels will be a composite of the reflectance of all the contributing materials present within the pixel. Endmembers are the individual constituent spectra of these distinct materials and commonly used endmembers include photosynthetic vegetation (PV), non-photosynthetic vegetation (NPV) and shade/moisture. This latter endmember reflects the roughness of the ground (with increasing roughness associated with increasing shade). Using techniques such as linear spectral unmixing (Adams et al., 1995), the relative proportions of these endmembers across the landscape can be estimated. The derived estimates can then be used subsequently to assist with classification of the landscape (Keshava, 2003; Bateson et al., 2000).

Within the UK, PV, NPV and shade/moisture are common elements of the landscape. For example, in the uplands of Wales, extensive tracts of land are dominated by Purple Moor Grass (*Molinia caerulea*) which is largely senescent in the winter and, to a certain extent, in the summer months. Bracken is another example but whilst this community supports a high proportion of NPV in the winter months, this is replaced by an equally large amount of PV during the summer months. The change from NPV to PV can be readily observed in optical sensor imagery acquired from late March though to late July. Differences between grasslands at varying levels of improvement are also reflected in shade/moisture fraction which tends to be greater in unimproved grasslands because of the greater amount of sur-

face roughness. Differences in the NPV and PV are also evident and suggest that discrimination of grassland types and growth stages may be achieved using these data. The use of endmember images can therefore provide unique information for discriminating and mapping a range of habitats.

2.1.4 Simultaneous acquisitions

LiDAR data only provide capacity for the retrieval of structural attributes of the landscapes and vegetation, but little insight into species composition can be obtained.

Optical and laser data acquired simultaneously, however, provide opportunities to combine the spectral and structural information derived from them and therefore increase the potential for differentiation of land cover. This is particularly beneficial in the case of vegetation with a pronounced vertical element, such as woodlands, but also other land cover types with a distinctly textured surface (Haack and Bechdol, 2000).

A further significant advantage of simultaneous acquisitions is the opportunity to create an accurate digital elevation model (DEM) from the laser data of the area covered by the imagery. This is very valuable as a tool in ensuring precise orthorectification of optical imagery, especially in regions with a pronounced topographic relief and applies to all types of land cover, e.g., forests and grasslands.

Increasingly studies are demonstrating, that by integrating data from different sensors, including optical (e.g., hyperspectral and, to an lesser extent, multispectral) and Interferometric Synthetic and Synthetic Aperture Radar (INSAR/SAR), forests can be better characterized in terms of their structure, biomass and species

composition (Hyde et al., 2005, 2006a; Chen et al., 2007a; Nelson et al., 2007) and over greater areas (Slatton et al., 2001), than by using LiDAR alone. Opportunities for detecting changes in these attributes over time and at various scales are also enhanced (Wulder et al., 2007a).

Approaches to integration have varied but have typically involved combining data and derived products from other sensors to better quantify forest attributes (e.g., Hyde et al., 2006a; Nelson et al., 2007; Lucas et al., 2008) or using LiDAR-derived information to better interpret data acquired by other sensors (e.g., Lucas et al., 2006a; Simard et al., 2008).

Studies are also increasingly incorporating data acquired by finer (typically < 1m) spatial resolution multi-/hyperspectral airborne (e.g., Compact Airborne Spectrographic Imager; CASI) and/or spaceborne sensors (e.g., Quickbird) to enhance descriptions of vegetation and land cover. The desire to simultaneously acquire complementary LiDAR and multi-/hyperspectral data-sets has also led to sensors being flown on the same platform (e.g., the Carnegie Airborne Observatory (CAO); Asner et al., 2008). More commonly, however, data are acquired using different platforms and on a similar or proximal date and algorithms for automatic rather than manual co-registration of data are then desirable.

Accurate co-registration of data-sets significantly increases the diversity of information that can be extracted. St-Onge et al. (2008), for example, used a LiDAR-derived digital terrain model (DTM) as a base for increasing the accuracy of tree height estimates generated from historical stereo aerial photography. Within co-registered data-sets, stand density can be estimated by counting a) extracted high points in LiDAR or 'bright points' in multi-/hyperspectral data (Wulder et al., 2000) and/or b) tree crowns/clusters delineated using algorithms ranging from

valley following to template matching (Bunting and Lucas, 2006). For open forests and orchard sites, retrieval accuracies have exceeded 70 % (Lee and Lucas, 2007b) and 99 % (Jang et al., 2008a) respectively. The advantage of having co-registered datasets is that trees identified within one can be attributed with measures (e.g., height or species; Chen et al., 2007a) from the other, thereby leading to better descriptions of the forest. As an example, Bunting and Lucas (2006) applied an algorithm developed within Definiens Developer software and CASI data to delineate tree crowns of varying dimension. Once delineated, crowns were associated with a species type using spectra extracted from the sunlit portions as input to a linear discriminant function.

Whilst hyperspectral data provide superior classifications of tree species, several studies have discriminated species or broad forest types using LiDAR intensity data (Antonarakis et al., 2008), relative height differences between the first and last vegetation returns (Moffiet et al., 2005) and directed graphs (Brandtberg, 2007). Holmgren et al. (2008) reported, however, best discrimination when using a combination of LiDAR and multi-spectral data.

While woodland environments form an obvious target for research into the advantages of integrated optical and laser data, such as LiDAR, other land cover type studies also benefit from such data integration. Bradbury et al. (2005) showed that crop and field boundary height could also determined from LiDAR data and combinations with land cover maps derived from optical remote sensing data would hence create a powerful tool for the structural description of farmed landscapes. This in turn could be used as a greatly improved input for organism-habitat models, such as for birds.

Kempeneers et al. (2009) used a combination of LiDAR and multispectral images

to map the vegetation of coastal dunes and assess its condition with regards to erosion risk. They found a considerable improvement in class differentiation ability and classification accuracy when using the data in synergy. Bork and Su (2007) found similar accuracy improvements while classifying heterogeneous rangeland vegetation.

The following sections provide an overview of how grasslands and forests have been characterized using various remote sensing data.

2.2 Remote sensing of grasslands

Using remote sensing data, important features of grassland functional community groups can be quantified including their biomass (Friedla et al., 1994; Boutten and Tieszen, 1983), productivity (Smita et al., 2008), living/dead matter ratio (Tucker, 1978) and structure (Guo et al., 2004). The information retrieved can subsequently be used to discriminate between different grassland types. Example of the manifestation of grassland types within remote sensing data are described by Hill (2004) and Trenholm et al. (2000) evaluated multi-spectral responses of selected grassland species.

Grasslands provide a unique challenge for remote sensing classifications since they are usually characterized by high variability (driven by species composition and proportional contents of forbs and grasses(Hill, 2004)), a lack of regular spatial

structure and an appearance of relative uniformity at the scale of satellite imagery.

Within the narrow range from ground level to approximately 1m in height, a wide diversity of vertical and spatial structures may be encountered. This structure is an important influence on the reflected or scattered radiation received by remote sensing instruments (Gamon et al., 1995).

Other factors affecting the reflectance of grasslands include terrain (which varies from steep slopes to flat expanses) as well as moisture content which varies from inundated (e.g., marshy grasslands) to dry (e.g., calcareous grasslands). Within many grasslands, the proportion of NPV can be substantial because of the contribution from standing litter and can vary from 100% (e.g., in *Molinia* dominated grasslands during the winter) to less than a few percent (e.g., very improved grasslands with a high proportion of *Lolium perenne*).

The relative components of live and dead tissue and the overall canopy structure are measurable in grassland swards and can be linked to variations in the features observed within hyperspectral and multispectral data.

2.2.1 Hyperspectral imagery and grassland properties

Many remote sensing studies of grassland properties specifically use either airborne or spaceborne hyperspectral imagery to obtain a more detailed understanding of grassland composition and properties. Hyperspectral data is well suited to this task due to its generally greater spectral and spatial resolution compared to multispectral sensors.

Research focuses specifically on a better understanding of grassland species composition, as well as grassland biomass and productivity.

Determining the species composition of grasslands, especially those of high diversity, is an important conservation priority, but is a time-consuming task to undertake over larger areas. There is a great need for accurate data on the distribution of natural resources as well as natural inventories and grasslands, due to their high prevalence in most ecosystems form a large part of this.

Studies which attempt to map grassland species include that of Jacobsen et al. (2000), who identified the spectral characteristics of a number of grassland species found in semi-natural grasslands through a canonical discrimination analysis of Compact Airborne Spectrographic Imager (CASI) and related floral composition to management practices. Yamanoa et al. (2003) and Schmidt and Skidmore (2001) used laboratory based spectroscopy methods to isolate unique hyperspectral characteristics of grassland species from two very different ecosystems in China and Kenya respectively and found that these were transferable to airborne hyperspectral imagery and hence formed a potentially effective tool for grassland mapping.

Grassland biomass estimation from remote sensing data is an area of great interest to agriculture as well as, increasingly, global carbon estimates (Jones and Donnelly, 2004). However, relationships between grassland productivity and diversity are also well documented (Guo, 2007) and reliable measures of biomass hence also contribute to the mapping and monitoring of biodiversity.

Studies commonly associate the red-edge and near-infrared (NIR) waveband regions with the best predictive ability of grassland biomass (Chen et al., 2009). Research hence further focuses strongly on the identification of narrow band ratio vegetation indices, as these overcome some of the saturation problems associated

biomass estimation (Cho et al., 2007; Mutanga and Skidmore, 2004).

2.3   Remote sensing of woodlands

The discrimination and mapping of forests is complex because of the diversity of tree species occurring and because of the deciduous nature of many. In particular, many broadleaved species and also Larch lose their leaves in the autumn and winter period but these reappear in the spring but often at different times during the growth period. Using single date optical imagery, discrimination and extraction of biophysical properties is best achieved during the full leaf period from high-resolution optical data, such as hyperspectral imagery (Bunting et al., 2006; Gong et al., 2003; Martin et al., 1998). Greater discrimination, however, can be achieved by considering time-series of optical sensor data which capture the seasonal phenology (Jing et al., 2009).

Low SWIR reflectance and a high shade fraction are two factors, which clearly distinguish forests from other habitats. Leaf angles, productivity, and seasonal change are other traits with which distinct spectral signatures of varying forest types can be explained.

A limitation of optical remote sensing for forest characterization is that they only provide a two-dimensional overview of the forest. However, to quantify the structure of forests, three-dimensional information is required. For this purpose, LiDAR data are most suitable and particularly if these are acquired at relatively fine (e.g., $< 1m$) spatial resolution.

2.3.1 Airborne LiDAR and forest structure

Remote sensing has been used to map and monitor forest extent (e.g., Botkin et al., 1984), type (e.g., Iverson et al., 1989) and condition (e.g., Rock et al., 1986) on a regular basis since the early 1970s. However, recent advances in sensor technology have allowed information on the three-dimensional structure of forests to be extracted allowing better descriptions of forests in terms of, for example, their above ground biomass (e.g., Drake et al., 2002) or biodiversity distribution (e.g., Warren and Collins, 2007). Synthetic Aperture Radar (SAR) has commonly been used for these studies (e.g., Lucas et al., 2004) as these data allow scaling across large areas. However, SAR is limited in its ability to quantify within canopy structures (i.e., number of layers or canopy depth) at high resolutions, although progress is being made in this area (Moghaddam and Lucas, 2003). For this reason, LiDAR data have been used preferentially for the extraction of detailed canopy attributes (e.g., height, crown volume). LiDAR also provides very high resolution three-dimensional information on the ground surface with typical point post spacings of 0.5 - 2 m. By removing vegetation returns from these data through appropriate filtering, highly detailed digital terrain models (DTMs) can be produced. Once generated, normalisation of vegetation points using the DTM allows creation of a canopy height model (CHM) and reliable measurement of vertical profiles and distribution of tree components within these.

Discrete return LiDAR data consist of the first and last returns from the laser pulse. Within a forested environment, the first return is typically associated with the upper canopy surface and the last with the ground surface or canopy elements (e.g., branches). More recently, multiple return LiDAR systems, which collect the first, second, third and last returns, have been used to provide increased information on

the structures in the upper parts of the canopy.

Measures that can be extracted from LiDAR data can be split into two categories, direct and indirect. The most common direct measure is height (Naesset, 1997) but also includes canopy cover (Lefsky et al., 1999a), depth (Chen et al., 2007b), openness (Lee and Lucas, 2007a), profile (Wulder et al., 2007b), outer ruggedness and crown dimensions (Hyppae et al., 2001). Indirect measurements establish relationships with those directly measured and include diameter at breast height (DBH), basal area and density (Hudak et al., 2008), timber volume and biomass (Naesset and Gobakken, 2008).

To further increase point densities and allow sampling across the whole vertical structure, full waveform systems have been developed. These systems record the intensity of the returned laser pulse as a function of time. Three methods have emerged for the processing of full waveform data. The first decomposes the waveform into discrete returns, with an intensity and width, allowing existing techniques to be applied in the processing of these data. Two common decomposition methods are threshold-based (Lin et al., 2008) and Gaussian decomposition techniques (Wagner et al., 2006). Recent studies (e.g., Lin et al., 2008) have highlighted the benefits of the Gaussian decomposition technique and developed extensions which allow overlapping pulses to be identified and decomposed, further increasing the number of points which can be retrieved and allowing smaller features to be identified. The second technique is to use the intensity and pulse width to model the geometry of the ground cover (Mallet and Bretar, 2009). These techniques have been most commonly used within urban environments where the geometry is relatively well understood. The third technique involves matching the waveforms to those that are known using signal processing techniques.

A number of studies have used full waveform LiDAR to extract and classify forest and vegetation. For example, Wagner et al. (2008) used the Riegl LMS-Q560 with a 25 cm footprint and mean pulse spacing of 0.5 m to classify vegetation and terrain within a set of formal gardens with an accuracy of ∼90 %. Reitberger et al. (2008) used full waveform LiDAR data to classify deciduous and coniferous trees within the Bavarian National Forest with accuracies of 85 % and 96 % in leaf-on and leaf-off conditions respectively. For classification, a tree crown delineation was performed on the canopy height model (CHM) and an average intensity computed for each crown; an unsupervised K-Means algorithm was applied to these data. To further describe the structure of the canopy, Hyde et al. (2006b) used the metrics outlined in Table 2.1 derived from full waveform LiDAR data. These structural parameters were then utilized to assess the landscape for wildlife habitat.

Algorithms have also been developed to derive measures such as basal area (Lefsky et al., 1999b; Means et al., 1999), canopy height profiles (Harding et al., 2001), canopy height (Kimes et al., 2006; Lefsky et al., 1999a), vertical distribution (Lefsky et al., 1999a), canopy cover (Means et al., 1999), canopy volume profile (Lefsky et al., 1999a), biomass (Hyde, 2005; Drake et al., 2002), mean stem diameter (Drake et al., 2002) and crown and stem volume from full waveform data (Mallet and Bretar, 2009).

By decomposing the full waveform data into discrete points, techniques and relationships previously derived for discrete return data are also valid. Such an approach allows algorithms developed for discrete return data to be applied to full waveform data with increased point densities. However, the retrieval is complicated by a number of factors including crown shape and leaf state (on/off; which vary within and between species), the location and spatial arrangement of trees

Table 2.1: Metrics derived from LiDAR waveforms (Hyde et al., 2006b)

Metric	Description
MINMAXHT	Minimum height of the top of the canopy (m)
MAXMAXHT	Maximum height of the top of the canopy (m)
MEANMAXHT	Mean height of the top of the canopy (m)
STDEVMAXHT	Standard deviation of the height of the top of the canopy (m)
MINCOV	Minimum canopy cover (%)
MAXCOV	Maximum canopy cover (%)
MEANCOV	Mean canopy cover (%)
STDEVCOV	Standard deviation of canopy cover (&)
MINHOME	Minimum height of the median energy of the waveforms (m)
MAXHOME	Maximum height of the median energy of the waveforms (m)
MEANHOME	Mean height of the median energy of the waveforms (m)
STDEVHOME	Standard deviation of the height of the median energy of the waveforms (m)

within footprints of varying dimensions, local slope, varying reflectivity of the ground and canopy, the LiDAR sampling intensity, atmospheric interference, and the reliability of ground measurement. These therefore need to be considered when applying any algorithm based on discrete return data (Yu et al., 2004; Harding and Carabajal, 2005; Hyde, 2005; Goodwin et al., 2006b; Hyde et al., 2006b; Wulder et al., 2007b; Jang et al., 2008b; Reitberger et al., 2008).

Hyde et al. (2006a), however, showed LiDAR data from the airborne LVIS sensor (Blair et al., 1999) alone to be effective in retrieving height and biomass of large trees and to be in this way superior to other sensors, such as InSAR, ETM+ and Quickbird.

A common limitation of airborne LiDAR data, however, is the expense of acquisition over large areas of forest (i.e., at the landscape level) and alternative

approaches (e.g., SAR interferometry) are often advocated as a solution.

2.3.2 Terrestrial Laser Scanning (TLS) and forest structure

TLS provide detailed reconstructions of trunk, branch and leaf distributions from which tree locations, diameter (Watt and Donoghue, 2005a), height (Maas et al., 2008b), timber volume by size class (Jupp et al., 2005), canopy gap fraction (Henning and Radtke, 2006b; Danson et al., 2007a) and Leaf Area Index (LAI; Jupp et al., 2009) can be quantified. Although limited by survey times and occlusion as a function of stand density, a particular advantage of TLS is that a permanent record of forest structure is provided.

Watt and Donoghue (2005a) used a Reigl LPM-300VHS TLS to map diameter at breast height (dbh) and tree height within Sitka spruce and lodgepole pine plantations in Kielder Forest, UK. Following capture, dbh and height were manually measured from the point data in Terrasolid software. A close relationship was observed with the field data providing R^2 values of 0.92, although point density, stem density and occlusion were identified as potential limitations of the process. Maas et al. (2008b) developed automated methods to identify individual trees and extract dbh and height for a range of forest types. 97.5 % of trees were successfully identified and dbh and height were identified with a root mean squared (RMS) error of 1.8 cm and 2.07 m respectively after outliners were removed. Tansey et al. (2009) compared three methods (circle fitting, cylinder fitting and Hough transform) for automating the extraction of dbh from the TLS data finding similar errors as Maas et al. (2008b) with RMS error ranging from 3.7 cm to 1.9 cm.

A close correspondence between forest height and, to a lesser extent, foliage profiles (Jupp et al., 2005) retrieved separately using co-registered TLS and airborne LiDAR has been reported. Linking TLS data with other remote sensing datasets (e.g., airborne LiDAR) does, however, require a high level of geolocational accuracy (Table 4.6). Hence, establishment of a comprehensive and precise network of ground survey points (Figure 4.11) and the use of high quality Inertial Navigation System (INS) for airborne systems is essential if all scan points are to be correctly located in three-dimensional space.

2.4 Biodiversity and remote sensing

Spatial indicators are required to assess habitats to support ecosystem integrity monitoring and to contribute to a more quantitative evidence base for monitoring and management of biodiversity in the UK and Europe. The Spatial Indicators for Nature Conservation (SPIN) project (Langanke et al., 2005) under the European FP5 programme recognized this need and endeavored to create and test a range of indicators at various sites in Europe (e.g., at selected sites in the UK and Northern Germany (Bock et al., 2005)).

The most obvious application of remote sensing for biodiversity assessment is the classification of land cover types from optical remote sensing images using their characteristic spectral properties. These classifications can potentially provide detailed information on the composition and distribution of vegetation, which is valuable in itself, and can often be used to define habitat suitability and the resulting faunal diversity.

Most maps produced for biodiversity assessment have been based on per-pixel classifications as opposed to object-based approaches. The benefits of an object-based classification include a greater ability to pre-filter objects of interest according to scale and mapping capacity.

Furthermore, most biodiversity assessments have been derived from two-dimensional information and ignored the additional benefit that three-dimensional data can provide.

Traditionally, all biodiversity assessment has relied on ground truth data, collected by field surveyors.

For forests, this has typically included direct measures, such as height, diameter at breast height (dbh) and stand density and habitat related surveys of associated species, such as birds (e.g., Common Bird Census). Whilst generally more accurate, such manual surveys are time and cost intensive and as such impractical and very inefficient at the landscape scale, particularly for ecological and conservation purposes. However, these measures are essential for many applications, such as timber and biomass estimations for commercial forestry and carbon accounting (Chen et al., 2007a), and structural assessments for biodiversity and habitat quality studies (Hyde et al., 2006a; Hill et al., 2004; Hinsley et al., 2006), which are rapidly gaining in importance.

The collection of grassland information is similarly work intensive and often involves detailed species identification work on the ground in a number of defined quadrats.

Whilst the level of detail in these type of surveys cannot be replicated from remote sensing data, there is increasing opportunity to do so through the use of new

technologies as indicated below:

- Terrestrial Laser scanning. Ground-based LiDAR provides highly accurate forest metrics, including height and vertical profile, but shares the disadvantages regarding large-area coverage with manual surveys (Tansey et al., 2009; Danson et al., 2007a; Watt and Donoghue, 2005a).

- Airborne LiDAR. The information provided by airborne lasers is very accurate, but also spatially limited. Statistical relationships between field, LiDAR and other sensors, however, allow the creation of spatially continuous maps at the landscape scale, even if the more detailed data is only available in the form of samples within the area (Hyde et al., 2006a).

  Indirect measures (e.g., basal area, timber volume and biomass) have been derived from the basic structural attributes, which are captured by terrestrial and airborne laser instruments (Lefsky et al., 2005; Tickle et al., 2006a; Goodwin et al., 2006a; Brandtberg, 2007; Popescu and Zhao, 2008).

- Hyperspectral sensors. Grassland productivity, biomass in particular and, to a lesser degree, species composition have been consistently assessed using airborne and terrestrial hyperspectral sensors, though the same spatial limitations apply as to terrestrial and airborne laser scanners (Yamano et al., 2003; Wamunyima, 2005; Cho et al., 2007; Psomas et al., 2007).

The advantages of using these data are that they provide opportunities for extrapolation of species information, either directly or through reference to measures of productivity (e.g., grasslands) or structure (e.g., forests).

Studies which have directly or indirectly assessed forest biodiversity from remote

sensing are Nagendra (2001) and Innes and Koch (1998).

The high diversity of fauna and non-tree flora associated with forests is attributable to the diversity of habitats, which, in part, is reflected in the spatial distribution and arrangement of structural elements within the volume space that trees create and occupy. Several studies have noted that the distribution and richness of bird species in particular are closely linked to forest canopy structure (Hyde et al., 2005) and heterogeneity (Goetz et al., 2007), both of which can be quantified using airborne LiDAR. Hill et al. (2004) and Hinsley et al. (2006) also reported a link between habitat quality (defined by forest canopy structure and height) and the breeding success of Great Tits (*Parus major*). Such assessments might be improved by integrating information on tree species and the age and condition of stands, as obtained using, for example, multi-/hyperspectral data (Hill and Thompson, 2005). Most studies focusing on biodiversity are confined to relatively small areas because of the limited coverage of airborne acquisitions. Extrapolation to regional areas requires the establishment of forest height and structural maps over larger areas, which can potentially be generated using SAR interferometry and/or IceSAT data. Such information would complement habitat maps generated at a commensurate scale using airborne/spaceborne optical data-sets.

Climate change will in the future precipitate changes in floral and faunal biodiversity. Remote Sensing is therefore expected to assume an increasingly greater role in the monitoring of the natural environment, which is a prerequisite for adapting to and mitigating for environmental changes expected in the decades ahead. The RSPB for example has listed a number of actions required which will help wildlife adapt to a changing climate (Avery, 2008) and one of the most urgent requirements is the creation of a national map of potential habitat creation sites (see

Section 1.2) to exploit these options fully, when the need and opportunity arises.

2.5 Summary

This review has provided an overview of

- Traditional habitat survey methods (e.g., Phase 1)

- The use of spaceborne remote sensing data for mapping habitats

- The lack of information on three-dimensional structure in land cover assessment

- Limited understanding of grasslands and their response in remote sensing data, particularly in relation to biodiversity.

This chapter has reviewed the types of Remote Sensing data and their use in retrieving biophysical properties and classifying the natural components of the landscape.

The chapter has also presented a theoretical review as to why certain properties can be retrieved. The use of Remote Sensing in biodiversity assessments has been demonstrated.

The next chapters will describe this in detail using the example of the present study.

Chapter 3

Study sites

Chapter 3 provides a brief overview of the main landscape features of Wales, focusing particularly on the climate, topography, soils and vegetation. A more detailed review of the grasslands at the two sites of Trawscoed and Pwllpeiran (Section 3.2.1) and the forests and heathlands at Lake Vyrwny (Section 3.2.2) is then provided.

The chapter justifies the choice of these study sites and provides a description of their context within the Welsh landscape.

3.1 Landscapes in Wales

3.1.1 Topography

Wales is largely a mountainous country, with much of its land lying above 150 metres. Yr Wyddfa (Snowdon) in the north-western national park of Snowdonia is

the highest mountain in England and Wales at 1085m. The major upland region in the south is formed by the Brecon Beacons, which rise to 885metres and the mountainous nature of the landscape means that large areas are only sparsely populated. Of the three million people living in Wales, over half are concentrated in the industrial areas of the south around the cities of Cardiff, Swansea and Newport, as well as Wrexham in the north-east.
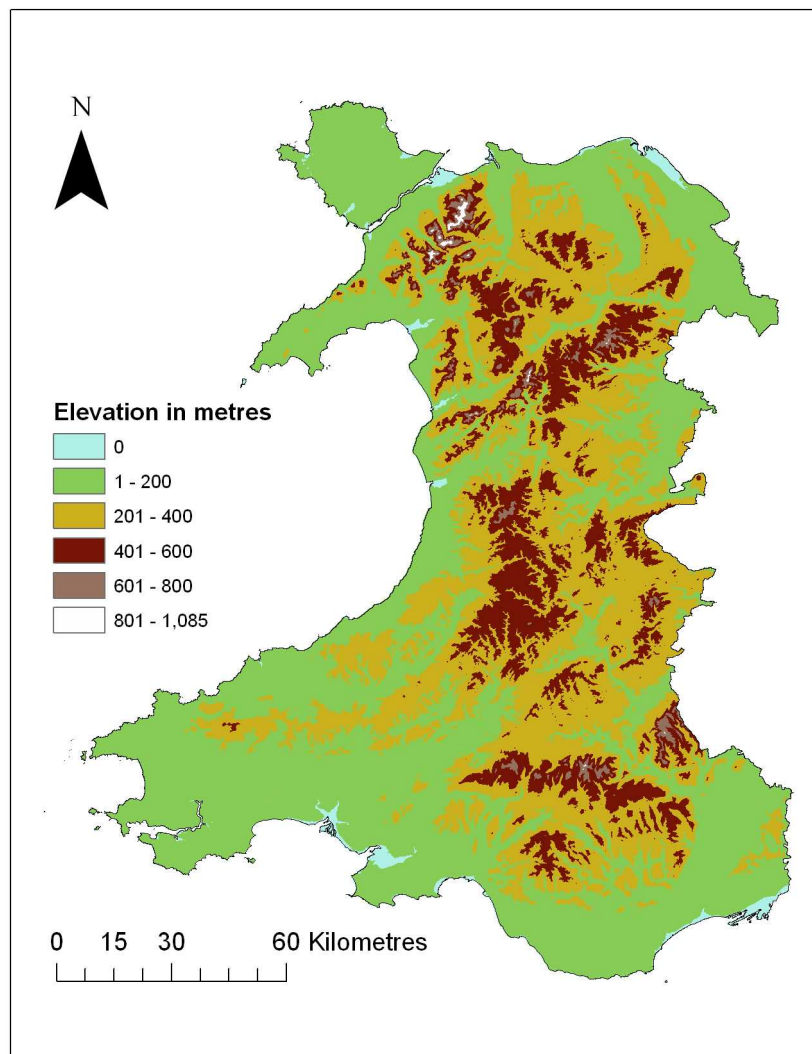
Figure 3.1: Digital Elevation Model (DEM) of Wales derived from NextMap Britain data

3.1.2 Climate

Wales has an essentially maritime climate, characterized by weather that is often cloudy, wet and windy, but mild. However, the shape of the coastline and the central spine of high ground from Snowdonia southwards to the Brecon Beacons introduce localized differences. Whilst some upland areas can experience harsh weather, the coastal regions have generally more favourable conditions and areas in east Wales are more sheltered and hence similar to neighbouring English counties.

Mean annual temperatures range from approximately 5 °C on the highest peaks of Snowdonia to 11 °C in the coastal areas (Figure 3.2). Mean daily minimum temperatures in January vary from just below 0 °C in the higher parts of north and mid-Wales to about 3 °C around the coast, while mean daily maximum temperatures are usually recorded in July and range from around 17 °C in the higher inland locations, to 18 °C along the west coast and 21 °C in the east of Powys and Monmouthshire along the border to England.

Wales' climate is primarily described as maritime, particular in the west and along the coastal regions. Rainfall varies considerably across Wales, but increases with altitude (Figure 3.3) and is greatest in the mountainous regions of the northwest, where the highest average annual totals are recorded. The wettest area is Snowdonia with average annual rainfall exceeding 3000 mm. In contrast, the coastal plains and regions close to the border with England are considerably drier, often receiving less than 1000 mm of rainfall a year.

The southern upland hill regions of the Brecon Beacons and the central hill range of the Cambrian Mountains divide the country between the climatically drier
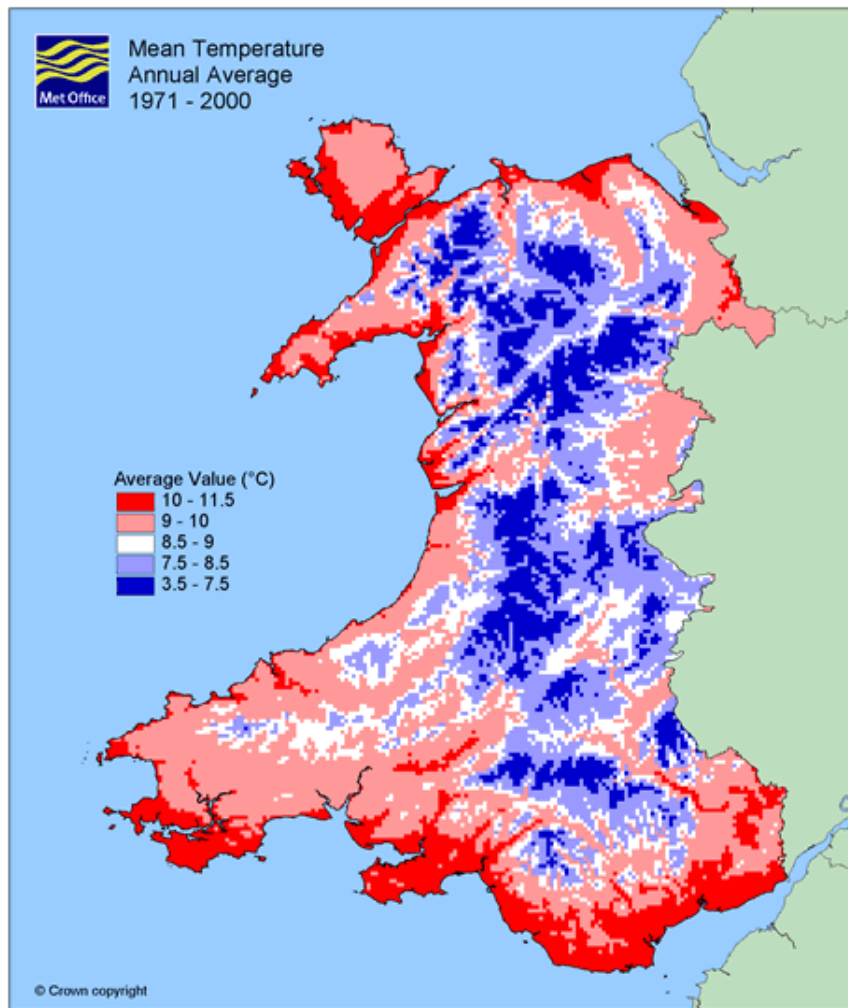
Figure 3.2: Mean annual temperatures across Wales (Crown Copyright/Met Office)

eastern stretches and the western areas descending towards the sea, which are more strongly influenced by the wetter Atlantic climate (Bendelow and Hartnup, 1980).
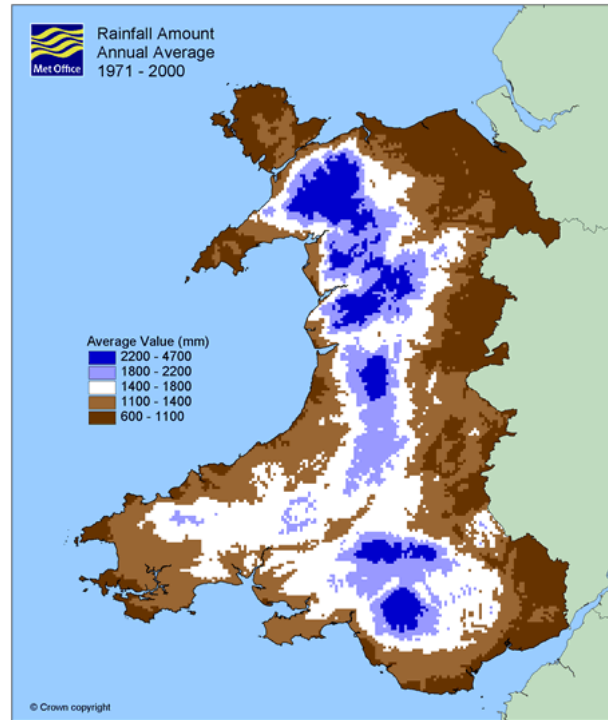
Figure 3.3: Mean annual rainfall across Wales (Crown Copyright/Met Office)

Climatic zonation

Previous studies (e.g., Bendelow and Hartnup, 1980) have attempted to divide Wales into biogeographical zones (Figure 3.4), giving consideration to location, continentality and elevation and their effects on climate and have directly correlated vegetation composition to climatic gradients (Yeo and Blackstock, 2002).

Table 3.1 lists the defining properties of the biogeographical zones outlined in Figure 3.4 by location, continentality and elevation Temperature gradients run
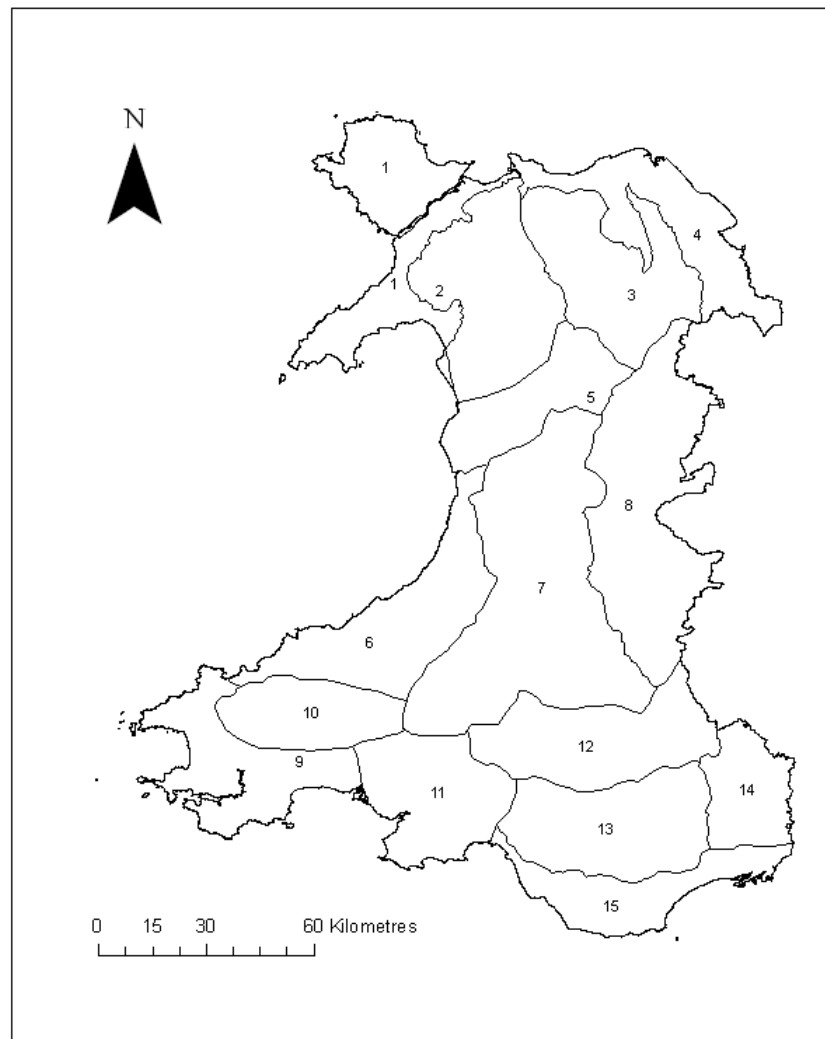
Figure 3.4: Biogeographical zones of Wales

from the north, the coastal areas and the uplands (coldest) to the south, inland regions and the lowlands (warmest), while precipitation is higher in the west and in the uplands than in the east and the lowlands.

Table 3.1: Biogeographical Zones in Wales

Map ID	Area	Location	Continentality	Relief
1	Anglesey and Llyn	Northwest	Coastal	Lowland and Upland
2	Snowdonia	Northwest	Inland	Upland
3	Mynydd Hiraethog	Northeast	Inland	Upland
4	North East Wales	Northeast	Coastal and Inland	Lowland
5	Cader Idris and the Mignant	Central West	Coastal and Inland	Lowland and Upland
6	Ceredigion and Coast	Central West	Coastal	Lowland
7	Cambrian Mountains and Elan Valley	Central	Inland	Upland
8	East Powys	Central East	Inland	Lowland
9	Pembrokeshire Lowlands	Southwest	Coastal	Lowland
10	Preselis	Southwest	Inland	Upland
11	Camarthenshire and the Gower	Central South	Coastal	Lowland
12	Brecon Beacons	Southeast	Inland	Upland
13	Head of the Valleys	Southeast	Inland	Upland
14	Monmouthshire	Southeast	Inland	Lowland
15	Gwent Levels	Southeast	Coastal	Lowland

3.1.3 Natural vegetation

In the past, a large majority of Wales' land area would have been covered by extensive broadleaf forests. Humans have, however, occupied the land for thousands of years and have impacted significantly on the distribution, composition and condition of vegetation.

In particular:

- extensive areas of deciduous forests have been cleared for agriculture or, in more recent times, have been replaced with coniferous plantations

- Uplands have been grazed by sheep for several 100 years, which has led to a change in the climax vegetation from forest to grassland

- Lowland marshes and fens have been drained and turned into arable land or intensive grazing

This focus on agriculture, and especially grazing, has resulted in a shift towards grasslands as the dominant land cover type within Wales and which today comprise over 60 % of the total land area (Table 3.2).

The Phase I Survey (Howe et al., 2005; JNCC, 2003) represents the most up-to-date mapping for Wales and defines 10 broad habitats (Table 3.2), within which over 80 land cover types are described.

Today, Wales contains a diversity of landscapes that extend from the coast to the mountainous regions. The coastal regions are diverse, supporting a range of estuarine habitats (e.g., salt marshes) and also sand dune complexes and coastal grasslands and heaths. Much of the lowland area below the enclosure boundary is

Table 3.2: Land cover distribution in Wales according to the Phase 1 habitat survey

Land cover type	Phase 1 code	Area (%)	Area (ha)
Woodlands	A	14.2	289818.7
Grasslands	B	62.2	1271633.2
Tall herb and fern	C	3.2	64804.6
Heathland	D	5.2	106452.0
Mire	E	3.0	61648.4
Swamp, marginal and inundation	F	0.1	2049.0
Open water	G	0.8	15713.9
Coastland	H	2.8	56451.9
Rock exposure and waste	I	0.7	13382.9
Urban and miscellaneous	J	7.9	161887.3

used for agriculture (primarily sheep and cattle grazing but also for arable crops) although extensive (albeit fragmented) areas of semi-natural habitat (e.g., mires, marshy grasslands) occur. Grasslands in Wales range from the intensively managed and strongly improved (i.e., reseeded and fertilized lowland pastures) to semi-natural, often single species, expanses of Purple Moor Grass (*Molinia caerulea*), Mat Grass (*Nardus stricta*) and Sheep's Fescue (*Festuca spp.*) in the less accessible upland regions. Even in the uplands though, these habitats are strongly modified by grazing pressure and their contribution to the overall biodiversity of Wales is therefore diminished.

Lowland grasslands of high conservation value in Wales often consist of wet 'Rhos' pastures and rare species-rich meadows, as well as unimproved neutral grasslands areas. Rhos pastures often support wet heath vegetation as well as rushes and grasses, which tolerate the waterlogged conditions. They were once so common that their Welsh name has been adopted in English as well.

A more detailed description of Welsh grasslands is given in Chapter 5.

Forests in Wales are diverse, but fragmented, with commercial coniferous planta-
tions in the uplands and broad-leaved and mixed forests in the lowlands. Many
forests are actively managed for either commercial harvesting, conservation or
recreation. Continously updated information about the size, distribution, compo-
sition and condition of Wales' woodlands are recorded in the National Inventory
of Woodlands and Trees (NIWT) compiled by the Forestry Commission. 14% of
the total land surface (20.779 km^2) of Wales is covered by forest, of which 57.8%
consist of commercial coniferous plantations made up mainly from Sitka Spruce
(*Picea sitchensis*) and Larch (*Larix decidua*), which is used to break up the vi-
sual impact of otherwise very large and monotonous, single-species stands. Other
commercial timber species present are Norway Spruce (*Picea abies*) and Douglas
Fir (*Pseudotsuga douglasii*). Only isolated and very small groves of semi-natural
conifer, such as Scots pine (*Pinus sylvestris*) can be found.

Apart from the coniferous forests, there are approximately 100.000 ha (30% of all
woodland in Wales) of broad-leaved woodland in Wales, of which around 34.000 ha
are ancient semi-natural forest, with Sessile Oak (*Quercus petraea*) the dominat-
ing tree species. Beech (*Fagus sylvatica*) is another species, which forms stands of
significant size and of a completely different structure. Furthermore there are im-
portant wet woodland habitats of willow (*Salix spp.*) and alder (*Alnus glutinosa*)
in the lowlands and upland stands of birch (*Betulus pendula*) and Mountain ash
or Rowan (*Sorbus aucuparia*) trees, especially along streams and on steep slopes,
where the grazing pressure is reduced. Hedges and scrub stands are further adding
to this range of important woodland habitats.

The mountain areas support some agriculture (primarily for sheep production)
but many are covered with semi-natural heaths, moors and bogs. Extensive, al-

beit fragmented areas of semi-natural habitat (e.g., mires, marshy grasslands and lowland heaths) remain in the lowlands. The most significant of these areas include Cors Caron National Nature Reserve (NNR) near Tregaron, Ceredigion, which is the largest area of near natural lowland raised bog habitat remaining in England and Wales, and also Borth Bog near Aberystwyth, Ceredigion. Remnant forest areas occur along the Ceredigion coast and in the Wye Valley.

The 1200 km coastline contains extensive areas of coastal cliff vegetation, sand dunes and saltmarshes.

Nationally rare alpine habitats occur in Snowdonia whilst the Berwyn Mountains are the southernmost habitat of the cloudberry (*Rubus chamaemorus*) in Britain and contain the greatest expanse of unmodified blanket bogs within Wales (Tallis, 1969).

3.1.4 Land use

About 80 % of the total land surface area in Wales is used for agriculture, with the majority being within the lowland areas (below 300 m elevation). Most consists of permanent grass pasture (for sheep and cattle production), which is interspersed with a smaller amount of arable land (less than 30%). The upland areas support extensive agriculture in the form of rough sheep grazing.

3.1.5 Landscape conservation value

Wales has three National Parks, Snowdonia, the Brecon Beacons and the Pembrokeshire coast, which are joined by a number of Special Areas of Conservation (SACs) and National Nature Reserves (NNR). There are also over a 1000 Sites of

Specific Scientific Interest (SSSI) in Wales, ranging from very small sites to large tracts of land, with over 50% located in the uplands. They cover just over 12 % of the land area of Wales. This illustrates the large amount of land with conservation interest that is present in the country.

3.2   Study sites

For this study two main sites were selected, with these chosen to represent grasslands and woodland sites respectively. Sites were selected for the diversity of habitats and vegetation types present.
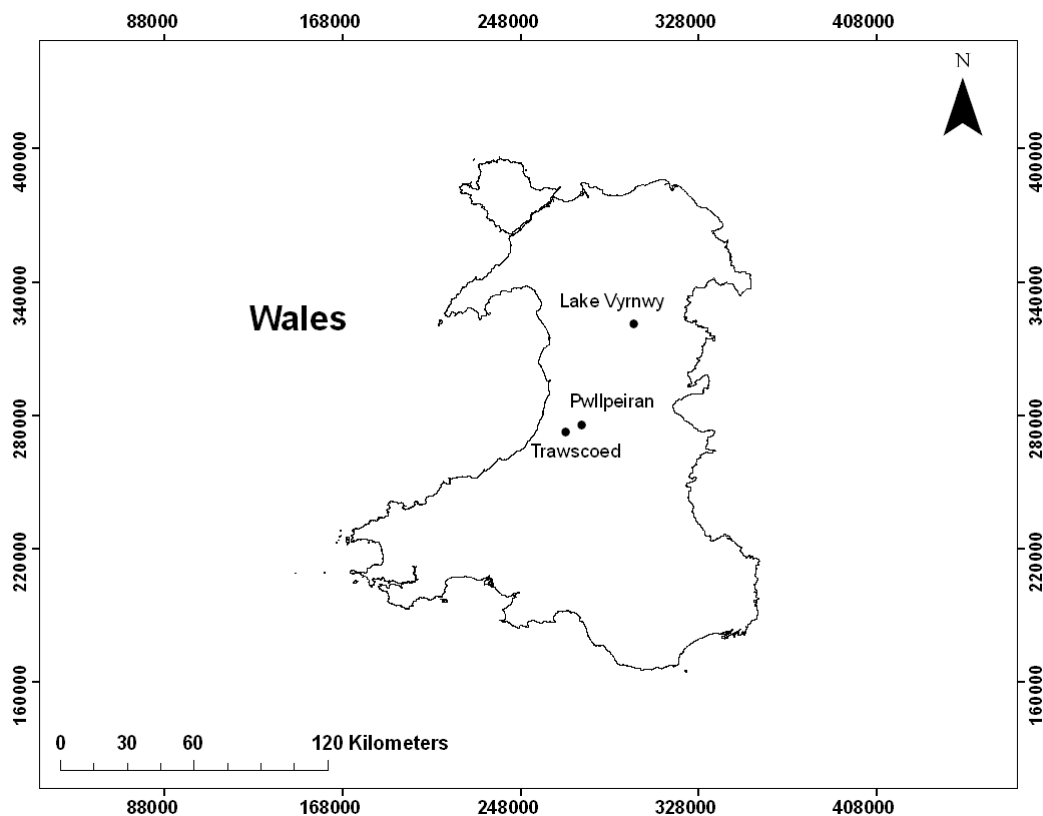
Figure 3.5: Study site locations within Wales

3.2.1 Grasslands: The Trawscoed and Pwllpeiran study areas

Trawscoed and Pwllpeiran are located near Aberystwyth (Figure 3.5) and are owned and managed by the Institute of Biological, Environmental and Rural Sciences (IBERS) at Aberystwyth University and the environmental consultancy ADAS respectively.

These two sites were selected, as together they supported grassland types ranging from lowland improved, Perennial Rye grass (*Lolium perenne*) dominated swards to upland semi-improved grasslands. Marshy grassland areas characterized by Purple Moor grass (*Molinia caerulea*) and Rushes (*Juncus spp.*) are occurring close to Pwllpeiran and the plots are considered to be representative of various grassland habitats occurring in the Welsh landscape.

These two sites were chosen especially because of their experimental design, as explained below, and the extensive records, which have been kept regarding their changing vegetation over the past 15 years.

Trawscoed

Trawscoed farm in Ceredigion lies at an altitude of 110 m above sea approximately 10 miles south-east of Aberystwyth. The study site was originally created in 1992 as part of a research experiment on the biodiversity restoration of previously intensely managed improved agricultural grasslands originally funded by the Ministry of Agriculture, Fisheries and Food (MAFF) which in 2001 was replaced by the Department of Environment, Food and Rural Affairs (DEFRA).

The site is comprised of a 3.6 ha hectare field divided into three blocks (see Fig-

ure 3.6), each containing six fenced 30 x 40 m plots for grazing control (see Figures 3.7 and 3.8). The site has received various management treatments (T1-T6), as outlined in Table 3.3, since its creation. Each treatment is represented once in each block, thus creating three replicates of each. T3 and T5 were merged in 2002 and are now managed identically; historically T5 sites were also cut for hay in early summer to decrease the nutrient content of the soil.

Figure 3.6: July 2006 Vexcel aerial photograph of the Trawscoed study site, treatment plots are outlined and labelled.

Figure 3.8 shows a south-west facing view of the trial plots at Trawscoed. The field on the right in the foreground of the image is the T6c plot, which is bordered by T5c to the left and T5b to the rear.

The management regimes as shown in Table 3.3, were continued by the Institute of Grassland and Environmental Research (IGER) after cessation of the initial funding in 1997, though monitoring of changes in the vegetation composition of the individual plots became sporadic and depended on available funds. Previous to
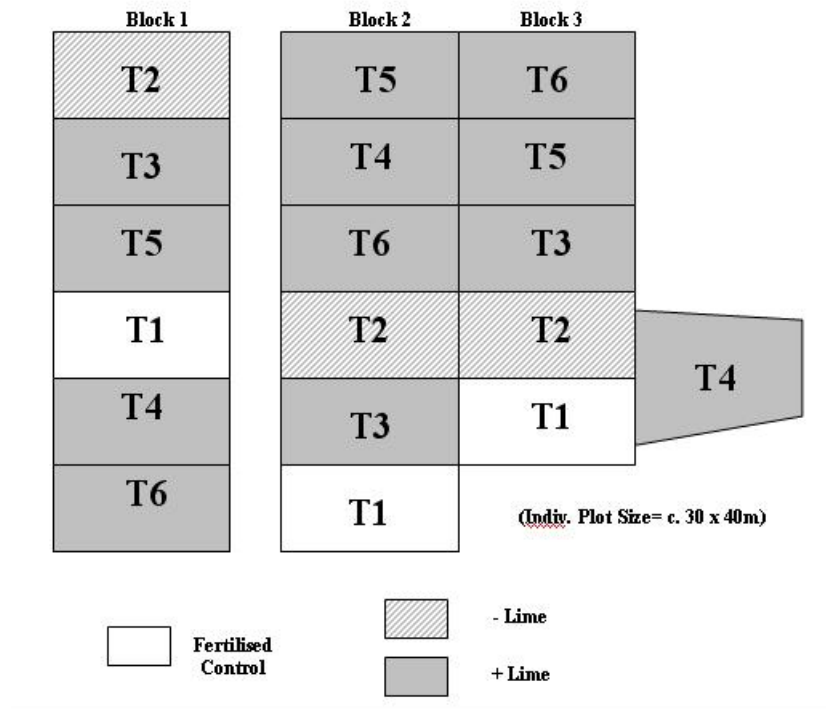
Figure 3.7: Trawscoed study site plot arrangement

Table 3.3: Trawscoed treatment regimes

Label	Sheep grazing	Hay cut	Fertilizer	Lime
T1 (Control)	continuous	-	yes	yes
T2	autumn/winter	July	no	no
T3	autumn/winter	July	no	yes
T4	no grazing	July	no	yes
T5	autumn/winter	July	no	yes
T6	continuous grazing	-	no	yes

Figure 3.8: Trawscoed study site plots

this, the site had been grazed by sheep with regular fertilizer inputs and the sward was dominated by *Lolium perenne* and *Poa spp.*. This status is still represented by the T1 control plots (Hayes and Sackville Hamilton, 2001).

After the merging of IGER with the Institutes of Biological Science (IBS) and Rural Science (IRS) of Aberystwyth University to form the Institute of Biological, Environmental and Rural Sciences (IBERS) in 2008, the treatments were discontinued and the fencing removed, though all fieldwork was completed at this time.

Pwllpeiran

Pwllpeiran is located near Devil's Bridge, approximately 13miles east of Aberystwyth in Ceredigion. The site lies at an elevation of approximately 300 m above sea level, near the main road leading to Cwmystwyth, adjacent to the historical Hafod estate. The trial plot arrangement at the site was created as part of the same DEFRA project as Trawscoed and shows a similar configuration (see figures 3.9 and 3.10) with the addition of one completely unmanaged plot and the P3 and P6 treatments sharing an enclosure. The management plan (see table 3.4) shows the same treatments as at Trawscoed with two additional plots at P2 and P3 where no lime was added to plots which are otherwise only grazed continuously or only cut for hay.

The fenced fields include one discard area in block 3, which is unmanaged and not grazed, but permanently fenced.

The experimental plots are part of an area of open, rough upland grazing dominated by a Sheep's fescue (*Festuca ovina*) sward and stocked predominantly with sheep and some Welsh Black cattle. Plot P2 in the experiment is identical in

treatment to the surrounding area.

There is a significant patch of *Juncus* on the eastern side of the experimental fields, just south of plot P1c. The practical management of the plots is undertaken by the local branch of the environmental consultancy ADAS, based at nearby Hafod and, as opposed to Trawscoed, continues to date (Summer 2009).

Figure 3.9: July 2006 Vexcel aerial photograph of the Pwllpeiran study site, treatment plots are outlined

Figure 3.11 shows plot P5c in the foreground and P4c adjacent to it. The fencing of block 2 (Figure 3.10) is visible on the hillside, rising beyond the plots.
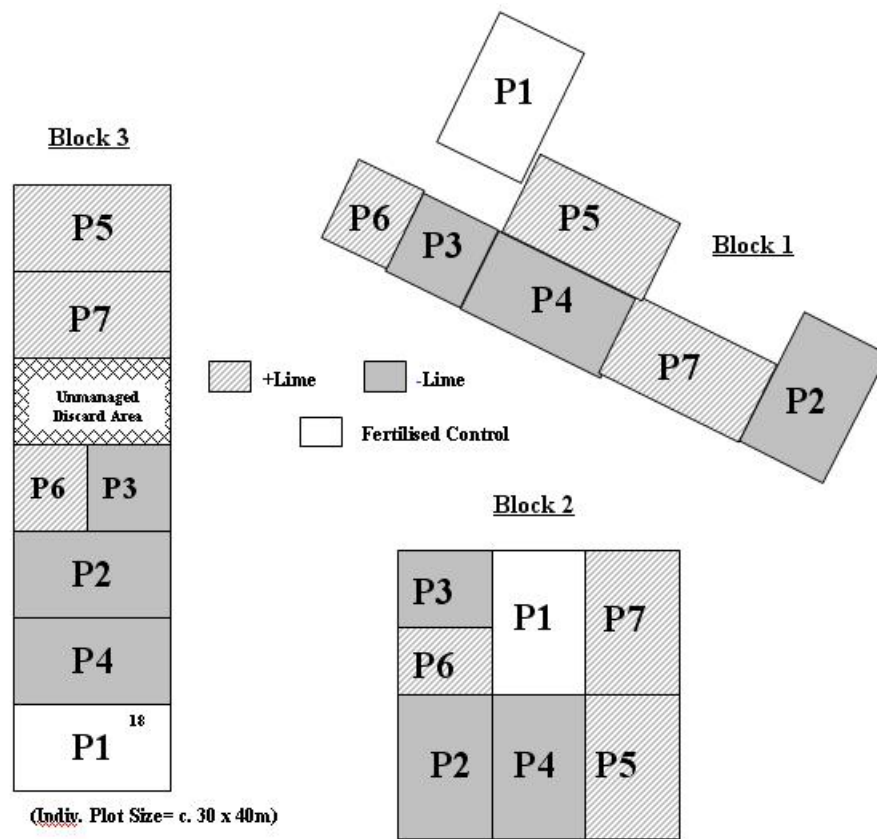
Figure 3.10: Pwllpeiran study site plot arrangement

Table 3.4: Pwllpeiran treatment regime

Label	Sheep grazing	Hay cut	Fertilizer	Lime
P1 (Control)	continuous	-	yes	yes
P2	continuous	-	no	no
P3	no grazing	July	no	no
P4	autumn/winter	July	no	no
P5	continuous	-	no	yes
P6	no grazing	July	no	yes
P7	autumn/winter	July	no	yes

Figure 3.11: Pwllpeiran study site plots

3.2.2 Forests: The Lake Vyrnwy study area

The forests at Lake Vyrnwy are diverse and consist of semi-natural broadleaved forest and coniferous plantations. The main forest types occurring in Wales are represented around the lake (Figure 3.12). Lake Vyrnwy is a manmade reservoir constructed in the late 19th century to supply the city of Liverpool with water. Today, the lake and surrounds form the centre of a RSPB reserve in the Berwyn Mountains in Powys, West Wales. Located just to the south of Snowdonia National Park at 52° 48' North and 3° 30' West, the lake has a surface area of 4.53 km^2, with a perimeter road of 11.75miles. It has an elongated shape in a East-West direction and a length of 4.75miles. Its primary outflow is the River Vyrnwy, which eventually joins the River Severn in Shropshire, while the reservoir is fed by up to 31 streams and rivers descending from the surrounding hillsides.

Lake Vyrnwy nature reserve is designated as a National Nature Reserve (NNR), a Site of Special Scientific Interest (SSSI), a Special Protection Area (SPA) and a Special Area of Conservation (SAC). The reserve and the area surrounding it are jointly managed by the RSPB and Severn Trent Water, the main landowner of the area, as well as the Forestry Commission. The boundary of the RSPB reserve is marked white in Figure 3.12.

The shores and adjoining hillsides of the lake are densely planted with about 5000 acres of mature commercial conifer plantations, interspersed by planted, as well as semi-natural broad-leaved forest woodlands. These consist of mature beech, semi-ancient sessile oak, as well as wet willow and alder stands and successional birch and mountain ash groves. The surrounding uplands are characterized by extensive heathlands and large areas of blanket bog on the hill plateaus, forming
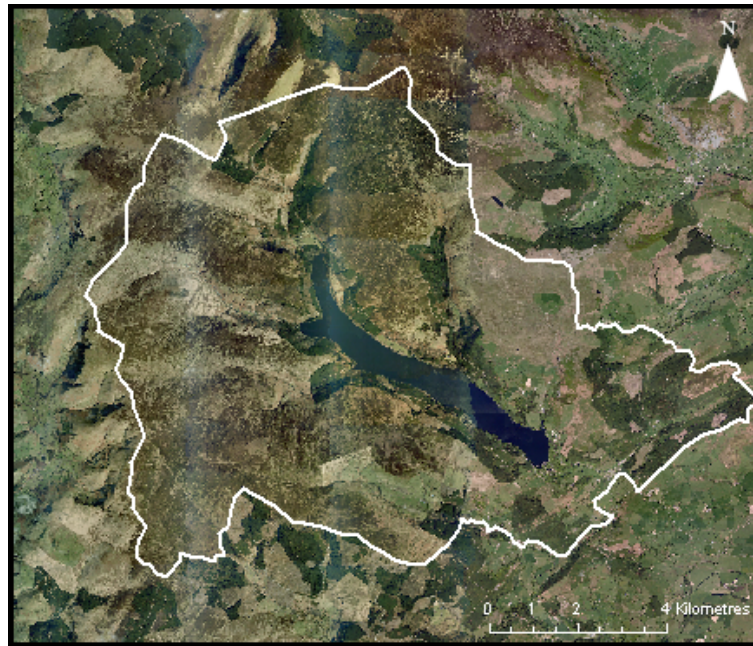
Figure 3.12: July 2006 Vexcel aerial photograph of the Lake Vyrnwy study site with RSPB reserve boundary outlined

the largest remaining continuous area of heather moorland in Wales. Farmland on the reserve consists mainly of rough upland sheep grazing with encroaching dry bracken-covered areas, while some cattle grazed grasslands and damp rough pastures can be found at the lower altitudes closer to the lake.

The bird life of the Lake Vyrwny catchment is diverse and resulted in the establishment of the area as a reserve for the Royal Society for the Protection of Birds (RSPB). The main bird conservation interest at the reserve derives from the wide variety of habitats surrounding the lake. Lake Vyrnwy is one of the RSPB's most diverse bird sanctuaries within the UK. Bird species of national importance include the Ring Ouzel (*Turdus torquatus*), Merlin (*Falco columbarius*) and Black Grouse (*Tetrao tetrix*)

The forested areas of the reserve contain a diversity of bird species, divided be-

tween those species which prefer coniferous forests, such as the Goldcrest (*Regulus regulus*), the Coal Tit (*Parus ater*) and the rare Siskin (*Carduelis spinus*) and Goshawk (*Accipiter gentilis*) and those which are predominantly found in broad-leaved woods, including Pied Flycatchers (*Ficedula hypoleuca*), Redstarts (*Phoenicurus phoenicurus*), Wood Warblers (*Phylloscopus sibilatrix*), Great Spotted Woodpeckers (*Dendrocopos major*), Nuthatches (*Sitta europaea*) and Tawny Owls (*Strix aluco*).

Since the Second World War a large percentage of heather moorland in the UK has been lost mainly to agriculture and forestry, which resulted in the increasing scarcity of birds which rely on this habitat for breeding, such as Red Grouse (*Lagopus lagopus*), Merlin (*Falco columbarius*) and Hen Harrier (*Circus cyaneus*). A large emphasis in the reserve management at Lake Vyrnwy is focused at retaining and restoring heather habitats to encourage these and other moorland species.

Finally the open farmland and especially the damp pastures are important habitat for Curlews (*Numenius arquata*) and Snipe (*Gallinago gallinago*), while Whinchats (*Saxicola rubetra*) and Tree Pipits (*Anthus trivialis*) can be found on the drier bracken-covered slopes.

Overall around 90 bird species have been recorded to be breeding on the reserve. Apart from avian diversity, a large variety of flowering plants, mosses, fungi, lichens and insects (e.g., butterflies and dragonflies) are also associated especially with the sessile oak woodlands and the less improved farmland. Six species of bat, including the pipistrelle and brown long eared bat have also been observed.

3.3 Summary

This chapter has provided an overview of semi-natural habitats and agricultural land in Wales and more detailed information on the selected grassland and forest study sites at Trawscoed and Pwllpeiran as well as Lake Vyrnwy.

It introduced the high diversity of vegetation types present in Wales which form the basic components of its biodiversity as outlined in Chapter 1, for example, grasslands important to conservation and a diverse array of forest types. The Welsh uplands and mountainous regions also are at the southernmost extent of several upland species within the UK.

The next chapter provides an overview of the field, airborne and spaceborne remote sensing data acquired for the study areas.

Chapter 4

Methods of data collection

This chapter describes the characteristics and acquisition of remote sensing data used for the study. The methods of collecting field data to support the interpretation of the remote sensing data and the validation of derived products (e.g., classifications) are also described. The chapter describes the spaceborne datasets available for the study regions and then focuses more specifically on the field and airborne remote sensing data acquired for grassland and forest sites respectively.

4.1 Spaceborne remote sensing data

The use of spaceborne optical sensors for classifying land cover and habitats across Wales has largely been limited by the high frequency of cloud occurrence in most areas. Many studies have also tended to select one sensor (particularly the Landsat series of sensors) for classification, but have not considered the use of other

sensors such as the SPOT-5 High Resolution Geometric (HRG), the Indian Remote Sensing Satellite (IRS) LISS-4 (P6) and the Terra-1 Advanced Spaceborne Thermal Emission and Reflection Radiometer (ASTER). However, utilizing data from several sensors observing at similar wavelength regions increases the number of cloud free observations of the land surface. To minimise differences between sensors as a function of radiometry, geometry, atmosphere and topography, however, a number of pre-processing steps are necessary. Clouds and cloud shadows also have to be identified within each of the images such that classifications of the land surface only can be undertaken (Section 4.1.1).

For this study, optical remote sensing data from the satellites listed in Table 4.1 were used.

Table 4.1: Satellites utilized in this study

Satellite	Sensor
Terra 1	Advanced Spaceborne Thermal Emissions and Reflection Radiometer (ASTER)
Satellite Pour l'Observation de la Terre 5 (SPOT)	High Resolution Geometric Sensor (HRG)
Indian Remote Sensing Satellite 1C, 1D & P6 (IRS)	Linear Imaging Self Scanning System (LISS)

For Wales, a near complete coverage of SPOT-5 HRG (10m spatial resolution) scenes was available for the years 2003-2007 (Figure 4.1).

Figure 4.1: Wales-wide mosaic of SPOT-5 HRG data

Coverage of IRS (23.5m spatial resolution) data was largely complete, apart from small areas in west Pembrokeshire, which are outside the area of interest for this study. ASTER images (15-30m spatial resolution), whilst often cloudy, also provided near complete cover of Wales for the years 2004-2006, with a cloud-free data strip available for the central region for March, 2004. The dates of acquisition for all scenes used in this study are compared in Table 4.2.

The different satellites and their sensors are described in detail, including individual wavelength regions, in Appendix A.2.2. These data were used as part of a larger project to support the revision of the Phase 1 Habitat Survey across Wales (Lucas et al., in press).

The following scenes in Table 4.2 were selected for use in land cover classifications

Table 4.2: Predominantly cloud-free SPOT-5 HRG, IRS LISS and ASTER scenes available for the studysites over the period 2003-2006

Sensor	Date	Site
SPOT 5 HRG	27.03.03	Lake Vyrnwy
SPOT 5 HRG	22.03.03	Lake Vyrnwy
ASTER	07.04.06	Lake Vyrnwy
IRS LISS IV	13.07.06	Lake Vyrwny
SPOT 5 HRG	27.03.03	Ceredigion
IRS LISS IV	13.07.06	Ceredigion

(Chapter 6) of the Lake Vyrwny and west Ceredigion sites as they were mostly cloud free and seasonally appropriate.

The two spring 2003 SPOT 5 HRG scenes, one summer 2006 IRS LISS IV and one spring 2006 ASTER image in Figure 4.2 cover both sites, but are shown here only for the extent of the study area over Lake Vyrnwy.

All scenes were provided courtesy of the Countryside Council for Wales (CCW). Orthorectification of the imagery using a fine spatial resolution digital elevation model, radiance calibration and atmospheric correction, cloud removal and topographic correction are considered in turn below.

4.1.1 Pre-processing of spaceborne sensor data

Radiometric correction

Radiometric correction from raw Digital Number (DN, 0-255) images at sensor radiance (R) was applied to each of the images.

Satellite sensors record pixel information in digital numbers, ranging from 0 to 255

(a) 27.03.03 SPOT-5 HRG   (b) 22.03.03 SPOT-5 HRG

(c) 13.07.06 IRS LISS IV   (d) 07.04.06 ASTER
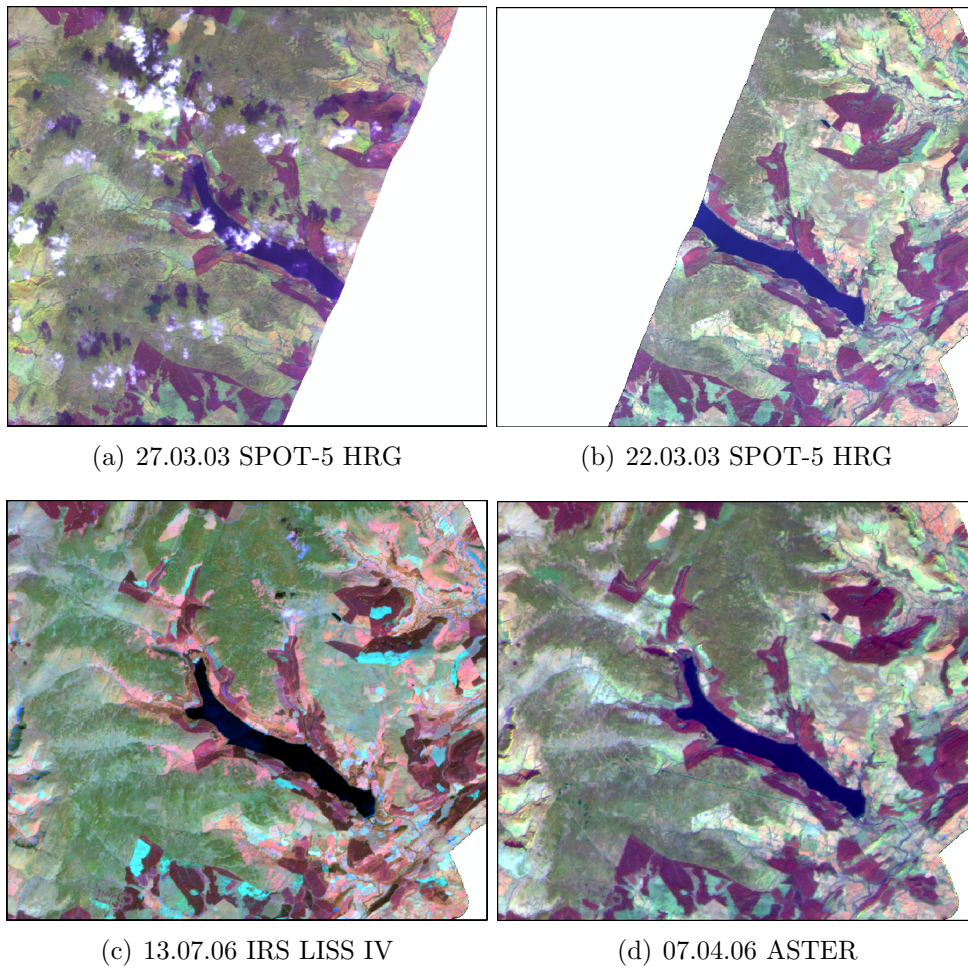
Figure 4.2: Multispectral Satellite imagery over the Lake Vyrnwy study site

and denoting the maximum and minimum measurable radiancies of the sensor. Calculation of spectral radiance is fundamental to converting data from multiple sensors into a common radiometric scale (Du et al., 2002). It takes the form of a simple linear regression to convert DN to radiance.

Equations 4.1 and 4.2 show the respective formulas for conversion of SPOT 5 HRG and IRS LISS data.

$$R = DN/CC \tag{4.1}$$

$$R = DN/CC * (L_{max} - L_{min}) + L_{max} \tag{4.2}$$

Where:

1. R = radiance $(Wm^{-2}sr^{-1}\mu m^{-1})$

2. CC = 255 for radiometrically corrected products

3. L_{max} = maximum saturation radiance

4. L_{min} = minimum saturation radiance

5. DN = the digital number of the image

CC denotes band-specific Conversion Coefficients for each sensor as described in Appendix A.2.2. The coefficients can be obtained either from the image metadata or published material (Abrams, 1999; Slater and Biggar, 1996; Chander et al., 2009).

As an example, Table 4.3 shows the calibration coefficients for a number of Spot 5 HRG images of Wales obtained from the metadata in the images' header file.

Table 4.3: SPOT 5 HRG sensor radiometric coefficients

Acquisition data	Band 1	Band 2	Band 3	Band 4
14/02/2003	0.8651	1.0264	1.1174	14.0118
17/03/2003	0.424789	2.877923	1.341774	14.0118
22/03/2003	0.287813	4.919843	1.784376	23.711787
04/09/2003	1.870249	2.231121	1.104	6.377
12/07/2005	2.903215	3.86682	1.308	8.225268

Geometric correction (Orthorectification)

Orthorectification is the process of correcting optical remote sensing image data for topographic relief and systematic sensor and platform-induced geometry errors (e.g., lens distoration and camera or sensor tilt). This procedure provides orthorectified images with the advantages of a uniform scale and true geometry, which in turn makes it possible to take direct and accurate measurements of distances, angles, positions and areas from the imagery, as if from a map. It also enables direct comparisons and overlay of different datasets (i.e., from different sensors or raster and vector layers).

Orthorectification is achieved through applying mathematical models of photogrammetry and requires a high quality digital elevation model (DEM). For this purpose, the 10 m spatial resolution NextMap Britain Digital Elevation Model (DEM) was used as a topographic reference. Between 1 (for ASTER) and 20 (SPOT, IRS) ground control points (GCP) were used, with these extracted from the VEXCEL true colour aerial photograph mosaic of Wales (see Appendix A.2.1). All satellite sensor data, regardless of their original spatial resolution, were resampled to 5m resolution using a nearest neighbour resampling algorithm. This was undertaken to better retain pixel values in the resampling process.

All SPOT 5 HRG images were orthorectified using the Leica Photogrammetry

Suite (LPS) of the ERDAS Imagine 9.1 software. The raw data SPOT 5 DIMAP (Digital Image Map) files were imported into ERDAS and subsequently orthorectified using the SPOT 5 specific Orbital Pushbroom geometric model within LPS, with the reference coordinate system set to United Kingdom and the British National Grid. The model further required the scene average elevation, a high resolution DEM (NextMap), as well as appopriately selected Ground Control Points (GCPs) and the reference image from which these were collected (in this case, the VEXCEL aerial photography). During the orthorectification process, the software determined the elevation of all GCPs from the DEM and used this information to correctly warp the input image to the map geometry.

The orthorectification process for IRS LISS III and IV data was identical to that for the SPOT 5 HRG data, with the only difference being, that the geometric model used in the Leica Photogrammetry Suite was the Polynomial Based Pushbroom.

ASTER scenes, in contrast to the SPOT and IRS data, were orthorectified using ENVI 4.3 software. The visible and NIR bands were orthorectified together, but separately from the SWIR band, because their original spatial resolution was coarser (30 m as opposed to 15m).

Only a single ground control point was required, which was located towards the centre of the image, away from either extreme of high or low elevation within the scene. Following selection of the GCP, its x/y coordinates were identified in the base (VEXCEL) and the warp (ASTER) image and the point elevation was extracted from the DEM. All images were orthorectified to the British National Grid.

Finally all bands were stacked into one final image at a spatial resolution of

15m.

Atmospheric correction

The objective of atmospheric correction is to compensate for variations between scenes in atmospheric conditions (e.g., water vapour and aerosols) that effect the signal the satellite sensor retrieves from the ground at the time of image acquisition. Atmospheric correction provides image data in units of surface reflectance (%), thereby standardizing the data and allowing comparison of images acquired on different dates, from different sensors, and also across different regions.

All satellite scenes were atmospherically corrected using ENVI's FLAASH (Fast Line-of-sight Atmospheric Analysis of Spectral Hypercubes) algorithm (Matthew et al., 2000). Prior to correction, each scene was converted to Band Interleaved (BIL) file format and a number of parameters had to be determined for each scene from the metadata before applying the algorithm:

- Scene centre location

- Sensor altitude (km)

- Average ground elevation across the scene (km)

- Image Pixel size (m)

- Image acquisition date and time

- Atmospheric model: Mid-latitude winter or summer

- Aerosol model - Rural

- Initial Visibility

- Zenith and Azimuth angle

- Output Reflectance Scale Factor

Topographic correction

In addition to the atmospheric and illumination effects compensated for during atmospheric correction, topographic effects also strongly influence the satellite signal by causing an enhancement of apparent surface reflectance values. Land surfaces oriented towards the sun appear to have higher reflectance values than the same surface cover oriented away from the sun if the influence of topography is neglected (Shepherd and Dymond, 2003). Topographic correction effectively approximates the reflectance of a surface as if occurring on flat terrain.

Topographic correction of the data was undertaken using ATCOR 3 software (Richter and Mueller, 2005; Richter, 2009) to minimise differences in reflectance as a function of slope and aspect, especially on north-facing slopes. However, the procedure was only successful when applied to images acquired in the spring or autumn months, where the shadowing effect of slope and aspect was also amplified by the seasonally low sun angle. When summer imagery were used, overcorrection of the imagery was observed. However, correction was deemed less necessary as the topographic effects were mostly neglible. All images used in this study were acquired close to solar noon.

Figure 4.3 shows a March SPOT 5 HRG image prior and following topographic correction and hence illustrate the importance of this pre-processing measure in enhancing the information content of previously shaded image areas.

(a) Original image   (b) After topographic correction
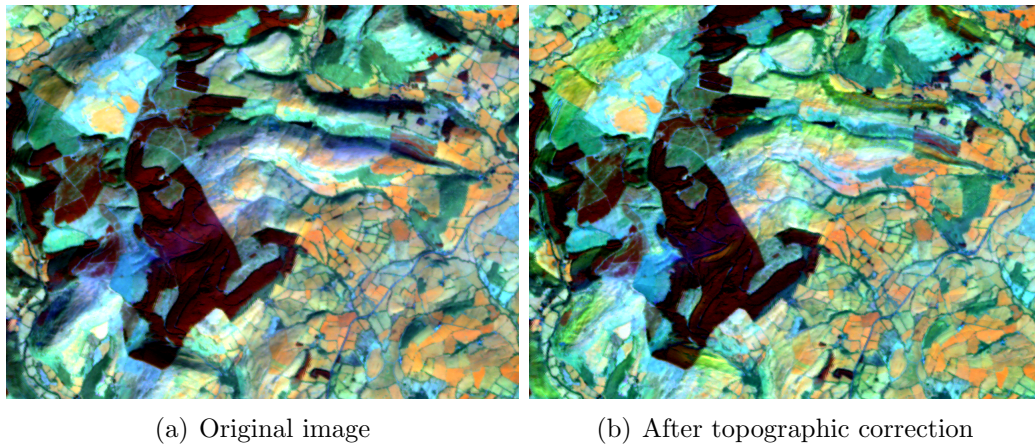
Figure 4.3: SPOT-5 HRG image (acquired on 27th March 2003) before and after topographic correction

Cloud removal

Cloud and cloud shadow screening was undertaken using procedures developed by Definiens AG. For each image, the algorithm was used to generate vector cloud masks, that were used either to indicate where a classification was unable to be undertaken or where the classification might be less reliable.

Derived products

Following atmospheric and topographic correction, a number of image products were derived including:

1. The Normalized Difference Vegetation Index

2. Estimates of the relative amount (fractions) of shade/moisture, photosynthetic (green) vegetation (PV) and non-photosynthetic (dead/senescent; NPV) vegetation

1. The NDVI has been related to vegetation productivity and phenology (Gamon et al., 1995; Weiss et al., 2001), the fraction of the Photosynthetically Active Radiation (PAR) absorbed by the vegetation canopy attributes (e.g., green biomass and Leaf Area Index, LAI) and the condition of the vegetation (e.g., stress; (Wang et al., 2001)).

The NDVI is calculated from the red and NIR bands an image using Equation 4.3.

$$NDVI = \frac{NIR - Red}{NIR + Red} \tag{4.3}$$

Values typically vary from -1 to 1, but the NDVI of vegetated surfaces exceeds 0 and values of closed and highly productive canopies can approach 0.6-0.7.

2. Due to the moderate (5-10m) spatial resolution of the satellite images used in this study and the heterogeneity of the landscape, many pixels contain a mixture of land cover types. The radiance detected by the sensor represents a combination of all object fractions present in the pixel. Non-photosynthetic, photosynthetic and shaded surfaces are, however, common to all images of vegetation. Fraction images can therefore be generated by deriving endmembers, defined as a spectral signature for a pure surface, for these three surfaces and using them as input into a linear spectral unmixing algorithm.

The linear spectral unmixing model is a technique that generates synthetic images where each channel represents the proportion (fraction) or each component of the mixing pixel (Lu et al., 2003). In linear spectral unmixing, the reflectance of each pixel in the image is assumed to be linearly correlated to the reflectance of each material (or endmember) present within the pixel (Adams et al., 1995). The model

then reduces the number of channels in the images to the number of components of the model. The number of endmembers must, however, be less (by one) than the number of spectral bands, and all of the endmembers in the image must be used. The SPOT-5 HRG, IRS LISS IV and CASI data used here are therefore well suited to this derivation as more than three bands are available. The model algorithms are described by Shimabukuro and Smith (1991).

Fractional images representing non-photosynthetic, photosynthetic vegetation and shade were therefore generated from the SPOT and IRS images used in this study. Within each image a small number of regions of interest (ROI) of each endmember type were selected, consisting of approximately 300 pixels each and spread equally across the image.

To ensure a good separation of the endmember fractions during the unmixing process, image regions with the greatest proportion of non-photosynthetic, photosynthetic vegetation or shade present were selected for the respective ROIs. For non-photosynthetic areas, bare ground areas like ploughed fields were used, while highly productive, agriculturally improved fields were chosen as samples for photosynthetic vegetation. Finally, regions of deep shade created by woodlands or buildings provided samples of the shade endmembers.

In each case the endmembers were defined through reference to the feature space plots of the Red, NIR and SWIR bands. Examples of the derived fractional images are given in Figures 5.10 and 5.11.

The advantage of fractional images generated using spectral linear unmixing is that they can be used to complement or supplement images used more traditionally as input to classification algorithms (Adams et al., 1995). Furthermore these synthetic images are often more representative of the physical properties of classes

(e.g., NPV in vegetation canopies) and for this reason also they are sometimes more readily interpretable.

4.1.2 Overview of spaceborne sensor pre-processing

By pre-processing, the following benefits to classification were provided:

- A high accuracy of orthorectification facilitated the overlay of vector layers (e.g., field boundaries, Figure 4.4) and also comparison of pixel values from different sensors and dates

- Radiometric and atmospheric correction allowed better comparison of pixel values from different sensors and dates

- The topographic correction allowed features within shadowed areas to be better discerned and their pixel values to be more comparable with those in non-shadowed areas

- The cloud and cloud-shadow screening allowed the study to focus only on the observable land surface but increased the utility of the sensors

- The derivation of data products (e.g., vegetation indices, fractions) allowed information on the productivity of vegetation as well as the proportion of different fractions (e.g., soil, photosynthetic vegetation and non-photosynthetic vegetation) to be extracted and used in subsequent analysis procedures (Figure 4.5, Bateson et al. (2000))
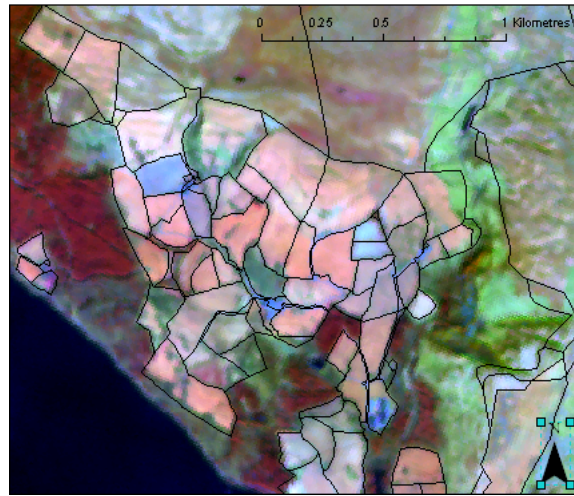
Figure 4.4: LPIS (Land Parcel Information System) boundaries superimposed on a orthorectified SPOT image

4.2 Airborne and terrestrial remote sensing data

4.2.1 Aerial photography and classification validation

For all of Wales, Vexcel aerial photography was provided courtesy of the Welsh Assembly Government (WAG) and the CCW. These data were acquired in 2006 at 1m spatial resolution in both the visible as well as the NIR wavebands. Where ground visits were not feasible, these data were the primary source for ground truth information and the consequent validation of the habitat classification by manual photography interpretation. The NIR photography highlighted variations in productivity across habitats and therefore provided a means of greater differentiation for the interpreter than the true colour photography alone.
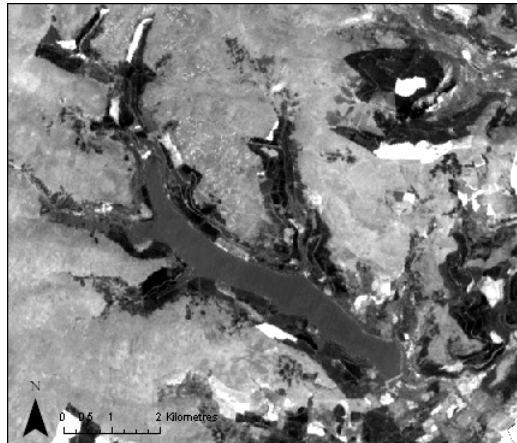
(a) NPV

(b) PV

(c) Shade

Figure 4.5: Non-photosynthetic (NPV), photosynthetic (PV) and shade endmember extraction of the July 2006 IRS scene around Lake Vyrnwy: a.) Lighter image regions indicate a higher proportion of non-photosynthetic vegetation. b.) Brighter areas of the image consist of stronger photosynthesizing vegetation. c.) Areas of high shade (mainly woodlands) are shown very light.

4.2.2 Compact Airborne Spectrographic Imager (CASI) data

Hyperspectral CASI data (1m spatial resolution) were acquired on 2nd June 2006 during two single overflights over the grassland plots at Trawscoed and Pwllpeiran. The spectral data were recorded in 12 bands covering the visible blue to NIR portions of the electromagnetic spectrum (Table 4.4), including several along the red edge.

Table 4.4: Pimhai CASI sensor (Grasslands)

Band	Centre wavelength (nm)	FWHM
1	449.3	12.6
2	487.4	11.7
3	551.0	6.2
4	668.4	8.2
5	696.0	7.2
6	708.4	6.3
7	736.1	7.2
8	749.5	7.2
9	761.0	5.3
10	778.2	9.2
11	817.5	8.2
12	863.6	8.2

In preparation for the flights, maps of the study areas were generated and the required course of the aircraft identified such that data were acquired over the key areas of interest (i.e., the grassland survey plots at Pwllpeiran and Trawscoed). The aircraft was held at an average height of 500 m above sea level to ensure that each image swath covered an approximate width of 500 m on the ground. Each image collected had an approximate length of 1.5 km of which subsequently only a subsection covering the actual field trial plots was used. Data collection followed the protocol outlined by Bunting and Lucas (2006). CASI position and Orien-

tation System (POS) data were acquired to compensate for aircraft position and movement. GPS base station data were acquired on the ground during the flights to facilitate geographical correction of the images. The CASI sensor acquired data in a north-south direction at approximately the time of the solar noon to avoid shadowing and minimize bi-directional effects (Schlaepfer and Richter, 2002).

During the overflights, one black, one white and one grey 4 x 4m calibration tarpaulin were laid out at one of the sites. As the aircraft passed, reflectance measurements were taken from each tarpaulin, using a field spectroradiometer, thereby allowing subsequent calibration of the data.

CASI scenes were provided corrected for roll and pitch and were geo-registered to Vexcel aerial photography data from July 2006. For the geo-registration process approximately 50 pairs of ground control points were collected at points which were easy to identify precisely in both the CASI image and the aerial photograph, for example at the corners of the sample plots or buildings. Following this, an image-to-image nearest neighbour warping algorithm in ENVI software was applied.

Registration accuracy was assessed by super-imposing both LPIS field boundaries and the boundaries of the trial plots, which were spatially defined using a differential GPS (Figure 5.8). Compared to these independent vector datasets, the result of the registration process was considered satisfactorily precise.

It would, however, be possible, to further improve the accuracy of the image registration by acquiring a high-resolution digital elevation model of the areas covered by the image strips, e.g., derived from LiDAR, to adjust for topographic relief. This particularly applies to the Pwllpeiran site, where the local topography is

very pronounced.

Empirical Line Calibration

The CASI scenes were provided in units of 'at sensor' radiance (L, W m^{-2}sr^{-2}?m^{-1}) but surface reflectance was estimated using the Empirical Line Calibration (ELC) procedure available within Environment for Visualising Images (ENVI) software (Inc, 2003). Empirical Line calibration is used to force spectral data to match selected field reflectance spectra. A linear regression was used for each band to equate DN and reflectance. This is equivalent to removing the solar irradiance and the atmospheric path radiance. Equation 4.4 shows how the empirical line gain and offset values are calculated. Through linear regression, the ELC forced the spectral radiance from the black and white tarpaulins (as measured by the CASI during the overflights, Jacobsen et al. (2000)) to match the corresponding field reflectance spectra. Through this approach, the effects of solar irradiance and atmospheric path radiance were reduced. From the ELC, a calibration file was generated which were used subsequently to convert the remaining CASI scene to estimated surface reflectance.

$$L = a + 6xDN \qquad\qquad (4.4)$$

This equals:

Reflectance (field spectrum) = gain x radiance (input data) + offset.

ENVI's empirical line calibration requires at least one field, laboratory, or other

reference spectrum; these can be obtained from spectral profiles or plots, spectral libraries, ROIs, statistics or from ASCII files.

Input spectra were automatically resampled to match the selected data wavelengths. When more than one spectrum was used, then the regression for each band was calculated by fitting the regression line through all of the spectra. If only one spectrum was used, then the regression line was assumed to pass through the origin (zero reflectance equals zero DN). The calibration can also be performed on a data-set using existing factors. In this study, images of all study sites were acquired in a single flight, which only allowed a narrow time window around solar noon. Due to limitations on human resources, field spectra from black and white could only be collected at Morfa (a third site flown close to Trawscoed and Pwllpeiran, near the Ceredigion coast and the village of Llanon, but not utilized in this study).

The empirical line calibration could therefore only be performed on the Morfa image. The Trawscoed and Pwllpeiran images were then calibrated using the calibration file obtained for this site. The trapualins at Trawscoed and Pwllpeiran were subsequently used to check how well the data were calibrated.

4.2.3 Airborne LiDAR data

Full waveform RIEGL LMS-Q560 LiDAR data were acquired over the Lake Vyrnwy forests in a series of adjacent passed to form a continuous mosaic in August 2006. The flightlines (approximately 500m swath width) were orientated parallel to the longest dimension of the Lake (Figure 4.7). This was undertaken to maximize the amount of forests sensed by the LiDAR.

Figure 4.6: A CASI image of Morfa showing the three tarpaulins to be used in the empirical line calibration circled in white. They are from the top: white, grey and black

The Riegl LMS-Q560 LiDAR is part of the LiteMapper-5600 system and provides access to detailed target parameters by digitizing the echo waveform of each laser measurement (Hug et al., 2004). After the flight, the digitized waveforms can subsequently be analyzed off-line. This approach proves especially valuable when dealing with challenging tasks, such as canopy height investigations or highly reliable automated target classification.

The waveform digitizing principle is illustrated in Figure 4.8.

In situation 1 in figure 4.8, the laser pulse first hits the canopy and creates three distinct echo pulses at various canopy layers. A fraction of the laser pulse also hits the ground giving rise to another echo pulse. In situation 2, the laser beam is reflected from a flat surface at a small angle of incidence yielding an extended echo pulse width. In situation 3, the pulse is simply reflected by a flat surface at normal incidence resulting in a single echo pulse with a similar shape as of the
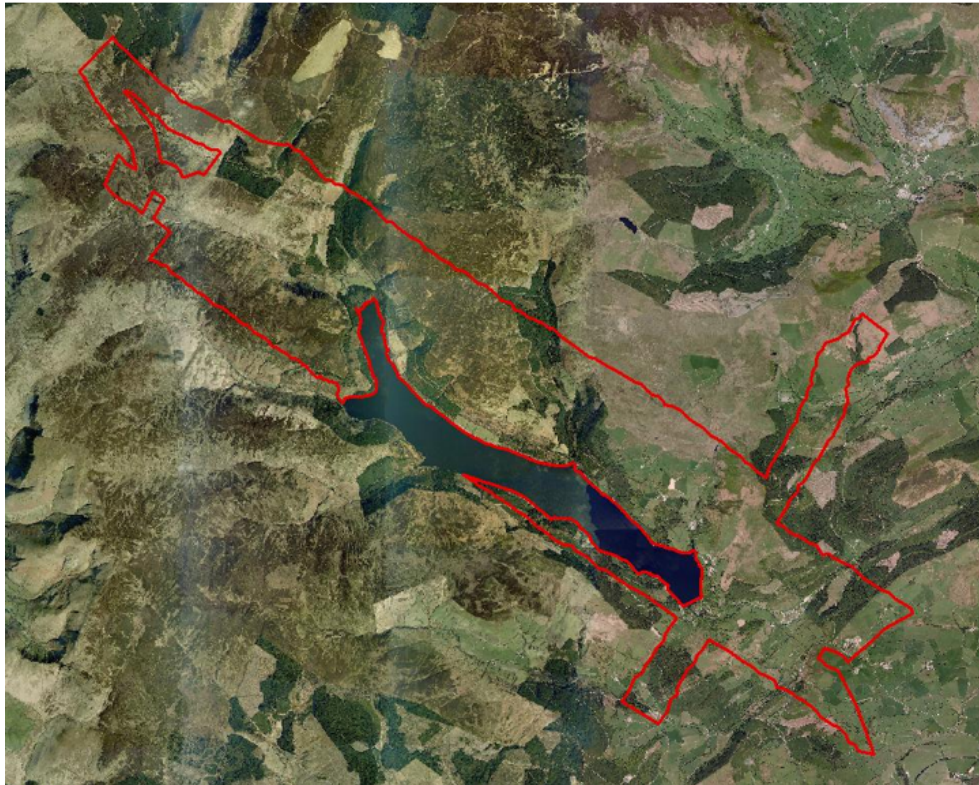
Figure 4.7: Area covered by the LiDAR acquisition over Lake Vyrnwy forests
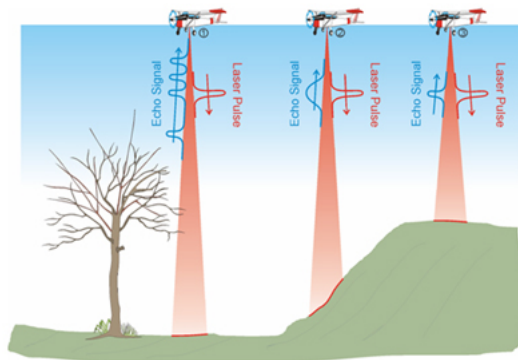
Figure 4.8: Waveform digitizing principle - Echo signals resulting from different targets (Rie, 2005)

outgoing laser pulse. The Riegl LMS-Q560 laser scanner with waveform digitization is especially well suited for forestry and agriculture monitoring.

In such applications, the digitized waveform information is valuable for deriving several ground and vegetation parameters, including surface elevation, tree/vegetation height, the openness of the canopy and the distribution of canopy elements within the vertical profile. Calculation of timber volume, biomass and other important vegetation descriptors is thus facilitated and made more precise (Grimm and Kremer, 2005).

The LiDAR data were preprocessed by the data provider and, as part of this, the waveforms were decomposed into discrete returns (a maximum of 4 per waveform). This is further explained in Chapter 7.

4.2.4 Terrestrial laser scanner data

Terrestrial Laser Scanners (TLS) provide detailed reconstructions of geometrically complex three-dimensional objects. In a forest context, data from the scanner can be used to describe the distribution of trunkes, branches leaves as well as the locations, diameters and heights of individual plants (Maas et al., 2008a; Watt and Donoghue, 2005b). Although methods are still being developed, additional attributes that are able to be retrieved include timber volume by size class (Jupp et al., 2005) and canopy gap fraction (Danson et al., 2007b; Henning and Radtke, 2006a). Potential exists also for retrieving the woody biomass of individual trees, either by considering the sizes of the stems scanned or multiplying the volume of scanned branches and trunks by wood density. Although limited by survey times and occlusion as a function of stand density, TLS provide a permanent record of forest structure. An advantage of this technique is the density and precision of

the spatial sampling at a high rate, particularly in inaccessible terrain and under adverse conditions (e.g., poor weather, time constraints due to tides, etc.). Observations are non-invasive, which is especially desirable in a conservation context. Initial labour investments in any study sites, particularly those under forest canopy, can be high due to the efforts required to geolocate the scans as described below, but repeat surveys would always be very efficient. The main challenges in the acquisition and application of TLS data in forested environments are the need for efficient computational engines to manage and model the resulting large datasets and the high acquisition and initial training costs required.

Terrestrial laser scanner

Terrestrial Laser Scanner data were collected using a Leica ScanStation 2 in 2007. The Scanner possesses a 270° vertical field-of-view of which 45° is below the horizontal. This enables the scanner to cover areas on the ground close-by to the set-up as well as increasing its utility on non-level surfaces. For the purpose of surveying forests, the ability to scan directly overhead is an added advantage.

Locations, vegetation characteristics and acquisition dates of the scanned sites

TLS data were acquired for sites representing a range of forest structures, which included coniferous plantations and broadleaved forests dominated by a range of species, as described in section 3.2.2. The locations of the scans around the lake
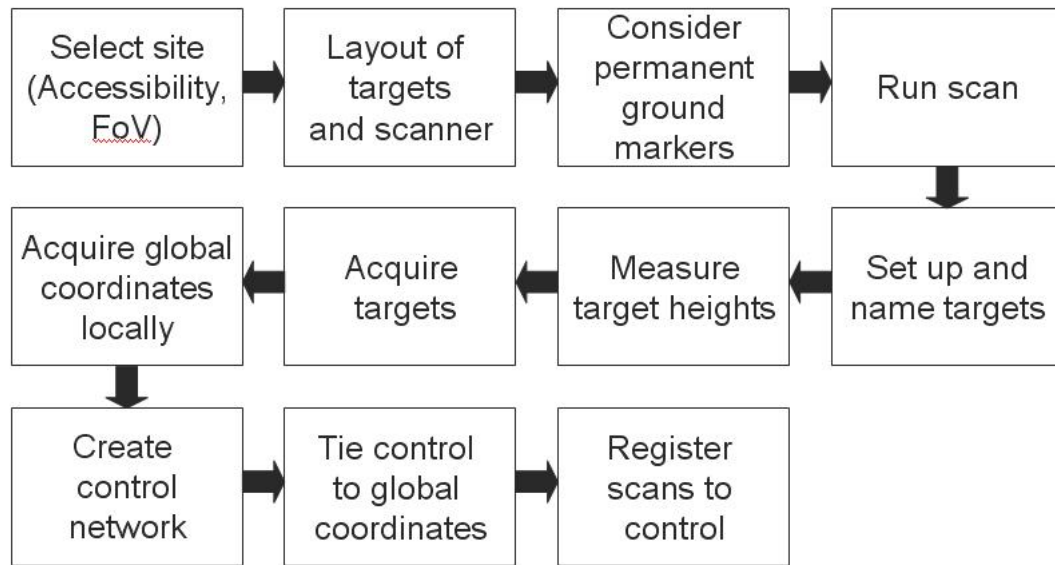
Figure 4.9: TLS data acquisition workflow

are illustrated in figure 4.10.

Data collection took place at 7 sites during August 2007.

Table 4.5: Terrestrial Laser Scans

Scan	Date	Scanner	Control Network	Dominant tree species
LV7	01.08.2007	Leica	Vyrnwy01	Douglas Fir
LV8	03.08.2007	Leica	Vyrnwy04	Sessile Oak
LV9	07.08.2007	Leica	Vyrnwy04	Sessile Oak and Sycamore
LV10	07.08.2007	Leica	Vyrnwy06	Sessile Oak
LV11	08.08.2007	Leica	Vyrnwy03	Larch
LV12	08.08.2007	Leica	Vyrnwy05	Sitka Spruce
LV13	13.08.2007	Leica	Vyrnwy02	Sitka Spruce
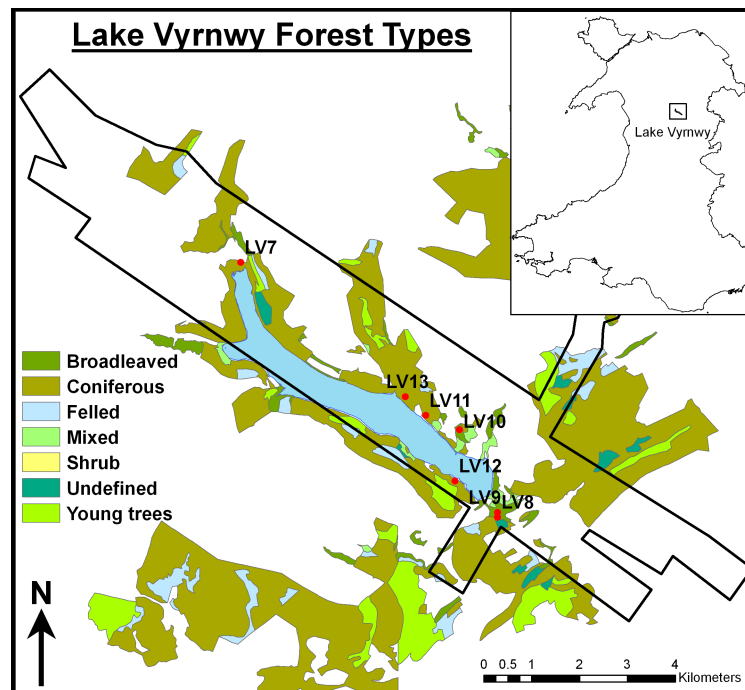
Figure 4.10: Locations of the 7 terrestrial laser scans around Lake Vyrnwy

The locations of the scanners for each forest plot (i.e., the triangular arrangement)

At each scan station point, a full 360°, hemispheric scan was performed, covering the entire area visible to the scanner, as defined by its view angle restraints.

Scanning

From each scan point a minimum of three targets where surveyed to aid subsequent geometric registration of the scans.

All scan points and target locations were marked with semi-permanent stakes and could subsequently be relocated for surveying with a total station.

Full-hemispheric scans taken with the Leica ScanStation took approximately 10

minutes. The time and effort required to obtain the targets greatly exceeded that of the actual scan, especially through view obstruction of branches and understory. The understory was included in the scanning, as this is considered a key habitat for certain bird species (e.g., blackcaps, bullfinches) and a significant forest structure attribute.

Geo-registration of scans

Due to the lack of penetration of a GPS signal through woodland canopy, which prohibited obtaining the global location of the scanner and target locations directly, it was necessary to set up control networks outside the forests. In several cases these were a considerable distance away from the site of the scans (see cp1, cp2 and cp3 in Figure 4.11). Each control network consisted of three points in a triangular arrangement, whose locations could be reliably established, using a differential GPS.

Starting at the control network, a local coordinate system (Figure 4.11) was subsequently created by using a Leica Total Station. All target and scanner locations were included in the local coordinate system.
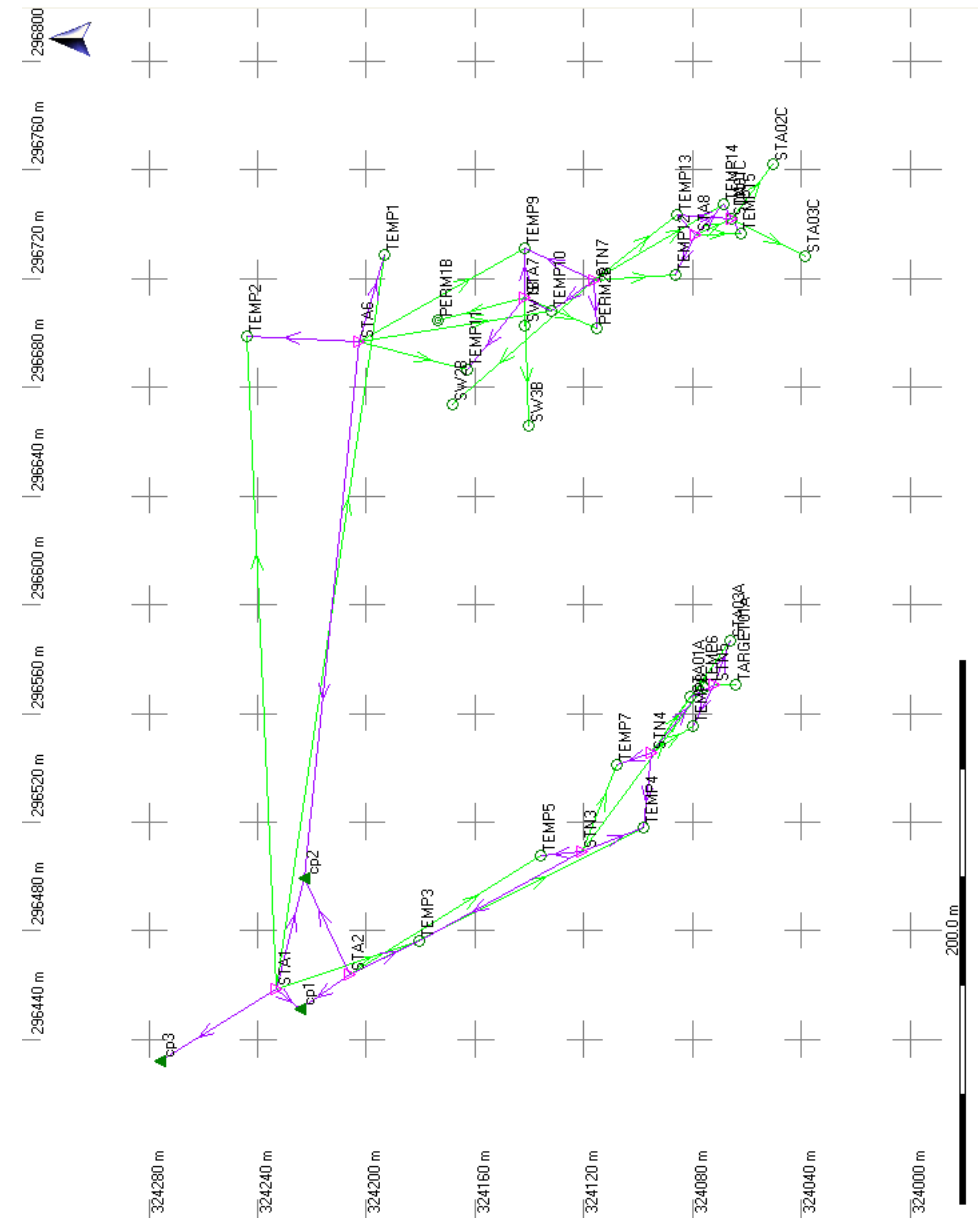
Figure 4.11: Control Network Vyrnwy01 (cp: Control Point, STA: GPS station location, Temp: temporary Total Station Location, all others are scanner and target locations)

To obtain exact global coordinates of all points, the local coordinate system was then registered to the known points of the control network using Leica Geo Office software. The comparison to the LiDAR data shows a good correspondence (Figure 4.12).
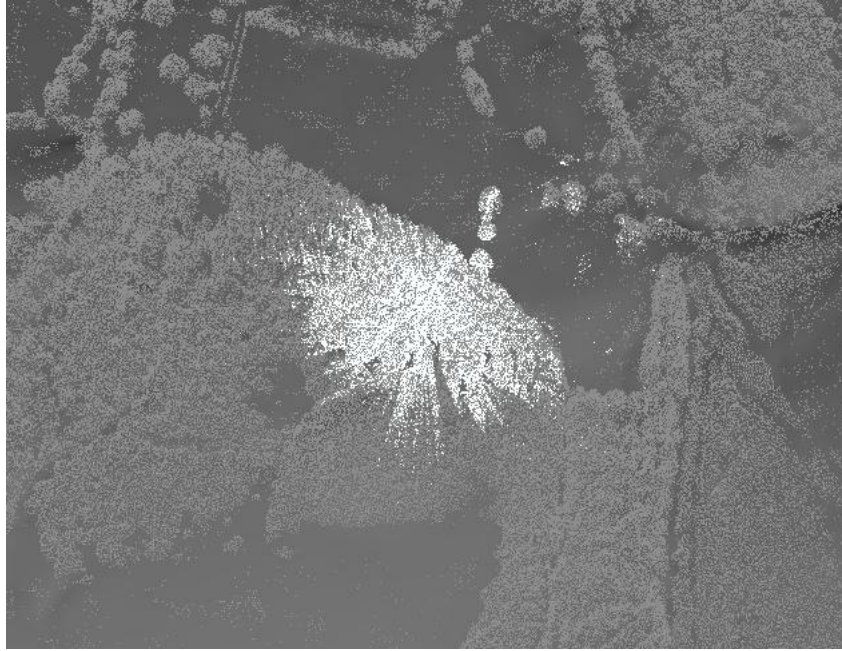
Figure 4.12: Co-registered airborne (full waveform) LiDAR point cloud (grey) and terrestrial laser scanner data (white)

Table 4.6 shows the registration accuracies for all target and scan points. The smallest (0.015m) and largest (4.708m) errors are highlighted in bold. The very large errors in LV13 were caused by a mis-function of the total station at the time as it failed to detect the target prism automatically. It was, however, decided to incorporate the scan in some of the analyses in Chapter 7 as outlined in Section 7.3.1.

Table 4.6: TLS registration error in meters

	LV2a	LV2b	LV2c	LV7	LV8	LV9	LV10	LV 11	LV12	LV13
1	0.021	0.119	0.422	0.088	0.221	0.256	0.132	0.044	0.203	3.134
2	**0.015**	0.155	0.837	0.069	0.065	0.374	0.217	0.294	0.276	**4.708**
3	0.026	0.274	0.420	0.034	0.216	0.048	0.267	0.046	0.187	1.648
4				0.656	0.374	0.077	0.174	0.271	0.288	
5							0.203	0.030		

4.3 Grassland field data collection

4.3.1 Biomass samples

During July 2006, 480 grass samples were collected from 30 0.25m x 2.5m strips in each of the field plots at Trawscoed . All plots were cut for hay by IGER staff using a tractor and standard hay mower. This mower cuts the hay along swaths approximating 2.5m and concurrently lays the hay in lines along the left hand edge of the swath. Against the management plan, the T1 and T6 treatment plots were also cut for thistle management, which facilitated the collection of a greater number of samples, as described below.

Samples were collected from the 2.5m wide swaths using a 25 cm wide wooden plank, which was placed across the swath. Exerting light pressure to hold the swath firm, the sample was cut either side of the plank with a sharp serrated knife. After removal of the plank, the cut cross-section of the swath was rolled up and collected in netted bags, which could be placed directly into the drying ovens. A label with plot identifier and sample number was placed inside each bag. Samples were collected in a regular pattern across each plot, mostly determined by the lay-out of the mowing swaths. Areas of swaths which were not uniform

because of mower blockage or repeated passes by the mower were avoided. This is a standard operating procedure (SOP) known as the 'bread knife technique', which was developed by ADAS for taking samples from hay swaths for monitoring purposes. The location of each biomass sample was recorded at either end and in the middle of the swath, using a differential GPS. This procedure was repeated at Pwllpeiran for a further 480 samples. At Pwllpeiran, however, the management plan was strictly adhered to, meaning that the P1, P2 and P5 plots were not cut by the mower. In these fields, corresponding sample strips were cut by hand using shears.

All grass samples were dried at 80° Celsius for 48 hours and then weighed to one decimal place to give an estimate of dry weight in grams.

4.3.2 Vegetation survey

As described in Section 3.2.1, the Trawscoed and Pwllpeiran grassland plots were originally created as part of a research experiment on the biodiversity restoration of previously intensely managed improved agricultural grasslands. An important component of the original experimental protocol was that regular vegetation surveys of all plots were carried out to monitor the expected increase in species richness over time. The plots were surveyed annually up to 1999, coinciding with the end of DEFRA funding for the research experiment (Hayes et al., 2000; Hayes and Sackville Hamilton, 2001), and thereafter approximately biannually, as some funding was available to maintain the experiment (Hayes 2006, personal communication). All surveys followed the protocol for the National Vegetation Classification (NVC) scheme and recorded species present and percentage coverage within ten randomly located 1m^2 quadrats in each trial plot. A full survey was carried out

at both sites in the summer of 2006 and these are the species data used in this study.

Figure 4.13: Vegetation surevy quadrat at Trawscoed

4.4 Bird census data

For the Lake Vyrnwy forests, the RSPB had conducted a comprehensive survey of the main forest areas during 2006. The method of the CBC involves the recording of birds on a paper map at regular intervals (often fortnightly) throughout the breeding season. Each bird species is given a code (see Appendix A.4) with a secondary code which indicates whether the bird is nesting, singing, not singing,

flying or fighting. At the end of the season, records are collated for each species on a new map such that territories can be discerned.

The CBC data were digitized and attributed within ArcGIS. Over 6000 observations were digitized and integrated within a Geographical Information System (GIS) project.

Bird species distribution data were collected by staff and volunteers in the woodland habitats of the RSPB Lake Vyrnwy bird reserve (see Section 3.2.2) between late March and early July 2006, following the territory mapping method of the Common Bird Census (CBC) for breeding birds of the British Trust for Ornithology (BTO). The CBC involves the recording of sightings of individual birds on a regular (e.g., weekly) basis during the breeding season. From information collated over the season, the occurrence of different species, their approximate nesting sites and also their territorial boundaries are mapped. Each site was visited six times, as compared to the usual ten times, due to a shortage of personnel. The protocol of this survey method is described in detail by Gilbert et al. (1998).

In total 6221 observations of 105 different species were recorded over the period. Many of these, however, were not specialist woodland species and are hence not considered in this study. Others were omitted because of insufficient sample sizes, which could be a result of itinerant, non-territorial individuals (see Chapter 8).

Figure 4.14: Bird observations of the 2006 Common Bird Census in the Lake Vyrnwy RSPB reserve

4.5   Summary

This chapter has provided an overview of the spaceborne, airborne and field (including TLS) data collected during the course of this project. Key elements of the work include:

- The acquisition and pre-processing of spaceborne optical data from a range of sensors to allow subsequent classification of the landscape

- The acquisition of airborne data by both hyperspectral and LiDAR sensors to provide more detailed information on land covers in both two and three dimensions

- The acquisition of TLS data to support the interpretation of LiDAR data, particularly in relation to forest structure (height)

- The collection of ground data in the form of biomass and broad species composition

- The collation and digitization of bird survey data collected by the RSPB during the same period as the LiDAR and CASI acquisitions over Lake Vyrnwy

The following chapters describe the methods of analysing these data with a view to:

1. The use of airborne hyperspectral data to better understand how spaceborne remote sensing data can be used to retrieve information on the level of improvement of grasslands

2. Classifying semi-natural habitats and agricultural land across selected regions in Wales (as part of a larger project)

3. To establish whether combinations of remote sensing data can be used to better quantify the diversity of grassland species and also bird communities inhabitating forests

Chapter 5

Spectral differentiation of grasslands

5.1 Introduction

Grasslands are valuable biodiversity repositories. Their inherent floristic and associated invertebrate diversity is an important component of Wales' total biodiversity and form the foundation for the habitat and food source requirements of many bird and mammal species.

The natural environment of Wales is predominantly characterized by its rural pastoral landscape in both lowlands and uplands and approximately 62% of its total area consists of grassland as established by the Phase 1 survey of Wales undertaken during the late 1980s and 90s (Howe et al., 2005; JNCC, 2003).

This chapter aims to establish whether different grassland types can be identified and discriminated using first airborne and then spaceborne remote sensing data.

This was achieved by establishing relationships between fine (< 1m) spatial resolution airborne CASI data acquired during 2006 at the Trawscoed and Pwllpeiran sites (Section 3.2.1) and field-based measures of grassland biomass and species composition. These relationships were further used to inform on the subsequent development of rules for the classification of grassland types using spaceborne data. The opportunities to acquire wide-area coverage of airborne CASI data are very limited, due to the narrow swath width and the effort and costs which would be incurred. For this reason it is important to identify the specific spectral characteristics of different grassland types also in large-scale, lower resolution multispectral satellite imagery such as SPOT 5 HRG. The potential for differentiating spectrally characterized grasslands of varying conservation value in the wider landscape using spaceborne SPOT data is therefore also discussed.

5.2 Review of grasslands

5.2.1 Grasslands in Wales

The conservation value of unimproved and semi-improved grasslands is determined by their floristic diversity and by their role as a habitat and food source for a wide variety of invertebrate (Rushton et al., 1989), bird (Barnett et al., 2004) and mammal species. Dry acid, neutral and lowland and upland calcareous grasslands, as well as Purple Moor Grass (*Molinina caerulea*) and rush (*Juncus spp.*) pastures are examples of grassland habitats that are listed as priority habitats for protection in the UK Biodiversity Action Plan (Maddock, 2008).

Conservation ecology and agricultural science commonly divide grasslands into improved, semi-improved and unimproved classes to categorize their nature conservation interest and grazing value respectively. Unimproved grasslands are of the highest interest and value to conservation and improved grassland of the lowest. Most grasslands in Wales have, at one time, been subjected to differing levels of agricultural improvement through grazing, fertilization with manure, slurry or inorganic fertilizers, drainage, re-sowing or harvesting of silage crops. To establish the conservation interest and potential for protection of grassland sites, it is important to distinguish unimproved and semi-improved from improved grasslands. However, different grassland types often form a continuum and the range of criteria for semi-improved grassland is especially broad, so that it is often not possible to define each type precisely. Critical indicator species, such as Bird's Foot Trefoil (*Lotus corniculatus* and Yellow Rattle (*Rhinanthus minor*), are often also only visible during certain periods of the growing season.

The following sections outline the grassland types occurring and, where appropriate, characteristics typical to Wales are highlighted. Features that may assist in their determination from remote sensing data are further described.

Improved Grassland

Agricultural grassland improvement typically causes a decrease in floral species diversity of the sward and dominance of competitive grasses such as Perennial Ryegrass (*Lolium perenne*), Yorkshire Fog (*Holcus lanatus*) and Red Fescue (*Festuca rubra*). Perennial Ryegrass (*Lolium perenne*) and White Clover (*Trifolium*

repens) commonly constitute more than 50% of the vegetation cover of improved fields. The actual sward composition is likely to vary with intensity of treatment, of which periodical application of selective herbicides, ploughing and re-seeding with a single species (most often the very productive Perennial Ryegrass) are the most severe.

Improved grasslands do not contain many of the forb species which are commonly found in an unimproved sward. The limited range of grasses and common herbaceous plants occurring are mainly those which require high levels of nutrients and are resistant to grazing. Crested Dogstail (*Cynosurus cristatus*), Common Sorrel (*Rumex acetosa*), Dandelion (*Taraxacum officinale*), Daisy (*Bellis perennis*) and Buttercup species (*Ranunculus spp.*) are commonly found. The presence of Dock (*Rumex spp.*), Common Nettle (*Urtica dioica*) and thistles (*Cirsium spp.*) indicate local nutrient enrichment of the soil through the manure of grazing animals.

Figure 5.1: Improved grassland plot at the Trawscoed study site. The uniform sward is dominated by *Lolium perenne*.

In Wales, the majority of improved grasslands are found in the lowlands and below the enclosure boundary. They are managed for sheep and cattle grazing with

the aim of providing an efficient fodder source. Semi-improved and unimproved grasslands are rare in the lowlands and often limited to either steep slopes, which hinder the use of agricultural machinery or areas of poor soil, especially marshy ground. In the uplands, improved swards are rarer, limited by access and the pre-dominant extensive grazing regimes.

Semi-improved Grassland

Semi-improved grasslands are a transition category created by partial improvement of previously unimproved sites, using the agricultural practices described above. Alternatively, if intensive agricultural treatment is not maintained, herbaceous species such as Knapweed (*Centaurea nigra*), Yarrow (*Achillea millefolium*) and Bird's Foot Trefoil (*Lotus corniculatus*) re-establish and the field can revert to semi-improved status. This usually takes place over a number of years. Fields that have been re-seeded in the past, but which have subsequently become more diverse again are included in this category. The diversity of species within semi-improved grasslands is generally lower and less compared to unimproved grasslands, although they still possess some conservation value.

Semi-improved grasslands span the widest part of the grassland continuum and therefore can vary considerably in appearance, making identification and mapping difficult. A key indicator of semi-improved grasslands is the generally lower species diversity compared to that of proximal unimproved grassland, but higher than improved fields. Semi-improved grasslands are therefore best categorized within their regional context.

Figure 5.2 illustrates a semi-improved sward at the Trawscoed study site, which has reverted from an improved field similar to that in Figure 5.1 since intense

management ceased. The seed heads of Plantain (*Plantago lanceolata*) are evident within the image.

Figure 5.2: Semi-improved grassland plot at the Trawscoed study site.

Unimproved Grassland

Species diversity in unimproved grasslands is often greater than that of semi-improved or improved fields, with species characteristic of the area and local soil type present, while agricultural species such as Perennial Ryegrass only make up a low percentage of the vegetation cover. Some extensive grazing, especially in the uplands, may take place, but is mostly not sufficient to alter the natural species composition of these grassland significantly. Fields may also be cut for hay. Unimproved grasslands are usually rare in the lowlands, because of the land demands of intensive agriculture.

The species composition and appearance of unimproved grasslands varies according to location (altitude), soil moisture and whether they occur on neutral, calcareous or acid soils, as determined by the underlying geology and soil depth. Improve-

ment often reduces the distinctive characteristics of acid, neutral or calcareous grasslands, making them difficult to differentiate.

Figure 5.3: Least improved grassland at the Pwllpeiran studysite

Acid Grassland

Acid grassland is often unenclosed and, in Wales, occurs mainly in the uplands and in the mountainous regions of Snowdonia. Underlying soils vary in acidicity, but commonly have a pH of less than 5.5. These grasslands are generally species poor, but contain species that are indicative of acidic conditions when frequent or abundant. These include Wavy Hair-Grass (*Deschampsia flexuosa*), Mat Grass (*Nardus stricta*), Heath Bedstraw (*Galium saxatile*), Tormentil (*Potentilla erecta*) and Sheep's Sorrel (*Rumex acetosella*). In Wales, the dominant grasses on dry, acidic soils are Sheep's Fescue (*Festuca ovina*) and Bents (*Agrostis spp.*) On wetter ground, these species will be replaced by expanses of Purple Moor grass (*Molinia caerulea*), particular in the Cambrian Mountains and wet acidic grasslands typified by species such as Heath Rush (*Juncus squarrosus*).

Calcareous grassland

These grasslands are also often unenclosed and occur on shallow soils with a pH above 7.0. In Wales, these grasslands are comparatively rare and confined to areas of limestone pavements in the uplands (e.g., above Llangollen in Powys). Indicator species of calcareous turfs are Crested Hair-grass (*Koeleria macrantha*), Downy Oat-grass (*Avenula pratensis*), Common Rock-Rose (*Helianthemum nummularium*), Salad Burnet (*Sanguisorba minor*), and Wild Thyme (*Thymus polytrichus*).

Neutral Grassland

This category is typically more intensively managed than acid or calcareous grassland and is often enclosed and occurring in the lowlands of Wales. The following species are indicative of neutral soils (pH 5.5-7.0), if they occur frequently: Meadow Foxtail (*Alopecurus pratensis*), False Oat-grass (*Arrhenatherum elatius*), Crested Dogstail (*Cynosurus cristatus*), Cocksfoot (*Dactylis glomerata*), Tufted Hair-grass (*Deschampsia cespitosa*), Yellow Rattle (*Rhinanthus minor*) and Meadow Fescue (*Festuca pratensis*).

Hay meadows usually fall within this category, as well as a range of grasslands which are inundated periodically or permanently wet. On such wet pastures grasses are dominant, but with species such as Marsh Marigold (*Caltha palustris*), Meadow sweet (*Filipendula ulmaria*) or Rushes (*Juncus spp.*) present.

5.2.2 Grassland manifestation within remote sensing data

Bright green, lush and even swards, dominated by grasses with a low diversity of herbaceous flowering plants usually indicate substantially improved grassland. Perennial Ryegrass (*Lolium perenne*) in particular and White Clover (*Trifolium repens*) commonly constitute more than 50% of the vegetation cover of improved fields. Within remotely sensed data, these swards typically exhibit a high and relatively uniform near infrared (NIR) reflectance (typically above 40%) and a high NDVI which often exceeds 0.4. These high values are attributable to the high density of grass blades, but is exaggerated by clover which has horizontally orientated leaves that are arranged in a relatively uniform layer. The NDVI is also high, because of the strong absorption of the green wavelengths by chlorophyll.

Within many grasslands, variability in reflectance is evident, both spectrally and spatially. Such variability is attributable to species composition and condition, which in turn are determined by a number of factors, listed in Table 5.1.

Table 5.1: Factors influencing reflectance variability in grasslands

Factors of spectral variability in grasslands	Effect
1. edaphic factors (soil type dominated communities)	Soil ph; clay, loamy or sandy soils
2. soil moisture conditions	water availability, drought and flood response
3. terrain factors	drainage and often influences soil depth
4. high stocking rates of grazing animals	low biomass / grass length through overgrazing
5. low stocking rates and selective grazing	variability in biomass and sward condition through grazing impact
6. other anthropogenic factors such as fertilizing, re-seeding and cutting regimes	

There is no precise divide in appearance between unimproved and semi-improved grasslands. Species composition usually is the over-riding criterion for distinguishing unimproved and semi-improved grasslands, which is difficult to detect in satellite images as most indicator species will occur at low frequencies, though their presence will make a difference to the overall appearance and hence reflectance of the sward.

Differentiating improved from semi-improved grasslands is difficult from remote sensing data, as on the ground, separation is based primarily on species composition. Many indicator species occur in low numbers and their presence cannot be detected remotely. Nevertheless, a number of factors suggest that fields are unimproved. These include:

1. lower productivity

2. reduced amounts of high reflectance (in the NIR), *Lolium perenne* and clover

3. increased structural variability associated with grass tussocks

These grasslands also exhibit characteristics that are midway between unimproved and improved grasslands (Figure 5.4). Hence by defining these characteristics first for these grassland types in spectral properties (e.g., NIR), vegetation indices (NDVI) or fractional images (e.g., shade), intermediate or overlapping areas can be associated with semi-improved grasslands.

Grasslands react, compared to other habitats such as forests, more readily to improvement by human intervention or climate change effects through changes in species composition (Robertson, 2010) and productivity (Zha et al., 2005; Holden and Brereton, 2002). It is therefore important to monitor them accordingly. While it is not possible to detect the presence of individual species, occurring with low
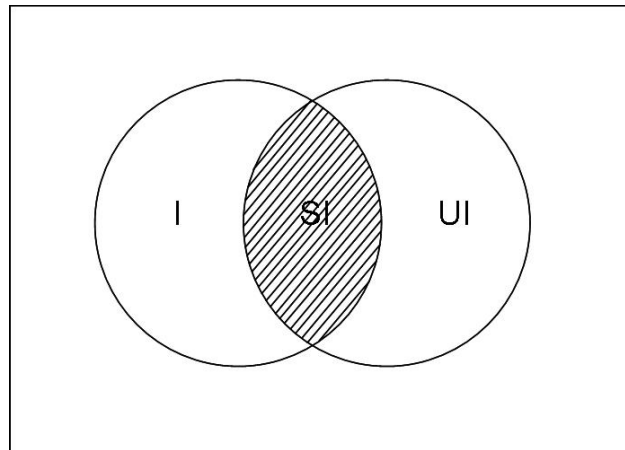
Figure 5.4: Feature distribution across different levels of grassland improvement

frequency, using low resolution satellite data, productivity and condition can be examined at the community level.

By focusing on grasslands at Trawscoed and Pwllpeiran, this chapter establishes whether differences in productivity and species community can be detected using remote sensing optical data. This was achieved by acquiring hyperspectral data at the same time as field based measures of biomass and species composition.

5.3 Methods of data acquisition and analysis

5.3.1 Grassland improvement levels

Under consideration of the management strategies described in Section 3.2.1 and the percentages of improvement indicator species present (Figures 5.5 and 5.6), all plot types were graded according to expected level of improvement through fertilization and grazing treatment. These gradients are illustrated in Figure 5.7 in ascending order of improvement for both Trawscoed and Pwllpeiran.
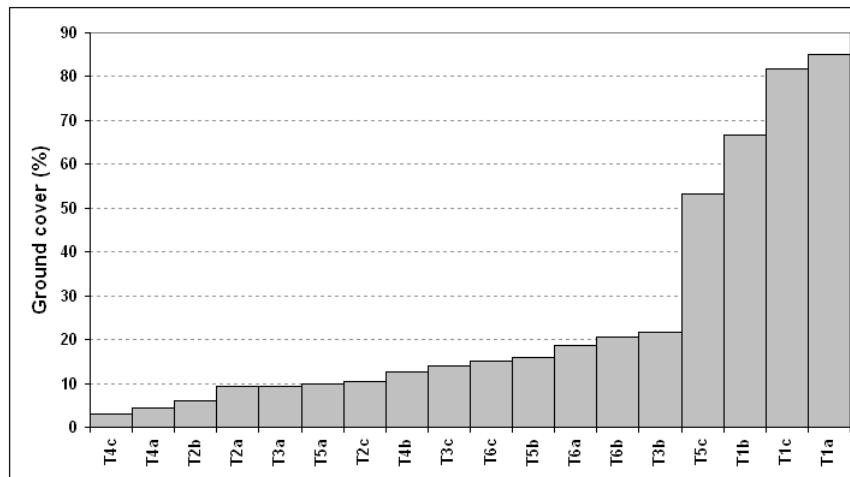
Figure 5.5: Percentage ground cover of *Lolium perenne* of the Trawscoed trial plots

5.3.2 Airborne data

CASI Image Data

Airborne CASI hyperspectral images were acquired over both the Trawscoed and Pwllpeiran study sites in June 2006 (Figures 5.8 and 5.9) during two single over-passes. All images were geo-registered using ground control points, with the VEX-CEL aerial photography used as a base image, and atmospherically corrected with the empirical line calibration process (Section 4.2.2).

Fraction Images

Endmember fraction images for non-photosynthetic (NPV) and photosynthetic vegetation (PV), as well as shade were derived through ENVI's linear spectral unmixing from the two CASI images (Figure 5.10 and 5.11, Adams et al. (1995)), using the process described in Section 4.1.1.
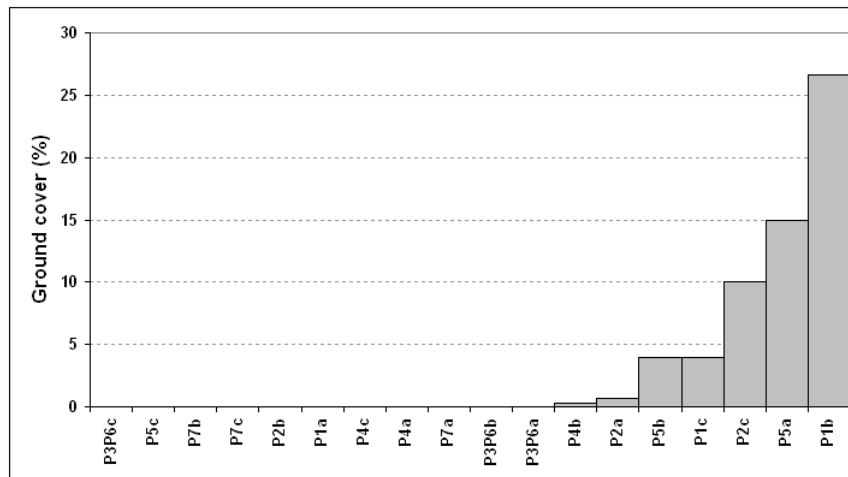
(a) *Lolium perenne*
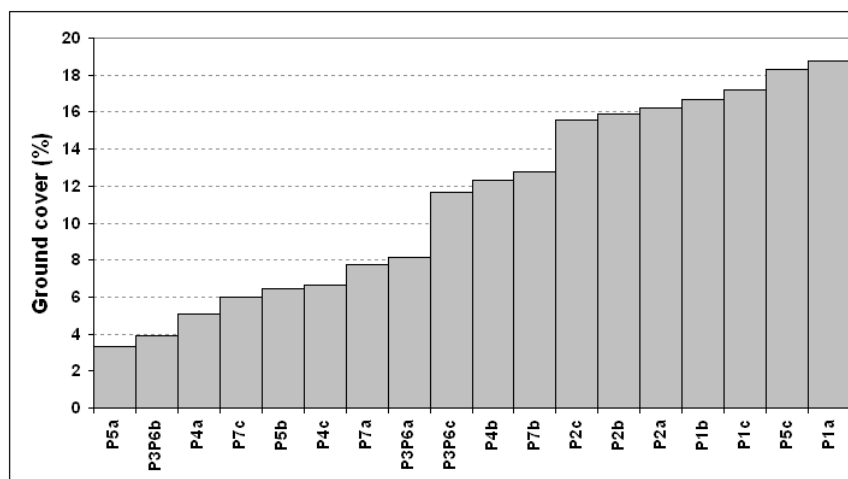
(b) *Festuca spp.*

Figure 5.6: Percentage ground cover of *Lolium perenne* and *Festuca spp.* of the Pwllpeiran trial plots

(a) Trawscoed   (b) Pwllpeiran
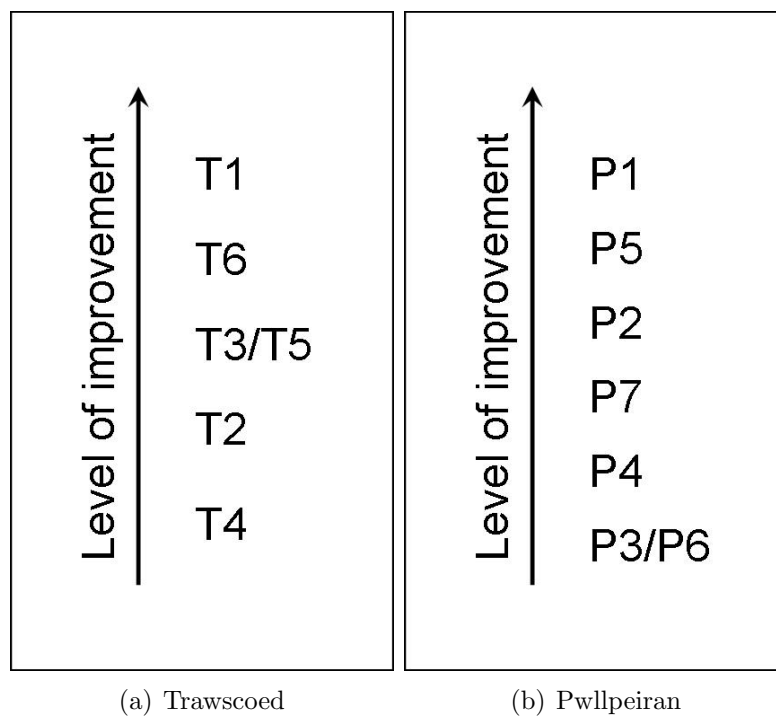
Figure 5.7: Grassland improvement in Trawscoed and Pwllpeiran study sites in increasing order of magnitude
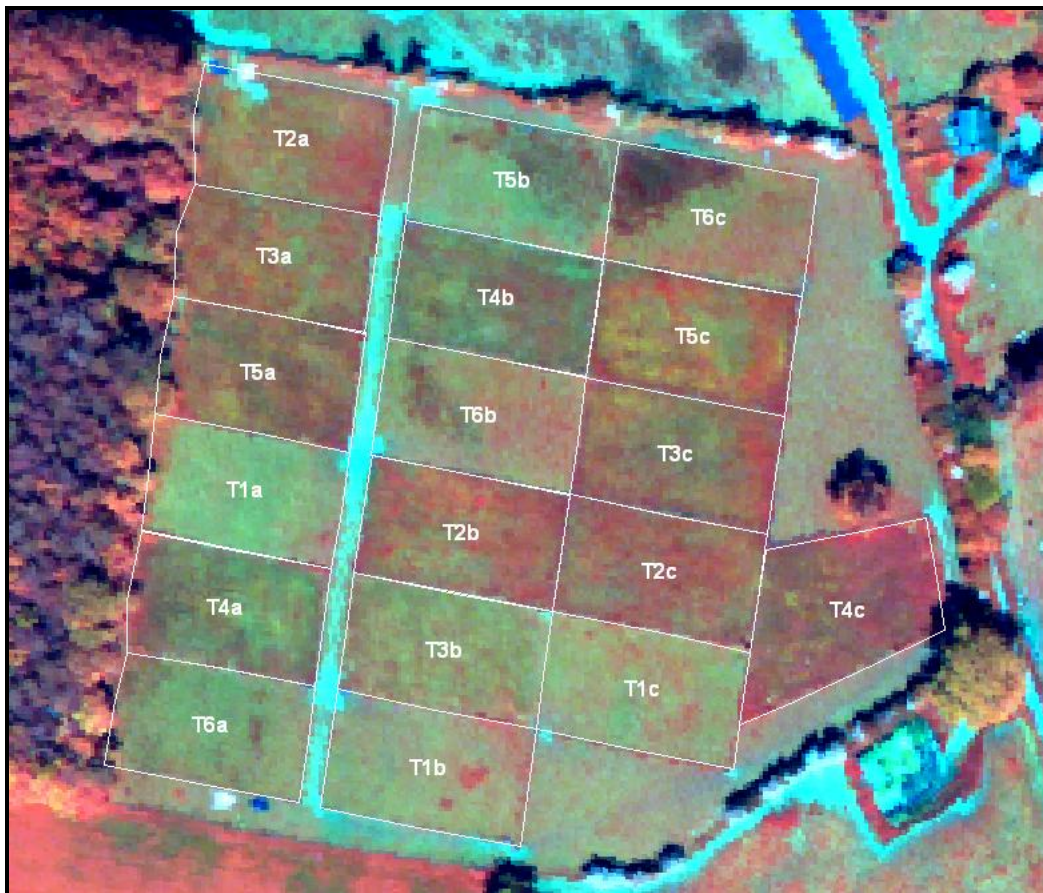
Figure 5.8: July 2006 CASI image of the Trawscoed study site, treatment plots are outlined and labeled according to the management treatments T1-T6 (see Table 3.3)

Figure 5.9: July 2006 CASI image of the Pwllpeiran study site, treatment plots are outlined and labeled according to the management treatments P1-P7 (see Table 3.4)

(a) NPV

(b) PV

(c) Shade
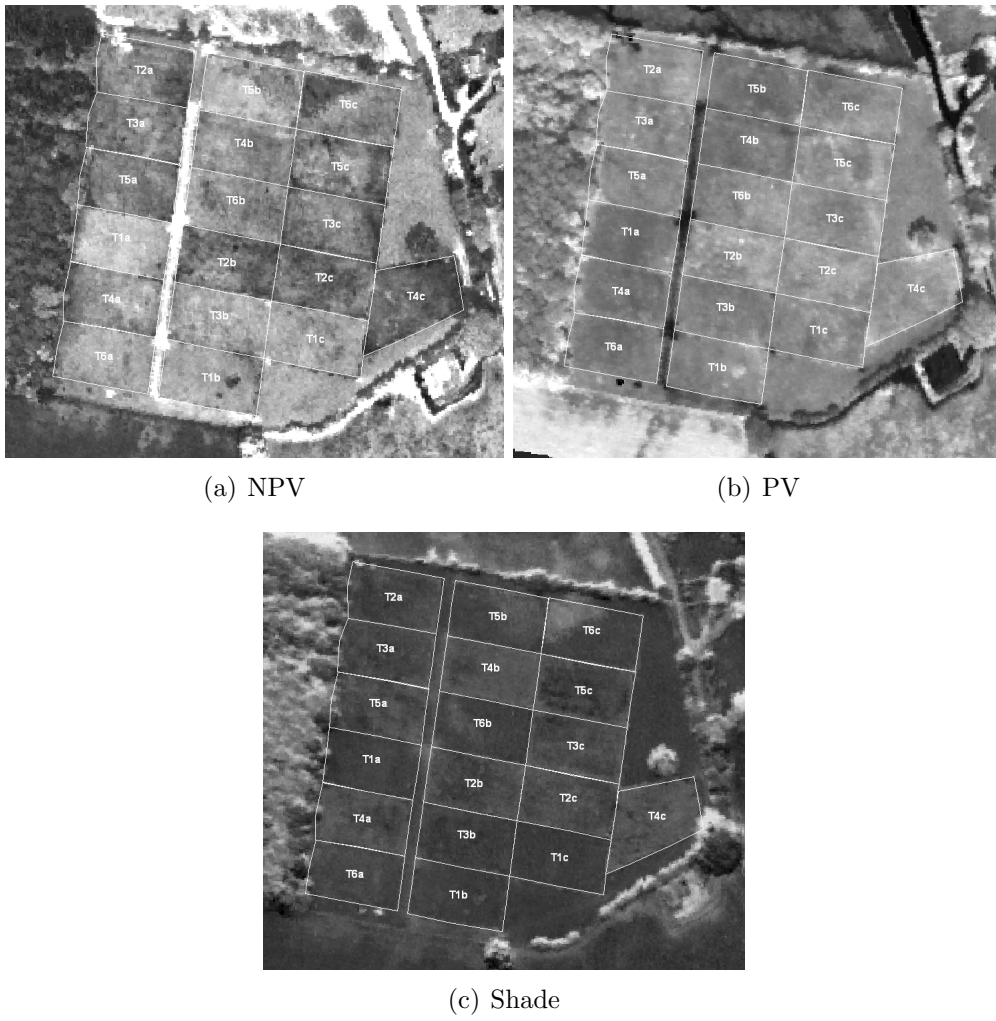
Figure 5.10: Endmember fraction images at Trawscoed

Vegetation Indices

The following five vegetation indices were calculated from the Trawscoed image only using band maths (Figure 5.12):

- Normalized Difference Vegetation Index $(NDVI) = \frac{\rho_{817.5} - \rho_{668.4}}{\rho_{817.5} + \rho_{668.4}}$

(a) NPV

(b) PV
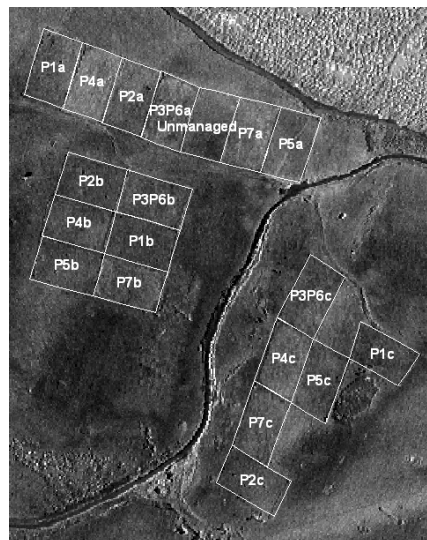
(c) Shade

Figure 5.11: Endmember fraction images at Pwllpeiran

- Ratio vegetation index $(RVI) = \frac{\rho_{749.5}}{\rho_{708.4}}$

- Renormalized difference vegetation index $(RDVI) = \frac{\rho_{817.5} - \rho_{668.4}}{\sqrt{\rho_{817.5} + \rho_{668.4}}}$

- Triangular vegetation index $(TVI) = \frac{120(\rho_{749.5} - \rho_{551}) - 200(\rho_{668.4} - \rho_{551})}{2}$

- Modified triangular vegetation index $(MDVI) = 1.2[1.2(\rho_{817.5} - \rho_{551}) - 2.5(\rho_{668.4} - \rho_{551})]$

The RVI, RDVI, TVI and MDVI were chosen for examination because they are described by Chen et al. (2009) in a detailed study of vegetation indices as most successful in estimating grassland biomass from hyperspectral data. The Normalized Difference Vegetation Index (NDVI) is a robust and very common measure of vegetation productivity from remote sensing data (Silleos et al., 2006; Wang et al., 2001), calculated from the red and near infrared bands. It is frequently applied in grassland environments (Goetz, 1997; Goodin and Henebry, 1998; Tieszen et al., 1997) and is hence also included here.

The airborne data acquisition and pre-processing are described in further detail in Section 4.2.2.

5.3.3 Data extraction

The location of the mid-point and both ends of each biomass sample, as determined by a differential GPS (Section 4.3.1), were buffered by a radius of 0.5m. The resulting shapefiles (Figure 5.13) were used to retrieve zonal statistics of the corresponding reflectance values for all bands, the NDVI and endmember fraction values within the plots for each biomass sample. At each location three values were extracted and the mean of these three was subsequently calculated.

(a) NDVI

(b) RVI

(c) RDVI

(d) TVI

(e) MDVI
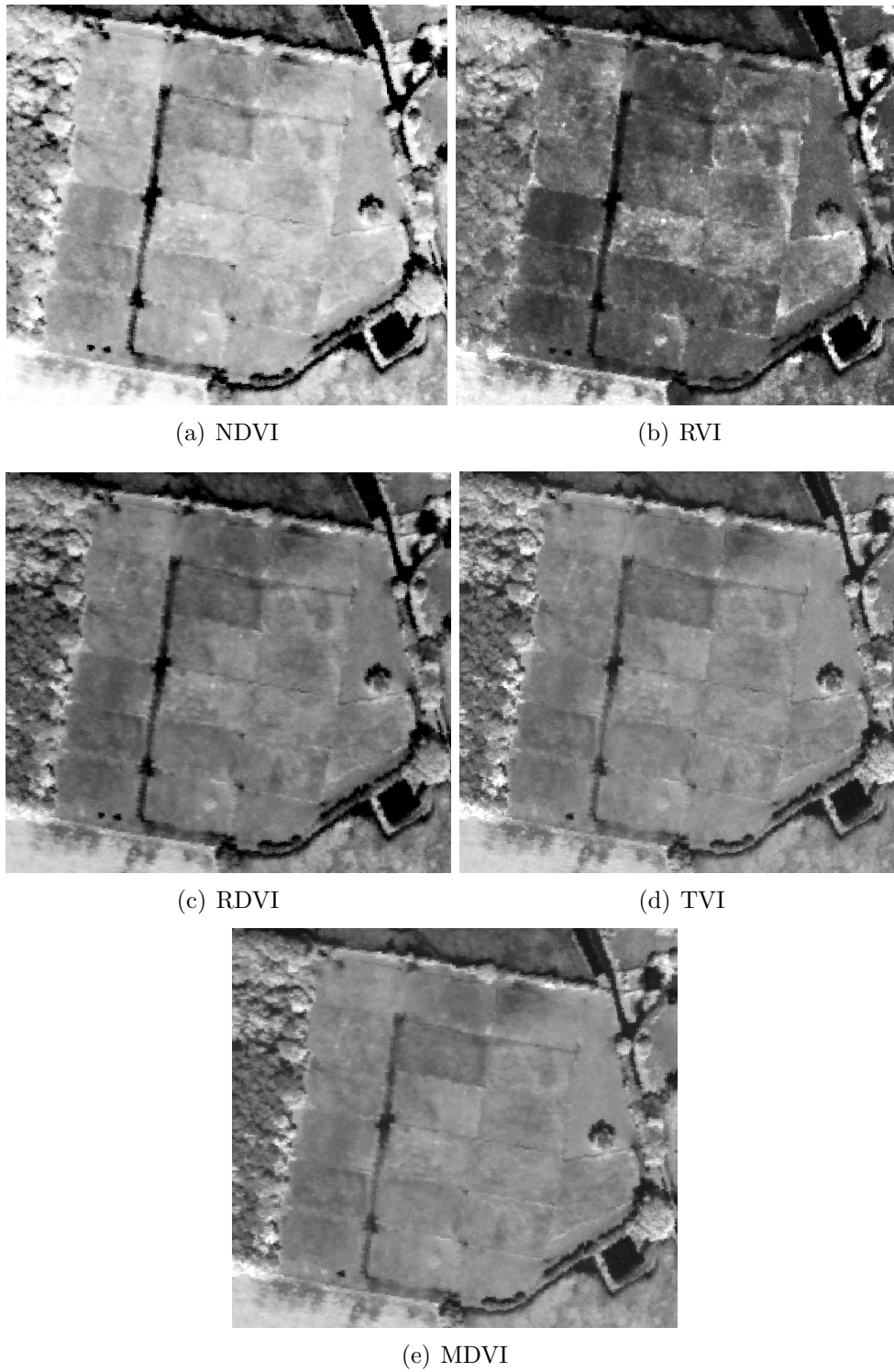
Figure 5.12: Vegetation Indices at Trawscoed
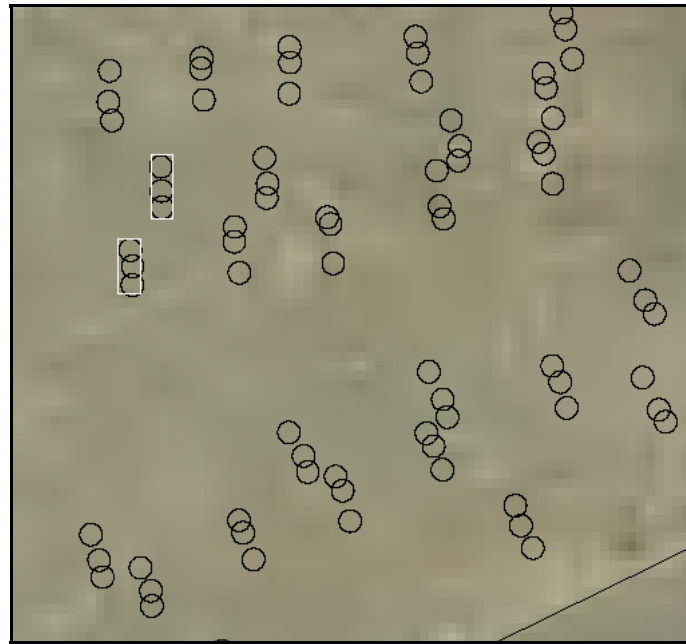
Figure 5.13: Buffered (0.5m) ends and midpoint (circles) of one sample swath and the area from which the biomass sample has been taken (rectangle)

Subsequently the outline of each plot was buffered inwards by 3m to avoid edge effects and data were extracted for the whole plot from the same datasets using zonal statistics as above. For Trawscoed the data for the additional Vegetation Indices listed in Section 5.3.2 were also obtained on a per plot basis.

One-way Analyses of variance (ANOVA) of the extracted reflectance (ranging from $\rho_{487.4}$ to $\rho_{863.6}$)of all trial plots from Trawscoed and Pwllpeiran were performed to establish whether the various plots differ significantly with regard to reflectance and in which bands the differentiation potential is strongest.

Further analysis explored the regression between reflectance data, NDVI and endmember fractions respectively and at each of the sample locations. The values for reflectance, endmember images and vegetation indices extracted from the sam-

ple locations were plotted against their corresponding biomass sample to establish their degree of regression and possible empirical relationships.

5.3.4 Vegetation and Biomass data

A survey following NVC protocol recording vegetation species occurring as well as percentage cover of species in ten $1m^2$ quadrats per plot was conducted during summer 2006 at both Trawscoed and Pwllpeiran.

Tha Shannon-Weaver diversity index ($H' = \sum_{i=1}^{S} p_i \ln p_i - [(S-1)/2N)]$) for each plot at Trawscoed were calculated from this data.

Biomass samples of all plots at both sites were collected during June and July 2006, in the three weeks after acquisition of the hyperspectral data (Section 4.2.2).

The mean, standard deviation and range of the biomass samples for all plots were calculated and compared (Tables 5.2 to 5.5).

One-way ANOVA tests of the biomass samples and species composition data respectively were performed for all trial plots at both Trawscoed and Pwllpeiran. This was done to establish the degree to which the different plots vary in relation to biomass and species compostion and how this variation can be related to the different management regimes.

A similar approach has been suggested by Jacobsen et al. (2000), to examine the connection between floristic composition and management of grasslands.

5.3.5 Spaceborne data

Through reference to the Phase 1 survey for Wales (Howe et al., 2005), as well as Vexcel aerial photography as a visual guide, grasslands at varying levels of agricultural improvement were identified in a range of temporally differing satellite images (SPOT-5 and IRS) across the whole of Wales. The spectral reflectance of these fields was subsequently extracted and compared both across time, as well as across grassland improvement levels.

The data collection and pre-processing, as well as the specifications of the spaceborne SPOT 5 HRG and IRS data utilized for the spaceborne analysis are outlined in Section 4.1 and Appendix A.2. The results for this experiment are described in Section 5.4.5.

5.4 Results

5.4.1 Grassland Biomass and management regimes

The tables below describe the biomass samples collected from the field plots at Trawscoed and Pwllpeiran on a per plot (Tables 5.2 and 5.4) and a summarized treatment basis (Tables 5.3 and 5.5).

Trawscoed Biomass

Figure 5.14 shows large variation of mean biomass samples across the individual treatment plots at Trawscoed. The most improved plots (Treatments T1 and T6) are found at the lower range of standing biomass. Two of the least improved

Table 5.2: Biomass sample measurements of the Trawscoed management treatment plots

Plot	Average weight (g/0.3m^2)	StDev	Range
T1a	20.9	10.6	25.9
T1b	14.4	32.7	126.4
T1c	12.1	6.3	40.3
T2a	112.6	29	136.6
T2b	134.4	44.02	98.9
T2c	116.8	28	196.3
T3a	129.6	41.8	428.4
T3b	97.2	31	119.7
T3c	102.7	28.2	122.4
T4a	154.4	39.2	122.4
T4b	120.6	32.7	88.8
T4c	216.4	66	152.5
T5a	138.9	32.3	146.4
T5b	69.4	53.7	192.6
T5c	141.5	34.9	119.1
T6a	43.6	22.4	167.6
T6b	37.6	34	129.4
T6c	84.6	111.2	283.2

Table 5.3: Average biomass measurements per treatment at Trawscoed

Treatment	Average weight (g/0.3m^2)	StDev	Range
T1	15.6	20.9	126.4
T2	120.9	35.1	202.5
T3	109.8	36.7	150
T4	163.8	62.1	317.6
T5	117.2	52.8	223.8
T6	55.3	70.8	443.6

plots (T4 treatment) are found to have the highest biomass occurring, with T4c noticeably higher than all other plots, though the third plot ranks considerably lower.

All other treatments (T2/T3/T5) occurr in the mid-range of values, with little variation evident. The standard deviations of plot T1b and T6c and to a lesser degree T5b are very high, indicating a wide spread of sample measurements around the mean.
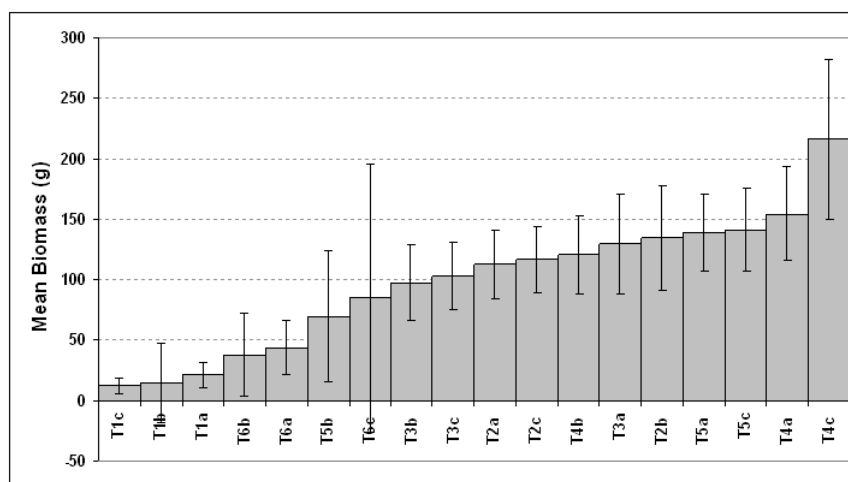
Figure 5.14: Biomass for the individual Trawscoed management plots (Table 5.2)

Figure 5.15 shows the mean biomass of each set of three plots being managed in the same way (Table 5.3). Comparing the treatments directly in this way, shows that the mean standing biomass for each treatment corresponds to the expected level of improvement, as indicated in Figure 5.7(a). T4, the least intensely managed treatment again shows the highest values and T1 the lowest.
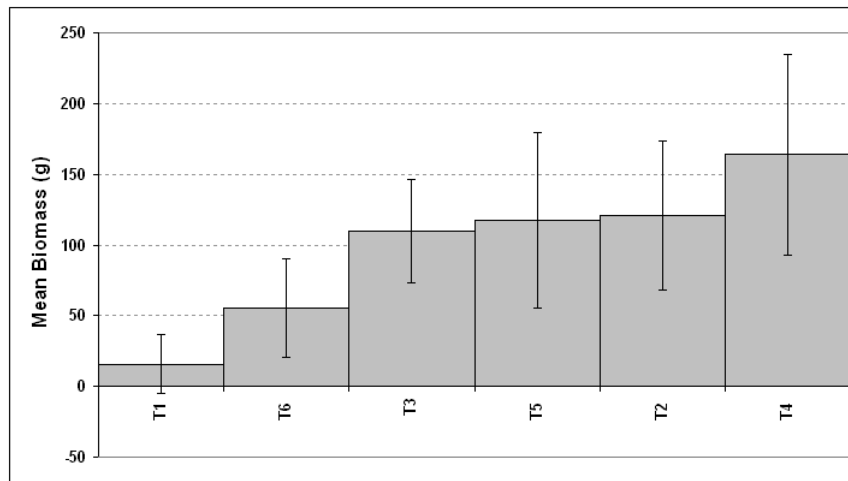
Figure 5.15: Average biomass measurements for the Trawscoed management regimes (Table 5.3)

Table 5.4: Biomass sample measurements for the Pwllpeiran management treatment plots

Plot	Average weight (g/0.3m^2)	StDev	Range
P1a	9.3	5.9	
P1b	9.9	10.3	
P1c	32.6	19.6	
P2a	12.6	7.9	
P2b	17.4	13.3	
P2c	21.19	17.5	
P3P6a	111.8	37.3	
P3P6b	144	38.2	
P3P6c	110.4	38.2	
P4a	29.3	18.8	
P4b	145.4	47.5	
P4c	94.5	38.9	
P5a	15.62	12.1	
P5b	27.8	19.3	
P5c	29.6	20.1	
P7a	94.6	29.3	
P7b	124.1	33.5	
P7c	110.6	37.4	

Table 5.5: Average biomass measurements per treatment at Pwllpeiran

Treatment	Average weight (g/0.3m^2)	StDev	Median	Maximum	Minimum
P1	17.3	17.1		81.7	0
P2	17.1	13.8		77.9	0.1
P3P6	121.7	40.6		235.3	30
P4	89.7	60.2		277.6	5.6
P5	24.4	18.4		96.3	0.9
P7	109.8	35.4		197	43.6

Pwllpeiran Biomass

Figure 5.16 shows a similar pattern of biomass distribution to Trawscoed. As illustrated in Figure 5.7(b), the treatments P3/P6, P4 and P7a are expected to produce the least improved fields and here also have noticeably higher biomass values than the more intensively managed fields (P1/P5/P2), though no single plot is showing a particular spike. The Standard Deviations also show little variation, indicating a high degree of uniformity amongst biomass samples from individual fields.
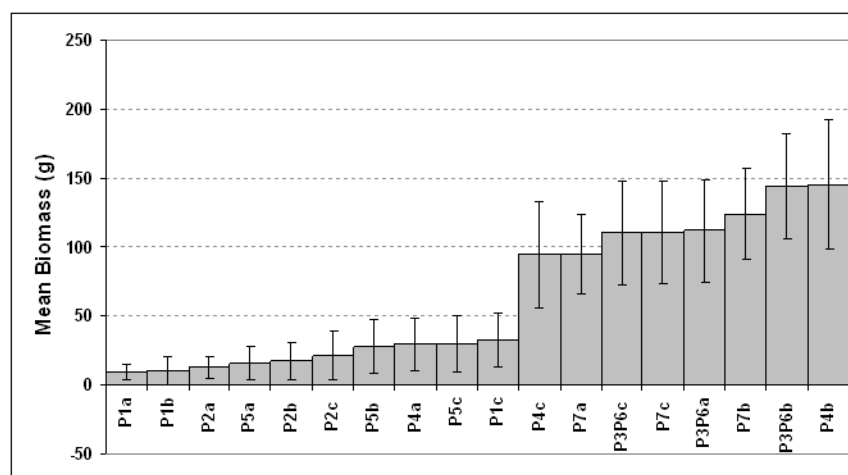
Figure 5.16: Biomass for the individual Pwllpeiran management plots(Table 5.4)

Figure 5.17 indicates the same trend. Though the increase in biomass per treatment does not correlate perfectly to Figure 5.7(b), with P2 showing the lowest value despite a semi-improved ranking, there are marked differences in standing biomass between the greater and less intensely treated plots.

These results suggest that lower levels of improvement are related to higher amounts of standing biomass within the sward.
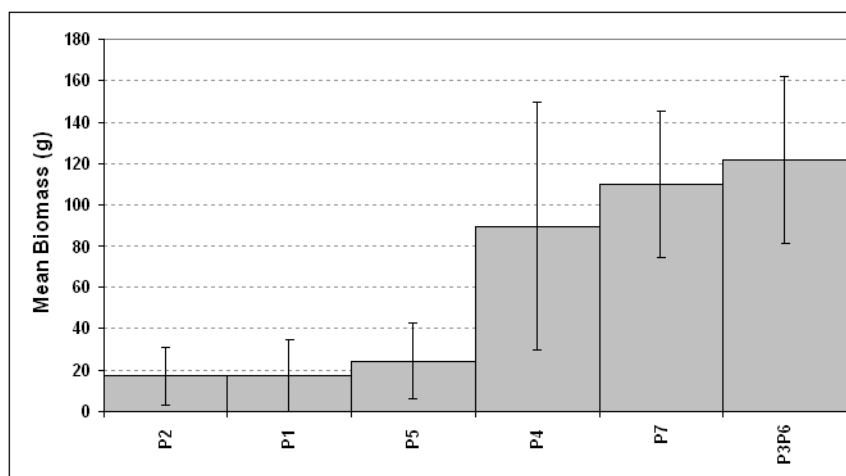
Figure 5.17: Average biomass measurements for the Pwllpeiran management regimes (Table 5.5)

further show the results of one-way ANOVA tests of the significance in biomass variation between treatment plots at the two sites. Both tests indicate that the variation of biomass between plots is higher than can be explained by chance alone, as this chance (p-value) is in both cases considerably lower than the statistically significant threshold of 5%. The high F-ratios also indicate that variability in biomass between plots is very considerable.

Table 5.6: One-way Analysis of variance (ANOVA) of the Trawscoed mean biomass between treatment types (T1-T6)

Source of Variation	SS	df	MS	F	P-value
Between Groups	41805.06944	5	8361.013889	9.754643556	0.000658244
Within Groups	10285.58	12	857.1316667		
Total	52090.64944	17			

Table 5.7: One-way Analysis of variance (ANOVA) of the Pwllpeiran mean biomass between treatment types (P1-P7)

Source of Variation	SS	df	MS	F-ratio	P-value
Between Groups	36258.42	5	7251.68	10.313	0.00051
Within Groups	8438.028	12	703.169		
Total	44696.45	17			

5.4.2 Variability of spectral reflectance across treatments and between trial plots

Figure 5.18 shows the greatest range of reflectance across treatments in the NIR band reflectance (736.1nm to 863.6nm). The T2 treatment shows the highest reflectance in this region, while the improved treatment type T1 reflects strongest in the visible and red edge region (449-708.4 nm). The T4 treatment consistently reflects at the lowest level, which is especially noticeable in the NIR region. This might indicate that the opportunity to distinguish between different levels of grassland improvement is greatest in the NIR region.

However, Figure 5.19 shows the results of one-way ANOVA analyses of the statistical significance of each image band in distinguishing between treatment types at Trawscoed. The graph illustrates that, with the exception of band 4 ($\rho_{668.4}$ / p=0.062), all image bands within the visible and red-edge regions ($\rho_{449} - \rho708.4$)
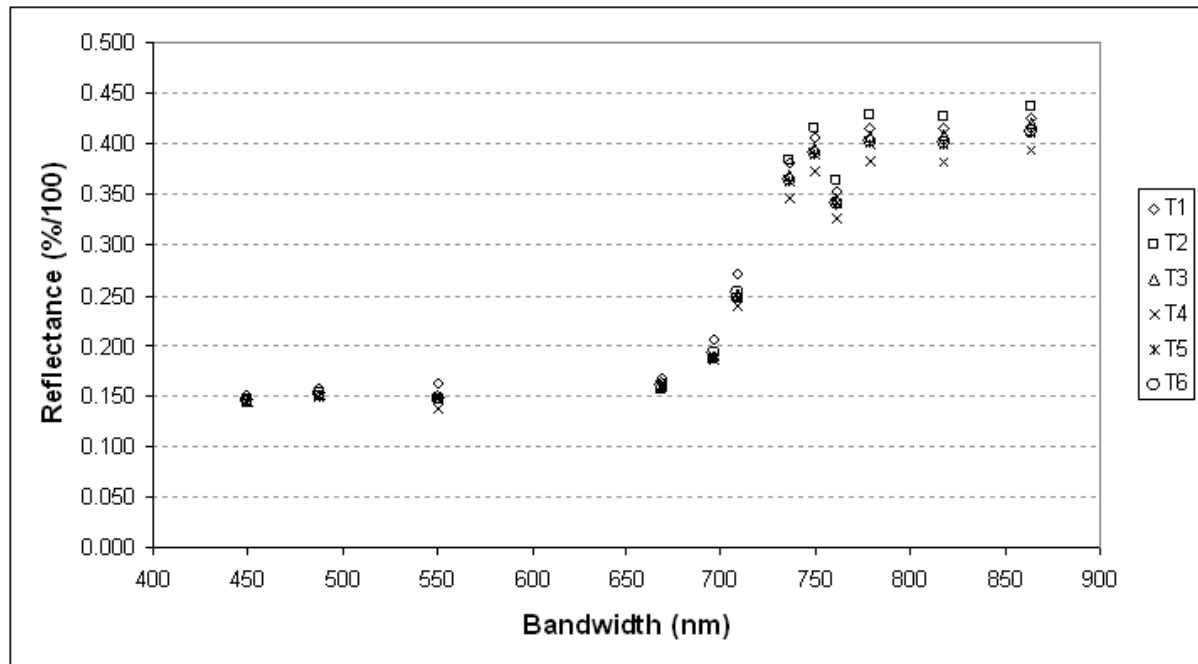
Figure 5.18: Reflectance of Trawscoed treatment types across the CASI bandwidth spectrum
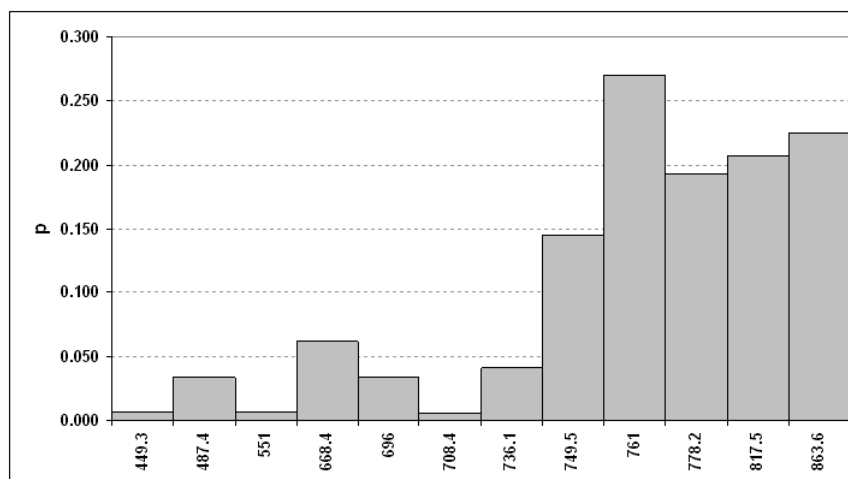
Figure 5.19: ANOVA test results across the CASI bandwidth spectrum for significant variability between treatments at Trawscoed

are statistically significant in explaining the variation between treatment types as manifested in the reflectance in these bands.

The null hypothesis tested in Figure 5.19 for each image band, states that there is no significant difference in reflectance between treatment types T1-T6, but the likelihood that the null hypothesis is true is below the standard significance threshold of 5% for six bands and is therefore rejected in this case.
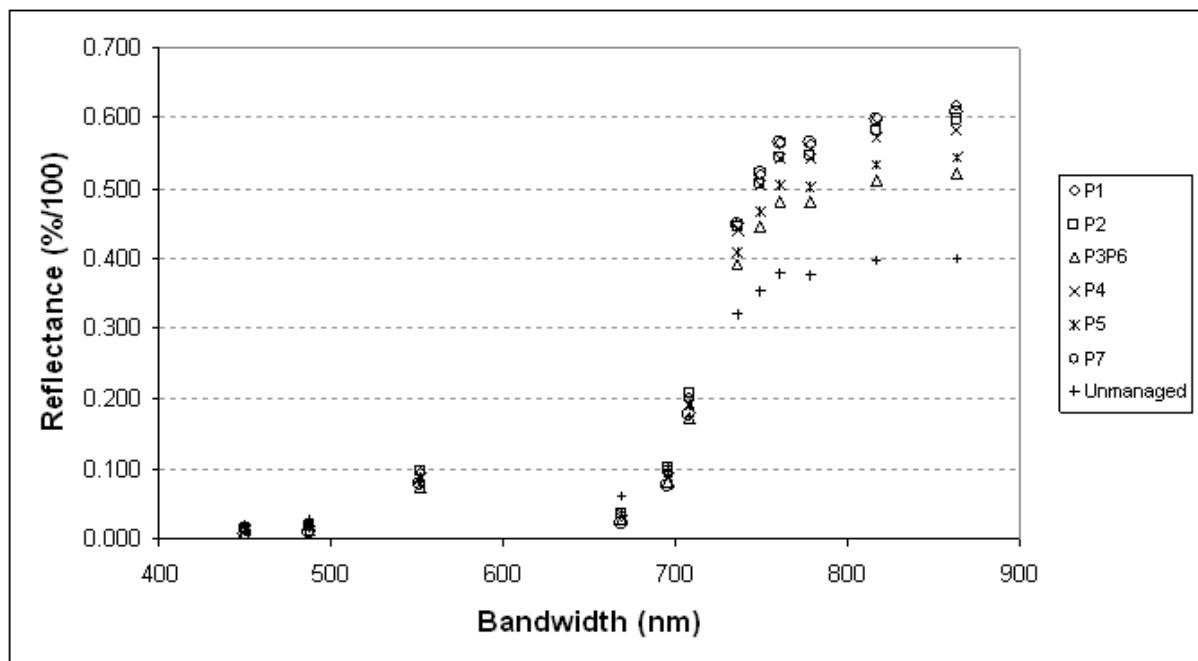
Figure 5.20: Reflectance of Pwllpeiran treament types across the CASI bandwidth spectrum

Figure 5.20 shows a similar pattern to Figure 5.18. The greatest range of average reflectance per treatment type is found in the NIR region ($\rho_{736.1} - \rho863.6$). The unmanaged discard plot at Pwllpeiran (Figure 3.7) exhibits a considerably lower NIR response than all other field types, but the greatest reflectance in band 4 ($\rho_{668.4}$). It is, however, not included further in the analysis, because no repeat

plots exist and it was not sampled for biomass.

P3P6, which is considered the least improved plot type, is then the lowest reflecting in the NIR bands, followed by P5, which is ranked as second most improved.
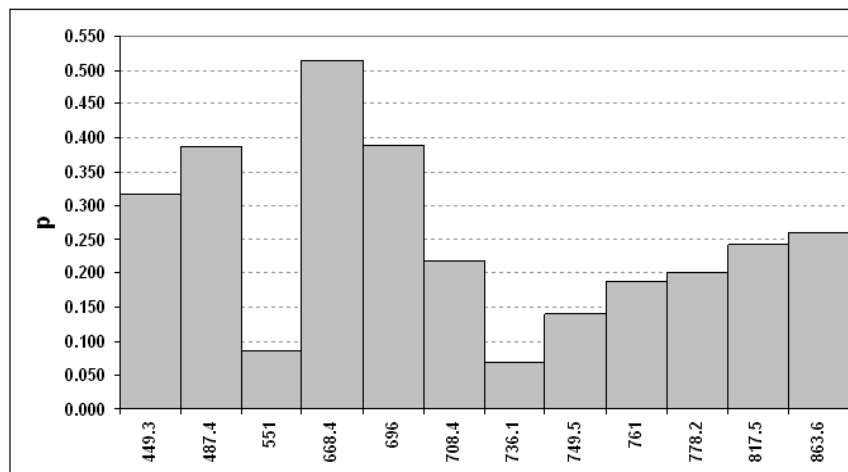
Figure 5.21: ANOVA test results across the CASI bandwidth spectrum for significant variability between treatments at Pwllpeiran

These results suggest a great similarity in the reflectance behaviour of the differently treated fields between Trawscoed and Pwllpeiran. The one-way ANOVA (Figure 5.21) conducted to test each band for significant differences in reflectance between all treatment types, however, shows that the significance threshold of 5% is not reached for any band. The null hypothesis can therefore not be rejected and the variation in reflectance between differently treated fields has to be considered not statistically significant.

Table 5.8, however, shows significant results of the same test when a smaller number of bands is considered. The result indicates that the spectral variation between the least and the most improved treatment types (P1 and P3P6) is significant in bands 3 and 6. A comparison of the same variation between the three least improved field types (P3P6/P4/P7) meanwhile indicates that they do not differ

significantly in band 3, but that there is a highly significant difference in band 6 (the red edge).

Table 5.8: ANOVA test result of spectral differentiation between selected treatment types at Pwllpeiran

Image band	P1/P3P6	P3P6/P4/P7
Band 3 (ρ_{551})	0.030	0.177
Band 6 ($\rho_{708.4}$)	0.040	0.0000029

However, as Figure 5.21 and Table 5.8 suggest that it is not possible to differentiate all treatment plots at Pwllpeiran spectrally, not all analyses below will be carried out for this site, but instead the study will focus primarily on Trawscoed. Possible reasons for the lack of separability are discussed in Section 5.5.5.

5.4.3 Species composition and coverage variability

Canonical Discriminant Analysis derives canonical variables that summarize between-class variation and finds the variables which optimize separation of the data groups, here vegetation survey data for each treatment type. The best two are represented on the two axes in Figure 5.22. As the the dataset only contains two variables, species and percentage cover of species, they are known to be represented here. The Canonical Discriminant Analysis in Figure 5.22 compares the similarity between the different management regimes with regard to species composition (Function 1) and coverage (Function 2). The distribution of quadrats indicates a high correspondence in the species composition and coverage in plots treated under the semi-improved management plans (T2, T3, T5). The improved (T1 and T6) plots display similarity with regard to percentage coverage (evenness of species distribution), but differ visibly in species composition. The least improved plots (T4),

in comparison, contain similar species to those which are semi-improved but they are distributed differently.
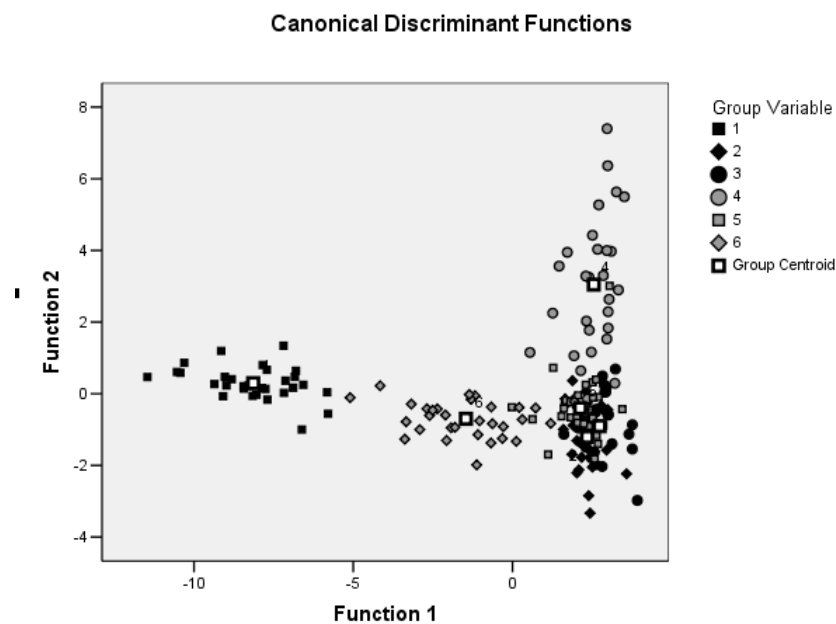
Figure 5.22: Canonical Discriminant Analysis of vegetation percentage cover at Trawscoed

Figure 5.23 shows the calculated Shannon-Weaver biodiversity index (H') for each of the indiviudal plots at Trawscoed. The most improved fields (T1) exhibit the lowest index, while all other plots do not seem to follow any particular order. T6b, one of the more improved fields shows the highest value for H'. The index, however, takes into account both species richness and evenness of vegetation distribution.

Figure 5.24 repeats the trend from Figure 5.23. The combined T1 treatments display the lowest biodviersity value, while the T6 plots are ranked highest and the
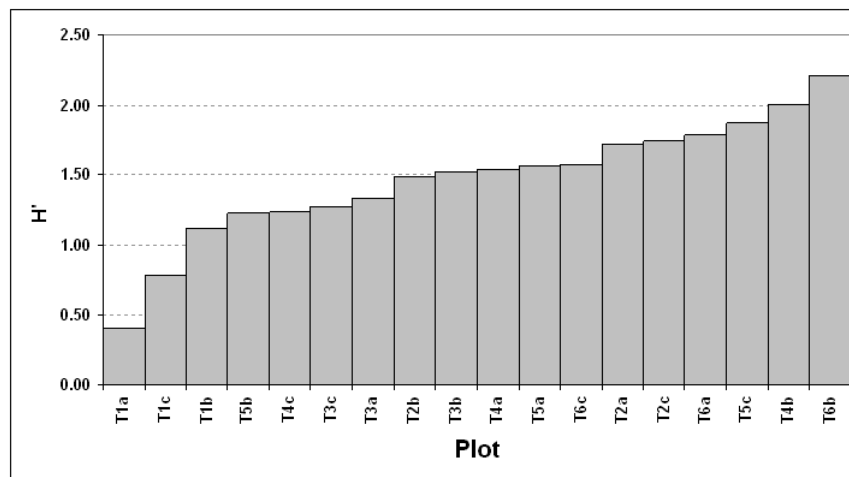
Figure 5.23: Shannon-Weaver diversity index (H') for Trawscoed experimental plots in ascending order

value of H' does not correspond to level of improvement with all other treatment types. One-way ANOVA tests on the separability of plots or treatments by the Shannon-Weaver Index showed that the variability between both plots and treatments with regard to this biodiversity indicator is not significant.

Two-way Analysis of variance (ANOVA) of the Trawscoed and Pwllpeiran vegetation survey data variability between treatments (Tables 5.9 and 5.10) further show that a statistically significant separation of the treatment types (here arranged in rows or samples) from the 2006 vegetation survey data is not possible and further that the interaction between treatment type and species is not significant.

Endmember fractions

Anova results for testing the separability of the treatment types using the endmember fraction images indicate that variation between treatments with regard to
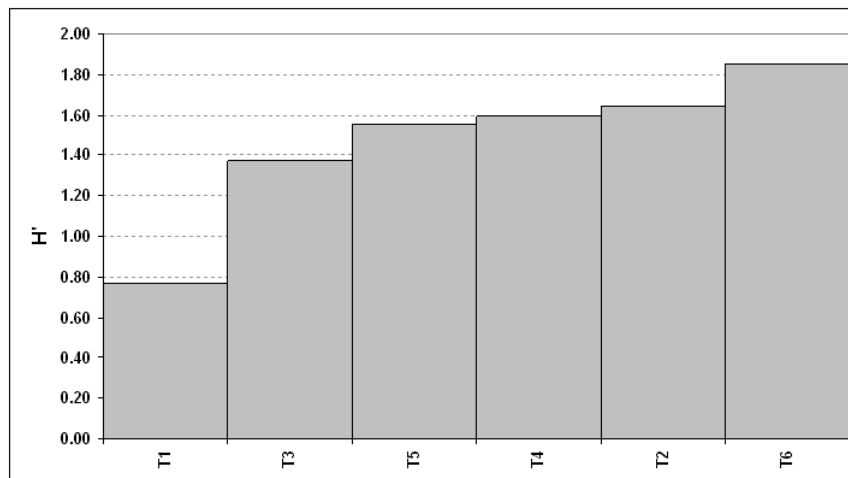
Figure 5.24: Shannon-Weaver diversity index (H') for Trawscoed treatment types in ascending order

Table 5.9: Two-way Analysis of variance (ANOVA) of the Pwllpeiran vegetation survey data variability between treatments (P1-P7)

Source of Variation	SS	df	MS	F-ratio	P-value
Sample	38.30276308	5	7.660552616	0.193393676	0.965033957
Columns	16308.72296	41	397.7737307	10.04195494	2.24666E-43
Interaction	7537.447237	205	36.7680353	0.928223573	0.730871015
Within	19964.03704	504	39.6111846		
Total	43848.50999	755			

Table 5.10: Two-way Analysis of variance (ANOVA) of the Trawscoed vegetation survey data variability between treatments (T1-T6)

Source of Variation	SS	df	MS	F-ratio	P-value
Sample	31.80348324	5	6.360696649	0.4301934	0.82766493
Columns	24417.79151	48	508.7039897	34.40520921	9.5936E-140
Interaction	16389.21966	240	68.28841527	4.618554723	1.45033E-51
Within	8693.972593	588	14.78566767		
Total	49532.78725	881			

the derived fraction images for non-photosynthetic and photosynthetic vegetation as well as shade is not significant, but that the variation between all individual plots is.

All plots show a very low standard deviation for their NPV, PV and Shade values respectively, indicating a low spread of samples around the mean.

5.4.4   Integration of field and airborne data

Biomass and Spectral data comparison

The graphs in Figure 5.25 to Figure 5.29 show the regression of biomass sample values against their corresponding spectral or derived values. There are three repetitions for each analysis, as each management treatment is repeated three times.

Figure 5.25 shows the results of a simple linear regression between biomass samples from all plots at Trawscoed and the reflectance at the corresponding sample point extracted from each image band ($\rho_{449.3}$-$\rho_{863.6}$). The greatest correlation between any band and biomass is found in band 6 (on the red-edge) with an r^2-value of 0.6. This corresponds with the result of the ANOVA analysis in Figure 5.19, which indicated that band 6 has the greatest potential to differentiate the treatment types spectrally.

The same result is included here for Pwllpeiran in Figure 5.26, to show that the correlation between spectral reflectance and biomass is indeed considerably lower than at Trawscoed, as suggested in Section 5.4.2 by the lack of significance of spectral variability between treatment types at Pwllpeiran..

(a) B1

(b) B2

(c) B3

(d) B4

(e) B5

(f) B6

(g) B7

(h) B8

(i) B9

(j) B10

(k) B11

(l) B12
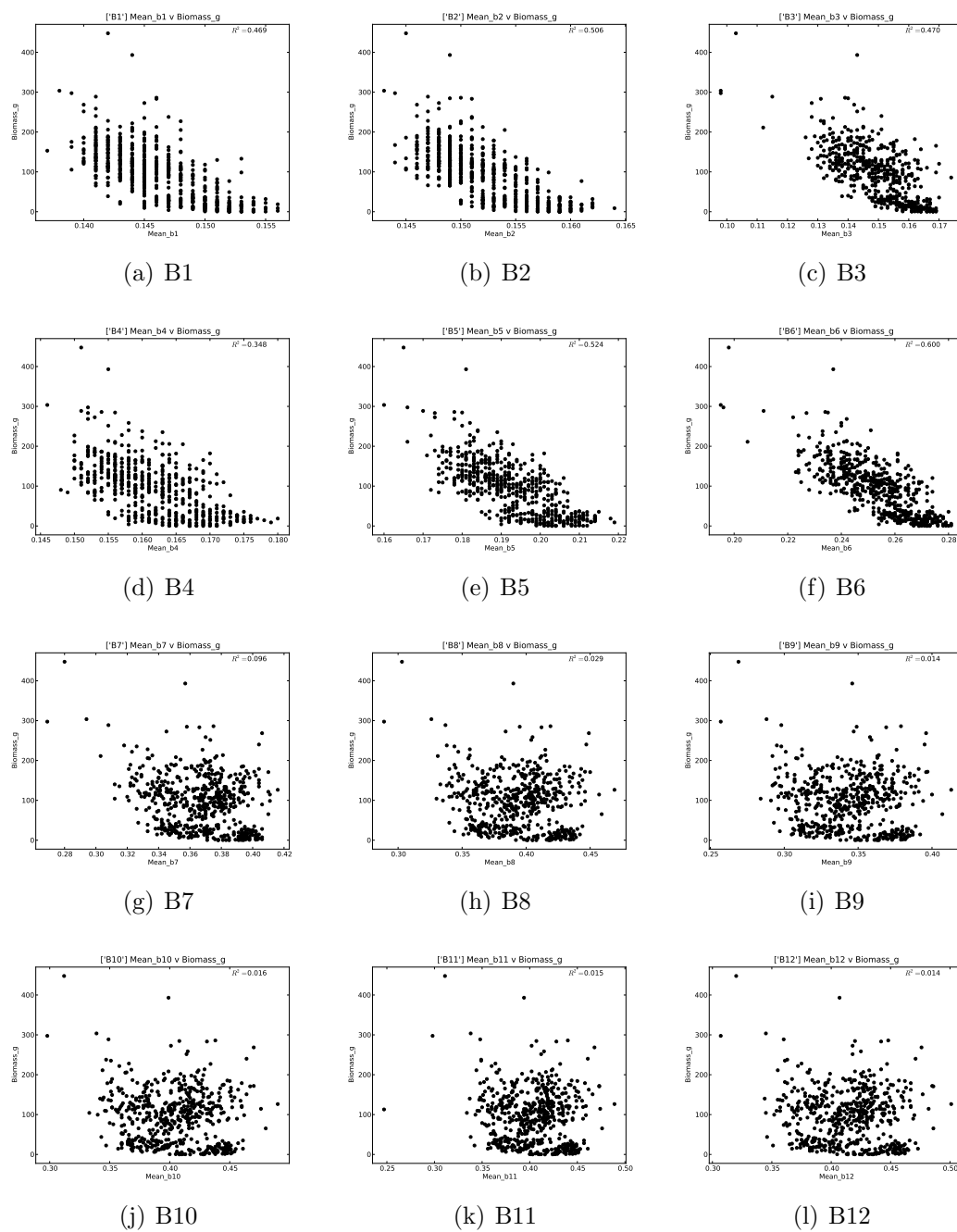
Figure 5.25: CASI image bands versus Biomass, Trawscoed

(a) B1

(b) B2

(c) B3

(d) B4

(e) B5

(f) B6

(g) B7

(h) B8

(i) B9

(j) B10

(k) B11

(l) B12
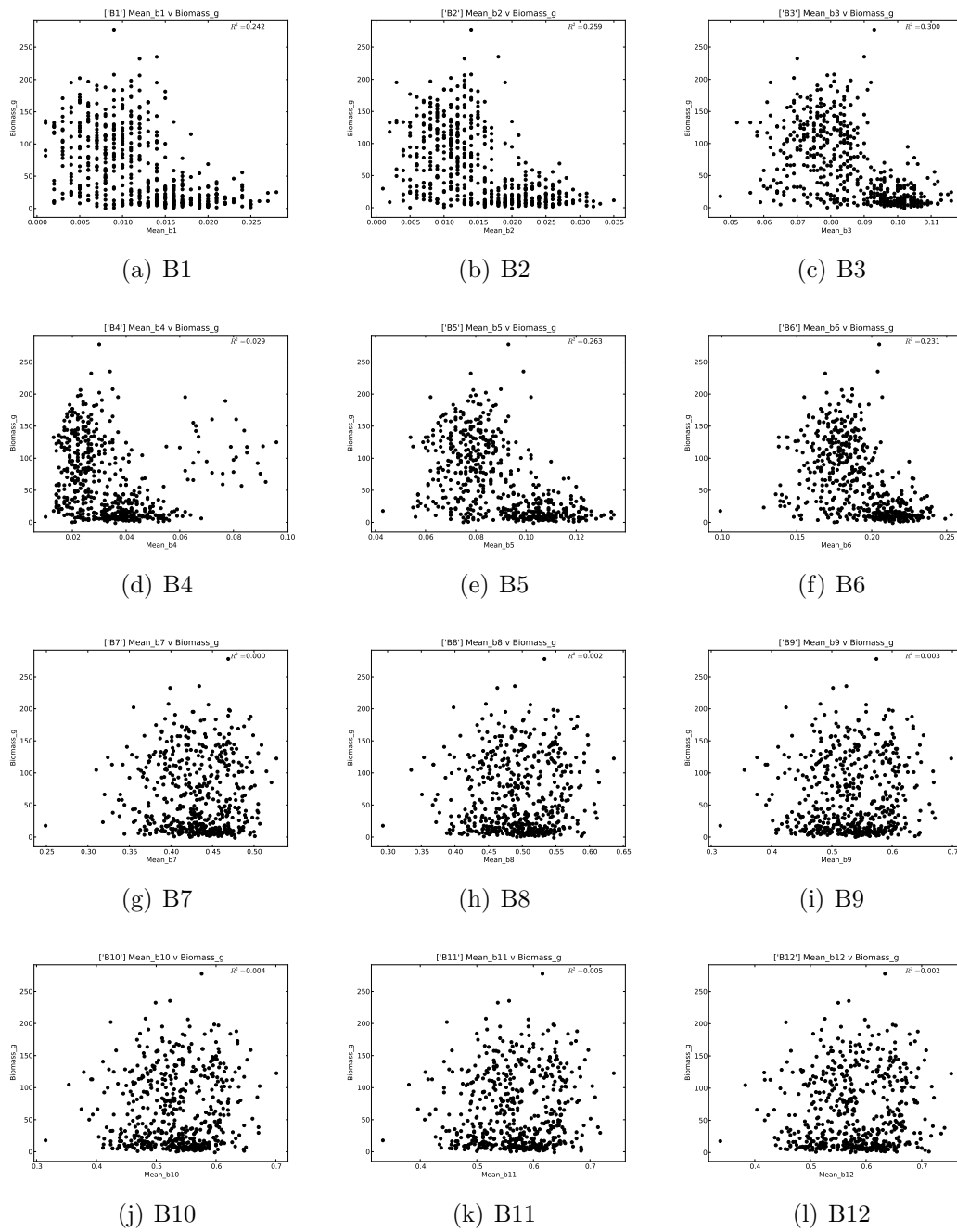
Figure 5.26: CASI image bands versus Biomass, Pwllpeiran

Figure 5.27 and Figure 5.28 compare the average per plot biomass with the corresponding spectral value also extracted from the whole plot for each band. Figure 5.27 shows strong correlations between biomass and reflectance in the visible bands at Trawscoed, particular again in Band 6 ($r^2=0.768$). This suggests that for Trawscoed biomass and spectral reflectance in the visible region of the wavelenght spectrum are highly correlated. However, the same is not the case at Pwllpeiran, even while the strongest correlation in Figure 5.28 reach r^2-values of nearly 0.5.

Figure 5.29 and Figure 5.30 illustrate the correspondence between the fractional image extracted from the CASI data and biomass at each sample location at Trawscoed and Pwllpeiran respectively. No correlation can be detected at for any fraction image at Pwllpeiran or the photosynthetic fraction at Trawscoed. The non-photosynthetic and shade fraction images at Trawscoed, however, show a small to moderate relationship with biomass.

Chen et al. (2009) suggest a range of vegetation indices derived from hyperspectral data obtained from a spectroradiometer to estimate grassland biomass. The four indices they indicated as most successful (MTVI, RDVI, RVI, TVI) were calculated in this study for Trawscoed (Figure 5.12) and are shown in Figure 5.31 correlated with the average biomass from each plot. The NDVI was also calculated and is compared against biomass samples at each sample location.

Apart from the RVI, the plots show no correlation between vegetation indices calculated from airborne hyperspectral data and grassland biomass. The correlation for the Ratio Vegetation Index is also weak at $r^2=0.248$, but it corresponds in so far with Chen et al. (2009), that this was also the best performing vegetation index in their study.

(a) B1   (b) B2   (c) B3

(d) B4   (e) B5   (f) B6

(g) B7   (h) B8   (i) B9

(j) B10   (k) B11   (l) B12
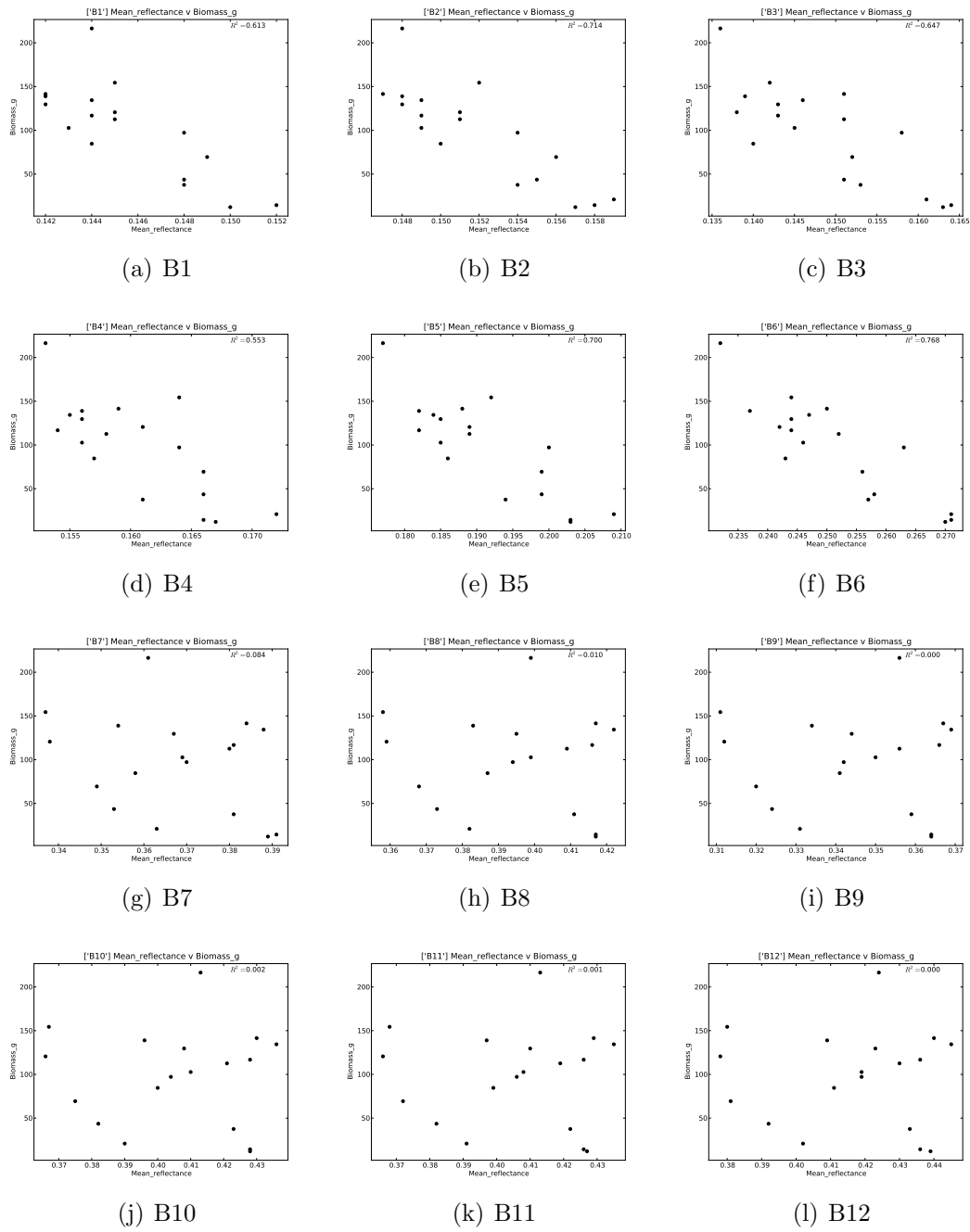
Figure 5.27: Comparison of average per plot biomass against spectral value per plot for each band, Trawscoed

(a) B1   (b) B2   (c) B3

(d) B4   (e) B5   (f) B6

(g) B7   (h) B8   (i) B9

(j) B10   (k) B11   (l) B12
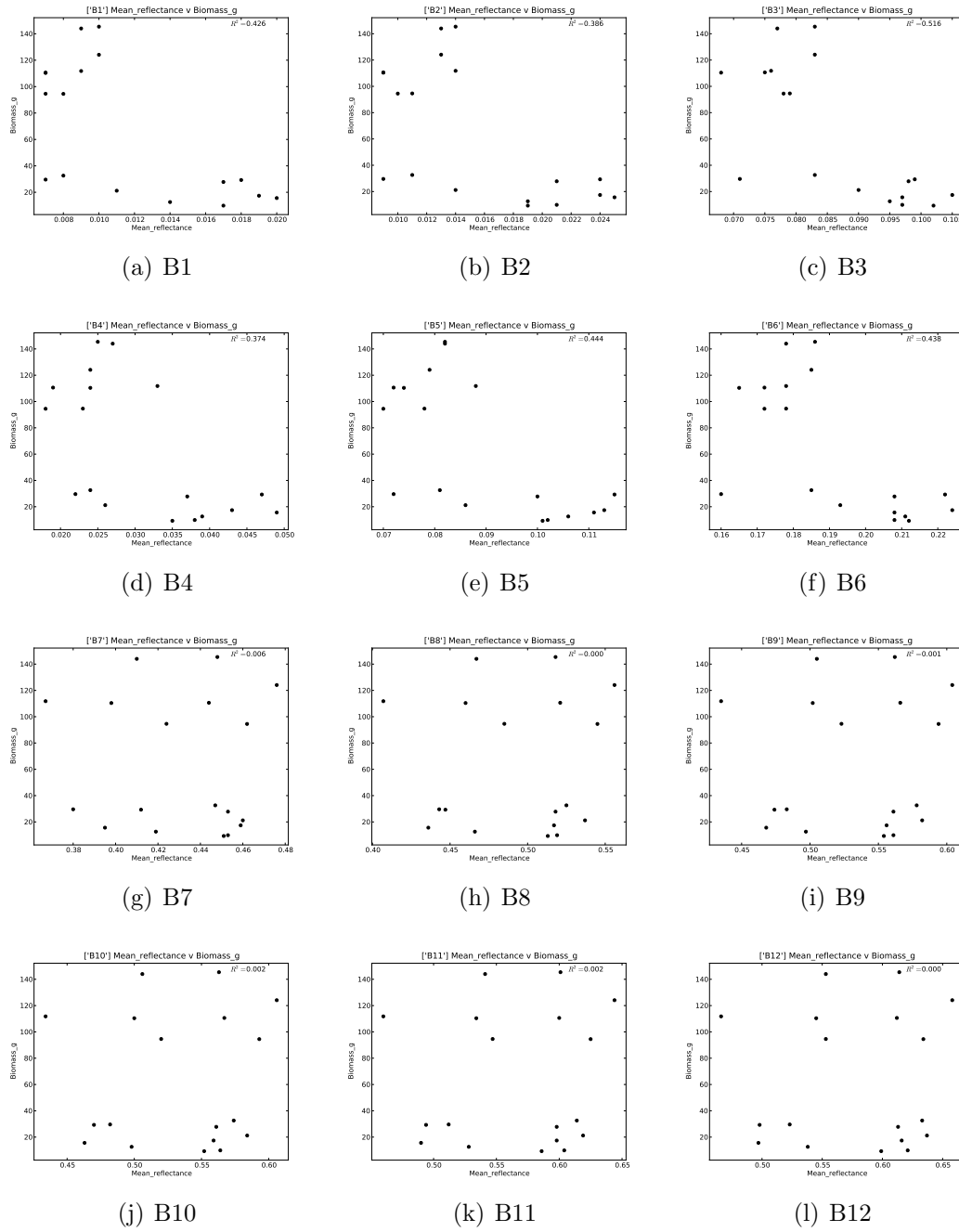
Figure 5.28: Comparison of average per plot biomass against spectral value per plot for each band, Pwllpeiran

(a) NPV

(b) PV

(c) Shade
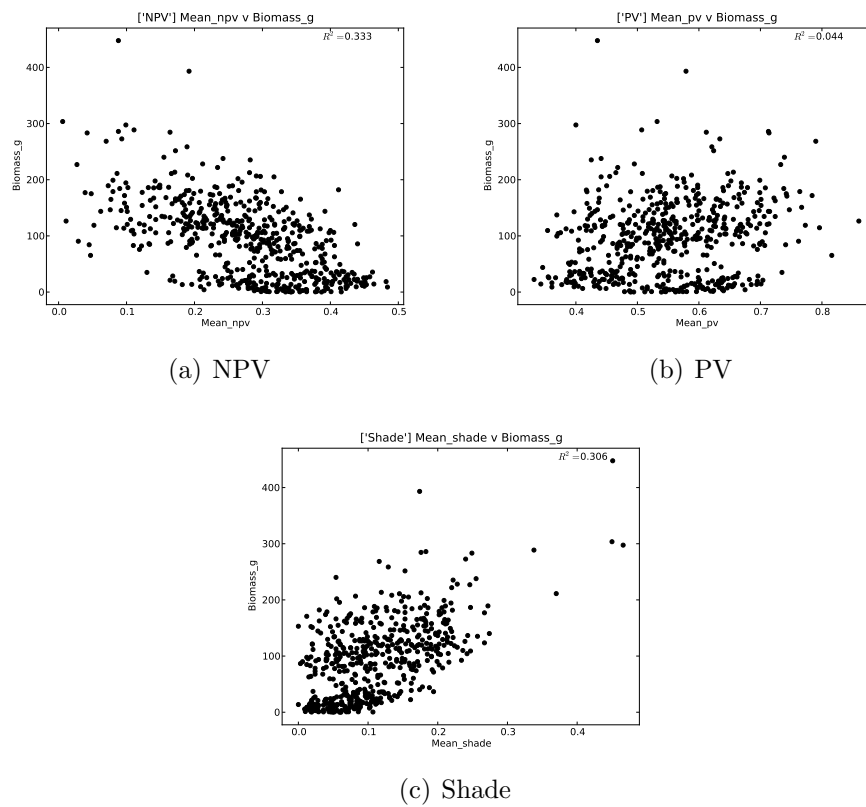
Figure 5.29: Endmember fraction values versus Biomass for each sample location at Trawscoed

(a) NPV

(b) PV

(c) Shade
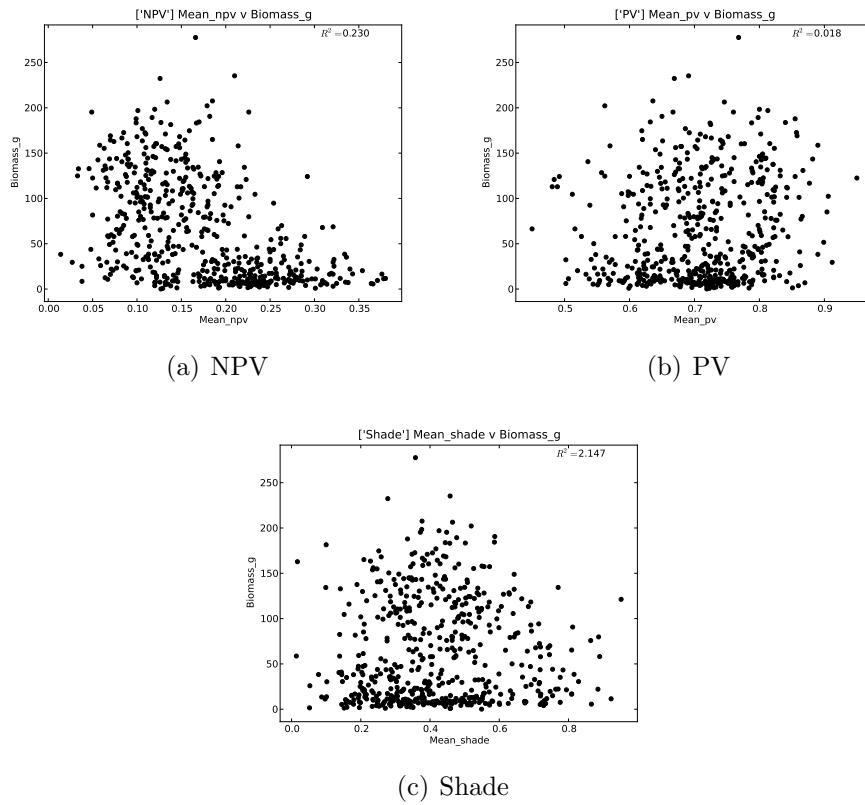
Figure 5.30: Endmember fraction values versus Biomass for each sample location at Pwllpeiran

5.4.5 Scaling up of grassland diversity using multispectral data

Figure 5.32 shows a 2003 March SPOT image of Trawscoed to illustrate the variability of coarser resolution (10m) multispectral data at the site.

Figure 5.33 then illustrates the results of a small scaling up experiment described in Section 5.3.5. It demonstrates that grasslands with different improvement levels can be differentiated also from multi-sensor and multi-temporal satellite data and that the NIR band has the potential to do so.

Differences in the reflectance of grasslands in Figure 5.33 were most evident within the NIR reflectance, with higher (> 30 %) reflectance observed for improved grasslands throughout most of the year, increasing to over 40 % (maximum 50 %) in late spring/early summer. By contrast, the NIR reflectance of unimproved acid grasslands was generally < 40 % and lower (by at least 10 %) in most months. Semi-improved grasslands supported a reflectance that was between these extremes.

The greatest potential for distinguishing between the different grassland types is between late February and early May, while improved grassland have a significant advantage in growth and productivity. Later in the year the differences are significantly reduced when less improved grasslands also reach higher growth levels and grazing and senescence take place to obscure productivity differences.

(a) NDVI

(b) MTVI

(c) RDVI

(d) RVI

(e) TVI
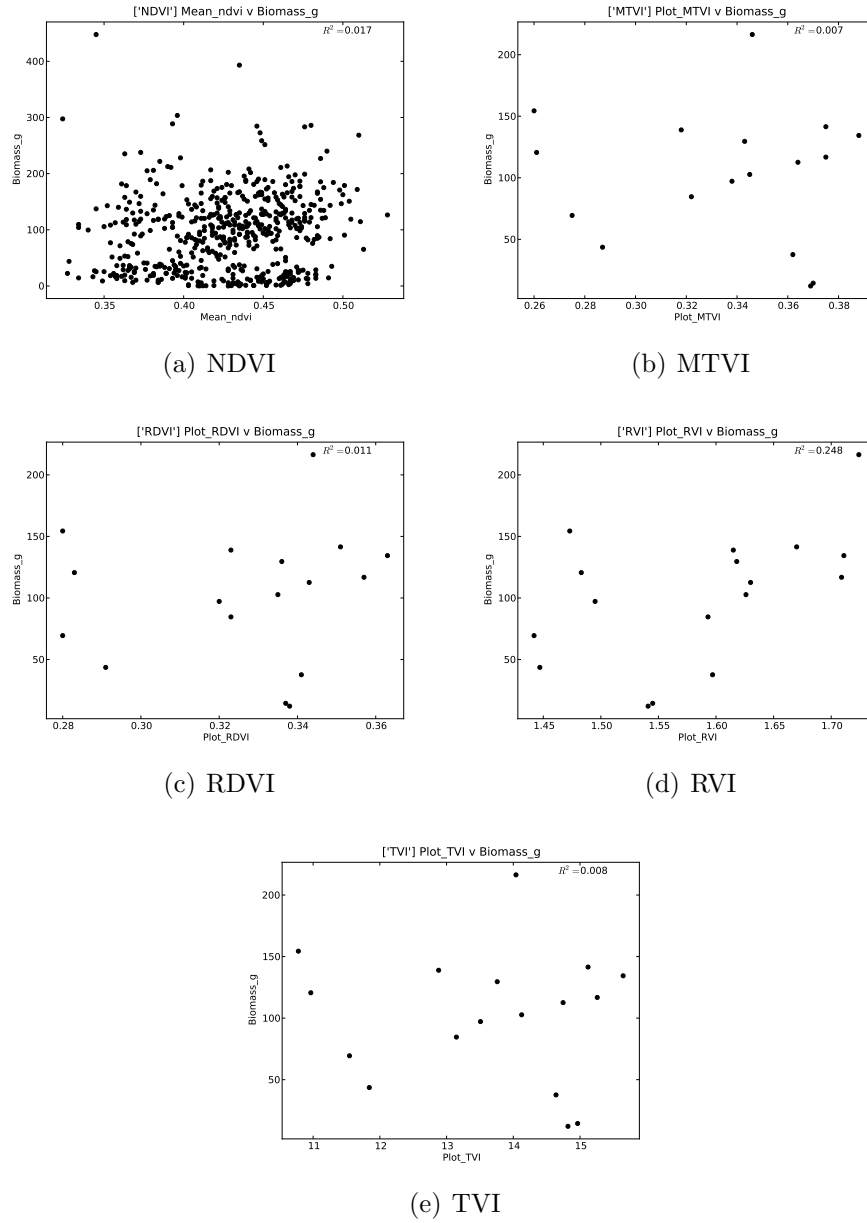
Figure 5.31: Comparison of average per plot biomass against vegetation indices, Trawscoed
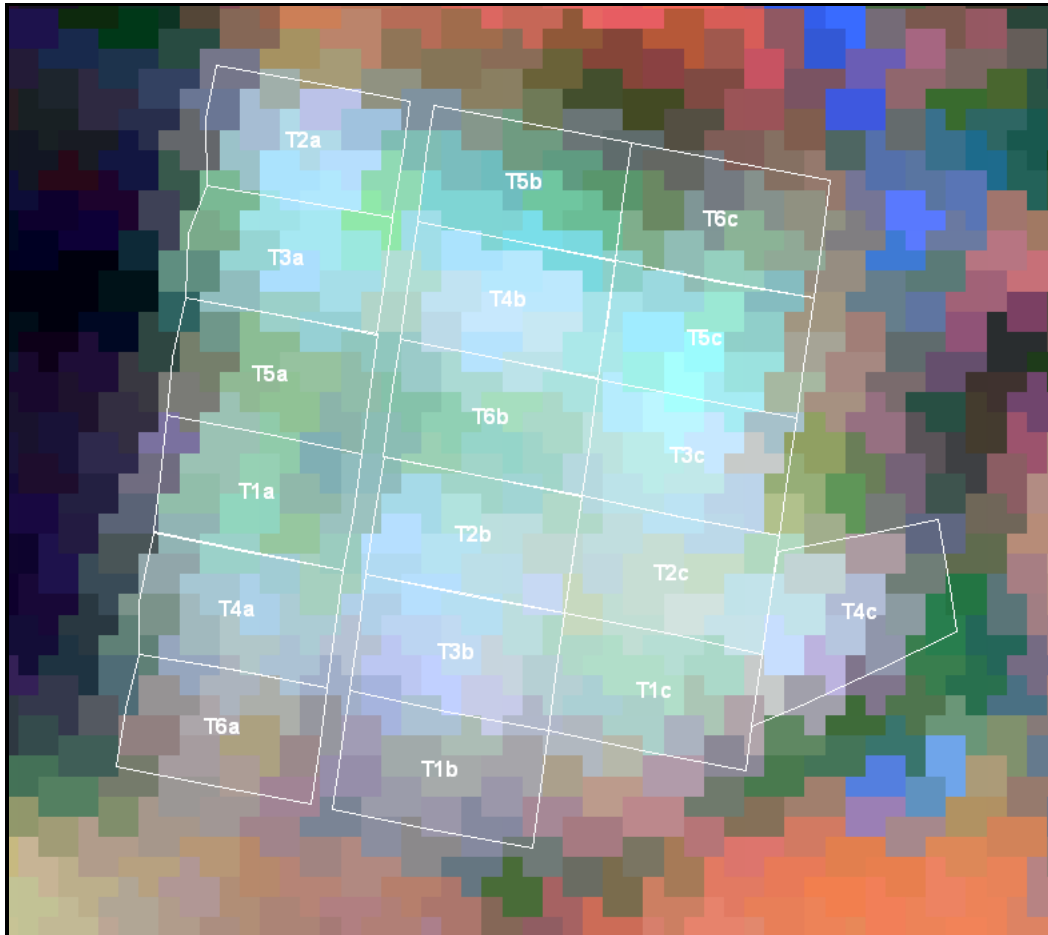
Figure 5.32: March 2003 SPOT image of the Trawscoed study site, treatment plots are outlined and labeled according to the management treatments T1-T6 (see Table 3.3)
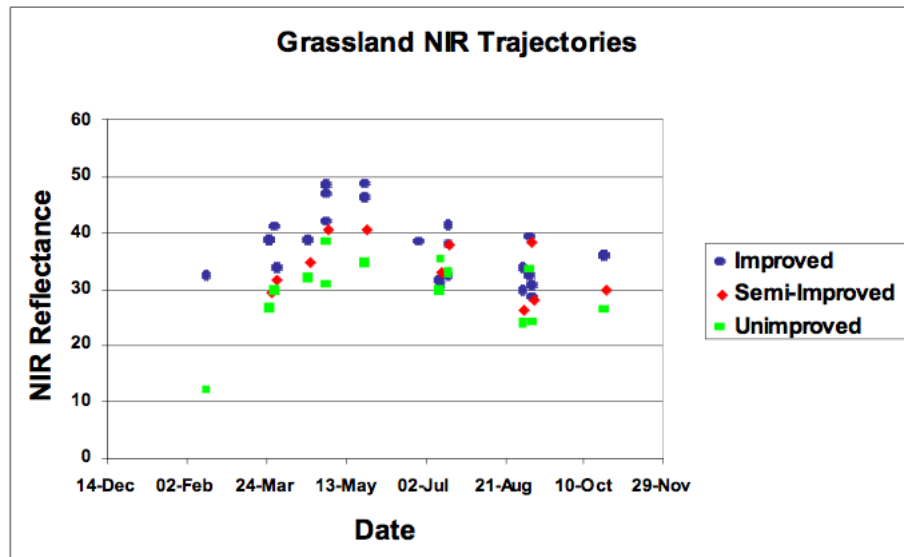
Figure 5.33: Variations in the SPOT NIR reflectance in grasslands of varying productivity throughout the growing season

5.5   Discussion

Diversity, biomass and productivity are key variables in community and ecosystem ecology (Guo, 2007), including that of grassland environments. Mapping grassland biophysical parameters such as biomass and Leaf Area Index (LAI) is hence fundamental to the understanding of ecosystem dynamics which directly influence biodiversity.

A large number of studies have established a positive relationship between plant species richness and productivity and biomass in grasslands (e.g., Jiang et al., 2007; Silvertown et al., 1994). Hector et al. (1999) stated that a loss of plant diversity could be related to a log-linear reduction of average above ground biomass, because of a reduction in functional diversity and therefore diminished uptake of niche spaces. Increased nutrient use efficiency at high species richness is an important mechanism in this relationship (van Ruijven and Berendse, 2005; Fargione

et al., 2007) and swards of high species richness have shown greater temporal stability of productivity levels (Tilman et al., 2006).

In direct comparison agricultural improvement, through re-seeding, fertilization and grazing of grasslands, leads to very low species numbers or even monocultures, mostly of *Lolium perenne*, in such swards and simultaneously to low productivity and biomass levels, often further reduced through intensive grazing.

Both for biodiversity assessment and subsequent conservation, as well as monitoring of a reliable and efficient supply of grassland products, such as livestock fodder, the reliable estimation of grassland biomass and productivity from remote sensing data is hence of great interest.

This discussion considers the differentiation of grasslands of varying degrees of agricultural improvement, as well as the estimation of related biomass levels and species diversity through the use of airborne hyperspectral remote sensing. This is an essential step in preparation for the large-scale mapping of habitats in Chapterr̃efchp6:AllHabitats, including different grassland types, from multispectral satellite data of a coarser spatial resolution.

5.5.1 Biomass

The high standard deviations of biomass samples for both individual plots and treatments for some of the experimental plots (Section 5.4.1) indicate a large range of sample values around the mean. This can be interpreted as a function of the heterogeneity of the vegetation within and between plots managed in the same way. Plot T1b for example has a uniform *Lolium perenne* sward, but contains a patch of

nettles *Urtica dioica*, which causes a number of samples to have considerably higher biomass values than the majority and hence increases the standard deviation of biomass samples for this plot.

The very high standard deviation in T6c biomass samples (Figure 5.14) is due to the presence of a large *Juncus spp.* patch in the NE corner of the plot next to a shorter, more homogenous swards. Incidentally this plot consistently exhibits the greatest correlation between reflectance and biomass, because a greater range of samples is available (Figure A.3(r) to Figure A.14(r)). The same is true for T5b, which shares this *Juncus spp.* area with T6c. There is a similar occurrence in T1b, where a large nettle patch occurs within the plot.

At Pwllpeiran the same phenomenon can be observed. Less improved plots have higher biomass levels (Tables 5.5 and 5.4). This is due to a lack of grazing on the less improved plots during the summer months (Table 3.3 and Table 3.4), which allows dead standing plant material to remain.

It has been shown that the differences in biomass between treatment types are highly significant (Tables 5.6 and 5.7) with regard to separability of the different management and that they relate well to levels of grassland improvement. It is therefore highly desirable to establish a good correlation between reflectance and biomass in order to be able to establish improvement levels reliably from remote sensing data for mapping and conservation purposes (Barnett et al., 2004; Breyer and Medcalf, 2006). If spectral reflectance and biomass are significantly related, the estimation of grassland biomass on a regional scale from airborne hyperspectral data would be a potential application of the connection (Jones and Donnelly, 2004).

5.5.2 Spectral wavelengths

This section regards the different wavelength regions and derived image products examined above in turn and assesses their information content with regards to their ability to discriminate grassland improvement levels and sward types within the landscape from remote sensing data.

Band 6 ($\rho_{708.4}$, in the middle of the red edge) has the greatest significance and hence the greatest potential to distinguish between different levels of grassland improvement at Trawscoed (Table 5.19). The red edge correlates closely with grass chlorophyll (Pinar and Curran, 1996).

The results above show a relationship between biomass and the reflectance obtained from hyperspectral CASI data. This has also been shown by other studies, such as Chen et al. (2009), Cho et al. (2007) and Psomas et al. (2007).

This study, however, differs from others in the experimental set-up of the studysites. Usually spectra are taken from open grasslands, where it is rarely possible to impose a consistent management regime, or alternatively, under laboratory conditions, where the simulation of natural conditions and grazing, for example, are difficult to simulate. Trawscoed and Pwllpeiran, however, offer a valuable opportunity for the study of grassland reflectance across a number of fields, which are subject to different treatments and hence differ in structure and species compostion.

5.5.3 Fraction images

Figure 5.29 indicates a weak relationship between the non-photosynthetic fraction image (r^2=0.333), the shade fraction image (r^2=0.306) and the standing biomass on the Trawscoed plots. The photosynthetic fraction image however does not display any relationship. This suggests that the non-photosynthetic proportion of the vegetation present is at this point in the season greater than that of the photosynthesizing, and hence alive, vegetation.

5.5.4 Vegetation Indices

With the exception of the RVI none of the vegetation indices showed any correlation with biomass in Figure 5.29. The RVI is, however, calculated from image bands on or close to the red edge (Section 5.3.2) which have been shown (Table 5.19) to have the greatest significance to distinguish between the individual treatment types and correlates strongest with biomass (Figures 5.27(f) and 5.27(f)).

5.5.5 Ecological causes of reflectance variation

Asner (1998) notes that grassland canopies typically have a low Leaf Area Index (LAI) and that leaf optical variability therefore plays a comparatively small role in determining canopy reflectance variation. Overall reflectance variability can be influenced by LAI or chlorophyll content (Pinar and Curran, 1996). However, sensitivity to this varies from the visible over the NIR to the SWIR reflectance. Leaf optical properties, and thus the biochemistry of leaf material, are generally un-

derrepresented at canopy scales, unless LAI is relatively high, which is an unusual scenario in grassland environments. The leaf orientation angle also has a strong effect on the expression of leaf optical properties at canopy scales and thus overall reflectance. Leaf angles vary between species, with most grasses having vertically orientated foliage. Forbs, however, which are more common in less improved grassland types, commonly have a higher LAI than grasses as well as horizontally orientated leaves and are therefore able to reflect light stronger, before senescence sets in.

Asner (1998), however, found that variability in surface reflectance was dominated by any presence of standing litter in the canopy and this has been confirmed here through the results in Table 5.6, which indicates that the predominant differentiating factor between the various plots is the standing biomass. The biomass subsequently shows a moderate correlation with the non-photosynthetic fraction image (Figure 5.29(a)).

Semi-natural vegetation, including grassland, is very rarely homogenous and the smallest scales and unimodal spectral classes for various vegetation types remain therefore the exception rather than the rule. Additionally, sites can be spectrally homogenous, but vegetationally heterogeneous. This can occur either as a function of the spatial resolution of the imagery available and the 'grain' of the vegetation mosaic on the ground or the inherent spectral similarity of different plant species and can be a feature within or between sites (Jacobsen et al., 2000). Spectral similarity between various grass species is especially pronounced, due to the structural similarity between species. However, grassland communities vary greatly in composition, distribution of species and associated non-grass species occurring, factors which provide distinct identification features of different communities and

plant associations.

Jacobsen et al. (2000) suggest the production of abundance maps, that could be interpreted at the succession stages from sown improved grassland to old, species-rich, well-established and successionally mature semi-natural grassland. This could be achieved through spectral unmixing of the images, using endmembers of different management and floristic classes.

The Trawscoed and Pwllpeiran grassland plots are considered to be in a successionally 'adolescent' stage (Mike Hayes, 2006, personal communication). Most of them are still in a process of reverting from formerly improved fields similar to T1/P1 plots. As this process is considered to be ongoing, it is possible that the significance of vegetation variability will rise in the future compared to those in Table 5.9, if the management regimes were maintained and a mature and stable stage in vegetation growth and composition is reached.

Effects on image features other than management to be considered are local topography and resulting microclimates (e.g., different moisture conditions on north and south-facing slopes). Topographic formations can also be the cause of spectral artifacts, such as shadow and BRDF effects (Jacobsen et al., 2000).

These factors could play a significant factor at Pwllpeiran, where the local topography is very pronounced and would partly explain the differing results between the two sites. Orthorectification of the Pwllpeiran image using a high-resolution digital elevation model is hence desirable to improve the georegistration of the scene, as it is likely inferior to that of Trawscoed, which is located on level ground. Pwllpeiran lies approximately 200m higher above sea-level than Trawscoed and is therefore part of a biogeographically subtly different area. Due to the greater elevation, exposure and accompanying factors, such as higher winds, lower temper-

atures and likely greater precipitation, the species composition of the site differs slightly to Trawscoed (Mike Hayes, 2006, unpublished vegetation survey), with a greater predominance of grassy vegetation and a considerably lower occurrence of forb species with a high LAI and is hence more homogenous in vegetation structure. Climatic factors also directly influence vegetation productivity (Wang et al., 2001) and it is likely that the more improved plots at Pwllpeiran would reach greater levels of productivity under more favourable climatic conditions, e.g., in the lowlands.

Furthermore, Pwllpeiran is not as regularly monitored as Trawscoed, due to a more remote location and it is likely that the grazing regime is not as well maintained. On several visits to the site, sheep were found in plots which were not due to be grazed. This could further reduce the spectral distinctiveness of the individual plots at the site, especially if this had been the case over the entire period of the experimental set-up.

Finally, as discussed below, spectral variation and differences in productivity between improved and unimproved grassland types are greater in the spring than in the summer, when the images were acquired, and this could be a further contributing factor to the less conclusive results at Pwllpeiran (Goetz, 1997).

5.5.6 Scaling up of grassland diversity

The productivity of grassland canopies varies throughout the year. Figure 5.33 illustrates the different annual growth curves of improved, semi-improved and unimproved grassland types by comparing their NIR reflectance, NDVI and non-photosynthetic and photosynthetic endmember fractions throughout the growing

season. Because of their intense fertilization and resulting growth advantage, as well as their lower content of dead vegetation matter, improved grassland have a much higher NIR response in the spring than less intensively managed swards. The differences in productivity are considerably less pronounced later in the year and early spring (late March) is therefore the point of highest separability between grasslands of differing improvement and composition. This is the crucial information for identifying grasslands of lower productivity, but higher conservation interest in low-resolution multispectral images.

The classification in Chapter 6 utilizes this information in order to differentiate different grassland types.

Considering this, the CASI image used in this study was captured at an disadvantageous time of year (June/July) for spectral grassland differentiation. Had it been acquired in late March/early April, it would have probably been possible to show greater differentiation between plots of differing improvement levels. Unfortunately it was logistically impossible to capture the imagery early in the season, but this should be considered a priority in any further studies.

The additional information available from the images due to the high spatial and spectral resolution of the hyperspectral data, however, balances this limitation somewhat.

It is likely that the spectral variability at Pwllpeiran in the spring is significant enough to differentiate between the treatment types.

5.6   Summary

This chapter has demonstrated the levels variability between grassland of various improvement levels according to spectral reflectance, biomass and vegetation cover. Empirical relationships between ecological parameters, such as biomass and species composition and spectral data and derived image products were also demonstrated.

Grassland types with different levels of agricultural improvement and hence different species compositions and sward structures were best differentiated based on the percentage of Red-edge reflectance followed by the ratio of non-photosynthetic material in the vegetation canopy.

The results of these analyses were related to the classification rule-base developed in Chapter 6 and used to inform the formulation of grassland specific rules, e.g., using the proportion of non-photosynthetic plant material within the sward to determine the level of agricultural improvement.

The following rules used information gained from the study in this chapter (Table 5.11):

Table 5.11: Grassland rules for discrimination within multispectral satellite data

Rule	Formula	Grassland habitats
1. NIR:Red (summer)	ρ_n/ρ_r	J. squarrosus/N. stricta (upland) grasslands
2. NIR-SWIR (spring)	$\rho_n - \rho_s$	Unimproved lowland grasslands
3. NIR-SWIR (summer)	$\rho_n - \rho_s$	N stricta/F. ovina (upland) grasslands
4. Red reflectance	$\rho_{r(spring)} - \rho_{r(summer)}$	F. ovina unimproved upland grasslands
5. NDVI	$NDVI_{spring} - NDVI_{summer}$	N. stricta/F. ovina unimproved upland grasslands
6. NIR (summer) & green (summer)	$\rho_{n(spring)} + \rho_{g(summer)}$	Improved grasslands (uplands)
7. Red/SWIR*SWIR (summer)	$\frac{\rho_r - \rho_s}{\rho_r + (\rho_s^2)}$	Lowland semi-improved grasslands

Chapter 6

Habitat mapping from multispectral data

6.1   Introduction

This chapter evaluates the use of spaceborne multispectral data for discriminating and mapping semi-natural habitats, with particular emphasis on different woodland types at the Lake Vyrnwy study site and grassland improvement levels in west Ceredigion. The chapter builds on the outcomes of Chapter 5 and is undertaken in preparation for Chapters 7 and 8. The chapter is structured as follows:

Sections 6.2.1 and 6.2.2 focus on the availability and pre-processing of multispectral data acquired by the TERRA-1 ASTER, IRS P6 and SPOT HRG sensors. These sensors were selected over the Landsat series because of their better spatial resolution. Temporally distinct combinations of these sensors were used to better capture the seasonal variability in the spectral reflectance of vegetation,

173

particularly given the persistent cloud cover occurring in the region.

Section 6.2.4 then outlines the approach to the segmentation of the landscape using the higher resolution SPOT data. Following this, Section 6.2.6 describes the development of a rule-based approach within Definiens software for classifying the landscape using combinations of the earth observation data. The outputs of the habitat classification for the Lake Vyrnwy and west Ceredigion areas are then illustrated in Section 6.3. The accuracy of the Lake Vyrnwy classification is further detailed in Section 6.3.2.

Finally, the results are discussed in Section 6.4 and put into context in relation to other land cover mapping schemes currently being undertaken in the UK.

Combining ecological knowledge and information from remotely sensed data into a rule-based classification method, Lucas et al. (2006b) suggested that remote sensing data could potentially be applied within an ongoing and continuously updatable habitat mapping and monitoring program. Such a method could subsequently be utilized to obtain urgently required information on the ecological implications of vegetation transformation attributed to both human interference and climate change.

6.2 Methods of data analysis

6.2.1 Available satellite sensor imagery

For the mapping of habitats, data acquired by the SPOT-5 High Resolution Geometric (HRG), Terra-1 Advanced Spaceborne Thermal Emission and Reflection Radiometer (ASTER) and Indian Remote Sensing Satellite (IRS) LISS 4 (P6) sen-

Table 6.1: Available Satellite Imagery for Lake Vyrnwy and west Ceredigion

Sensor	Date	Site
SPOT 5 HRG	27.03.03	Lake Vyrnwy
SPOT 5 HRG	22.03.03	Lake Vyrnwy
ASTER	07.04.06	Lake Vyrnwy
IRS LISS IV	13.07.06	Lake Vyrwny
SPOT 5 HRG	27.03.03	Ceredigion
IRS LISS IV	13.07.06	Ceredigion

sors were used (see Table 6.1 for a complete list of scenes and Appendix A.2 for a description of the sensors used). The images chosen were the best, i.e.; cloud free, available for a three year period between spring 2003 and summer 2006. Scenes outside of this time window were not considered, as it was found that land cover change was too great after three years as to enable a consistent classification.

There are two spring March SPOT 5 HRG scenes which cover the area of interest around Lake Vyrwny (Figure 4.2), though neither the whole area alone. The 27.03.03 scene was used wherever possible, with the image from the 22.03.03 substituted over the eastern part of the classification area. Where scattered cloud is found on the primary SPOT scene (Figure 4.2(a)), the second SPOT scene was used if an overlap existed. In the north-west area of the classification the ASTER scene was then utilized in the rule-set, where neither SPOT image could be used. As the two SPOT-5 HRG scenes were acquired only five days apart (see Table 6.1), under similar atmospheric conditions, it was possible to create a seamless classification.

For Ceredigion only one IRS and SPOT scene were available respectively (Figure 6.1). However, as they both provide cloud-free, complete coverage and were acquired at the optimal time for habitat differentiation, i.e., late spring (March)

(a) 27.03.03 SPOT-5 HRG   (b) 13.07.06 IRS LISS IV
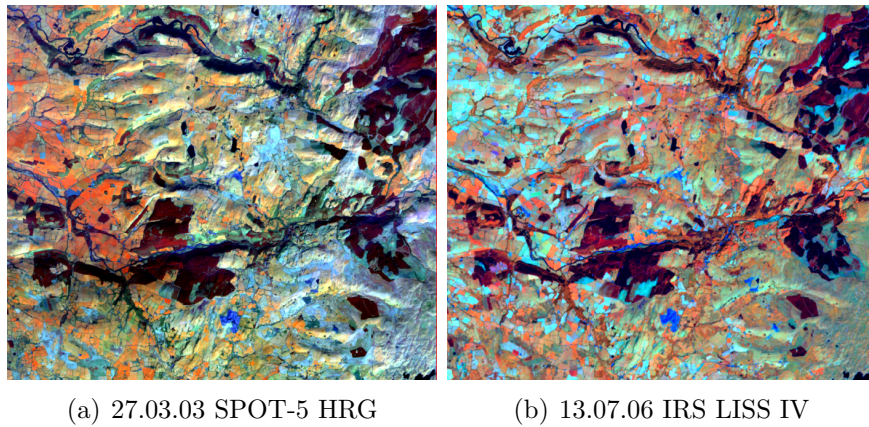
Figure 6.1: Multispectral Satellite imagery over the Ceredigion study sites

and mid-summer (July), they are sufficient.

The shadowing effects of topography can be clearly seen in the Ceredigion SPOT scene (Figure 6.1(a), though they are diminished by topographic correction (Section 4.1.1).

Within spaceborne remote sensing data, regional variability in the phenology and dynamics of vegetation was evident, even when acquired on the same date. For example, an IRS scene acquired in May 2007 revealed extensive stands of bracken emerging in the south but not yet in the north of Wales as a result of a shorter growing season with a later start date.

This study focused on two areas around Lake Vyrnwy and in Ceredigion, which are highlighted grey in Figure 6.2. Each classification area is approximately 12km^2 in size.
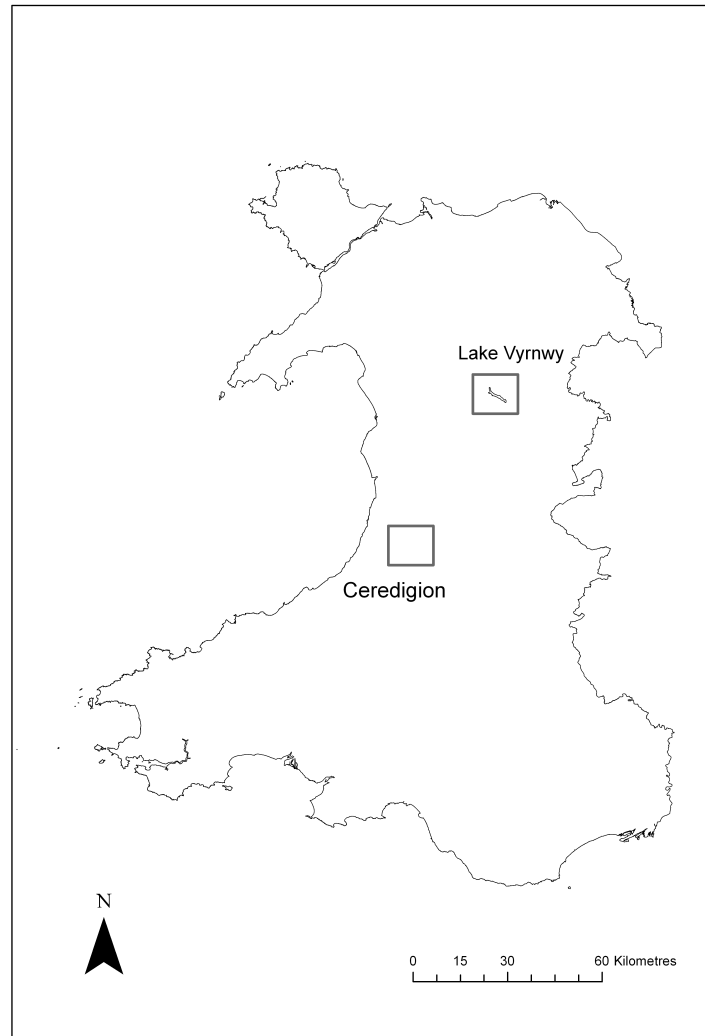
Figure 6.2: The classification project areas for this study are outlined around Lake Vyrnwy and in Ceredigion

6.2.2 Image pre-processing

Prior to mapping, a range of pre-processing was necessary to allow integration of the available satellite sensor data. Separate procedures were implemented for the SPOT, IRS and ASTER data and focused primarily on radiance calibration, atmospheric correction and orthorectification, as well as the correction of topographic shadowing. All images were orthorectified using 10 m spatial resolution NextMap Britain Digital Elevation Model (DEM) as a topographic reference. Between 1 (ASTER) and 20 (SPOT, IRS) ground control points were used for each image registration, with these extracted from a 2006 true colour aerial photograph mosaic (see Appendix A.2.1) of Wales.

All satellite sensor data, regardless of their original spatial resolution, were resampled to 5m resolution using a nearest neighbour resampling algorithm. Atmospheric correction was undertaken to provide image data in units of surface reflectance (%), thereby allowing comparison of images acquired on different dates, from different sensors, and also over different regions. Topographic correction of the data was undertaken using ATCOR 3 software to minimize differences in reflectance as a function of slope and aspect, although the procedures were only successful when applied to images acquired in the spring or autumn months, where strong shadowing occurred due to low seasonal sun angles.

Following atmospheric and topographic correction, a number of image products were derived, including:

- Estimates of the relative amount (fractions) of shade/moisture, photosynthetic (green) vegetation (PV) and non-photosynthetic (dead/senescent; NPV) vegetation.

- Vegetation indices, including the Normalised Difference Vegetation Index (NDVI; derived from visible red and near infrared bands).

Cloud and cloud shadow screening was undertaken using procedures developed by Definiens AG. For each image, the algorithm was used to generate cloud masks that were used either to indicate where a classification was unable to be undertaken or where the classification might be less reliable.

All image pre-processing procedures and the generation of the fractional images and the NDVI outlined above are described in detail in Section 4.1.1.

6.2.3   Thematic layers

Following processing, the images were stacked within Definiens Developer software in preparation for segmentation and classification.

Additional thematic layers representing infrastructure (roads and buildings), water, the coast, Land Parcel Information System (LPIS) boundaries and also elevation, slope and aspect (as derived from NextMap Britain Digital Elevation Model (DEM) data) were included. As the visible (green and red), near infrared and shortwave infrared bands were common to all sensor data, only these wavelengths were used in the classification.

Digital soil maps were investigated for inclusion in the classification but none were found to be of sufficient spatial resolution.

Table 6.2: Thematic layers utilized in the land cover classification

Layer	Origin	Use
Urban	OS MasterMap	Exclusion of buildings and roads from the classification
Water	OS MasterMap	Exclusion of permanent water features from the classification
LPIS	WAG	Field delineation
Elevation	NextMap Britain	Distinction of lowlands and uplands
Slope	NextMap Britain	Exclusion of habitats not occurring on slopes, e.g., blanket bog
Aspect	NextMap Britain	Identification of shadowed north slopes

6.2.4 Image segmentation

The segmentation and classification processes were necessarily developed using subsets (training areas) of each project, as the software can only process each project completely during a tiling procedure, with the tile size set at 500x500 pixels (1 pixel = 5m x 5m = 25m^2).

Initial segmentation of the images into objects was undertaken within Definiens Developer software and differed depending on whether the landscape was enclosed (e.g., by hedges or within the LPIS boundaries) or pre-classified as urban, water, arable, coastal, upland or lowland (e.g., as determined by elevation thresholds or overlap with the relevant thematic layer (Table 6.2)). The objects varied in size from individual pixels to entire fields, the extent of which was determined from the LPIS thematic layer. The segmented image was then duplicated to form a layer above (hereafter referred to as the super-level) and below (sub-level) the original layer (Level 1, Figure 6.3).

In the super-level, segments were redefined using the Land Parcel Information

Service (LPIS) vector layer and were typically larger compared to Level 1, although the same boundaries were maintained, where these were common to both layers. Many of the segments were equivalent in size to the fields defined using the LPIS. The sub-level was segmented such that objects were of the size of one pixel each (i.e., $25m^2$). In both projects, the segmentation was undertaken using the image values themselves and the SPOT 5 HRG data were used in preference to others because of the greater spatial resolution.
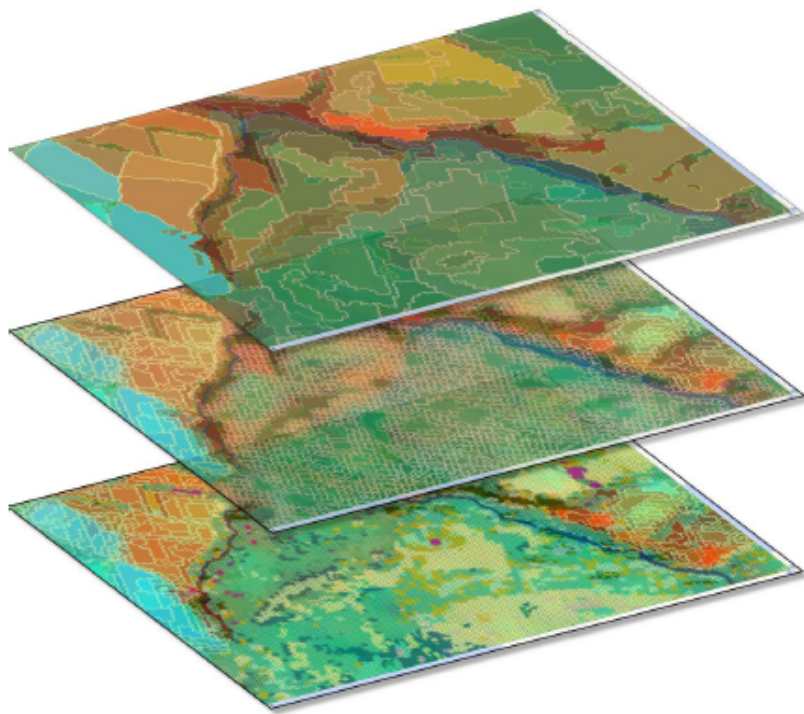
Figure 6.3: Image segmentation on three levels

6.2.5   Class selection and definition

The Phase 1 Habitat Survey defines 10 broad types of habitats (lettered A to J; Table 6.3) and within these, over a 100 different habitats are described (JNCC

(2003), Section A.5).

Table 6.3: Broad Phase I habitats defined for Wales

Code	Description
A	Woodlands
B	Grasslands
C	Tall herb and fern
D	Heathland
E	Mire
F	Swamp, marginal and inundation vegetation
G	Open water
H	Coastal land
I	Rock exposure and waste
J	Miscellaneous

A more detailed classification of habitats than listed in Table 6.3, but often distinct from the 80 Phase 1 sub-classes was undertaken for the following reasons:

1. The 80 Phase 1 habitat classes have been found to be often insufficient in detail for many ecological applications (e.g., for the assessment of biodiversity in the landscape).

2. Many Phase 1 habitats cannot be mapped directly from remote sensing data as a single class, because they represent a number of sub-habitats. However, the subhabitats themselves may be spectrally distinct,because of differences in phenology and structure and able to be discriminated from remote sensing data.

As indicated by Fuller et al. (2005a), the definitions of habitats can be too broad or variable to be extracted from remote sensing data in a single class. A number of Phase I habitats are associated with a single species (e.g., bracken (C1.1)) and are extensive and hence well-suited to classification.

However, a greater number are comprised of a mix of species, either occurring

within the same community or as discrete and separate communities. For example, Bilberry (*Vaccinium myrtillus*) and Ling heather (*Calluna vulgaris*) often occur together and are both constituents of the Phase I class Dry Dwarf Shrub Heath (D1) whilst Larch (*Larix decidua*) and Sitka Spruce (*Picea sitchensis*) commonly occur separately (and often in discrete homogeneous stands) but are still referred to jointly as coniferous woodland (A1.2). Another example is scrub (A2), which combines wet willow, gorse and hawthorn scrub, amongst others, into the same class.

Therefore, any attempt at mapping Phase I classes from remote sensing data needs to either combine maps of these different species based on relative proportions or commonalities in the grouping of species.

The composition and dynamics of habitats also varies as a function of, for example, seasonality and the physical environment. Between and even within biogeographical zones (Figure 3.4), several habitat classes can vary with regard to their timing of leafing, flowering and senescence, but also in their overall structural and species composition. For example, in the north of Wales and particularly on colder north-facing slopes, bracken fronds appear later in the year compared to southern zones and south-facing slopes. Across the country, broadleaved woodlands are often dominated by different species (e.g., Rowan (*Sorbus aucuparia*) or Sessile Oak (*Quercus petraea*)), depending on whether they occur in the uplands or lowlands or on different geological substrata. As the reflectance of vegetation varies as a function of the response of vegetation to environmental factors, consideration of this variability is a pre-requisite to mapping.

Given the seasonal phenology of plant species in Wales, the development of a new

approach to mapping necessarily required the use of satellite sensor data acquired at different points in the growing season. A spring and summer image respectively allowed the exploitation of maximum differences within and between vegetation types, e.g., between coniferous and broadleaved trees before leafing in the spring or large seasonal changes in productivity and reflectance, due to growth or senescense, such as in bracken (*Pteridium aquilinum*) stands.

Consideration also needed to be given to the different phenological and growth responses of plant communities to the physical environment, such as elevation, geology, soils, slope and aspect (Yeo and Blackstock, 2002). Understanding this seasonal and geographical variability in appearance of habitats is a prerequisite to mapping from reflectance data and derived measures.

6.2.6   Classification of land cover and vegetation communities

The classification of habitats was undertaken in Definiens eCognition software (Definiens, 2008), which allows the formulation of a knowledge based rule-set to classify imagery.

Rules that were based on thresholds of reflectance data or derived layers were applied progressively in a defined hierarchy described in nine steps below. For this purpose, a large number of additional image-based indices were developed which assisted the discrimination. They are listed in Table 6.5, together with the habitat classes which they differentiate. Table 6.4 further lists the single channel data which has been used to distinguish habitats and the key habitats they were used for.

Table 6.4: Single channel data used for classifying land cover classes within the rule-based classification

Channel	Key habitats
1. Green (summer)	Broadleaved woodland, lowland wet heath, uplands bogs and dry heath (*Calluna*-dominated)
2. Red (summer)	Non-vegetation, ploughed fields, felled coniferous forest, *Molinia*-dominated marshy grasslands in lowlands and uplands
3. NIR (summer)	Water, bracken, hedgerows, improved grassland
4. SWIR (summer)	Bracken, coniferous forest, improved grasslands, lowland mires and fens. *F. ovina* upland unimproved grasslands.
5. Green (spring)	Broadleaved woodland, hedgerows, lowland marshy grasslands (*Juncus*-dominated), rock
6. Red (spring)	Water, lowland mires and fens, lowland scrub, *Juncus*-dominated marshy grasslands upland heaths (*Calluna*-dominated)
7. NIR (spring)	Water, improved grasslands, *F. ovina* upland unimproved grasslands, rock
8. SWIR (spring)	Water, coniferous forests, *Molinia*-dominated marshy grasslands in lowlands and uplands, unimproved grasslands in lowlands. *N. stricta/F. ovina* upland unimproved grasslands
9. Shade (spring)	*Ulex* and other scrub

10. PV (spring)	Bare ground, semi-improved upland and lowland grasslands
11. NPV (spring)	Lowland wet heath, upland bogs and dry heaths (*Calluna*-dominated)
12. Shade (summer)	Rock features, coniferous forest
13. PV (summer)	Bracken, semi-improved lowland and upland grasslands.
14. NPV (summer)	Bare ground
15. Elevation	Bracken, coniferous forest, coastal habitats
16. Slope	Bracken, coniferous forest, *Molinia*-dominated marshy grasslands in lowlands and uplands, lowland mires and fens and wet heath, bog (*Eriophorum*-dominated and unmodified)

Table 6.5: Indices used for classifying land cover classes within the rule-based classification and based on reflectance (ρ) in the green (g), red (r), near infrared (n) or shortwave infrared (s) wavelength regions

Index	Formula	Key habitats
		Standard Indices
17. NDVI (spring)	$\frac{\rho_n - \rho_r}{\rho_n + \rho_r}$	Lowland scrub, upland marshy grasslands (*Juncus*-dominated), improved grasslands (uplands).
18. NDVI (summer)	$\frac{\rho_n - \rho_r}{\rho_n + \rho_r}$	Lowland flushes and marshy grasslands, gorse and improved grasslands, Broad-leaved woodland and larch plantations. Acid flushes, non-vegetation, unmodified bogs (*Eriophorum* dominated), dry heath (*Calluna*-dominated)
		Band ratios
19. Green:SWIR (summer)	ρ_g/ρ_s	Broadleaved woodland, rock
20. NIR:Red (summer)	ρ_n/ρ_r	*J. squarrosus* and *N. stricta* (upland) grasslands
21. NIR:Green (summer)	ρ_n/ρ_g	Rock features
22. Red:SWIR (summer)	ρ_r/ρ_s	Rock features

Index	Formula	Key habitats
Band differences and products		
23. NIR-SWIR (spring)	$\rho_n - \rho_s$	Unimproved lowland grasslands
24. NIR-SWIR (summer)	$\rho_n - \rho_s$	*N stricta* and *F. ovina* (upland) grasslands
25. SWIR-NIR (summer)	$\rho_s - \rho_n$	Wet bog with *Eriophorum sp.*
26. SWIR-NIR (ASTER)	$\rho_s - \rho_n$	*Sphagnum bog*, coniferous forest
27. SWIR-Green (ASTER)	$\rho_s - \rho_g$	Coniferous forest
28. NIR*GREEN	$\rho_n * \rho_g$	Gorse and other isolated or contrasting patches of vegetation, hedgerows
29. NPV-PV fraction (spring)	$NPV - PV$	Hedgerows
30. Normalized seasonal red difference	$\frac{\rho_{r(spring)} - \rho_{r(summer)}}{\rho_{r(spring)} + \rho_{r(summer)}}$	Gorse and other isolated or contrasting patches of vegetation, hedgerows
Relative difference to neighbours		
31. NIR reflectance (summer)	$\frac{\sum_{i=1}^{n} \rho n - \rho ni}{n}$	Gorse *Ulex* and other isolated contrasting patches of vegetation, hedgerows
32. Green reflectance (summer)	$\frac{\sum_{i=1}^{n} \rho g - \rho g_i}{n}$	Hedgerows

Index	Formula	Key habitats
33. SWIR (spring)	$\frac{\sum_{i=1}^{n} \rho s - \rho s_i}{n}$	*Juncus*-dominated upland marshy grasslands
	Seasonal difference images	
34. Green difference	$\rho_{g(spring)} - \rho_{g(summer)}$	*Juncus* flushes
35. Red difference	$\rho_{r(spring)} - \rho_{r(summer)}$	*F. ovina* upland unimproved grasslands, *Ulex* scrub.
36. NIR difference	$\rho_{n(summer)} - \rho_{n(spring)}$	*F. ovina* grasslands with bracken, hedgerows
37. SWIR difference	$\rho_{s(summer)} - \rho_{s(spring)}$	Lowland mires and fens, felled woodlands
38. NDVI difference	$NDVI_{spring} - NDVI_{summer}$	*N. stricta/F. ovina* grasslands, unimproved grasslands, felled woodland
39. PV fraction difference	$PV_{pv(summer)} - PV_{pv(spring)}$	*M. caerulea* grasslands (lowland/upland), bracken, mature *Calluna*
40. NPV fraction difference	$NPV_{npv(summer)} - NPV_{npv(spring)}$	*Larix decidua* forests
41. Green difference/SWIR difference	$\frac{\rho_{g(spring)} - \rho_{g(summer)}}{\rho_{s(spring)} - \rho_{s(summer)}}$	Hedgerows, *Juncus squarrosus* and *Nardus stricta* grasslands, gorse clusters
42. NIR (spring) + Green (summer)	$\rho_{n(spring)} + \rho_{g(summer)}$	Improved grasslands (uplands)

Index	Formula	Key habitats
43. NIR (spring) + SWIR (spring)	$\rho_{n(spring)} + \rho_{s(summer)}$	*N. stricta* upland unimproved grasslands.
Other indices		
44. Spring	$\frac{\rho_r - \rho_s}{\rho_r + (\rho_s * \rho_r)}$	Hedgerows, Larch
45. Summer	$\frac{\rho_r - \rho_s}{\rho_r + (\rho_s * \rho_r)}$	Lowland mires and fens and *F. ovina* grasslands (steep slopes, lowlands and uplands) Unmodified bogs (*Eriophorum*-dominated), dense scrub and broadleaved woodland, Dry heath (*Vaccinium* dominated)
46. Spring	$\frac{\rho_r - \rho_s}{\rho_r + (\rho_s^2)}$	Lowland semi-improved grasslands
47. Summer	$\frac{\rho_r - \rho_s}{\rho_r + (\rho_s^2)}$	Lowland semi-improved grasslands
48. Red/SWIR*Green (summer)	$\frac{\rho_r - \rho_s}{\rho_r + (\rho_s * \rho g)}$	*Vaccinium*-dominated dry heath
49. Spring	$\rho_n * \rho_g$	Hedgerows, broadleaved woodland, gorse, Lowland/ upland marshy grasslands (*Juncus*-dominated), upland dry heath (*Calluna*-dominated), *F. ovina* upland unimproved grasslands

Index	Formula	Key habitats
50. Heath detection	$\frac{\rho_s - \rho_r * \rho_n}{100}$	Lowland gorse and scrub
51. Gorse detection	$\frac{\rho_{g(spring)} - \rho_{g(summer)}}{\rho_{s(summer)} - \rho_{s(spring)}}$	Gorse *Ulex*

Indices in Table 6.5 are based on SPOT-5 HRG spring (March) and IRS summer (July) images, as listed in Table 6.1.

Rules were developed initially to discriminate and map the distribution of different land covers (e.g., forest, grasslands and heath) or dominant species within vegetation communities (e.g., Purple Moor Grass (*Molinia caerulea*), Ling Heather (*Calluna vulgaris*) or rushes (*Juncus spp.*), comprising many of the Phase I habitats. In each case, rules were based on ecological knowledge with regard to, for example, relative differences in moisture content, surface roughness, woody biomass or productivity, and the manifestation of these within remotely sensed data.

Rules were developed sequentially and applied separately within each of the three separate levels, according to the scale appropriate to the respective land cover class, and the resulting classification was subsequently transferred to the level above or below. As an example, arable croplands were classified at the super-level using objects approximating the size of fields (Figure 6.3). The classification was then transferred to objects created on the lower levels. All woodland types were classified within Level 1 and their classification was then transferred to objects in the sub-level.

6.2.7 Classification steps and workflow

The classification was applied progressively within 9 stages focusing first on man-made infrastructure, other non-vegetated areas and forests and then on lowlands and upland habitats. The classification is based on optimized rules combined from the indices listed in Table 6.5 and specifically calibrated for each class. The individual steps of the calibration process are described in detail below and also

summarized in the flowchart in Figure 6.4.

Stage and level	Classification action	Knowledge source for rule base
Step 1 (Level1)	Classification of water bodies, built-up area and roads	OS Mastermap
Step 2 (Level1)	Identification and separation of uplands and lowlands	Elevation data from NextMap DEM
Step 3 (Level1)	Classification of non-vegetated areas	NDVI, visible reflectance and shade fraction from image data
Step 4 (Sub-level)	Classification of bracken	Seasonal PV and NIR differential in the image data
Step 5 (Level1)	Classification of woodlands and scrub	SWIR, NIR, Red and Green image bands, NPV and NDVI differential
Step 6 (Sub-level)	Classification of hedgerows	Object reflectance contrast, spring green/summer NIR differential
Step 7 (Super-level)	Classification of arable and improved land	Spring NIR, NIR and NDVI seasonal differential
Step 8/9 (Sub-level)	Classification of lowland and Upland semi-natural habitats	Image data (detailed bands and indices listed in Tables 6.4 +6.5)

Figure 6.4: Flowchart of individual classification steps undertaken on the three different levels to create the land cover classification

Step 1: Water bodies, urban areas and infrastructure were mapped with reference to the OS Mastermap layers such that recognizable features that constituted the framework on the landscape were accurately represented.

Step 2: Upland and lowland areas were differentiated on the basis of elevation. Areas that were enclosed (or otherwise) were defined with reference to the LPIS boundaries.

Step 3: Non-vegetated areas were classified using the image data themselves and primarily the NDVI, visible reflectance and shade fraction data, e.g., large spoil

features. Adjacent objects of the same class were merged to create larger fused objects.

Step 4: The extent of bracken was primarily defined by considering differences in PV fraction and NIR reflectance between the spring and summer periods. Separate modified rules were also developed to account for differences in the timing and appearance of bracken growing on north and steep facing slopes.

All bracken rules were applied to unclassified objects in the lowlands and uplands.

Step 5: Woodlands (including areas of felled plantations) were defined using reflectance data and region-growing processes from core areas. Coniferous forests (plantations) were largely confined to areas outside of the LPIS and exhibited lower SWIR reflectance in the spring and summer months. Separate rules were developed for *Larix decidua* (European Larch) because of the deciduous nature of this tree species, with these based largely on differences in the NPV fraction between the spring and summer imagery.

Felled woodlands exhibited greatest differences in the red, NDVI and SWIR bands between dates of satellite data acquisition. Where woodlands had been felled previous to data acquisitions, these exhibited low summer NDVI and red reflectance values and were often in proximity to existing woodlands. Broadleaved woodlands typically exhibited a low green reflectance in both spring and summer and occurred primarily outside of the LPIS. Similar rules to broadleaved woodland, but with lower thresholds, were applied to map dense scrub.

Within the woodland classes a small number of single-species broadleaved and coniferous classes were subsequently distinguished at Lake Vyrnwy.

Step 6: Hedgerows were identified largely by exploiting the contrast in reflectance

with surrounding open fields, particularly the relative difference in visible green in spring or NIR in summer. Subsequent rules were implemented to allow objects to grow the hedgerows along the field boundaries.

Step 7: Agricultural land was identified by classifying the larger objects contained within the upper layer first as either ploughed, harvested, mown or grazed fields. The classes were then merged and transferred to the smaller objects contained in the layers below. As many of these objects had already been classified previously (e.g., as bracken or woodland), the transfer was only applied to those classes that had not been assigned a habitat class previously. All areas remaining unclassified were then assigned to an umbrella class representing semi-natural habitats.

Steps 8 - 9: Lowland and upland habitats (including, e.g., heaths, bogs, semi- and unimproved grasslands) were classified using fuzzy membership functions (defined primarily on the basis of the remote sensing data, (Benz et al., 2003)) in a single simultaneous classification step for all lowland and upland habitats respectively.
The rules were applied separately for habitats occurring in both the lowlands and uplands (e.g., heaths and semi-improved grasslands).

Once developed, the segmentation and classification processes were evaluated on other subsets taken from different parts of the project areas and then refined where needed. This process required several iterations as rules used to discriminate habitats in one part of the project area were often found to lead to confusion in other parts, particularly where additional habitats occurred. Once developed, the final process was then applied to the entire image area using Definiens Developer workspace and server engines, which use a tiling and stitching process to apply the ruleset to the entire project area.

6.3 Results

This section is divided as follows:

Section 6.3.1 shows the two classifications for the Lake Vyrnwy (Figure 6.5) and east Ceredigion (Figure 6.6) study sites, with a full colour legend in Figure 6.7. Table 6.6 lists all habitat classes occurring in the two maps and gives a description of each with regards to predominant species, location (e.g., upland/lowland) and other characteristics, such as age or structure, if appropriate.

Section 6.3.2 then outlines the results of a rigorous accuracy assessment of the Lake Vyrnwy classification.

6.3.1 Habitat classifications

Table 6.6: Lake Vyrwny and Ceredigion habitat classes

Classname	Description
Acid flush	Wet flushes on upland grassland slopes,
Arable	Land under arable cultivation
Ash gulleys	*Sorbus aucuparia* along stream gulleys in the uplands
BareGround	All non-vegetated, non-urban surfaces
BirchAsh wood	*Betulus penduala* and *Sorbus aucuparia* stands on steep hillsides in the uplands
Bog_OldCv	Blanket Bog with mature, continuous *Calluna vulgaris* cover
Bog_youngCv	Blanket Bog with scattered or young *Calluna vulgaris* cover

Bracken	Dense, continuous stands of bracken
Broadleaved	All broadleaved woodland not classified by species
Coniferous Plantation	All coniferous woodland not classified by species
Cv_cont_old	Mature *Calluna vulgaris* or very dense younger stands which form complete ground cover
Cv_Et_Short	Mixed *Calluna vulgaris* and *Erica tetralix* stands
Douglas Fir	*Pseudotsuga douglasii* single species plantation
Et_Mc_Cv_wet	Wet heath vegetation with *Molinia caerulea,,* *Erica tetralix* and *Juncus sqarrosus*
Felled woodland	Felled Coniferous Plantation (pre and post 2003)
Fo_At_grass	Dry *Festuca ovina/Agrostis spp.* upland grassland
Fo_Ns_moss	Dry banks with frequent *Polytrichum spp.* carpet amongst the fescue and some *Nardus stricta*
Hedge	All hedges below enclosure line
I_upland	Improved acid grassland in the uplands above the LPIS boundary
Je_flush	Wet *Juncus spp.* dominated flushes in the uplands
Jsq_Ns_grass	Wet acid grasslands in the uplands dominated by *Nardus stricta* and *Juncus spp.*, relatively unproductive
Larch	*Larix europaeus* plantations
LowL_I	Intensively improved pasture in the lowlands, mostly dominated by *Lolium perenne*

LowL_Je_flush	Lowland *Juncus spp.* flushes and marshy grassland
LowL_SI_acid	Lowland semi-improved grasslands
Mature Oak	Semi-ancient, species-rich *Quercus petraea* woodland, grazed or ungrazed
Mature Spruce	Core of conifer plantations and mature stands (usually Sitka Spruce (*Picea sitchensis*))
Mc_upland	Dense *Molinia caerulea* grassland, complete ground cover
Ns_Fo_grass	Less productive acid grassland, with more dead matter but still dry - looking like Nardus dominated grassland
Scattered scrub (gorse)	Gorse scrub close to bracken
Scattered scrub (trees)	Hawthorn/Blackthorn scrub and other young broadleaved woodland
SI_acid_upld	Semi-improved (mostly by grazing) upland acid grassland
Sph_bog	*Sphagnum spp.* dominated blanket bog
Ue_scrub	Gorse scrub
Urban	All man-made surfaces
Water	All waterbodies visible to sensor or recorded in OS Mastermap
Wet woodland and Scrub	Willow carr or alder on very wet

	or periodically flooded terrain
Young Spruce	Younger, less dense plantations and plantation
	edges with wind damage (usually *Picea sitchensis*)

Figure 6.5 is the detailed habitat classification of the area of interest around Lake Vyrnwy. At the bottom right hand corner of the map a small part is missing, where no cloud free imagery was available.

The map shows the Lake surrounded by commercial Spruce plantations (dark green, Figure 6.7) and a number of small stands of mature oak, ash and birch woodlands, as well as larch and Douglas Fir. There are large areas of recently felled conifer plantations (grey), both in the southern as well as the eastern part of the image.

The only agriculturally managed land of the area is to the east of the image, in the lower lying regions. The network of hedges can be clearly distinguished.

From the lake the land rises steeply to the upland stretches of the Berwyn Mountains. Bracken (light-orange) and *Molinia* grassland (turquoise) are found in extensive stands in the upland fringes. The upland plateaus are completely dominated by a combination of blanket bog and large areas of *Calluna vulgaris* heath (pink and dark purple). Semi-improved and unimproved grasslands (light yellow) are found mostly in the western part of the map, at a lower elevation than and at fringes of the upland heath and bog complex.

Figure 6.6 shows a habitat classification for the predominantly lowland region between the Trawscoed and Pwllpeiran grassland studysites (highlighted in red) examined in detail in Chapter 5. Both sites are, on this scale, correctly classified as lowland and upland semi-improved grassland respectively.

The eastern part of this map shows some extensive areas of semi- and unimproved
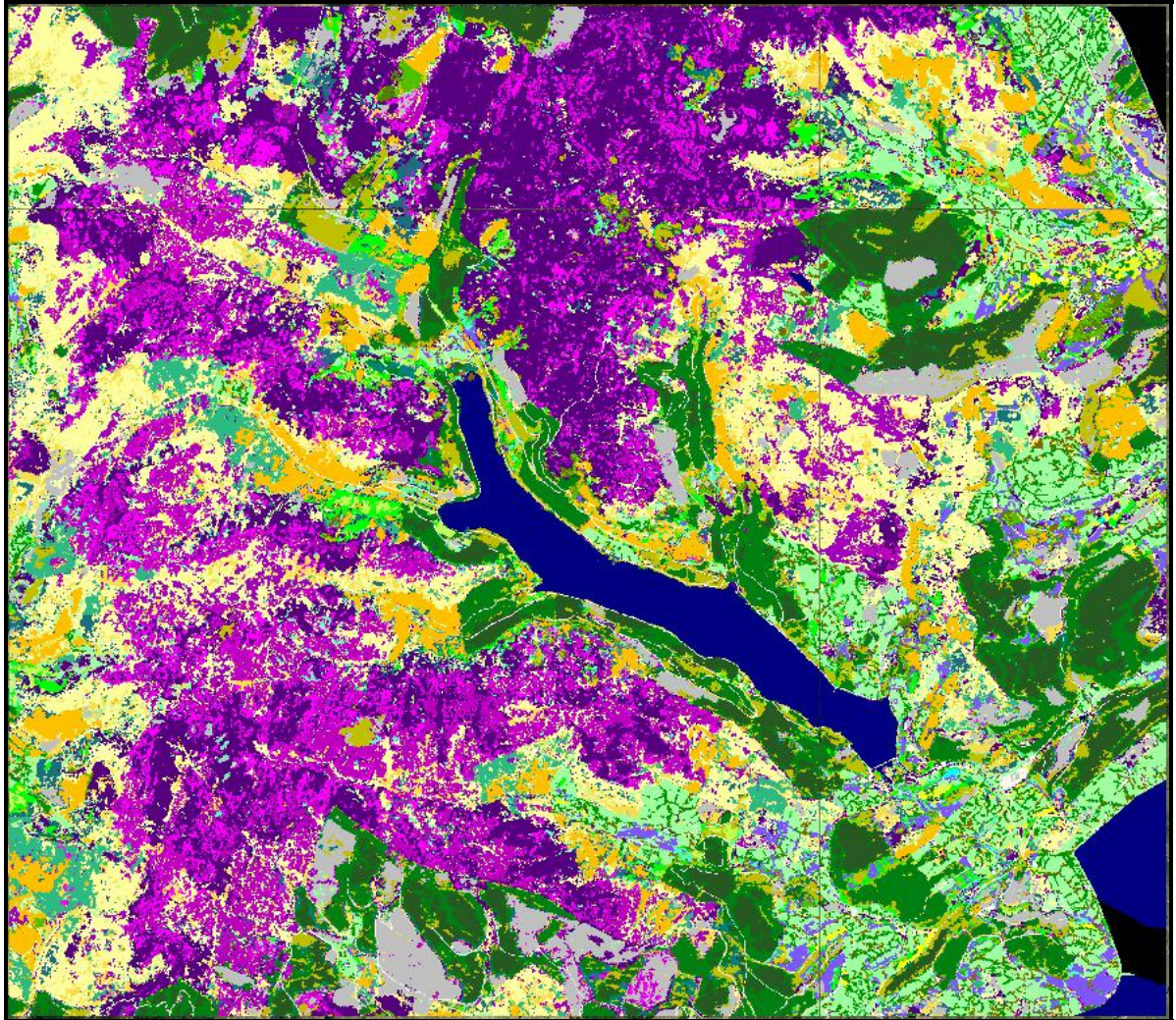
Figure 6.5: Classification of forests, grasslands, lowland and upland habitat types around Lake Vyrnwy (A colour key to the classes is provided in Figure 6.7)
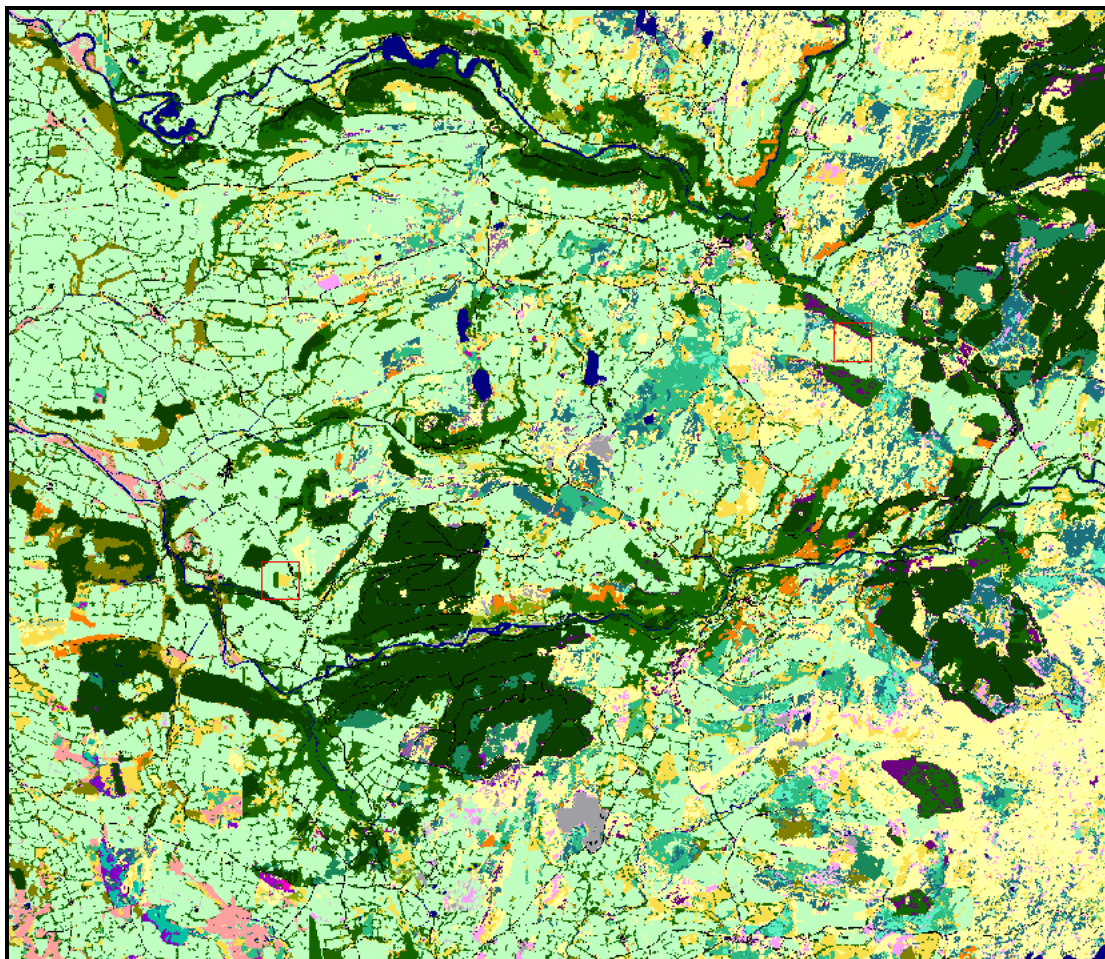
Figure 6.6: Classification of grasslands, lowland and upland habitat types in east Ceredigion. (A colour key to the classes is provided in Figure 6.7.) The Trawscoed and Pwllpeiran grassland study sites (Chapter 3) are outlined in red.

upland grasslands, with some areas of *Molinia* and *Juncus spp.* dominated marshy grasslands on the upland fringes. The majority of the area is, however, classified as improved grassland, with an increase in connected hedges towards the west. Other features of interest are the broadleaved woodlands, which are spread along rivers descending from the uplands and an area of lowland bog (light pink) in the south western corner of the map.

6.3.2 Lake Vyrnwy classification accuracy

If classification-based maps are used in decision making processes, such as policy development and resources management, a measure of their accuracy has to be given, so as to establish the degree of confidence with which these thematic maps can be used (Stehman and Czaplewski, 1998).

The accuracy of the Vyrnwy classification only was assessed by creating an error matrix (see Table 6.7 for results) and using this to calculate the overall, as well as the user's and producer's accuracy. These are standard methods for the accuracy assessment of remote sensing classifications (Story and Congalton, 1986; Congalton, 1991).

For the error matrix a 100 x 100m grid was superimposed on the classification, creating 9000 points at which the predicted habitat class was visually compared to 2006 Vexcel 1m resolution aerial photography. Each point was exactly located in the centre of a pixel, which is also the Minimum Mapping Unit (MMU) of $25m^2$, to ensure association with only one predicted class.

It is important though to remember that the images were not pan-sharpened after orthorectification, but simply re-sampled to 5m square pixels, using a nearest-neighbour algorithm. This means that the during a per-pixel classification the

- Acid_flush
- Arable
- Ash gulleys
- BareGround
- BirchAsh wood
- Bog_OldCv
- Bog_youngCv
- Bracken
- Broadleaved
- Coniferous Plantation
- Cv_cont_old
- Cv_Et_Short
- Douglas Fir
- Et_Mc_Cv_wet
- Felled woodland
- Fo_At_grass
- Fo_Ns_moss
- Hedge
- I_upland
- Je_flush
- Jsq_Ns_grass
- Larch
- LowL_I
- LowL_Je_flush
- LowL_SI_acid
- Mature Oak
- Mature Spruce
- Mc_upland
- Ns_Fo_grass
- Scattered scrub (gorse)
- Scattered scrub (trees)
- SI_acid_upld
- Sph_bog
- Ue_scrub
- Urban
- Water
- Wet woodland and Scrub
- Young Spruce

Figure 6.7: Class legend

effective MMU is still 100m^2. However, due to the segmentation approach employed here, the four quarters of any original 100m^2 pixel can be apportioned to different objects and there exists therefore a possibility that they would be classified differently.

Due to the number of classes, the error matrix was too large to be displayed here. The results were hence summarized by class in Table 6.7.

The overall accuracy for the classification is 63.69%. The individual user's and producers' accuracies for each class assessed are listed in Table 6.7.

The producer's accuracy for each category describes the percentage of grid points at which the predicted class was judged to be correct during the accuracy assessment, i.e., the total number of grid points apportioned to this class during photo-interpretation. The producer's accuracy therefore describes the percentage of each class on the ground correctly identified. The user's accuracy shows the same value divided by the column total of each class, i.e., the total number of grid points predicted to be the class heading the column (Congalton and Green, 1993). This therefore indicates the proportion of each predicted class which has been classified correctly.

The reverse values of producer's and user's accuracy hence respectively describe the percentage of under- and over-estimation of each class in the classification. These values are usually called omission and comission error.

Figure 6.8 ranks each class with regard to their user's and producer's accuracy, as listed in Table 6.7, respectively. The classes Arable and Ue_scrub have very low values in both cases, which is due to their very rare occurrence in the classification. Another unusual feature is a 100% User's accuracy for the urban class. This is explained by the fact, that it is exclusively classified from the OS MasterMap the-

Table 6.7: Accuracy assessment results for the Lake Vyrnwy study site (Figure 6.5)

Classname	Number classified	Number groundtruth	User's accuracy (%)	Producer's accuracy (%)
Acid flush	233	87	27.90	74.71
Arable	2	1	0.00	0.00
Ash gulleys	190	47	18.42	74.47
Birch-Ash wood	119	65	32.77	60.00
Bog_OldCv	649	415	58.71	91.81
Bog_youngCv	400	485	72.00	59.38
Bracken	408	410	69.12	68.78
Broadleaved forest	141	164	51.77	44.51
Cv_cont_old	1130	1017	67.08	74.53
Douglas Fir	58	2	1.72	50.00
Et_Mc_Cv_wet	154	356	50.65	21.91
Felled woodland	451	556	76.27	61.87
Fo_At_grass	347	352	58.50	57.67
Fo_Ns_moss	297	221	62.29	83.71
Hedges	167	95	37.72	66.32
I_upland	56	128	57.14	25.00
Je_flush	68	77	29.41	25.97
Jsq_Ns_grass	27	151	62.96	11.26
Larch	355	213	32.11	53.52
LowL_I	549	755	89.44	65.03
LowL_SI_acid	37	58	59.46	37.93
Mature Oak	176	71	22.73	56.34
Mature Spruce	502	528	86.45	82.20
Mc_upland	184	213	55.98	48.36
Ns_Fo_grass	187	303	68.45	42.24
Scattered scrub (gorse)	22	50	27.27	12.00
Scattered scrub (trees)	67	34	47.76	94.12
SI_acid_upld	323	259	51.39	64.09
Ue_scrub	5	29	0.00	0.00
Urban	209	248	100.00	84.27
Water	458	454	98.69	99.56
Wet woodland and Scrub	126	309	52.38	21.36
Young Spruce	881	852	77.19	79.81
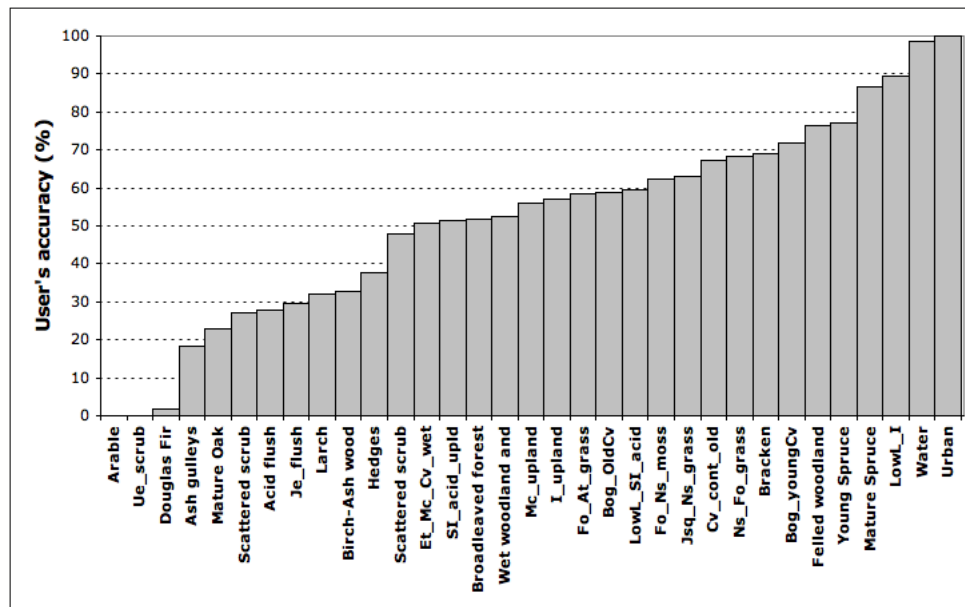
(a) User's Accuracy
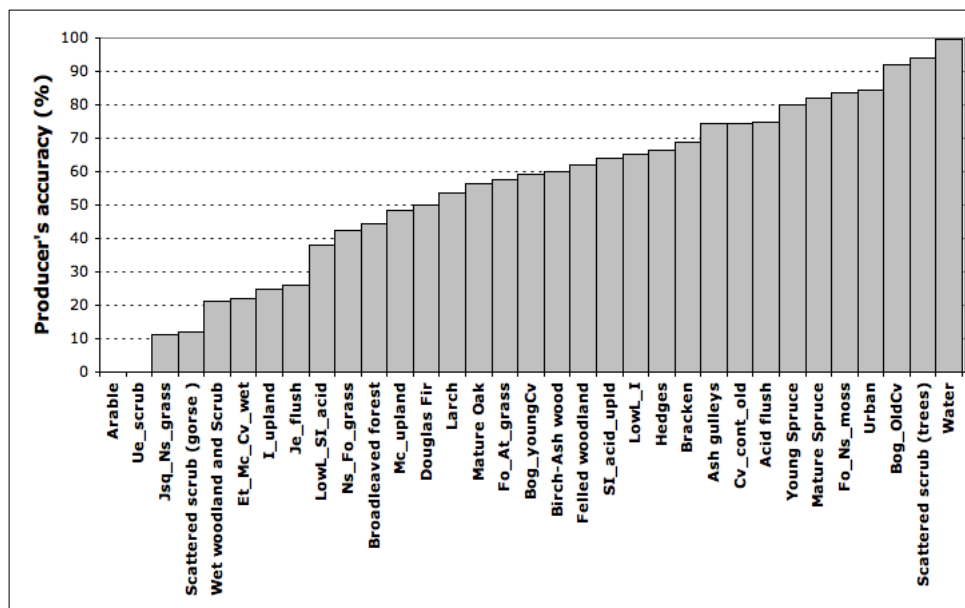
(b) Producer's Accuracy

Figure 6.8: User's and Producer's Accuracy for the Lake Vyrnwy classification ranked in order of magnitude (Table 6.7)

matic layer and hence does not confuse with other classes. It does though still show a 15.73% omission error, indicating that the MasterMap layer is not completely comprehensive and some man-made features are hence not classified.

Classes such as Ash gulleys, Birch-Ash wood, Hedges and especially Douglas Fir have quite low user's accuracies, compared with their high producer's accuracy. This indicates that, while they are not differentiated well, these classes also are not confused a lot with other classes. Water in comparison is classified from a combination of the OS MasterMap water data and a satellite based rule and performs very highly for both types of accuracy.

In contrast many classes, which are comparatively successfully classified, also show a high percentage of comission error, which suggests that the rules used to classify them are not class-specific enough and probably should be revised. A good example is Jsq_Ns_grass, which has a comparatively good user's accuracy and a very high producer's accuracy.

While 63.69% is not a very high accuracy for the whole of the classification, several individual classes achieve considerably higher values of user's accuracy, such as Bog_youngCv, Felled woodland, LowL_I, as well as Young and Mature Spruce. Both types of spruce also achieve high scores for producer's accuracy and are hence the best performing classes solely differentiated from remote sensing data.

Fo_Ns_moss is further remarkable, as it scores high for both accuracies, but particular producer's accuracy. In turn I_upland's values are lower than could be expected in comparison to Lowl_I and the homogenous appearance of improved grassland in comparison to an unimproved grassland type, such as Fo_Ns_moss.

It was decided not to undertake a separate accuracy assessment in Ceredigion in favour of collecting the very large set of assessed points described above at

a high spatial density over the Vyrnwy site. It is therefore not possible at this stage to provide similar figures for the Ceredigion classification. However, it was created by applying a near-identical set of rules to the Vyrnwy classification to the same spring SPOT 5 HRG and summer IRS scenes and is hence assumed to be of comparable accuracy.

Transferability of the rules to other areas further away from the training sites is an important consideration though for the validation of the approach and an accuracy assessment should hence be undertaken, when time allows.

6.3.3   Spatial error distribution

The spatial distribution of errors is not random, but can in many cases be related to certain image and ecological phenomena as suggested above. In the context of accuracy assessment during change detection, van Oort (2007) found that spatial error distribution is often temporarily correlated and consistent, thus further supporting the argument above.

Figure 6.9 illustrates the spatial distribution of errors in two areas around Lake Vyrnwy.

The images indicate that errors are clustered on the boundaries between well defined habitats and across ecotones, e.g., blanket bog and upland dry heath (Figure 6.9(b) *2*), as well as flushes and gulleys (Figure 6.9(a) *3+4*). There are no errors over the lake itself, but several along the shore(Figure 6.9(b) *1*), where narrow bands of different tree species are common. A similar tendency can be found along woodland edges(Figure 6.9(b) *3*). The error associated with steep north-facing slopes is very well illustrated in Figure 6.9(a) *1+2*.

Ecotones are characterized by a mixture of species and/or habitats and therefore
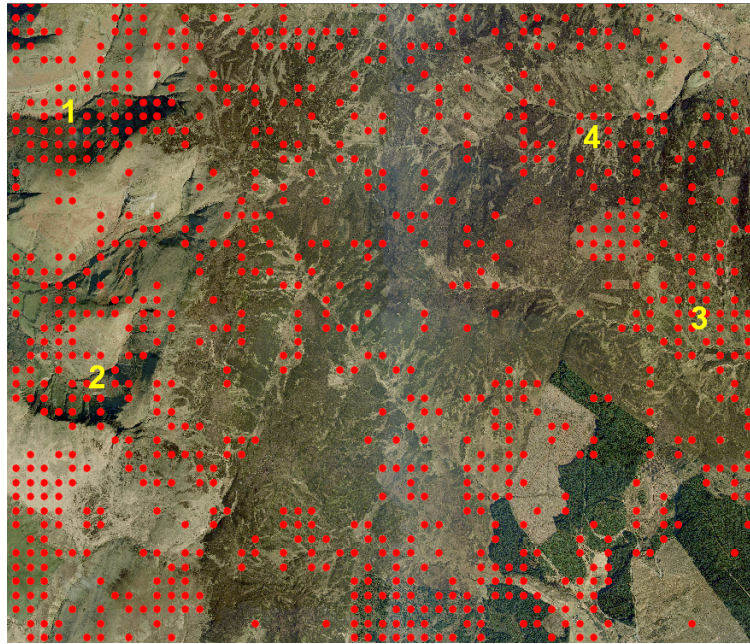
(a) Example 1
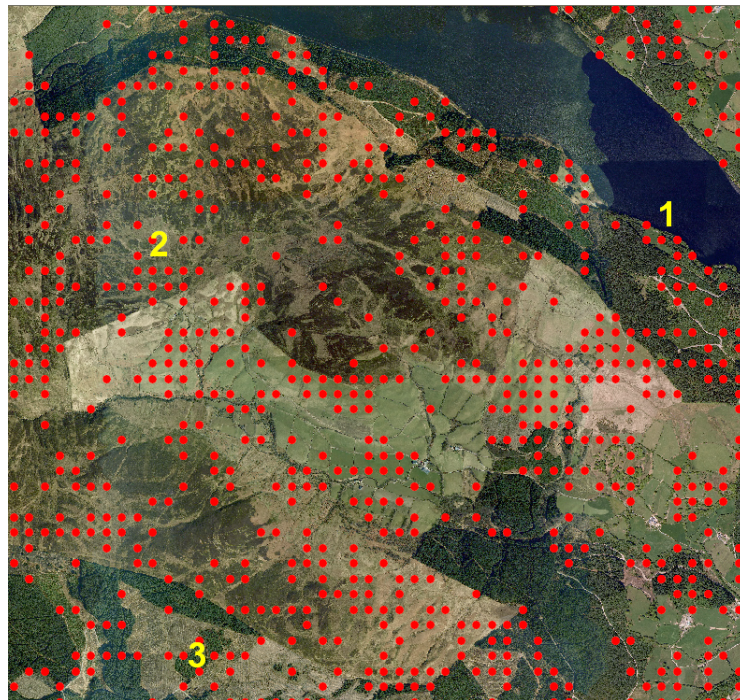
(b) Example 2

Figure 6.9: Spatial error distribution across an upland landscape. Dots (red) indicate grid points tested for accuracy and judged to be wrongly classified. The numbers (yellow) refer to different scenarios where error clustering occurs and these are outlined in the text above.

prove challenging for a rule-based classification, particular one that is based on the assumption that it is possible to divide the landscape into a fixed number of clearly defined classes. In some classes, this ambiguous character has been taken into account in the rule-base by making allowance for stands occurring on north-facing slopes (bracken) or different levels of productivity in grasslands, which are nevertheless all considered to be improved.

However, despite the pixel level segmentation and fuzzy classifications taking the possibility into account that an object can feasibly have a membership to one or more classes, in the final and crisp map this membership cannot be displayed and a final decision has hence to be made with regard to a single class.

6.4   Discussion

The high level of detail obtained in the classification was largely attributable to the use of the 10 m SPOT HRG data for segmenting the landscape and the application of fuzzy membership functions for describing complex communities (e.g., heath mosaics) in the uplands. The use of optical data acquired prior to and during the growing season allowed the seasonal phenology of habitats to be better captured, thereby increasing opportunities for their discrimination. Whilst a greater number of satellite acquisitions during the year would lead to further enhancement of the classification, those acquired prior to the spring flush of growth (late March) and following this flush (July) were considered sufficient. Imagery acquired early (before February) or late (after November) was of limited use, particularly in mountainous areas and primarily because of the low sun angle.

While the point based approach to accuracy assessment used here is the most

rigorous,the object based approach is arguably more appropriate for the following reasons:

1. habitats are traditionally defined and described at the patch level

2. many 'patches' consist of mosaics that are comprised of a range of species (e.g., Ec_Mc_Cv_wet; see Table 6.6)

3. others can be interpreted as belonging to several habitats (in terms of their Phase 1 description). For example, broad-leaved woodlands may support a bracken understory and, depending on openness and height of the canopy, maybe interpreted as being dense scrub, rather than forest.

4. a number of habitat patches may be at various stages of degradation, succession, species invasion or extinction processes and their classification is therefore open to interpretation

6.4.1   Classification error

An overall accuracy of 85% is considered a standard requirement for remotely sensed land cover maps (Foody, 2002; Fuller et al., 2003), which is considerably above the accuracy achieved in this study. The classification accuracy could, however, be considerably improved through a meaningful combination of related classes. This would particularly apply in the case of an amalgamation of all woodland classes into a single broadleaved and coniferous class respectively, as well as the creation of a single class for upland bogs. While this would lead to a simplification, confidence in the usability of the map would increase considerably.

Laba et al. (2002), however, question the usefulness of the 85% accuracy standard and argue that accuracies approaching 80% are only feasible through the use of sensors with higher spectral, spatial, and temporal resolution than utilized in this study. The required overall accuracy of any map is further dependent on its intended use (Wulder et al., 2006), while the proportional distribution of its component classes determine the weighting of individual class accuracy requirements (Czaplewski and Patterson, 2003).

The five classes (Bog_youngCv, Felled woodland, LowL_I, Young and Mature Spruce) highlighted in Section 6.3.2 for their high accuracy values all have in common that they form large, homogenous and continuous areas with well-defined borders and are hence less likely to mix with other vegetation types, which could reduce classification accuracy.

Figure 6.9 shows that there are few errors associated with large and even land cover types.

Douglas Fir has an exceptionally low user's accuracy. This is probably due to the fact that only one small stand exists in the study area (Number of points tested for accuracy = 2), though this has been classified correctly. The class otherwise is commonly confused with other conifer species and the rule for Douglas Fir should be revised, where it is more commonly found.

Classification errors can be divided into several distinct types of varying severity, corresponding to error source. Accordingly there are low severity errors, which are confusions between related classes, e.g., Mature and Young Spruce, as well as high severity errors (e.g., grasslands confused with forest).

More important though than awarding a degree of severity to the error, is to establish whether a reason for the error can be identified.

There are many possible sources for errors in the classification and confusions be-tween categories and not all of them are caused by the classification rule-base. The accuracy assessment therefore benefits from the identification of these confusion sources and the subsequent opportunity to control and limit their impact in future classifications. Confusions caused by such external factors are referred to by Con-galton and Green (1993) as non-error differences to distinguish them from the true classification errors in the confusion matrix. The accuracy values derived from the confusion matrix, as described above (see Table 6.7) are based on the assumption that all mismatches in the matrix derive from the remotely sensed classification and/or segmentation and while segmentation based errors are discussed below, the following other possible error sources were identified and considered.

It is further difficult to obtain a complete correspondence between habitats ob-served in the field or from aerial photography interpretation and those classified from remote sensing data for the following reasons:

The reference data (in this case the Vexcel aerial photography from 2006) post-dates some of the imagery (2003 SPOT data) used in the classification by three years and the land cover can therefore have changed significantly in the intervening period. Examples include the harvesting of commercial conifer plantations and the burning of heathlands and bracken stands as well as fluctuations in grassland improvement levels due to changing management regimes.

A specific problem in this study is also that the aerial photography was acquired over several seasons in 2006 and while the whole mosaic is seamless, the appear-ance of a category in the reference data can change suddenly (e.g., from leafleass broadleaved woodland in the winter to leaf canopy present in spring and summer) and demands the interpreter to be alert to this (Figure 6.10). This is particularly

apparent in larch stands and in bracken covered areas, as well as all other habitats, which change their appearance seasonally.

Congalton and Green (1993) also mention registration differences between the reference data and the map classification as a potential error source. This does not apply here as the Vexcel was used as the registration basis for all remotely sensed data utilized in the classification. Accurate co-registration of the various data layers used is indeed a prerequisite for a successful classification.

Photo-interpretation varies with individual interpretation bias and it is therefore important that assessments are carried out by the same interpreter, or the minimum number possible to ensure the highest consistency possible (Wyatt, 1991). Each interpretation based on the skills and experience of the interpreter and the degree of familiarity with the classification area and the classes.

An absolute decision from the aerial photography is also often difficult to justify and it is therefore important to consider the surrounding habitats and to take ecological knowledge of the communities present into account.

Objects often can reasonably be attributed to more than one class and a considered decision has to be made, but this might justifiably vary between different interpreters. Categories with low accuracy values were often associated with regions that were comparatively cloudy or shadowed by cloud. The 27th March 2003 Spot scene used at Vyrnwy is covered in scattered cloud (Figure 4.2(a)), which causes difficulties where a spring image is required for the differentiation of a habitat class, though the ASTER and second SPOT scene have often been successfully substituted here.

Very steep north facing slopes are similarly problematic to areas obscured to cloud, as the sun illumination is often not sufficient to differentiate habitat classes. This

Figure 6.10: Seasonal discrepancy in the 2006 Vexcel Aerial Photography. While all individual photograph tiles form a very well constructed mosaic of this part of North Wales, a clear vertical boundary is visible in the centre of the image. This is due to the images of the left of the boundary to have been taken during the summer (note the brighter green appearance) and those to the right of it being acquired during the winter after deciduous trees had shed their leaves and during a time of lesser productivity for grasslands.

effect is especially pronounced where imagery were acquired in the winter and is well illustrated in Figure 6.9.

6.4.2 Habitat scale and homogeneity

Homogeneity across patches of the same class cannot be assumed and therefore decisions regarding deviation have to be made early on to avoid later discrepancies in the assessment.

Categories here are constrained in scale by the limitations, and especially by the resolution of the remote sensing data on which the classification is based and are therefore sometimes forced amalgamations of classes which should be separated from an ecological point of view and which are not homogeneous. They form the 'smallest common denominator'. It is therefore paramount that these limitations are considered during the accuracy assessment.

In effect, whilst some classes are homogenous (e.g., coniferous plantations) and can be classified with relative confidence, where more heterogeneous and complex habitats occur, assignment to a particular class then becomes more difficult, particularly across ecotones. For this reason, criteria for separating classes have to be established a priori in order to arrive at an appropriate classification scheme, but also to establish which classes are acceptably confused when evaluating accuracy.

The scale of observation is also important. As an example, a confusion between improved grassland and hedges was commonly observed. These two categories are spectrally sufficiently distinct to make this an unexpected occurrence. However, neither is classified at the sub-level, but segmented to and classified at Level 1.

Hence the elongated shape of the hedges and the relative coarseness of the re-sampled pixel resolution ($25m^2$) is causing the objects which delineate them, to often include a small area of the adjacent improved grassland. The predominant category in the object is then assigned to the whole of the object. However, this is not reflected in the accuracy assessment on a point basis.

Furthermore it was found that the rate of error, in the classes predicted on the object level, decreased with increasing distance of the checked grid point to the edge of the object. This can be related to the core and edge habitat definitions in spatial ecology as outlined in Chapter 1. Core habitat is always assumed to be more representative of a habitat class than the edge and this can be translated into a remote sensing context as the increasing likelihood to encounter mixed pixels closer to the the edge of a habitat patch or object, which will influence the classification accuracy in this area. The greater the contrast between two habitats and the more defined their edge (e.g., between coniferous forest plantations with predominantly straight, man-made borders and adjacent grasslands), the less this type of confusion occurs, as the segmentation closely follows the borders and the occurrence of mixed pixels at the edge is less likely.

However, natural and semi-natural habitat patches often have very poorly defined edges and transitions between habitats are typically gradual and not abrupt. In cases where mixed pixels are abundant, classes are decided by the majority of one habitat in the object or the MMU. Whilst the MMU in this case is only $25m^2$, this resolution is still too coarse to capture precise boundaries of many habitats, for example hedges and small flushes, and hence confusion using a point-based approach to accuracy assessment will be greater.

6.4.3 Other land cover classification schemes

Neither the Phase 1 or Phase 2 Surveys utilized satellite sensor data. However, these data have been used for more timely mapping of land cover and largely for reporting at the national (UK) and European level.

Using 30 m spatial resolution Landsat Thematic Mapper (TM) data for the period 1988-1989, the first satellite derived map of land cover of Wales was created as part of the United Kingdom(UK) Land Cover Map (Fuller et al., 1994). A maximum likelihood classification of 25 classes representing broad and nationally consistent vegetation categories was applied at the pixel-level, with mapping undertaken in conjunction with a sample based countryside survey (CS1990). A follow-up map (LCM2000) for 2000 again used Landsat-sensor data acquired during the winter and summer months but these were segmented to better identify relatively homogeneous areas (e.g., fields, water bodies; Fuller et al. (2002, 2006)). Knowledge-based algorithms that integrated ancillary data, such as soils and elevation, were also applied. The mapping identified 72 classes, which were subsequently grouped into 24 thematic subclasses. A further update is expected using a generalization of the UK Mastermap GIS objects (Smith and Wyatt, 2007). Fuller et al. (2005a) noted several limitations to the land cover maps. Many of the broad vegetation classes selected were not ideal for detection using remote sensing data as these had often been defined by combinations of plant species, by the substratum or by elements of land use not discernible in images. Some vegetation categories typically occurred in stands that were rare, localized or smaller in area than the spatial resolution of the imagery. While limitations on the separability of classes in the imagery could be partially resolved by only mapping broad habitats, many users required more detailed information on classes beyond these.

The approach used in this study is an extension to the method suggested by Lucas et al. (2006b) as part of a pilot study commissioned by the Countryside Council for Wales (CCW) and the British National Space Centre (BNSC). Lucas et al. (2006b) used a time-series of Landsat TM/Enhanced TM data from four dates (March, April, July and September) as input to a rule-based segmentation and classification procedure developed within eCognition (Definiens, 2008). The approach differed from the traditional methods in that the landscape was first segmented into objects of sizes that varied from individual pixels to entire fields (as defined using Land Parcel Information System (LPIS) boundaries). Numerical rules, designed to capture known correspondences between the distribution of habitats in the landscape and their manifestation within remote sensing data, were then applied. The sequential application of these rules allowed semi-natural habitats and agricultural land cover classes to be discriminated, in some cases, to a level comparable to or better than those mapped previously using Phase 1 Survey field methods.

This study further develops the approach used by Lucas et al. (2006b) and the Land Cover Map, by using higher resolution spaceborne satellite data (SPOT 5 HRG and IRS LISS IV, resampled to 5m pixel size) than Landsat and by integrating further thematic layers (Table 6.2), beyond the LPIS boundaries, into the classification. The segmentation and classification procedures within the rule-base are further refined by undertaking them at three separate levels to allow for differences in habitat scale and homogeneity to be taken into account.

The number of classes identified has been increased from Lucas et al. (2006b) and the classification focused more on single-species dominated habitats, such as *Calluna vulgaris* heath and particularly a greater number of woodland classes

(Table 6.6).

6.4.4 Advancements to land cover classification

One of the most important advantages of this mapping approach is its capability to be updated on a regular basis, as new imagery becomes available.

Whilst the classifications were generated using satellite sensor data acquired between 2003 and 2006, the rule-base can be adjusted to allow updates for any reference year and/or refined as and when new imagery becomes available. The approach can be adapted and expanded to provide continual monitoring of the extent, distribution and state of habitats across Wales, where imagery of sufficient quality is availaible.

The original Phase 1 survey did not map hedgerows in Wales, except in the county of Powys. The ability to map hedgerows from spaceborne remote sensing data is hence a significant advancement of this mapping method.

With regards to the accuracy assessment, it has been shown that errors are more likely to occur in ecotone regions, i.e., along the edges of relatively homogenous habitat stands, rather than in their core area.

While the classifications in this study have shown encouraging results, particular with regard to more detailed tree species, blanket bog and unimproved upland grassland identification, the classification needs to be improved further, especially with regard to more complex habitat mosaics. This should be done by a revision of the classes used and the rules applied under considerations of the accuracy assessment and spatial error distribution demonstrated in this study. The inclusion of a class for Bilberry (*Vaccinium myrtillus*), for example, would increase the

accuracy of the map, but it is limited by its seasonal appearance and can only be detected in the remote sensing imagery during small windows in time. Gorse (*Ulex europaeus/Ulex gallii*) is also poorly classified so far and suffers from strong spectral similarities with mature Ling heather (*Calluna vulgaris*) and other scrub types. As a common and distinct land cover class within Wales, it would be desirable to improve the differentiation of gorse significantly.

The segmentation approach has been improved by using three differently scaled levels, in order to create habitat-scale appropriate objects. However, as described above, especially with regards to hedgerows, there is further potential for a better delineation of objects to reduce confusion with neighbouring habitat patches.
Preliminary tests have shown, that a segmentation based on a high resolution dataset such as the 2006 Vexcel NIR aerial photography of Wales (1m spatial resolution) greatly improves object definition and hence classification accuracy from coarser remote sensing data. This is, however, to be explored in a further study.

6.5 Summary

Land cover maps as described in this study can be used to support various environmental and natural resource applications, such as change analyses, resource inventories, flood modeling and as input into habitat suitability models (see Chapter 8 (Stehman and Czaplewski, 1998)). Reliable and consistent vegetation data is an important component of many ecological studies, but it is time-consuming and expensive to collect. A widely available large-scale map of acceptable accuracy, based on a consistent rule-base would therefore provide an invaluable resource for

a great number of further studies of individual habitats and species and would help to reduce the element of assumptions in much research regarding land cover.

This chapter has described how spaceborne remote sensing data can be integrated within a rule-based approach to map semi-natural habitats, including grasslands and woodlands and how to distinguish these from other habitats (e.g., heaths and moorland).

Key elements, that allow classification, are:

1. accurate geometric correction, which allows intercomparability with other data layers (e.g., aerial photography and MasterMap derived thematic layers)

2. atmospheric correction, which allows the creation of a range of indices to exploit seasonal variation for habitat differentiation (e.g., difference in photosynthetic vegetation proportion of bracken between spring and summer images)

3. a hierarchical segmentation approach that segments and classifies at three levels (super-level, sub-level and Level 1) and therefore gives consideration to relative differences in the scale and homogeneity of habitats (e.g., arable fields through to complex heath mosaics)

4. a careful definition of classes to be defined from the remote sensing data, according to how they manifest themselves within the data. A correspondence of any class system to existing survey class definitions (such as the Phase 1 habitat survey) is desirable to ease comparison and utility of the classification. However, many existing field survey classes can not be directly translated into a remote sensing class and the classification might suffer in accuracy, if this is not taken into account.

The following chapter describes the structural characteristics of different woodland types as derived from full-waveform LiDAR and Terrestrial laser scanner data.

Chapter 7

Forest structural attributes from laser data

7.1 Introduction

In recent years, significant advances in the use of Light Detection and Ranging (LI-DAR) have occurred with the development of full waveform LiDAR and Terrestrial Laser Scanners (TLS). Independently, these datasets have been shown to provide opportunities for quantifying the structure of forests (e.g., Watt and Donoghue, 2005a; Koetz et al., 2006; Coops et al., 2007; Hudak et al., 2008; Tansey et al., 2009). However, few studies have compared TLS and airborne LiDAR to understand the extent to which structures occurring within the vertical profile are being captured by the airborne LiDAR and the interaction of LiDAR pulses with different tree components (leaves, branches and trunks).

The primary objective of this chapter is to couple small footprint full-waveform

airborne Light Detection and Ranging (LiDAR) data with terrestrial laser scanner (TLS) and forest inventory data for purposes of evaluating the level of forest structural information that can be retrieved from the former.

Focusing on the RSPB reserve of Lake Vyrnwy (see section 3.2.2), research in this chapter seeks to analyse forest structure by retrieving parameters such as tree height, canopy openness and canopy layers from full-waveform LiDAR data. Integrating the LiDAR and terrestrial laser scanner data also provides an in-depth assessment of the capacity and accuracy of airborne LiDAR for retrieving sub-canopy forest structural attributes at scales ranging from the tree to the landscape.

An objective of this research therefore is to establish whether these data can be used realistically to estimate forest stand height and other structural parameters, particularly in relatively undulating terrain.

Many studies (e.g., Todd et al., 2003; Chen et al., 2005; Lefsky et al., 2005; Suarez et al., 2005), have focused on the use of LiDAR data for retrieving forest structural attributes. However, none have coupled these data, and specifically full-waveform LiDAR, to terrestrial laser scanner (TLS) data acquired at the ground level for purposes of better understanding the attenuation of LiDAR pulses through the vertical profile and their interaction with different tree components (leaves, branches, trunks). For this project TLS data for selected forests stands has been obtained for which airborne LiDAR data have also been acquired, thereby facilitating a direct comparison between the two datasets.

The chapter is structured as follows. The acquisition of LIDAR and TLS data and methods used to retrieve the ground elevation and structural data are outlined in Section 7.2. In Section 7.3, accuracies in the registration of the LiDAR and TLS data and comparisons between the two datasets are presented. The discus-

sion (Section 7.4) outlines the implications for the retrieval of forest structural attributes from both sensors. The study is concluded in Section 7.5.

7.2 Methodology

For the Lake Vyrnwy area, airborne LiDAR and TLS data were acquired in August 2007, details of which are provided in the following sections. In linking the remote sensing datasets (i.e., airborne LiDAR and TLS), a high level of geo-locational accuracy was required. Hence, a comprehensive and precise network of ground survey points was established in conjunction with TLS data acquisition and a high quality Inertial Navigation System (INS) was used during the airborne LiDAR acquisitions. This ensured that all points were correctly located in three-dimensional space. For processing, all point data were converted to the Sorted Point Data (SPD) file format (Bunting, 2009) and processing was undertaken within the Remote Sensing and GIS software library (RSGISLib; Bunting and Clewley, 2009) unless otherwise stated. The acquisition and processing steps are outlined below.

7.2.1 TLS data acquisitions

Leica Geosystems Scanstation 2 TLS data were acquired for seven forests representing a range of structural formations (one to multiple layers, with or without understory) and species types (Table 7.1), including forests dominated by douglas fir, sessile oak, larch, or mixtures of these. This terrestrial laser scanner is well suited for scanning forests as it supports a 270° vertical field of view which extends

45° below the horizontal but only records a single first return per pulse. The sensor operates to a range of 250-350m (300m at 90 % reflectivity) and generates three dimensional (x, y and z) point cloud data. For each site, a single scan was acquired from the centre with a point spacing of 3cm at 30m providing a hemisphere of data around the scanner that covered approximately a 50×50m plot.

Table 7.1: The location and forest type for each of the seven TLS sites.

Scene	Eastings	Northings	Dominant tree species
LV7	296702	324141	Douglas Fir
LV8	302082	318823	Sessile Oak
LV9	302078	318934	Sessile Oak and Sycamore
LV10	301273	320647	Sessile Oak
LV11	300583	320963	Larch
LV12	300786	319826	Sitka Spruce
LV13	300209	321227	Sitka Spruce

For each site, tilt and turn targets (flat or hemispheric) were mounted on tripods and orientated towards the TLS. The TLS itself was mounted on a plumb tribrach which allowed leveling of the target over a specific point on the ground (marked with a permanent marker). Site markers were put in place at all sites so that repeat measurements could potentially be taken in future years. For each plot, at least three targets were set up around the TLS and named appropriately. The height of each target above the marker was then recorded for later geo-registration.

To precisely locate the TLS in x, y and z coordinates, a GPS base station and control network were first established within an open area close to the site of each scan. An open area was required as a reliable RTK GPS signal could not be obtained under the forest canopy. Therefore, following the establishment of the control network, a total station was used to move into the forest and survey the TLS and target locations. To move within the forest with the total station,

a series of resections were required, with each resulting in an x, y, z location fix. In total 196 points were surveyed within the airborne LiDAR scenes, 42 of which overlapped with the TLS surveys. The GPS data were processed using the Ordnance Survey of Great Britain's active GPS RINEX data (within Leica GeoOffice). The total station survey data were then converted into the UK national grid coordinate system. Using these survey points, the scanner target locations were identified within each scan and matched to the appropriate survey point. This process allowed geo-registration of the complete scan, which was undertaken within Leica's Cyclone software.

7.2.2   TLS data analysis

Following geo-registration, returns associated with the ground were identified to derive a fine spatial resolution (2m) Digital Terrain Model (DTM). DTM generation was limited as the point spacing provided by the TLS varied as a function of range and shadowing occurred within the scene because of occlusion by trunks, branches and foliage. For this reason, the data were first binned to a 2 m grid whereafter the algorithm attempted to identify a single ground return for each bin. Ground returns were identified using a plane fitting (least squares) approach whereby a window of bins 10m either side of the central bin was first selected. Within this larger column (22×22m), a plane was iteratively fitted to the data. Following fitting, the deviation of the points from the plane was quantified. Where the deviation was below a user defined threshold (e.g., 0.5m), the plane was deemed to be well fitted with the points along the plane corresponding with the ground surface. The lowest point below the plane in the central bin was then identified and classified as a ground return. Where the deviation was above the user-defined

threshold, then the plane was deemed to be poorly fitted, the points above the plane were removed and the plane refitted to the remaining points. This process was continued iteratively until either the points fitted to an identified plane or the number of points remaining was below 4. In the latter case, the process was ceased and no ground point was classified. These thresholds were found to be suitable as, although the point densities from the TLS were high, the number of ground returns were spatially variable with range from the instrument and ground cover (i.e., as a function of understory).

7.2.3   LiDAR processing

The airborne LiDAR data were captured by the Natural Environment Research Council (NERC) using the Riegl LMS-Q560 full waveform laser scanner, with a 20 cm footprint size and a post spacing of approximately 2m. Following capture, the data were processed by NERC, using the Riegl RiAnalyze software to decompose the waveforms into discrete returns (a maximum of 4 per waveform). Registration was undertaken using Terrasolid software. The LiDAR data were supplied in LAS format but converted to the SPD format (Bunting, 2009) for processing. From these data, a DTM was derived using the same algorithm and parameters as applied to the TLS data (binned to a 2m grid, a window of bins 10 m either side of the central window (creating a 22×22m window) and a threshold of 0.5 m defining whether the points fitted the plane). These thresholds were determined experimentally through a visual assessment of the derived DTMs to minimize any incorrectly classified ground points and were found to be suitable for both the TLS and airborne LiDAR.

7.2.4   DTM and CHM generation

Following classification, the ground returns identified were used to form a delaunay triangulation from which a 2 m resolution raster DTM was produced. The final stage of processing produced canopy height models (CHM) for each TLS scene and the airborne LiDAR. This was achieved by normalizing the ground surface to a height of zero for each point where the intersecting DTM height was removed. Therefore, the CHM contained all the points within the scene, including the ground returns normalized for the ground surface topography. From these data, the vertical profiles and heights of the forest from both the airborne LIDAR and TLS could be observed. For this purpose, each TLS scene was subset to field plots of 50×50m with the scanner positioned at the centre of the scene. The scenes were subset to extract a core of data with sufficient point densities (< 3cm at 30m) for later processing and interpretation. Subsetting was undertaken following DTM and CHM generation to avoid boundary effects within the areas of interest.

7.2.5   Integration of airborne LiDAR and Terrestrial Laser Scanner data

As the TLS data was referenced using differential Global Positioning Systems (dGPS), each tree imaged on the ground was associated with the position of the LiDAR waveform in relation to the TLS. Recorded returns in three-dimensional space were then related through position.

A number of analyses were subsequently undertaken, including comparisons at the individual tree, tree cluster and stand level of the frequency of LiDAR returns by height above the ground surface. Previous studies in Australia (Lee and Lucas,

2007b) have established that the relative penetration of pulses into the forest canopy can be described using a Height Scaled Crown Openness Index (HSCOI) and that the lower values of the HSCOI can be associated with trunk locations. Further testing of this has been carried out as part of this research, but in a different environment.

7.3 Results

7.3.1 Registration accuracies

Through the registration process, within the Leica Cyclone software, the residual errors for each target used to register the TLS data were identified (Table 7.2). For the majority of targets, the error was less than 30 cm with the lowest being just 3 cm.

LV13 was the exception where, because of equipment failure, manual targeting of the total station was required within a dense forest and across undulating terrain which lead to greater residual errors. Data from this site were included in the subsequent assessment of the ground surfaces (DTM) derived from both sensors as the ground points were identified within a radius of 7m around each survey point (Section 7.3.2). The terrain at site LV13 was level and the canopy height comparatively uniform and the site was further included in the comparison of both DTMs and canopy top height (Figures 7.3 and 7.4) without leading to a notable decrease in correspondence compared to the high impact of inclusion of a single non-ground point in Figure 7.3. The site was, however, not included in the generation of two-dimensional plots of the forest vertical profile in Section 7.3.4,

because of the higher registration accuracy required for a visual comparison of canopy profiles at precise locations.

Table 7.2: TLS residual errors (in metres) for the TLS target positions.

Target	LV7	LV8	LV9	LV10	LV11	LV12	LV13
1	0.088	0.221	0.256	0.132	0.044	0.203	3.134
2	0.069	0.065	0.374	0.217	0.294	0.276	**4.708**
3	**0.034**	0.216	0.048	0.267	0.046	0.187	1.648
4	0.656	0.374	0.077	0.174	0.271	0.288	
5				0.203	0.030		

7.3.2   Resolving the ground Surface

To assess the accuracy of the DTMs derived from the TLS and airborne LiDAR datasets, the elevation data from survey points collected to geolocate the TLS data were compared. To ascertain whether the laser strikes were reaching the ground surface, the lowest point within a radius from each survey point was first identified within both the TLS and airborne LiDAR datasets. Radii of 1 to 25m, at 1m intervals, were considered to identify the density of points reliably reaching the ground surface. The survey data were then compared to the raster DTMs generated from the filtered point data. This test aimed to demonstrate that the filtering and interpolation algorithm deployed worked appropriately. Finally, the DTMs from the TLS and LiDAR were compared.

Survey and points

The comparison of the survey data with the minimum TLS and airborne LiDAR data (within a radius from the known survey point) indicated similarities in the

surface elevation for both sensors, with errors reducing with increases in the search radius. Differences between the elevation were minimal at a radius of 7m and increased for radii >7m because of topographic variations (Figure 7.1). The radius of 7m was the distance at which the ground returns could be identified for a particular point without errors introduced from any changes in the adjacent topography (radii greater than the optimal) or non-ground returns such as those associated with the understory (radii less than the optimal). This analysis reinforced the decision to use the same parameters for the TLS and airborne LiDAR to retrieve the ground returns and generate the DTM as the ground returns were similarly spaced.
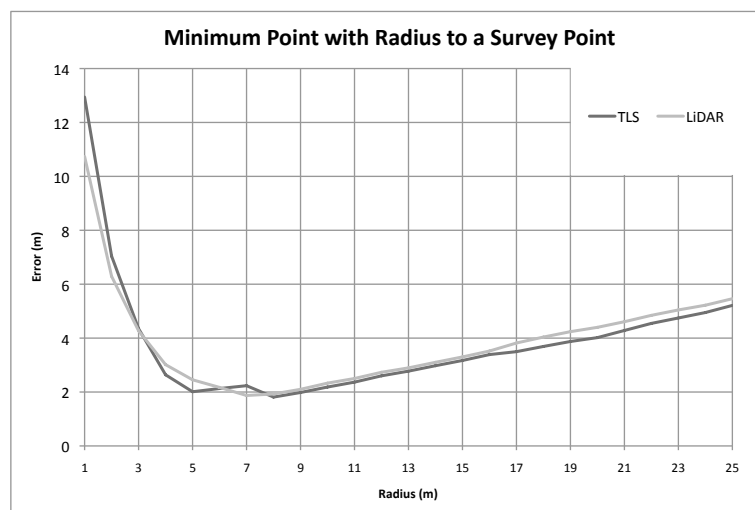
Figure 7.1: This graph demonstrates that the LiDAR points match the ground survey with an average error of 2m at a radius of 7m from the survey point.

Survey and DTM

When compared to the survey data, the DTMs derived from the TLS and airborne LiDAR showed residual errors of ± 0.99m and ± 1.17m respectively, (Figure 7.2).

Survey heights were derived from the 196 and 42 survey (GPS and total station) points for the airborne and TLS respectively whilst base heights were established from a corrected RTK-GPS control network.

TLS DTM and LiDAR DTM

A close correspondence was also observed between the DTMs from both datasets (Figure 7.3), with the overall error being $\pm$ 0.58 m. However, a notable error occurred in scene LV9, where a single incorrect ground point had been identified in the TLS data which resulted in the generation of an incorrect surface in the surrounding pixels of the DTM. This leads to a deviation of the otherwise close correspondence of the two surfaces visible at the lower end of the graph in Figure 7.3. In the future, this problem will be solved by integrating an additional step into the DTM filtering process where points which form a vertex to steeply sloping triangles (within the delaunay triangulation) will be removed.

7.3.3 Canopy top height

A comparison of canopy top heights derived from both the TLS and airborne LiDAR (Figure 7.4) indicated a close correspondence ($\pm$ 4.44 m, R^2=0.65) and were consistent with previous measures of tree height from TLS data (e.g., Maas et al., 2008b). The differences can be explained by the different viewpoints and characteristics (e.g., sampling rates) of the sensors resulting in different levels of penetration. The TLS data were captured from the ground looking up and therefore the majority of the points were intercepted by the lower parts of the canopy. By contrast, the strongest returns decomposed from the airborne LiDAR were
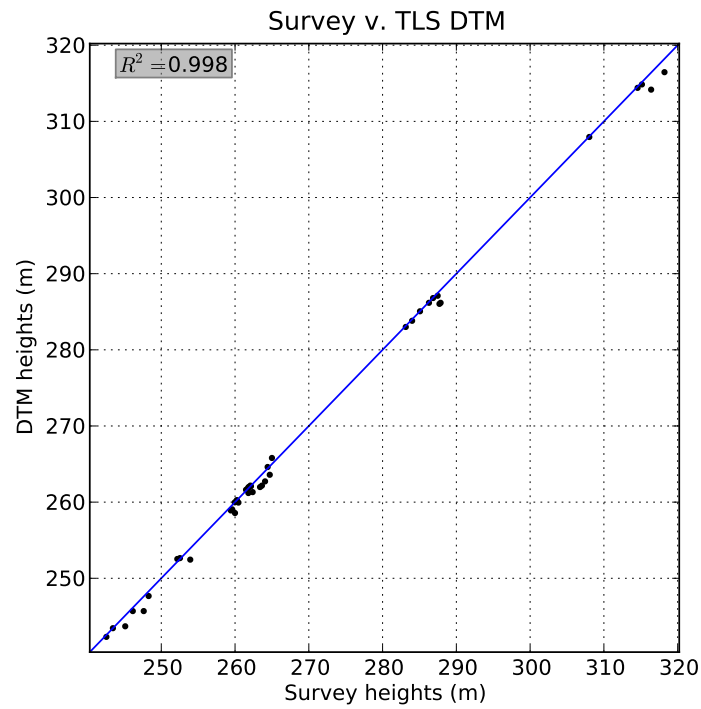
(a)
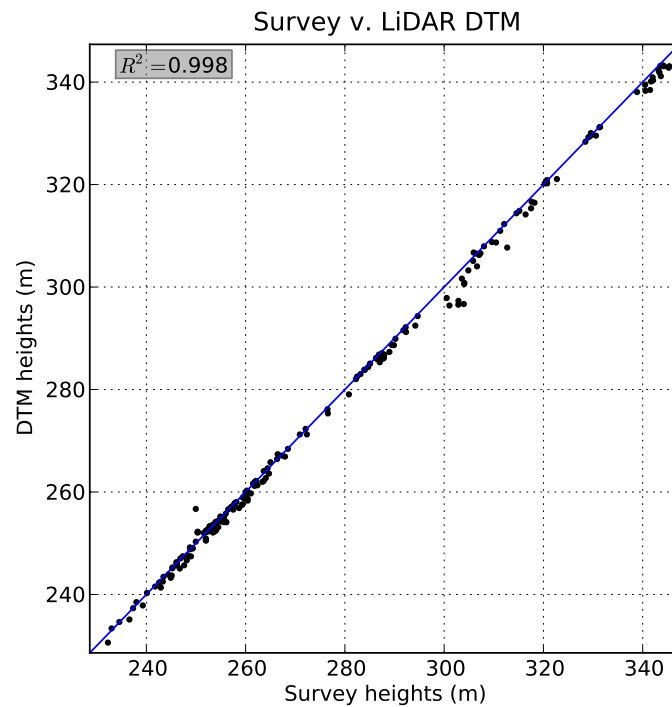
(b)

Figure 7.2: The survey data compared to the DTMs derived from the (a) TLS and
(b) LiDAR data. Heights are metres above sea-level.
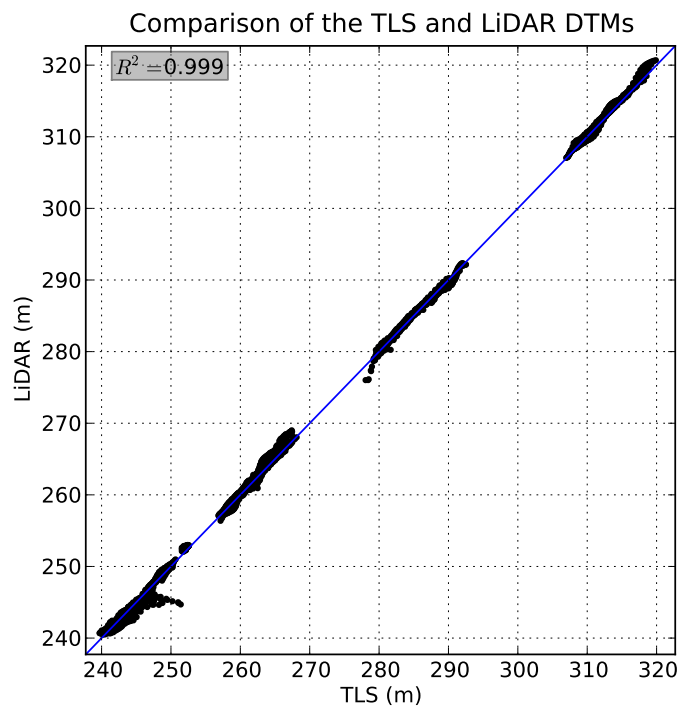
Figure 7.3: Correspondence between DTMs derived from the TLS and LiDAR datasets respectively. The outliers at the lower end of the graph are caused by a non-ground point, which was missed during filtering and created an artificial peak in the surface of the DTM in its vicinity.

concentrated in the upper parts of the canopy and also on the ground. Therefore, the forest structure represented by the LiDAR profile was biased towards the top of the canopy and under represented the canopy depth and volume.
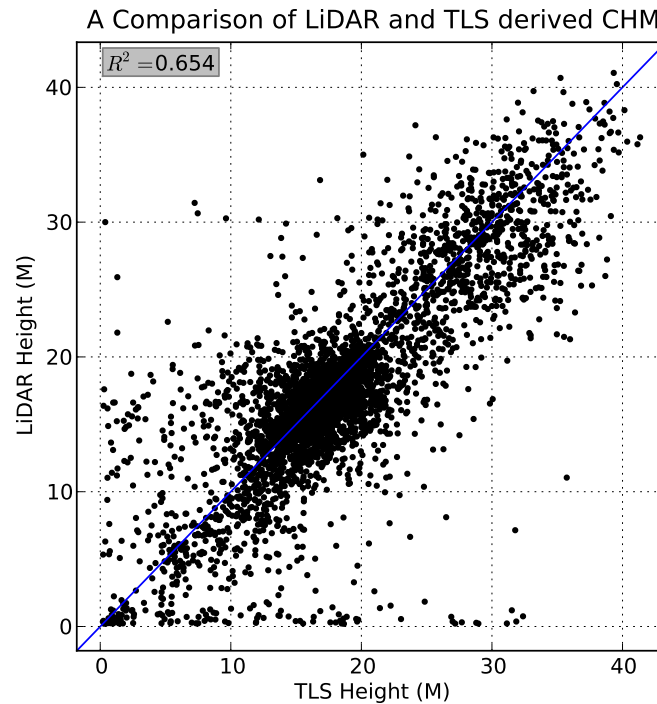
Figure 7.4: Comparison of canopy height models derived from TLS and LiDAR data respectively.

7.3.4 Forest structure

To understand the differences in measured canopy height and profiles and interpret the structures represented by the two systems, the TLS and airborne LiDAR data were compared visually. Two-dimensional plots, using the X and Z axis, were used for visualization where variable width slices were taken through the TLS data such that each slice contained approximately 100,000 TLS points. The intersect-

ing airborne LiDAR points were identified for these slices and plotted alongside the TLS data. Additionally, for the data within each slice, binned profiles were generated using a vertical bin width of 1 m and visualized alongside the point data (Figure 7.5). The plots demonstrated the penetration of both the TLS and LiDAR data through the forest canopy and their capacity to represent the vertical structure within the forest volume. Figure 7.5a illustrates a forest stand dominated by Douglas fir (LV7). The dense upper canopy results in an offset of the resulting profile structures. The profiles for the TLS and airborne LiDAR were similar to one another in shape and form but neither had captured the full vertical profile of the canopy and the TLS data underestimated the canopy height. For an oak stand (LV9; Figure 7.5b) with a dense canopy, the LiDAR pulse was able to penetrate through the more open canopy but the form of the generated profiles differed between the two. The TLS profile was biased towards the bottom while the airborne was biased towards the top of the canopy. Therefore, these profiles would be interpreted as representing different forest structures. For an oak stand with an open canopy (LV8; Figure 7.5c), the laser returns were observed throughout the canopy resulting in profiles with a strong correspondence even though sensors characteristics and viewing angles differed.
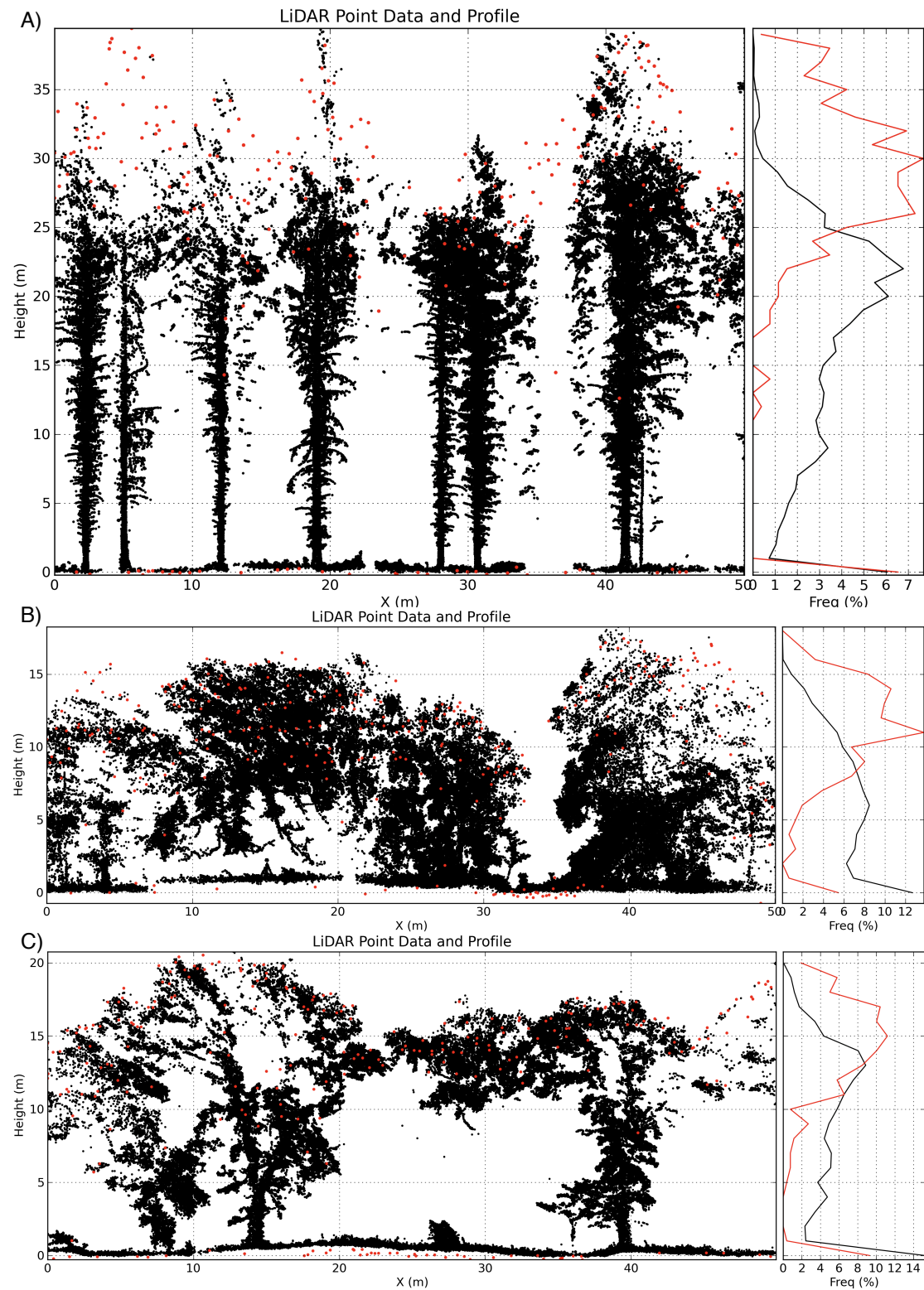
Figure 7.5: Comparison of TLS (black) and LiDAR (red) data points and profiles. A) LV7: dense Douglas Fir stand, B) LV9: dense sessile Oak canopy, C) LV8: open sessile oak canopy

7.4 Discussion

7.4.1 Retrieval of forest structural attributes from TLS data

Despite the resolution of the TLS, the number of pulses reaching the upper canopy was significantly reduced in denser forest stands because of occlusion from trunks, branches, and leaves. The resulting shadowing had a signifiant effect on the profiles and therefore the structures represented (Henning and Radtke, 2006b). To overcome the problem of occlusion, multiple scans from different view points could be captured and the individual scans registered for use as a single combined point cloud. However, this solution is time consuming during data capture, although options should improve with new developments in sensor design (e.g., multiple return or full waveform systems). The Leica ScanStation 2, which was used for this study, only records the first return and in complicated environments with many small overlapping elements (e.g., forest), the vegetation elements behind cannot be observed. Therefore, the amount of information that can be obtained is limited.

Measurement of the forest vertical profile from the TLS is limited to visual interpretation. However, these data provide good representation of the individual vegetation elements occurring within the forests. Therefore, future studies will focus on extraction and direct measurement of key structural attributes (e.g,. trunk diameter; Gorte and Pfeifer, 2004) and the development of relationships between the point cloud distribution and canopy metrics (e.g., canopy gap fraction, leaf area index, foliage projected cover and branch angles). The present study in-

dicates that the TLS is best used for retrieving attributes that are closer to the scanner (e.g., dbh) with the exception of more open forest types where penetration to the upper canopy can be achieved.

7.4.2 Retrieval of structural attributes from airborne LI-DAR

From the airborne LIDAR, a close correspondence with the maximum tree height derived from the TLS data where penetration was sufficient to reach the upper canopy was observed. However, descriptors such as canopy depth and the number of layers (e.g., sub-canopy and understory) were either significantly underrepresented or not represented at all within the data. Generally, the height estimates were considered to be more accurate than those obtained using TLS data. However, because of the lower sampling rate of the airborne LiDAR, the upper canopy was not always sampled and therefore the measured top of canopy heights could be underestimated (e.g., Figure 7.5a; Tickle et al., 2006b; Hyppae et al., 2008).

In terms of within canopy structures, reliable profiles were only extracted for the top half or third of the canopy, depending on the density of branches and foliage in the canopy. Therefore, reliable measures of canopy parameters such as depth or layers could not be retrieved from these data, although the profiles do illustrate differences between the dominant forest structural types (Figure 7.6).
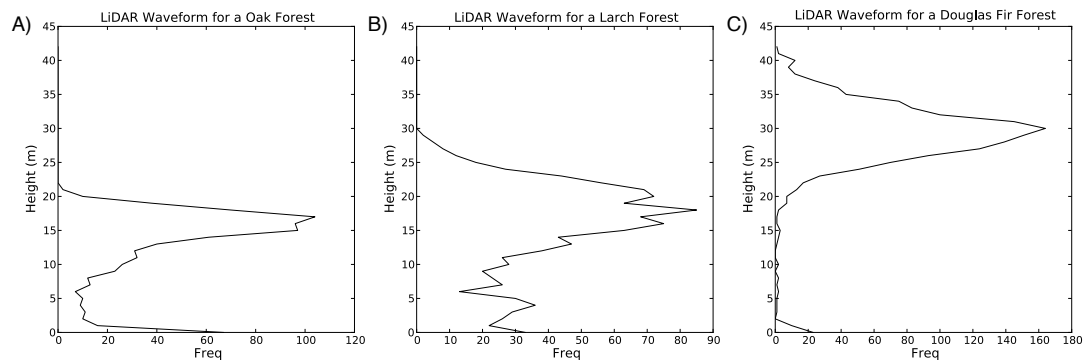
Figure 7.6: Comparison of LiDAR vertical canopy profiles for a) Oak, b) Larch and c) Douglas Fir woodlands.

7.4.3 Parameterization of the canopy vertical profile

The results here differed from those obtained from previous work (e.g., Andersen et al., 2005; Hyppae et al., 2008), which have demonstrated the ability to extract various canopy parameters (e.g., canopy depth). However, these studies used data acquired with higher sampling rates and hence the point density was increased significantly. The research presented in this study has demonstrated that low sampling density airborne LiDAR data are primarily characterizing the upper sections of the canopy while TLS data provide a better representation of the lower sections. These discrepancies are largely attributable to the different viewing geometries.

However, these datasets might be more comparable if higher numbers of pulses/returns were extracted from the full waveform data and one possibility for future work therefore consists of investigating the potential of these data at other sites using improved pulse extraction algorithms (e.g., Lin et al., 2008).

Further research is also needed to better establish the influence of changing LiDAR system specifications, and specifically point density on the retrieval of structural

attributes. The use of TLS data acquired at a similar time as the airborne LiDAR is recommended in such investigations in order to independently assess the degree of signal attenuation between the top of the canopy and the ground. The degree of attenuation in itself might provide a useful measure of canopy density (Wright et al., 2008).

While the comparative profiles of extracted TLS and LiDAR waveforms shown in this study are interesting in itself, they do not allow a parameterization of the canopy vertical profile and future research should also concentrate on the extraction of quantitative measures of forest structure at the site from the data available. This would be particularly interesting with regard to the different woodland types present in the dataset and hence offers an opportunity to quantify structural variation between forests of various species composition. An integration of the two datasets should be considered, to explore the possibilities for mutual compensation of their respective limitations (Tansey et al., 2009).

Potential further analyses of the data therefore should include the following:

1. The thresholds of canopy openness should be related to dominant forest species and growth stage or maturity. The proposed scale of openness should be further reviewed with regards to its suitability.

2. Quantification of signal attenuation of either sensor related to canopy openness, depth and density, as well as forest species composition.

3. Possible fusion of the waveforms extracted from TLS and LiDAR data in order to compensate for the respective upward and downward signal attenuation. For this the decreasing point density of the TLS with increasing distance from the scanner needs to be calculated and the different point densities of both sensors have to be compensated for.

4. Refinement of the canopy height model through integration of the TLS data and utilization of known allometric relationships for the calculation of forest biomass from tree height.

5. If the resolution of the TLS data allows identification of diameter at breast height (dbh) or basal tree areas then this would allow further precision in any biomass calculation (Ni-Meister et al., 2010).

6. Vegetation density at regular, ecologically meaningful height intervals could be calculated for the different sites by assessing and comparing horizontal as well as vertical profiles of selected sites.

7.5 Conclusions

For a range of temperate forest structures, comparison of TLS and airborne LiDAR concluded that:

1. The height of individual trees was identified to a higher degree of accuracy using airborne LiDAR when compared to TLS data. This was attributed to the inability of the TLS to penetrate the upper sections of the canopy. The 2 m post spacing of the airborne LiDAR led to some loss of returns from the crown tops and an underestimation of height.

2. The full waveform LiDAR penetrated the forest canopy to retrieve ground returns consistently across all the forest types represented in this study.

3. The ability to characterize the full canopy was limited for both datasets as the majority of points were associated with interaction with elements closer

to the sensor. This resulted in insufficient penetration to characterize the remaining parts of the canopy.

4. Similarities between the observed structures was greatest for more open broadleaved forests.

5. Future work is focusing on the use of the RAW full waveform data rather than decomposing the signal to a series of discrete returns.

This chapter has highlighted a number of issues associated with the retrieval of structural attributes through the interpretation of vertical profiles from TLS and airborne LiDAR. Even so, information on forest structure can be extracted. In particular, TLS represents an opportunity to extract individual elements from the canopy, such as stem diameter and branch distributions. Airborne LiDAR needs to be captured at high point densities and new methods which are directly applied to the RAW full waveforms data should be sought to allow further extraction of structural information.

Chapter 8

Forest structure associations with bird distributions

8.1 Introduction

As indicated in Chapter 7, airborne LiDAR provides unique information on the three-dimensional structure of forests, including the height, openness and the distribution of plant elements such as branches and trunks within the vertical profile. The inclusion of such information with the two-dimensional information on the distribution of forests can significantly enhance the capacity to assess distribution of biodiversity elements (particularly mammals, birds and insects) across the Welsh landscape. The Nextmap Intermap DSM is regarded as unsuitable for this purpose because of inaccuracies in the retrieval of stand height as well as ground returns and the inability to retrieve information on, for example, the number of layers within the forest vertical profile (i.e., upper canopy, sub-canopy, understory

(< 10 m) and shrub layer (< 2m)).

Airborne LiDAR, particularly if acquired at a finer (< 1m) post spacing, are however recommended although these data are unlikely to be acquired in large quantity in the foreseeable future due to the high costs involved and the large area needed to be covered. However, with sufficient justification, data may be acquired. For this reason, this chapter focuses on demonstrating the potential of using airborne LIDAR for assessing three-dimensional elements of biodiversity, focusing specifically on the bird species typical to forests, woodlands and the fridd in Wales. The fridd is a complex mosaic of habitats that occurs at the margins of the upland moorlands and typically consists of bracken, shrub (e.g., gorse, blackthorn) and scattered trees (e.g., hawthorn, mountain ash).

The chapter is structured as follows. Section 8.2 outlines a dataset of bird populations that was acquired for Lake Vyrnwy forests during the summer of 2006 using techniques adopted in the British Trust for Ornithology's (BTO) Common Bird Census (CBC). Section 8.3 outlines how these observational data, LiDAR structural attributes and profiles were extracted for a range of species common to woodlands. Section 8.4 describes and compares typical profiles for forest types common to the study site whilst Section 8.5 considers structural attributes associated with different bird species and discusses these in relation to forest type and the habitat (structural) preferences of these species. Section 8.6 discusses the utility and limitations of using structural information derived from LiDAR as input to species distribution models. Section 8.7 then outlines optimal approaches for integrating the three-dimensional information from LiDAR with the satellite habitat mapping for quantifying bird species diversity across the wider landscape in Wales.

8.2 Bird species data

8.2.1 The Common Bird Census

The British Trust for Ornithology (BTO) initiated the Common Bird Censuses (CBC) with the primary aim of establishing baseline distributions of breeding birds during the spring and summer periods against which to assess changes in population and habitat use over extended periods (Marchant et al., 1990). This method involves visits of pre-defined areas by personnel skilled in the recognition of birds, both visually and from calls, during which the location of each sighting and information on bird activity (e.g., nesting, territorial fighting, flying) is recorded. The methods of the CBC are well established (Snow, 1965; O'Connor and Marchant, 1990; Fuller et al., 1985). In 2000, the CBC was superseded by the Breeding Bird Survey (BBS) which records data along line transects rather than the territory-mapping method employed by the CBC (Freeman et al., 2003).

8.2.2 RSPB Lake Vyrnwy Survey

Using the original CBC methods, the RSPB conducted as many as six repeat surveys of birds between March and July 2006 within a range of small woodlands surrounding Lake Vyrnwy. These included coniferous (fir, spruce and larch) plantations at various stages of maturity and semi-natural broadleaved woodlands dominated either by oak, birch or beech or of mixed species composition. For the period 2006, RSPB staff made 6221 observations of 72 bird species.

8.2.3 Data used

Through reference to existing Ordnance Survey mapping and VEXCEL aerial photography, the locations of all 6221 bird sightings were digitized within a Geographical Information System (GIS) and attributed with information on bird activity (e.g., nesting, flying, fighting). However, many observational data were subsequently excluded for the following reasons:

1. They represented water birds (e.g., Mallard, Kingfisher, Dipper, Grey Wagtail) or birds (e.g., Raven) flying overhead and not within or in close proximity to the forest. The only exception was Buzzards, where most observations were associated with birds flying in proximity to forests.

2. They were observed on less than 20 occasions although some that were rare or elusive (e.g., Cuckoo, Crossbill, Firecrest, Green Woodpecker, Jay, Tawny Owl and Willow Tit) were retained.

3. They were located outside of the area captured in the LiDAR overflight.

The final dataset therefore included 4906 observations of 36 species, with 7 species having less than 20 observations (Table 8.1). The location of the observations is given in Figure 8.1.

8.3 Extraction of data

LiDAR data were extracted to associate structure attributes with different forest types, but also the observation locations of different bird species. More specifically, data were extracted from:

1. Regions representing common forest types and structures (conifer plantations, mature semi-natural woodlands of varying species composition, dense and scattered scrub), with areas selected identified through classification of each of the forest types occurring (see Chapter 6), as well as field visits.

2. Locations associated with observations of birds of different species. In this latter case, the number of observations ranged from two (for cuckoo) to 702 (chaffinch).

The extractions from different forests types, as classified using the rule-based approach (Chapter 6), were undertaken specifically to give an indication of differences in the mean canopy height, canopy openness and canopy profiles (the distribution of canopy elements). For the forest types, data were extracted from large polygons representing discrete areas of each type. However, for the bird observation locations, data were extracted from buffered areas of 20 m radius to overcome limitations connected to low point density, as described in Chapter 7.

8.3.1 Forest type classification

Within the area of the LiDAR overflights, a wide range of forest types were classified but the most extensive were coniferous plantations (primarily Sitka Spruce, Douglas Fir and European Larch) and broadleaved woodlands dominated by oak, ash, birch or beech or combinations of these. The forests were at various stages of growth and maturity and included young (< 10 year old) coniferous forests planted on previously felled areas.

Table 8.1: Bird species associated with semi-natural vegetation with woody components

BTO code	Common Name	Scientific Name	Count
B	Blackbird	*Turdus merula*	289
BC	Blackcap	*Sylvia atricapilla*	192
BF	Bullfinch	*Pyrrhula pyrrhula*	34
BT	Blue Tit	*Parus caeruleus*	250
BZ	Buzzard	*Buteo buteo*	35
CC	Chiffchaff	*Phylloscopus collybita*	68
CH	Chaffinch	*Fringilla coelebs*	702
CK	Cuckoo	*Cuculus canorus*	8
CR	Crossbill	*Loxia curvirostra*	2
CT	Coal Tit	*Parus ater*	146
FC	Firecrest	*Regulus ignicapillus*	6
G	Green Woodpecker	*Picus viridis*	4
GC	Goldcrest	*Regulus regulus*	104
GS	Great Spotted Woodpecker	*Dendrocopos major*	76
GT	Great Tit	*Parus major*	143
GW	Garden Warbler	*Sylvia borin*	45
J	Jay	*Garrulus glandarius*	14
LR	Lesser Redpoll	*Carduelis cabaret*	33
LT	Long-tailed Tit	*Aegithalos caudatus*	38
M	Mistle Thrush	*Turdus viscivorus*	27
MT	Marsh Tit	*Parus palustris*	21
NH	Nuthatch	*Sitta europaea*	97
PF	Pied Flycatcher	*Ficedula hypoleuca*	135
R	Robin	*Erithacus rubecula*	521
RT	Redstart	*Phoenicurus phoenicurus*	145
SF	Spotted Flycatcher	*Muscicapa striata*	56
SK	Siskin	*Carduelis spinus*	64
ST	Song Thrush	*Turdus philomelos*	201
TC	Treecreeper	*Certhia familiaris*	91
TO	Tawny Owl	*Strix aluco*	7
TP	Tree Pipit	*Anthus trivialis*	43
WO	Wood Warbler	*Phylloscopus sibilatrix*	94
WP	Wood Pigeon	*Columba palumbus*	91
WR	Wren	*Troglodytes troglodytes*	646
WT	Willow Tit	*Parus montanus*	4
WW	Willow Warbler	*Phylloscopus trochilus*	474
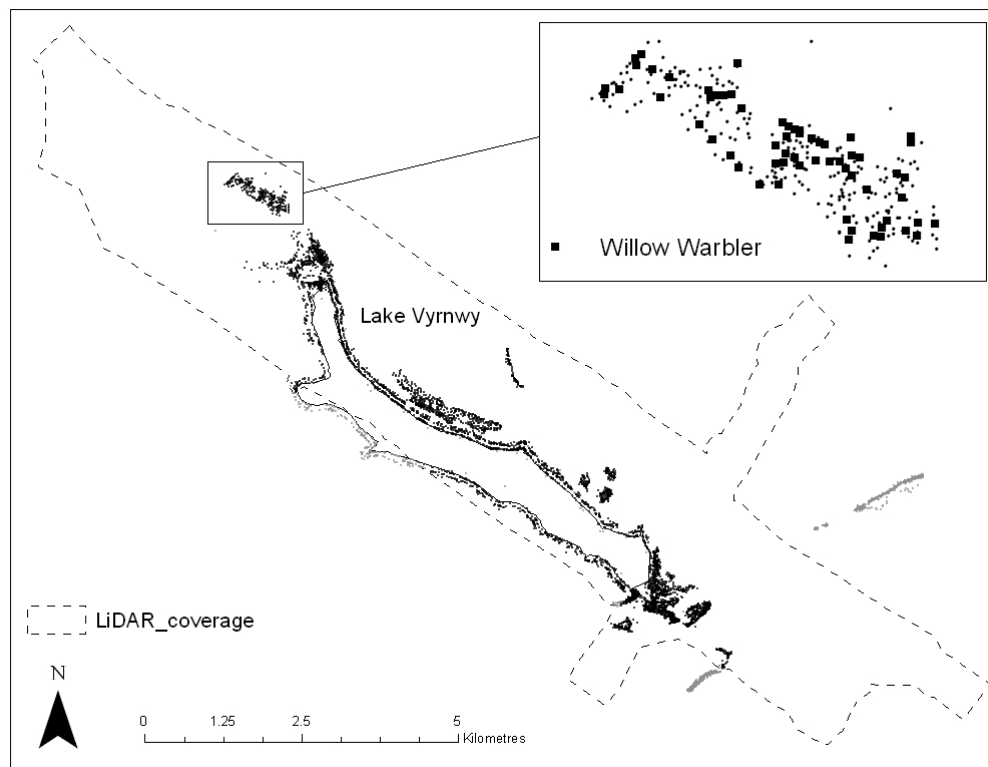
Figure 8.1: The location of RSPB bird observations around Lake Vyrnwy

8.3.2 Canopy height and openness

As measures of canopy height, both the maximum and mean were extracted from the polygons associated with discrete forest stands and observation locations. A measure of canopy openness, the local maximum Height Scaled Crown Openness Index (HSCOI; Lee and Lucas (2007b)) was also calculated for each polygon. The HSCOI translates point measurements into a measure of relative penetration of LiDAR pulses by scaling these from the top of the canopy. Values range from 0 (no penetration) to 100 (full penetration). The HSCOI is a weighted summation of a proxy variable of the inverse of canopy density (i.e., 1/number of voxels (n_{voxels}) containing returns per 1m^2 vertical column). The weighting used is the relative height of the voxel (H_{voxel}) with respect to the maximum height (H_{max}) within an n x n kernel window such that:

$$HSCOI = \sum_{n=1}^{n_{voxels}(i)>0} ((\frac{H_{max} - H_{voxel}}{H_{max}}) * \frac{1}{n_{voxels}}) * 100 \qquad (8.1)$$

where the summation uses only those voxels that contain LiDAR returns. This is achieved with a variable (i) that counts the LiDAR voxels (containing returns) up to the maximum number of levels (i.e., maximum height of the column). The maximum height can also be that of the stand, although this was not used here.

8.3.3 Canopy profiles

Extraction of canopy profiles from bird observation points was undertaken to establish whether these were reflective of the habitat preferences of species. For each of the 4906 bird observations, data were extracted from areas of variable area

(circles of, respectively, 2, 5, 10 and 20 m radius), with each area centred on the location of the observed individuals. From each, the number of points in each 0.5m height interval in turn (up to a maximum of 50 m) was summed as:

$$N_j = \sum_{i=1}^{i=n} O_i \qquad (8.2)$$

where N_j represents the count of LiDAR returns in height interval j (range 0.5 to 50 m) for all observation points (O) with n being the number of observations for the bird species considered. Once extracted, the data were combined to produce a frequency profile such that:

$$N_p = N_i / \sum_{j=0}^{j=50} N_j * 100 \qquad (8.3)$$

where N_p represents the number of returns in each 0.5m height interval as a percentage of the total. The profiles represented the distribution of scattering elements within the vertical column.

Comparison of the profiles extracted suggested that areas with radii of 2 and 5m respectively were too small to give representative profiles, with no clear distinction between layers (Figure 8.2). However, those from 10 m and 20 m radii were more similar and differences between the upper canopy, subcanopy, understory and shrub-layer were discernible. As the profiles based on a 20 m radius fell largely within the forest area, this buffer size was used for all extractions, although some overlap with different forest types (e.g., coniferous plantation, broadleaved forest) and other land covers (e.g., grasslands at various levels of improvement) was evident.
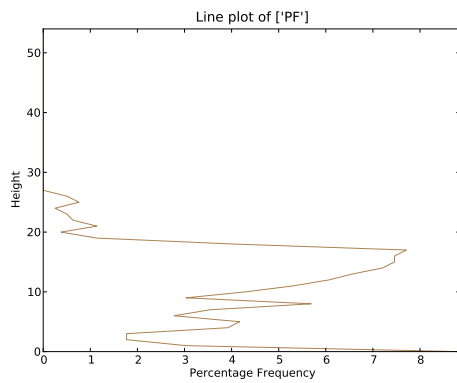
(a) 2m radius
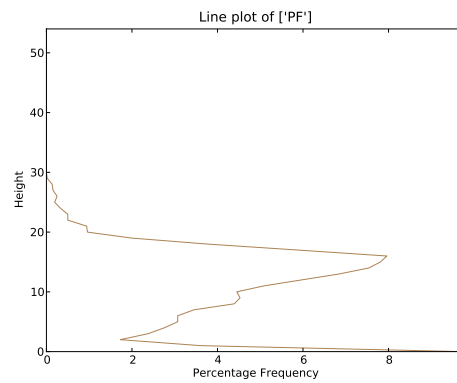
(b) 5m radius
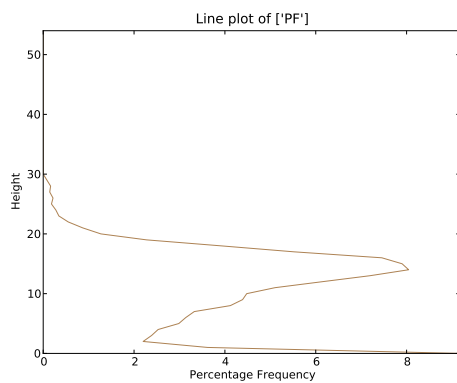
(c) 10m radius
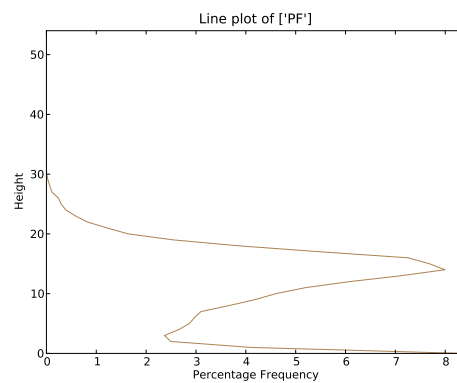
(d) 20m radius

Figure 8.2: Vertical profiles based on LiDAR points extracted from circular areas of 2m, 5m, 10 m and 20 m radius and associated with the locations of pied flycatcher observations (Sessile oak woodlands)

8.4 Structural characteristics

8.4.1 Height (mean and maximum)

The image representing the height of forests at Lake Vyrnwy is given in Figure 8.3. The tallest forests (> 35m) were associated with Douglas Fir plantations, although the range of height classes reflected the different age classes of plantations in the area. The majority of broadleaved forests were between 10 and 35m in height, with the tallest associated with beech forests north of Lake Vyrnwy.
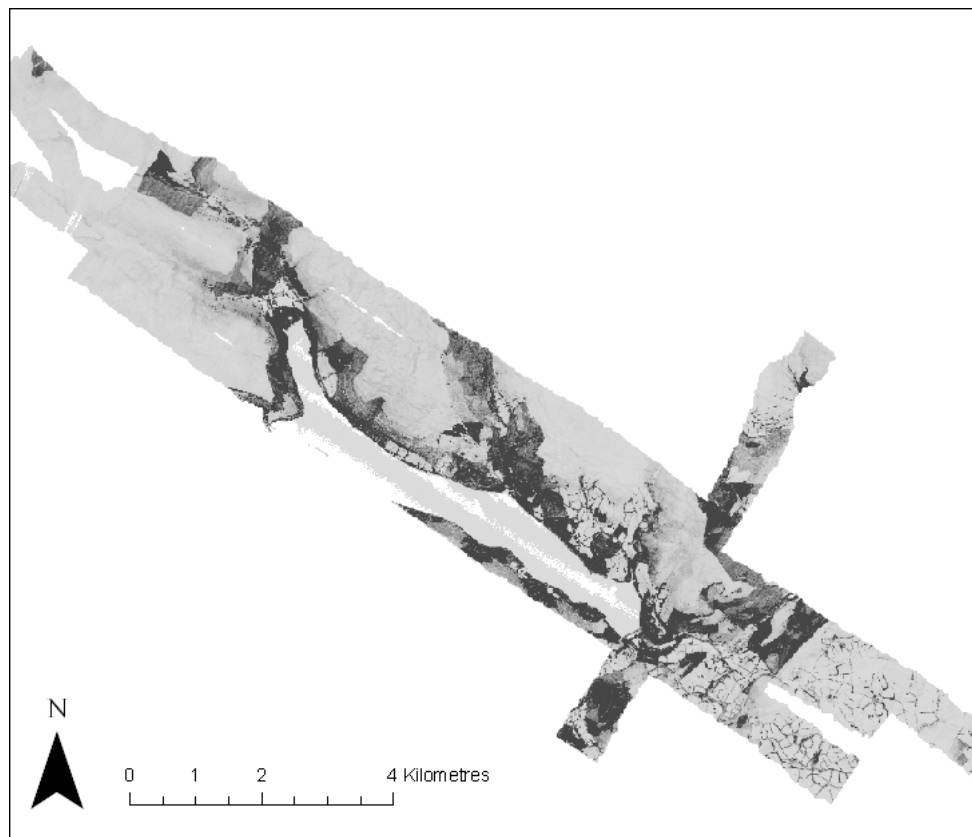
Figure 8.3: Tree height at Lake Vyrnwy (ground returns are not filtered out and are hence shown in light grey)

8.4.2 Openness

The image representing the openness of forests at Lake Vyrnwy is given in Figure 8.4. Most forests supported an openness of < 40 %, with greater openness associated with the sessile oak woodlands. Within the fridd zone, extensive areas of bracken, gorse and scattered or dense tree scrub were observed, with these generally being < 10 m in height. These forests were also more open (typically > 80 %) compared to the forest areas. The younger coniferous plantations observed were also less than 10 m in height.
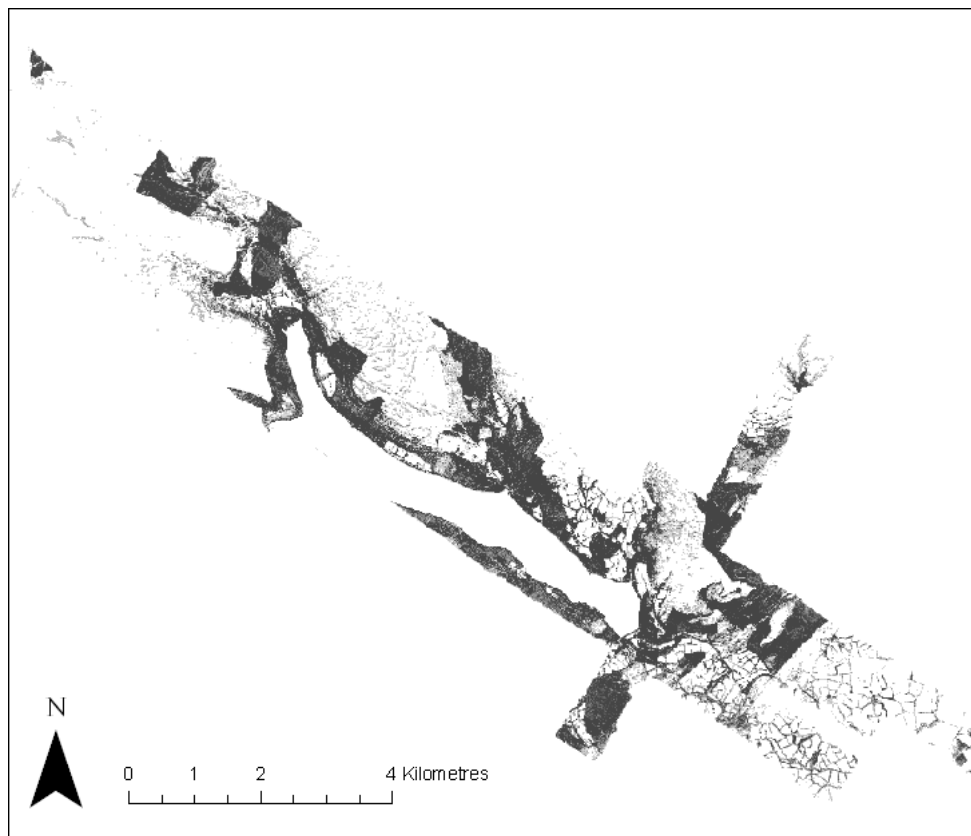
Figure 8.4: Canopy Openness at Lake Vyrnwy

8.4.3 Canopy profiles

Examples of canopy profiles for a range of forest types are given in Figure 8.5. Monospecific and relatively mature coniferous plantations (typically dominated by Douglas Fir, Sitka Spruce and Scots Pine) tended to be single layered with no sub-canopy and a limited understory. The majority of returns from within these forests were in the height range 20 - 30 m, 15 - 25m and 15 - 20 m respectively. Profiles associated with approximately 30 m high larch plantations indicated an understory (of <10 m), which was attributed to regrowth beneath the upper canopy. An example of a regrowth conifer plantation (10 m in height) is also given for comparison. For broadleaved woodlands, profiles were generated for woodlands dominated by oak, beech, birch and willow/alder (wet woodlands). Some differences were observed between sessile oak woodlands of lower stature (< 20 m) and with and without a shrub layer (Figures 8.5(g) and 8.5(h)). Within woodlands dominated by either beech and birch and also the wet woodlands, neither the shrub layer nor understory were well established which reflected field observations (Figure 8.5(i) and 8.5(j)). Within woodlands dominated by mountain ash in the fridd, most of the trees and associated shrub were < 15m in height with a few larger individuals occurring. In each case, the profiles reflected observations in the field although caution needs to be taken in their interpretation, given the discrepancies observed between the profiles obtained using the TLS and airborne LiDAR (see Chapter 7).

(a) Douglas Fir   (b) Sitka Spruce   (c) Scots Pine

(d) Larch   (e) Regrowth   (f) Gorse Scrub

(g) Mixed Oak with sparse understory   (h) Mixed Oak with understory   (i) Beech forests

(j) Birch   (k) Wet woodlands   (l) Mountain Ash
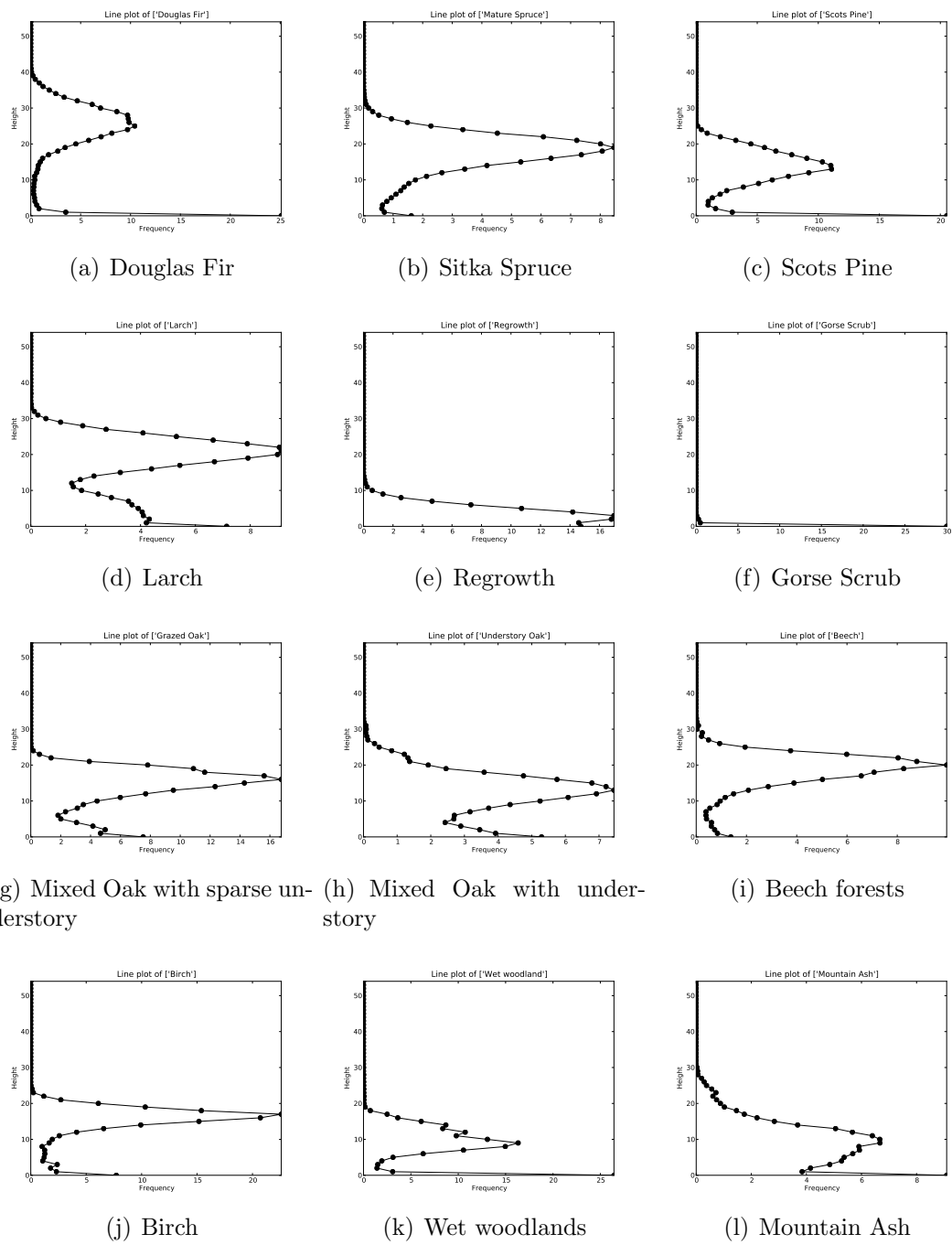
Figure 8.5: Canopy profiles of common forest, woodland and shrub types. Dominant species are indicated where appropriate.

(a) Sparse understory

(b) Understory

(c) Birch woodland

(d) Beech woodland

Figure 8.6: Panoramic photographs of sessile oak woodland with a) sparse understory and b) understory, c) birch and d) beech woodlands

8.5 Links between forest type and structure and bird species distributions

8.5.1 Forest type

As expected, general associations between forest type and bird species occurrence were observed. For example, within the mature oak forests (Figure 8.7), common species included pied flycatcher, green woodpecker, nuthatch, redstart and greater spotted woodpecker. This was in contrast to the mature spruce forests where the most commonly observed species were firecrest, siskin and goldcrest. These species are typically associated with coniferous forests. Within mixed forest types, the presence of bird species more typical to coniferous forests was generally dictated by the existence of coniferous tree species within the stand.

8.5.2 Forest structure

Height

With increases in mean height (Figure 8.8), bird species typically associated with woodland communities were more prominent, with these including tawny owl, nuthatch, treecreeper and greater spotted woodpecker. Some species (e.g., spotted flycatcher and chiff chaff) were associated with taller stands, although observations were generally at the margins with cleared or more open areas. A number of species occurring in the taller forests generally favoured the understory and ground layers (e.g., blackbird, robin, blackcap, song thrush) and hence were generally not exploiting the full vertical profile. Birds associated with lower stature forests
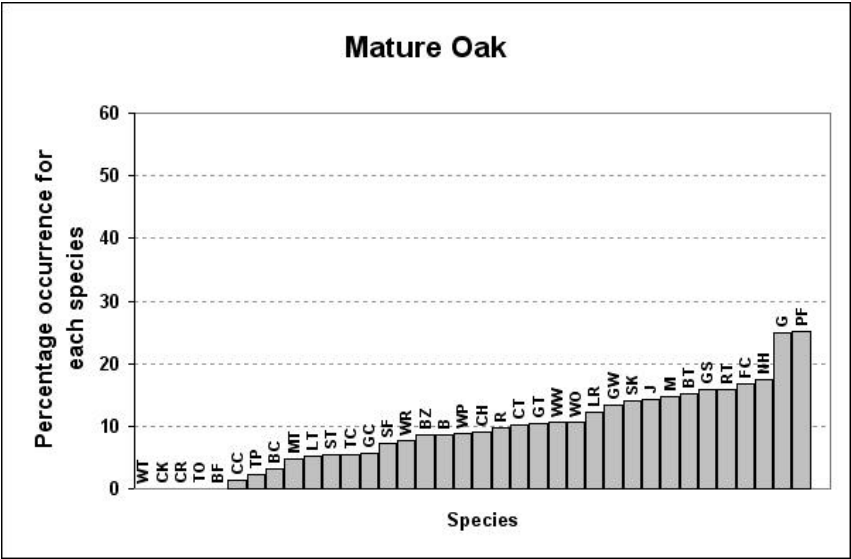
(a)
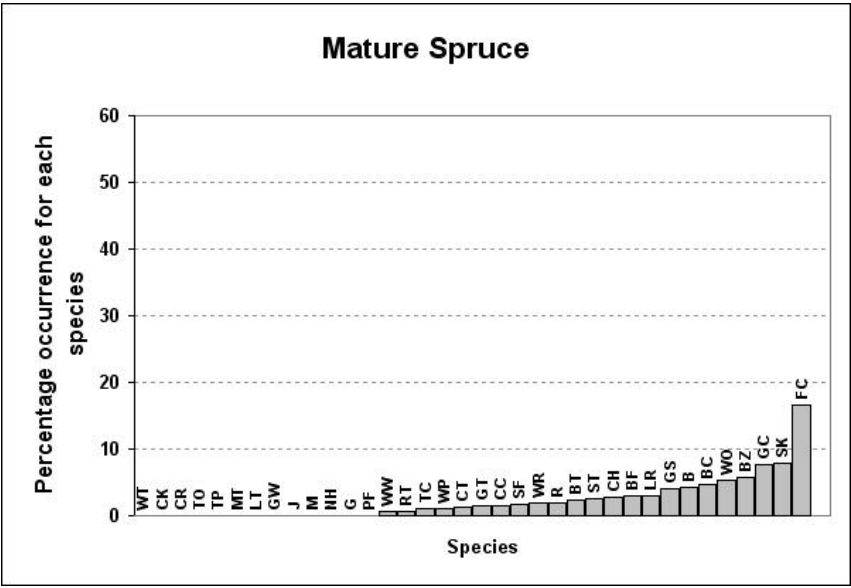
(b)

Figure 8.7: Relative frequency of bird species within (a.) mature oak and (b.) spruce forests.

included tree pipits, green woodpeckers, cuckoo, lesser redpoll, willow warbler and willow tit. However, whilst species such as tree pipit and cuckoo favoured open areas, larger isolated trees were often present. Linkages between tree height and species distributions therefore need to be treated with some caution and should take account of specific use of the forested landscape (e.g., for nesting, feeding, roosting). For all forests, maximum height was less appropriate as a measure because of bias towards larger trees where these existed (Figure 8.9).
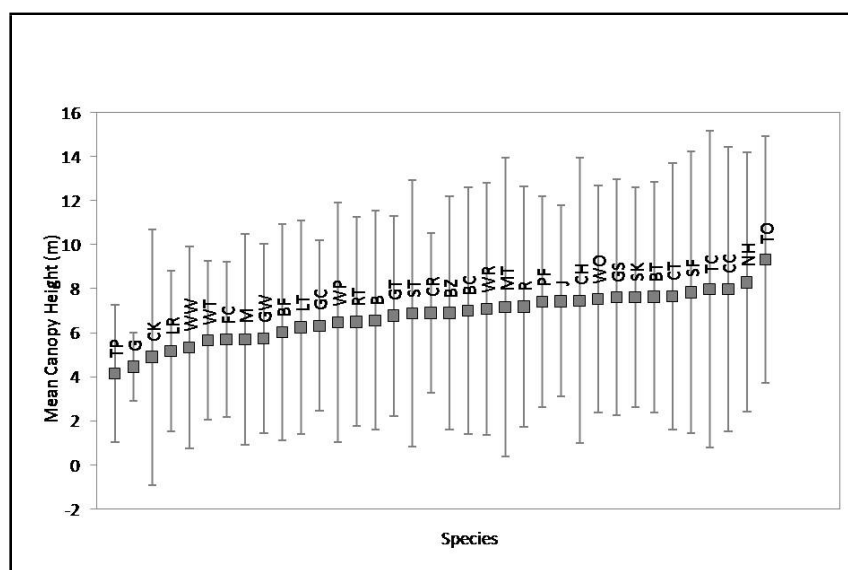
Figure 8.8: Distribution of bird species occurrences within woodlands of increasing mean canopy height

Canopy openness

Species preferring more open canopy forests (Figure 8.10) included jay, mistle thrush, tawny owl, blue tit, lesser redpoll, nuthatch and siskin whilst the more open forests were favoured by firecrest, cuckoo, green woodpecker, tree pipit, carrion crow and whinchat. These observations generally align with known species
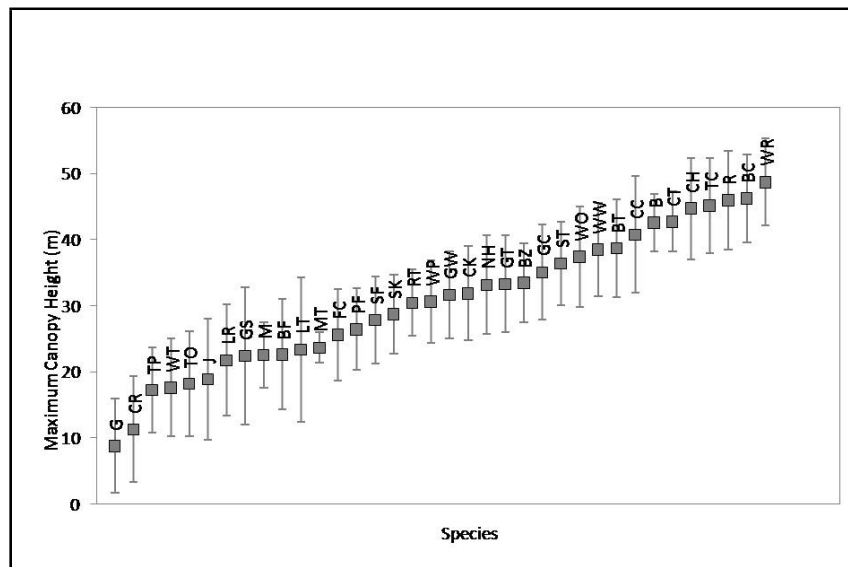
Figure 8.9: Distribution of bird species occurrences within woodlands of increasing maximum canopy height

preferences.

Canopy profiles

For bird species with territories confined largely to the area occupied by forest, woodland or fridd, canopy profiles were generated and compared. Within the coniferous plantations, bird species that were most common included goldcrest, firecrest, siskin and coal tit (Figure 8.11). Firecrest, which has a preference for nesting in tall trees, was found largely within the mature Douglas Fir plantations. Goldcrest and siskin were more common within a lower stature forests, where most of the returns were between 10 and 20 m. These included broadleaved forests with coniferous trees as a component. Coal tits were associated more with forests with a sub-canopy occurring between 10 and 20 m and overstory up to 30-35m.

A large proportion of bird species were more common to the broadleaved forests,
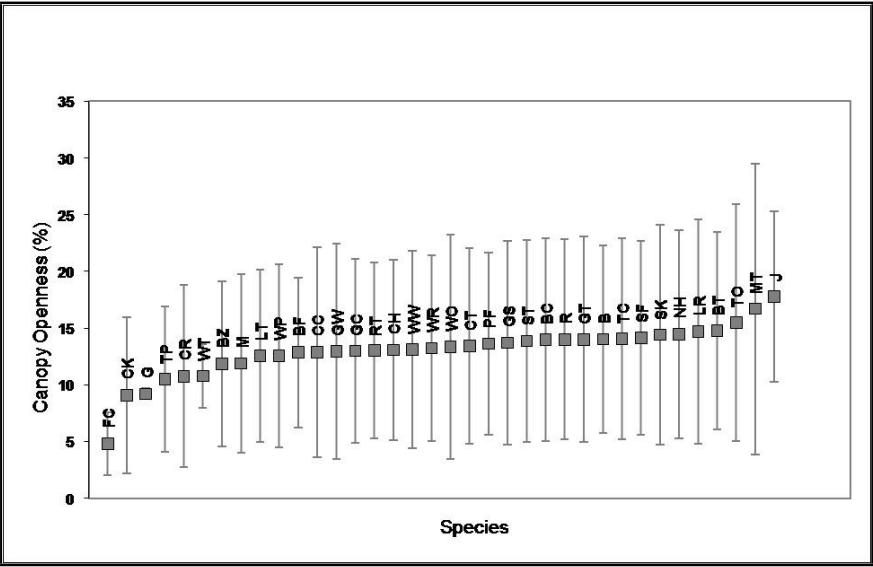
Figure 8.10: Distribution of bird species occurrences within forests of varying canopy openness
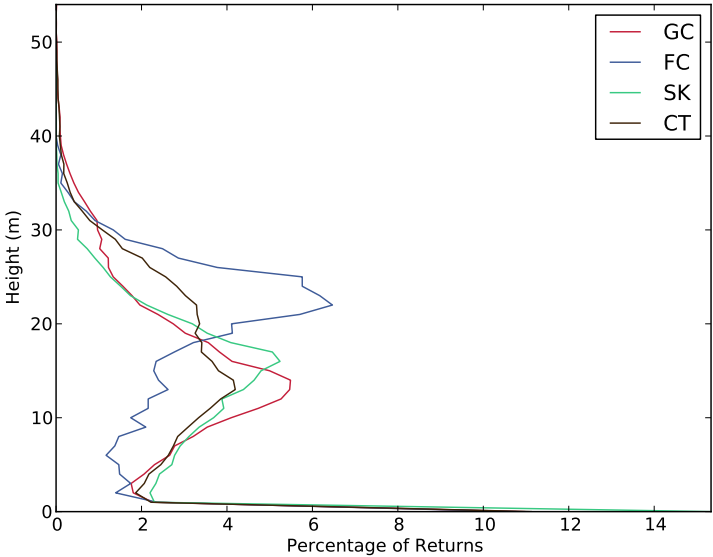
Figure 8.11: The percentage of LiDAR returns by height (m) for goldcrest (GC), firecrest (FC), siskin (SK) and coal tit (CT).

although some frequented coniferous forests. Greater spotted woodpecker, green woodpecker, treecreeper and nuthatch are species that require trees above a certain trunk diameter size in order to breed and also obtain food (e.g., insect larvae). The vertical profiles associated with these four species were remarkably similar with each occurring in forest up to 40 m in height but with a dominant of returns between 10 and 15m (Figure 8.12(a)). These species also preferred a relatively sparse understory. Other species that are typically associated with larger trees and which were observed at Lake Vyrnwy included tawny owl, mistle thrush and wood pigeon (Figure 8.12(b)). These species favoured forests with a more established sub-canopy and understory.

Pied flycatchers, wood warblers and redstarts are typical to upland woodlands in Wales and particularly those dominated by or including sessile oak. Pied flycatchers in particular are common in sheep-grazed woodlands or those with a limited understory. This species nests in holes in trees and hence are more frequent in older woodlands where branch and trunk sizes are sufficiently large. The nesting material often includes honeysuckle and hence the occurrence of this plant within the understory often favours this species. Wood warblers are also common in oak and also taller beech woodlands. This species often remains in the upper canopy but nests on the ground. To access the nest site, individuals move from the upper canopy to the ground by using the lower branches of larger trees but also sub-canopy trees (e.g., beech) as cover. Redstarts prefer more open woodlands and dense to scattered scrub and nest in hollow trees or buildings. The different preferences of these three species were reflected in the vertical profiles (Figure 8.13). In particular, wood warblers were found in taller forests (dominated by beech and/or oak) up to 45m, with a sub-canopy of 10-25m and relatively sparse understory.
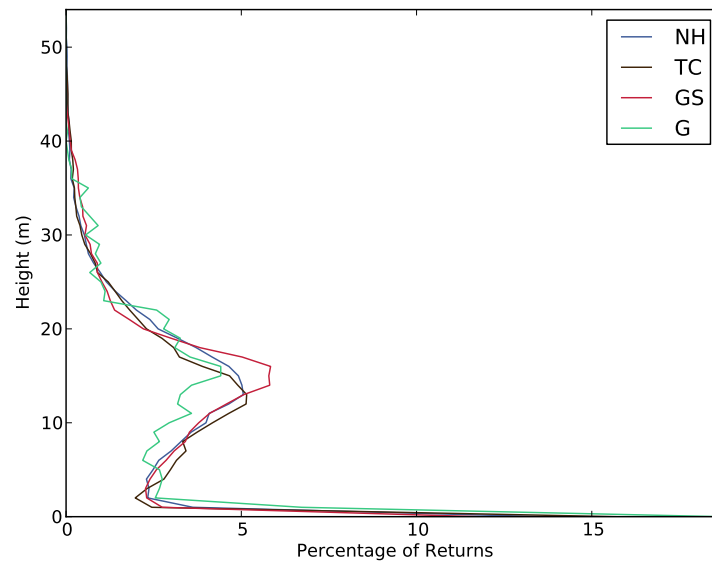
(a)
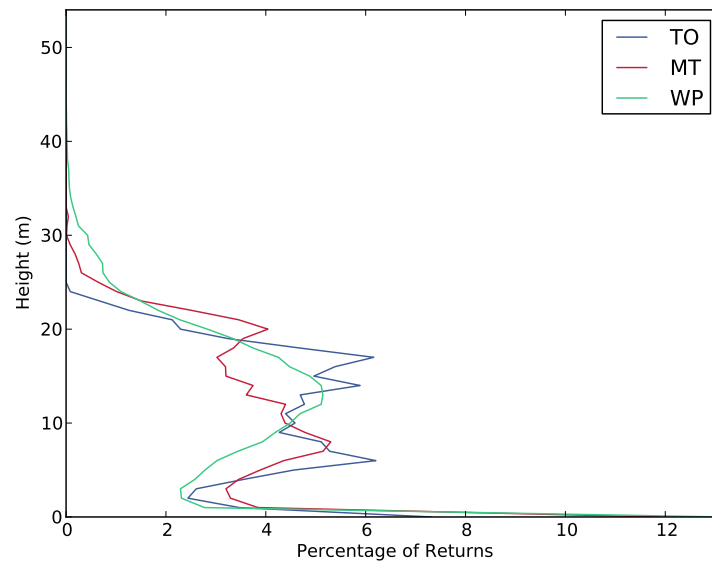
(b)

Figure 8.12: The percentage of LiDAR returns by height (m) for a) nuthatch (NH), treecreeper (TC), greater spotted woodpecker (GS) and green woodpecker (G) and b) tawny owl (TO), mistle thrush (MT) and woodpigeon (WP).

Pied flycatchers and redstarts were found within woodlands of lower stature, with the former associated with those with a reduced understory layer. Redstarts were associated with a more open canopy and a more established understory.
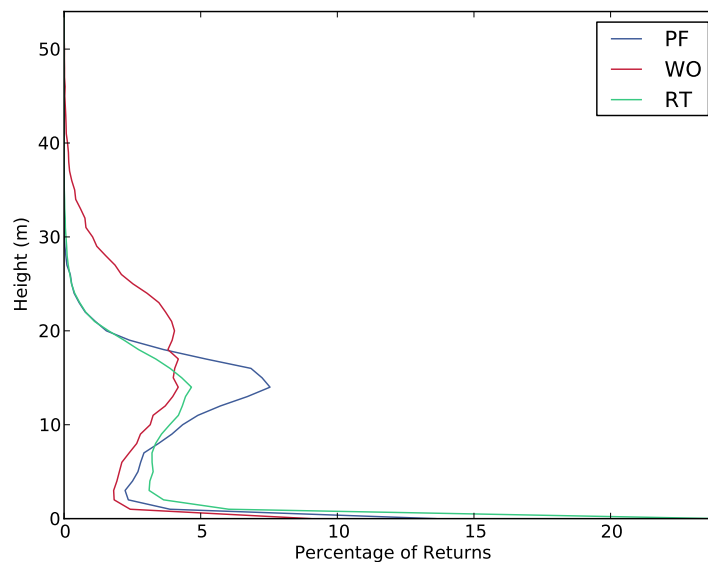
Figure 8.13: The percentage of LiDAR returns by height (m) for pied flycatcher (PF), wood warbler (WO) and redstart (RT).

Blackcap, bullfinch and garden warbler occur across a range of woodland types (coniferous or broadleaved) of varying height but require a dense shrub layer for nesting. Both blackcaps and garden warblers typically nest about 0.5 to 2m above the ground whilst bullfinches often nest 1 - 2m above the ground. Nests are often located in brambles and other dense shrub-layer species. All three species also feed within the understory or lower layers of the canopy. The vertical profiles for these species (Figure 8.14) reflect their occurrence across forest structures ranging from > 40 m high coniferous forest (BC) to lower stature woodlands with an established sub-canopy and understory (including dense scrub).
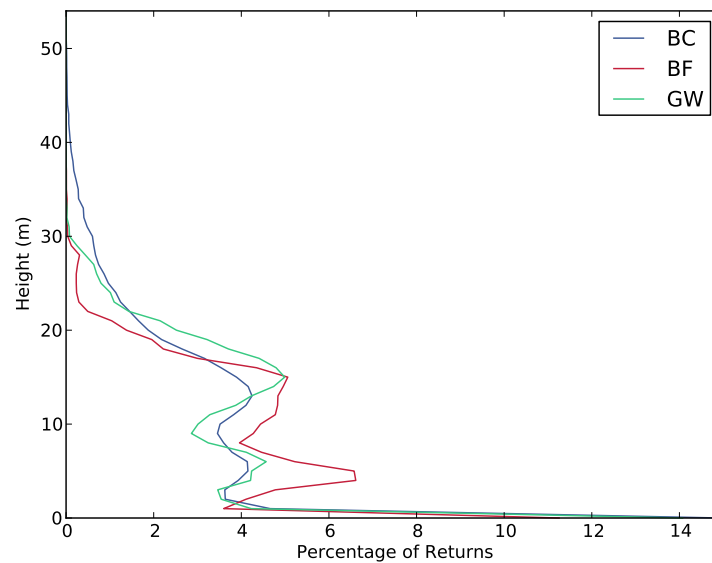
Figure 8.14: The percentage of LiDAR returns by height (m) for blackcap (BC), bullfinch (BF) and garden warbler (GW).

A number of bird species were associated with more open woodlands and scrub (typical to the fridd). Both tree pipit and cuckoo favour open areas with low scrub but scatterings of tall trees, with these including felled coniferous plantations where mature deciduous trees are often retained. Spotted flycatchers also prefer these habitats as well as the edges of forests from where they make frequent flights from their perch, catch insects and then return to the same or a nearby perch. Willow warblers and chiff chaffs are associated with more open forests and often favour willow/alder carr or regenerating forests (including plantations with a high proportion of birch). These preferences are again reflected in the vertical profiles (Figure 8.15), with all indicating a dominance of returns within the lower height classes (with the exception of spotted flycatchers). The profiles reflected the preference of these species for low stature woodlands (including regrowth) and the occurrence of large individual trees but a lack of a distinct overstory.
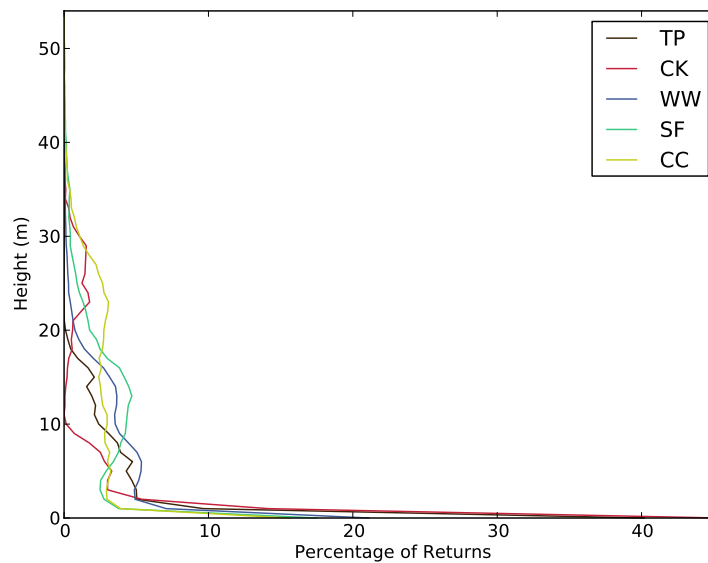
Figure 8.15: The percentage of LiDAR returns by height (m) for tree pipit (TP), cuckoo (CK), willow warbler (WW), spotted flycatcher (SF) and chiff chaff (CC).

A number of bird species were widespread and generalist, occurring across a range of forest types and often associated with human habitation (e.g., gardens, out-buildings, farmyards). As examples, blackbirds and song thrush are woodland birds that are frequent within more open areas. However, these species prefer a dense understory for cover and also for nesting but often sing from tall trees, hence their occurrence within the woodlands that were mature or contained larger individual trees. Robins and wrens are ubiquitous throughout the Lake Vyrnwy forests but typically feed and breed in the lower canopy and ground layers. Chaffinches occur in the upper canopy where they both nest and feed but also make frequent visits to the ground layer. The vertical profiles (Figure 8.16) indicate preference for a sub-canopy and ground layer but also their occurrence across a range of forest statures (including > 40 m high coniferous forests).
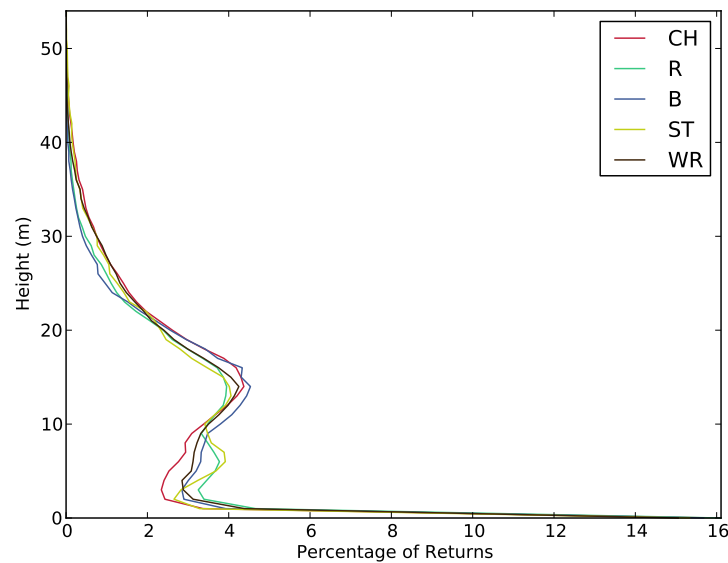
Figure 8.16: The percentage of LiDAR returns by height (m) for chaffinch (CH), robin (R), blackbird (B), song thrush (ST) and wren (WR).

To better illustrate differences between vertical profiles, those obtained for titmice (Paridae) and warbler (Sylviidae) families are compared (Figures 8.17 and 8.18). Great tits and blue tits are common to woodlands, particularly those dominated by oak species which provide an abundance of food (e.g., caterpillars). Long-tailed tits are more characteristic of woodlands and dense scrub of medium height, particularly that dominated by birch, willow and alder. Both marsh and willow tits occur across a range of broadleaved woodlands although favour an understory or shrub layer; both nest at a relatively low level in the canopy. These preferences are reflected in the profiles, which were similar for great tit and blue tit (Figure 8.17), with both occurring within forests > 30 m in height but with a dominance of trees within the 10 - 20 m height range. Long-tailed tits were absent (or not observed) within forests > 30 m but with a distinct upper canopy layer. Marsh tits were observed within forests up to 30 m but were more abundant within lower stature

forests and those with an established understory. Willow tits were associated with forests with a distinct overstory with some understory, although this could have reflected the lower number of observations for this species.
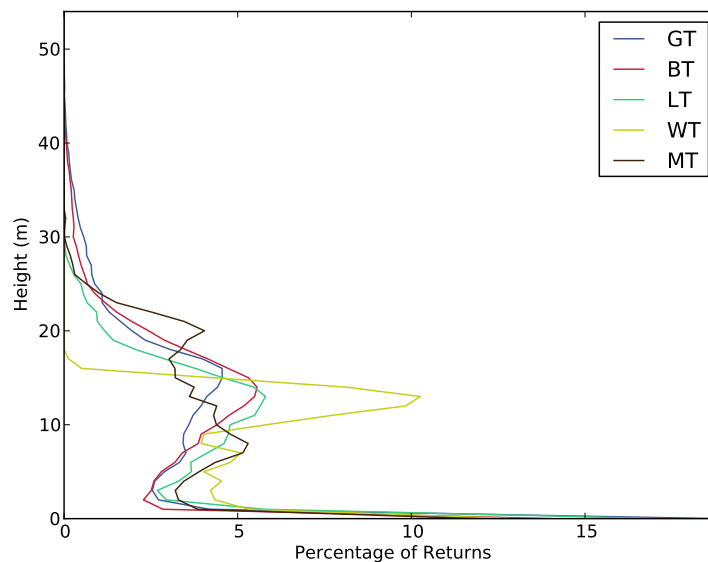
Figure 8.17: The percentage of LiDAR returns by height (m) for great tit (GT), blue tit (BT), long-tailed tit (LT), willow tit (WT) and marsh tit (MT).

For the different warbler species, the profiles varied. Wood warbler favoured the taller forests (as outlined earlier) with a sparse understory whilst chiff chaff preferred a more substantial understory. Garden warblers occurred in woodlands with an overstory at approximately 10 - 20 m and an understory of 2 - 8m. Willow warblers preferred a more open forest of < 20 m in height with an established understory. In this case, the profiles for each of these species reflected the different habitat preferences.

Whilst the profiles for the bird species illustrated are as expected, it should be noted that observations of birds occurring in the upper canopy may be less than
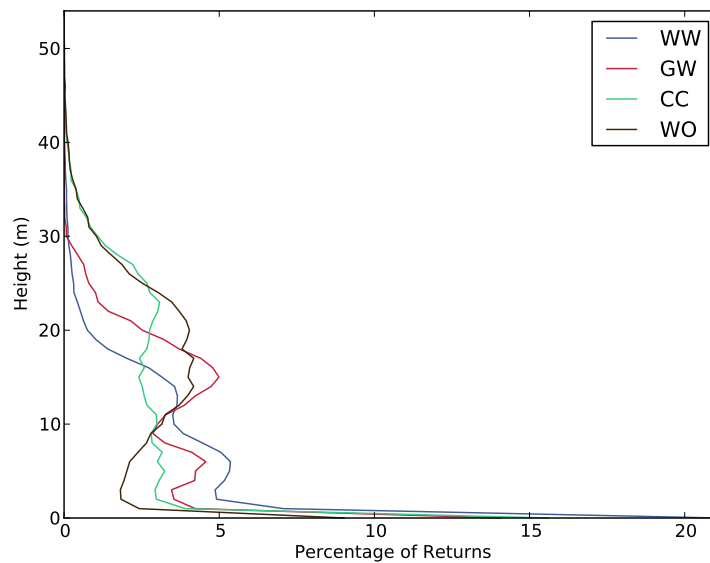
Figure 8.18: The percentage of LiDAR returns by height (m) for willow warbler (WW), garden warbler (GW), chiff chaff (CC) and wood warbler (WO).

in the lower canopy, particularly when these are not singing and their identification is less certain. Therefore, some care needs to be taken in characterizing the vertical profiles for different bird species. Canopy profiles were generated for all species, but only those associated with species confined largely to the forest area are illustrated and discussed. However, Table 8.2 indicates the dominant layer and the number of layers associated with all species observed.

Table 8.2: Association of common bird species with the dominant layer and number of layers in the forest.

BTO code	Common Name	Dominant layer (depth in m)	No. layers
B	Blackbird	0-18	1
BC	Blackcap	0-15	1
BF	Bullfinch	< 10	1
BT	Blue Tit	3-17	1
BZ	Buzzard	0-20	1
CC	Chiffchaff	0-10,10-30	1
CH	Chaffinch	0-15	1
CK	Cuckoo	2-7	1
CR	Crossbill	0-15	1
CT	Coal Tit	0-15	1
FC	Firecrest	15-30	1
G	Green Woodpecker	10-18	1
GC	Goldcrest	3-20	1
GS	Great Spotted Woodpecker	5-20	1
GT	Great Tit	0-18	1
GW	Garden Warbler	0-5, 10-17	2
J	Jay	0-8, 15-20	1
LR	Lesser Redpoll	< 7	1
LT	Long-tailed Tit	3-16	1
M	Mistle Thrush	0-5, 10-20	2
MT	Marsh Tit	3-20	1
NH	Nuthatch	8-18	1
PF	Pied Flycatcher	10-19	1
R	Robin	0-5	1
RT	Redstart	3-15	1
SF	Spotted Flycatcher	4-20	1
SK	Siskin	4-22	1
ST	Song Thrush	0-15	1
TC	Treecreeper	0-16	1
TO	Tawny Owl	8-20	1
TP	Tree Pipit	0-5	1
WO	Wood Warbler	10-23	1
WP	Wood Pigeon	0-20	1
WR	Wren	0-15	1
WT	Willow Tit	< 5, 10-15	2
WW	Willow Warbler	< 5	1

8.6   Discussion

8.6.1   Links between bird distributions and forest structure

Within the Lake Vrywny catchment, several bird species were confined primarily to either coniferous (e.g., firecrest) or broadleaved forest (e.g., pied flycatcher, wood warbler). These broad habitats can be mapped using satellite sensor data (as indicated in Chapter 6) and their classification from these data infers a relatively mature forest. Fridd habitat can also be classified from satellite sensor data. However, better knowledge of the distribution of some forest types (e.g., those dominated or containing sessile oak, beech and/or birch) is necessary to better indicate the distribution of the habitats of some bird species (e.g., pied flycatcher, wood warbler). Other bird species were associated with mixtures of broadleaved and coniferous forests. For example, willow warblers were often observed within younger coniferous plantations, where birch is commonplace, whilst goldcrest occurred within broadleaved forests where coniferous species (e.g., pines) were a component. In the former case, classification from satellite sensor data can be achieved, particular if time-series datasets were introduced (i.e., to document the history of felling and replanting).

The inclusion of structural information benefits the characterization of forests and their association with bird species distributions. In particular, differences in the vertical profiles associated with distinct species groups were evident. For example, bird species that utilize the larger trunks and branches of trees (e.g., woodpeckers, treecreeper and nuthatch) were more frequent within taller forests with a sparser understory. Below a certain mean tree height, observations of these species reduced

and other species became more prevalent (e.g., blackcaps, garden warblers, marsh tits). Many species (e.g., firecrest, wood warbler) were confined largely to more closed canopy forests whilst others (e.g., tree pipit, redstart, cuckoo) favoured more open areas with scattered trees or the edges of the forest.

Defining a 'typical' profile for bird species is nevertheless problematic as this depends on a number of factors including scale (i.e., of data extraction) and also more specific requirements of species (e.g., nesting sites). Nevertheless, the profiles reflected the known preference of many species in terms of their use of the vertical profile of forests.

The limitations of using LiDAR data to retrieve canopy profiles have been highlighted in Chapter 7. Nevertheless, a broad correspondence can be observed in many cases, although this depends on the number of plant elements occurring within different parts of the vertical profile. Figure 8.19 gives examples of TLS and airborne LiDAR profiles for the forest types observed at LV7 - LV13. In most cases, the overstory and sub-canopy are well represented within the airborne LiDAR data (although less so by the TLS).

These data may be less suited though for identifying differences in habitat for species favouring the understory (e.g., blackcap, bullfinch, marsh tit, garden warbler) and Figures 8.11 to 8.18 therefore have to be considered with this limitation. However, discrimination also depends upon the relative openness of the top canopy of each woodland type and the capacity for LiDAR pulses to transmit through to the underlying layers, which would increase with greater pulse frequency. The profiles in Figures 8.11 to 8.18 are furthermore not based on single laser pulses, but on a large number of profiles extracted from a 20m radius around each bird sighting. Assuming the relative structural homogeneity of each separate woodland

type, a proportion of any understory present would be represented in each profile through those fewer laser pulses which penetrated the canopy to the ground, though the exact proportion cannot be accurately determined here.

A number of studies have similarly identified a link between forest structural measures and bird species diversity. For example, Goetz et al. (2007) suggested that the distribution and richness of bird species was linked closely to the structure and heterogeneity of the forest canopy structure. Hill et al. (2004) and Hinsley et al. (2006) also reported a link between habitat quality (defined by canopy structure and height) and the breeding success of great tits in UK woodlands. A number of studies have linked LiDAR-derived measures of forest structure to bird species distributions (e.g., Bradbury et al., 2005; Davenport et al., 2000; Hyde et al., 2006a). Hill and Thompson (2005) also advocated the inclusion of additional information on tree species as well as stand age and condition (e.g., as determined from multi- or hyper-spectral data). However, whilst a broad correspondence may be observed, there are other factors which determine the distribution of bird species that cannot be quantified from LiDAR, including the occurrence of nesting sites (hollows in trees), food availability and competition between individuals and species. Other species may be more generalist in habitat generalization and occupy both forests and adjoining habitats. For this reason, many studies have focused on a particular bird species or group of species (Goetz et al., 2007).

8.6.2 Species distribution models

For conservation purposes, spatial information on both the actual and likely occurrence of species is a requirement and has been obtained primarily by linking field-observations with environmental surfaces, including habitat maps. For this
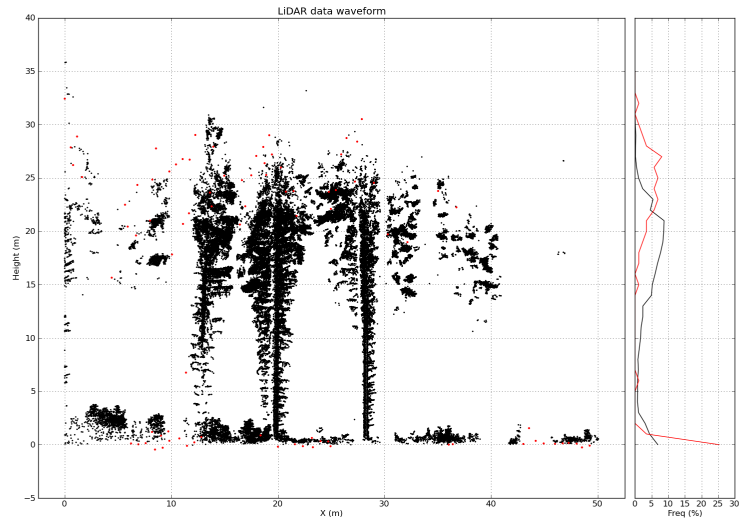
(a) LV7 (Douglas Fir)
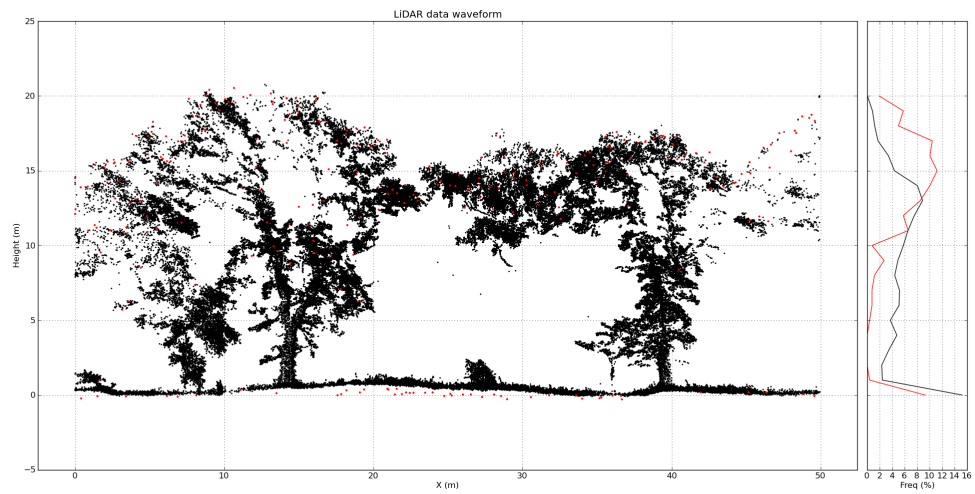
(b) LV8 (Open Sessile Oak)

Figure 8.19: Comparison of vertical profiles obtained for coniferous and broad leaved woodlands from both TLS (black) and airborne LiDAR (red)
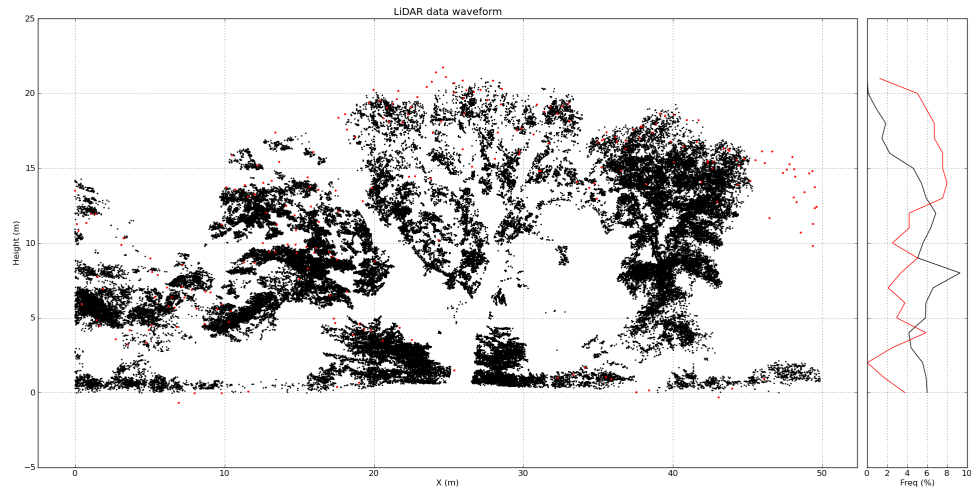
(c) LV9 (Open Sessile Oak with understory)
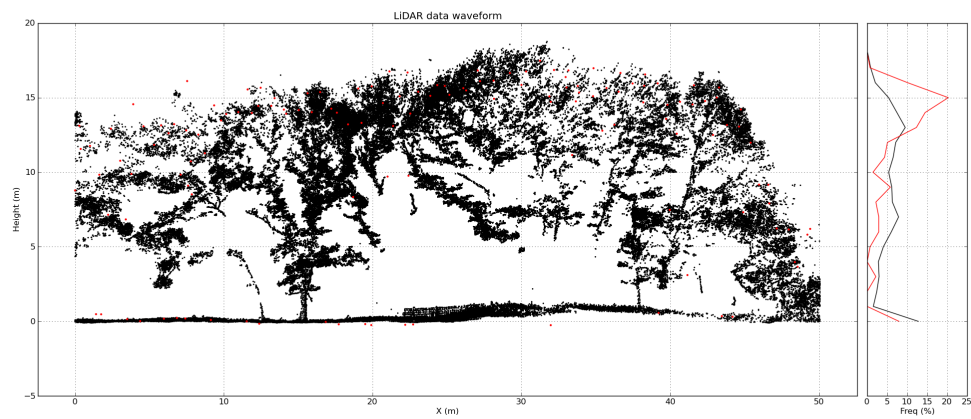
(d) LV10 (Grazed Sessile Oak)

Figure 8.19: Comparison of vertical profiles obtained for coniferous and broad leaved woodlands from both TLS (black) and airborne LiDAR (red) (cont.)
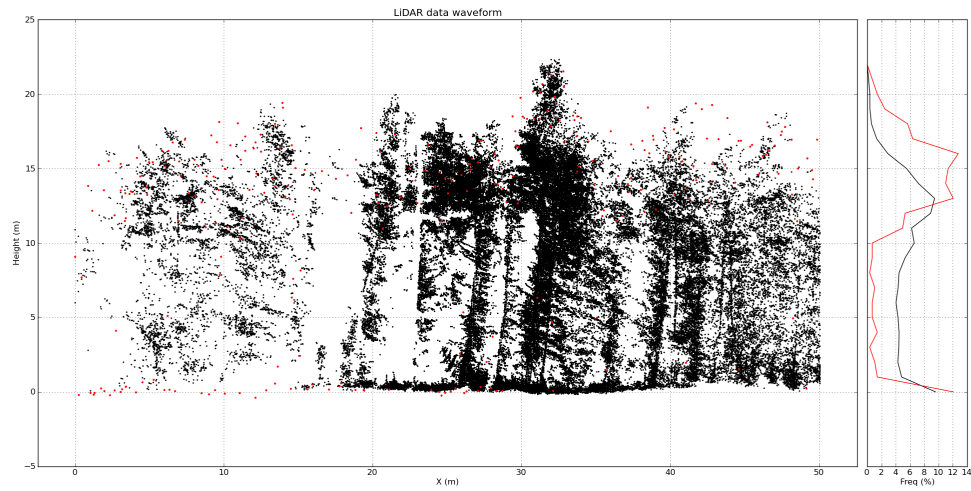
(e) LV11 (Dense Larch)
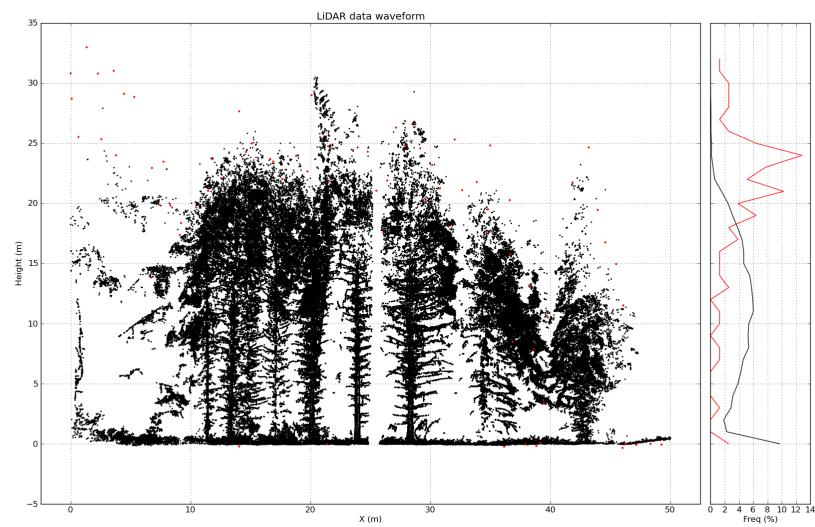
(f) LV12 (Dense mixed coniferous wood)

Figure 8.19: Comparison of vertical profiles obtained for coniferous and broad leaved woodlands from both TLS (black) and airborne LiDAR (red) (cont.)
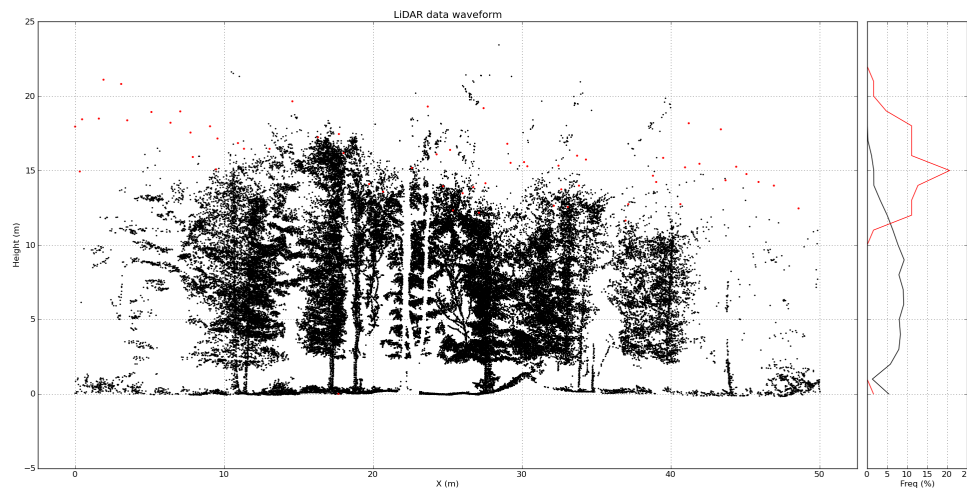
(g) LV13 (Dense Sitka Spruce)

Figure 8.19: Comparison of vertical profiles obtained for coniferous and broad leaved woodlands from both TLS (black) and airborne LiDAR (red) (cont.)

purpose, a wide range of species distribution models (SDMs), or habitat suitability models, have been developed (e.g., GARP, BioMapper, Maxent). SDMs provide an opportunity to combine field-based observations (presence, presence-absence or abundance) of the distribution of flora and fauna with vegetation maps and environmental information (e.g., terrain and climate variables, disturbance or energy resources; (Guisan and Thuiller, 2005)) to predict their distribution in unsampled areas. In many cases, these models use existing or new or updated mapping based on the classification of satellite (primarily optical) sensor data. A number of SDMs are commonly used including DesktopGARP (Stockwell and Peters, 1999; Stockwell, 1999) and Biomapper (Hirzel et al., 2001, 2008).

The majority of SDMs have relied on two-dimensional mapping of habitats and other biophysical properties (e.g., vegetation productivity). However, few have

used quantitative information on the three-dimensional structure of vegetation, particularly forests. Potential LiDAR-derived inputs to such model include forest top height, mean height and openness as well as the number of layers within the vertical profile. However, a number of issues have been identified which still limit the use of these LIDAR-derived measures in SDMs.

1. Comparison of canopy profiles derived from both the airborne LiDAR and TLS indicated discrepancies associated with attenuation of the pulses by elements within the canopy volume. Hence, components of the sub-canopy and particularly the understory may not be captured accurately.

2. Many bird species may be associated with distinct profiles but other components of the habitat (e.g., availability of nesting sites or prey) may be more important.

For these reasons, careful consideration needs to be given to the inputs into SDMs.

8.6.3   Assessing bird habitat suitability across Wales

To assess the suitability of habitats for different bird species across Wales, detailed habitat maps are needed. For this purpose, the revised Phase I map (Lucas et al., in press) provides detailed land cover mapping at 10 m spatial resolution and at a sub-object level for complex environments (e.g., upland mosaics). For habitats low in height (e.g., heathlands, grasslands), the requirement for structural information is relatively low and hence these data may be well suited for SDMs, particularly in relation to birds. However, for forests, the use of three-dimensional information to assess structural heterogeneity can contribute to a better assessment of bird

species distributions. Although Wales-wide coverage is provided, the Nextmap Britain DSM has already been discounted, because of inaccuracies in the retrieval of stand height and low spatial resolution.

Whilst discrete dual return LiDAR data (2m nominal resolution) have been acquired for much of Wales, and particularly along the river network, by the Environment Agency, these data are also considered to be of insufficient spatial resolution. As full waveform data were not acquired, the number of structural attributes able to be extracted is also more limited, particularly in relation to descriptions of the vertical canopy profile. Even so, measures such as mean and maximum stand height and the HSCOI should be retrievable. On this basis, the study recommends the use of full waveform data acquired at $< 1m$ post spacing at a Wales-wide level.

8.7 Summary and conclusions

For the Lake Vyrnwy forests, woodlands and fridd habitats, 4906 bird observations (36 species) were made in 2006. For each of the 36 species, information on the forest type, height, openness and vertical profiles was summarised. The main conclusions were:

1. The vertical profiles reflected the known habitat preferences of most species, particularly those that were more specialised (e.g., wood warbler, pied flycatcher, greater spotted woodpecker, garden warbler, tree pipit).

2. Profiles were less easy to interpret for species that were more generalist (e.g., blackbird, robin, chaffinch) but still reflected the habitat use by these species.

3. Confidence in the use of profiles for the interpretation of bird distributions was reduced for forests where the density of plant components led to attenuation of the airborne LiDAR pulses such that information on the sub-canopy or understory was reduced.

4. Whilst structural attributes derived from airborne LiDAR data may be used as input to species distribution models, consideration needs to be given to attenuation of the LiDAR pulse, the post-spacing of the LiDAR data used and the presence of other factors (e.g., nesting opportunities, food availability and competition) that might influence species occurrence and use of the landscape.

For regional assessment of bird species distributions, the Phase 1 Survey revised with satellite sensor data is regarded as more useful for those species specific to habitats such as grasslands and heaths. However, to assess distributions within forests, information on their three-dimensional structure is required. Whilst maps of forest height at a national level can be generated from NextMap Britain data, these are considered unreliable because of the difficulty in obtaining a DTM from below the forest canopy. For this reason, acquisition of full waveform LiDAR data of fine (< 1m) post spacing, even if only across important forested areas (e.g., reserves or areas with actual or planned management actions), is recommended.

Chapter 9

Discussion: Remote Sensing of biological diversity

The discussion focuses on the benefits obtained through the integration of space-borne multispectral, airborne hyperspectral and LiDAR data for better land cover mapping and the characterization of grasslands and forests in particular. The benefits for the assessment of biodiversity in terms of grass species (inferred from habitat type) and bird species associated with forests are conveyed. Potential benefits and measurements for mapping across Wales are highlighted.

9.1   Object-based classification of Welsh landscapes

The research undertaken has established, through reference to hyperspectral data, that different grassland types and levels of improvement, can be discriminated from spaceborne optical sensor data. Such knowledge has been evaluated over west

Ceredigion and incorporated into the mapping of habitats across Wales. For assessing the species diversity of grasslands, the spectral information can allow mapping of broad categories (e.g., grasslands dominated by *Molinia caerulea*, *Nardus stricta* and *Festuca ovina*) and different levels of improvement. The classification scheme has been expanded to include forests (coniferous and broadleaved) and also upland heaths. For discriminating tree species, some success was obtained using spectral data (e.g., for oak) but this was considered insufficient for wide area application. For assessing the diversity of bird species within forests, the use of three-dimensional information (namely from LiDAR) is advocated as a close correspondence in metrics (e.g., height, distribution of elements within the vertical profile and canopy openness) with the known distribution of some species observed. The following sections discuss in more detail the contribution that remote sensing data acquired at various scales and modes can make to the assessment of biodiversity in Wales.

9.1.1 Classification of semi-natural habitats

The object-based classification of semi-natural habitats and agricultural land represents a significant advance in land cover mapping. This research has contributed to the development of a map by focusing on Ceredigion grasslands and Lake Vyrnwy forests.

Habitat mapping across Wales has been, as indicated previously, associated with field survey with support from targeted aerial photography interpretation. Satellite derived mapping has been relatively coarse and not at the level of detail, in terms of resolution or discrimination of habitat types, as to be useful for conservation purposes.

The research conducted for this PhD has established that better mapping can be achieved from spaceborne remote sensing data, particularly through the integration of SPOT 5 HRG data.

In particular:

1. habitats can be mapped in greater detail

2. rules are consistent in terms of their sequence but values change between regions. The mapping benefits from

   a. hard (boolean rules)

   b. soft (fuzzy based rules)

   This allows both discrete and relatively homogenous areas of the landscape to be mapped and differentiated from complex mosaics.

3. The method utilizes field boundary information which assists documentation of habitats, etc.

9.1.2   Classification of grasslands

Across the Vyrnwy and Ceredigion study areas, grasslands were categorised primarily as improved, semi-improved or unimproved. The latter category largely belongs to upland acid (Sheep's fescue (*Festuca ovina, Agrostis spp.*) or calcareous grasslands and marshy grasslands (dominated primarily by Purple Moor Grass (*Molinia caerulea*) and/or rushes (*Juncus spp.*) as well as Mat Grass (*Nardus stricta*) and these could be discriminated spectrally.

Improved grasslands

At a regional level, improved grasslands were defined by the presence of some species (e.g., *Lolium perenne*). Using spaceborne data, areas of improved grassland were also associated with a relatively high near infrared reflectance, photosynthetic fraction and/or NDVI during the growing seasons. In the uplands, improved grasslands were associated with a high spring NDVI and also a high NIR reflectance. Based on the data collected at Trawscoed and Pwllpeiran, improved grasslands exhibited a higher near infrared reflectance which was associated with greater structural and species homogeneity, as well as increased productivity through fertilization. Similarly, the greater proportion of photosynthetic vegetation compared to non-photosynthetic vegetation because of constant grazing was evident.

Productivity in improved fields is high and so there is a reduction in reflectance in the visible wavelengths (as a consequence of chlorophyll absorption) and an increase in scattering in the near infrared wavelengths. In many improved swards, clover (*Trifolium repens*) is present and the leaves are horizontally orientated and held in a relatively uniform 'floating' layer. Hence shadowing is reduced (and hence the shade fraction) and the proportion of non-photosynthetic vegetation (NPV) is minimal.

Unimproved grasslands

The drier unimproved grasslands were generally less productive, which was reflected in a greater SWIR reflectance (particularly in the spring) and lower NDVI compared to more improved grasslands in the spaceborne data. Unimproved grass-

lands also often have a high level of non-photosythetic vegetation present, as the grazing levels are less intense than those of improved fields and there is subsequently less removal of biomass before senescence. At Pwllpeiran and Trawscoed, the increase in reflectance in the SWIR and reduced NDVI was attributed to a greater species diversity and hence sward heterogeneity, but also a greater proportion of non-photosynthetic material in the vegetation.

Semi-improved grasslands

Semi-improved grasslands were generally more productive, as indicated by greater proportions of photosynthetic vegetation in the spring and summer. Discrimination of these grasslands is difficult as though, even in the field, there is contention as to their classification.

Differentiation of improved, semi-improved and improved grasslands was problematic as these are effectively gradations of each other.

Other grassland types

A number of other grassland types were discriminated with these being dominated by one or several species. Wet grasslands dominated by *Juncus* species were identified primarily using the visible green and red wavebands because of contrasts with many surrounding habitats, often improved grasslands. These grasslands also exhibited lower NIR reflectance and NDVI compared to those that were more productive.

Molinia caerulea is widespread throughout Wales and is the dominant species of many upland marshy grasslands. Typically, the diversity of other grass species is

very low were *Molinia* is widespread. Differences in the photosynthetic fraction between the spring and the summer months as well as red (summer) and SWIR (spring) reflectance and knowledge of slope preferences were used primarily to distinguish *Molinia*-dominated grasslands from adjoining habitats (e.g., bracken and other unimproved upland grasslands). Vegetation indices incorporating the SWIR and red reflectance in the spring and summer were also used. Unimproved grasslands associated with *Nardus stricta* exhibited low differences in the NDVI between the spring and summer. This occurred because of the low proportion of non-photosynthetic vegetation with *Nardus* dominated swards as the species is very slow-growing and has a comparatively low primary productivity (Perkins, 1968).

Festuca spp. grasslands (with short turf) typically exhibited a high spring SWIR and NIR reflectance.

Overall, individual species can only be mapped if they are spatially dominant and occupy large areas and are spectrally distinct. However, the species diversity can also be inferred. For example, within improved fields, species diversity is low but increases within semi-improved fields. Acid grasslands tend to be of lower diversity than neutral or calcareous unimproved grasslands (Krauss et al., 2004), because they are confined generally to the upland areas where conditions permit less species to establish themselves.

Comparisons with other classifications indicate that a wider range of grassland types have been mapped. The land cover map of 2000 (Fuller et al., 2002) only mapped broad grassland classes, for example. It was possible to make improvements to the grassland classifications by utilizing the relationships established between grassland improvement and reflectance. Similarly, the proportion of non-

photosynthetic vegetation within the grassland provides a good indication of productivity and improvement levels. Use of multi-temporal imagery further allowed observation of the seasonal variation in these parameters for different grassland types (Tateishi et al., 2004).

The key indicators for level of grassland improvement in multispectral data are:

- NDVI - productivity

- NPV - proportion of dead material

- Shade - roughness of grasslands

- NIR - biomass/grass length and living, photosynthesizing material

- Seasonal differences in the above

Some grassland species information can be inferred from multi-spectral remote sensing data, especially where swards are dominated by a single or very few species, e.g., *Molinia*-dominated grasslands.

Improved grassland supports few species, but those that occur (*Lolium perenne, Trifolium repens*) are very productive and the sward, more importantly for classification, is very homogenous in appearance and reflectance. Unimproved grasslands have a high proportion of NPV, though this varies with different types of unimproved grasslands. *Molinia*, for example, produces a large amount of non-photosynthetic vegetation and complete ground cover, while acid and calcareous swards which are commonly closely grazed do not contain much dead material. The amount of NPV present also varies by species composition of the unimproved sward, for example *Festuca ovina* in the uplands, and this can be discriminated.

The points made above give some indication of species present, when remote sens-

ing information is combined with ecological knowledge. The greater the area of one type of grassland or habitat, the greater the chance to detect and identify it correctly, because a greater homogenous core will be present. This, for example, has been shown to improve the species discrimination within semi-natural grasslands (Jacobsen et al., 2000; Lauver, 1997).

9.1.3   Classification of forests

Across Wales, according to the Phase 1 survey (Howe et al., 2005), forests represent about 14 % of the landscape, with these split between broadleaved (5 %), coniferous (7 %) and mixed (2 %). Scattered and dense scrub cover approximately a further 6% of the landscape.

The segmentation and classification procedures resulted in two different levels of information relating to the distribution and scale of habitats. These included complex mosaics such as moorlands and lowland grasslands where objects were associated with values representing the fuzzy membership of selected sub-habitats. Within Level 1, habitats were associated with one class only (e.g., coniferous forest). The rule-base was extended to attempt classification of more detailed forest types by species but was only moderately successful because of spectral similarities between different tree species and insufficient segmentation of different forest type objects from their surrounding habitats. Similar rule-based approaches to classification have been applied previously with variable success (Czaplewski and Patterson, 2003).

For forestry, mapping requirements are varied and range from broad type classifications (coniferous, broadleaved, mixed) to individual tree mapping.

As an example Bunting and Lucas (2006) used 1m spatial resolution hyperspectral data at the individual tree level, as well as co-registration with LiDAR data to allow each mapped tree to be assigned a structural measure (e.g., height, crown area).

An object-orientated rule-based classifications of forests (broadleaved, coniferous and some single species dominated woodlands) was undertaken as part of a larger programme aimed at classifying habitats across Wales. Classification of other habitats (e.g., bracken) was necessary to facilitate the discrimination but also to place the forests in the context of the wider landscape.

The rules accommodated imagery from different sensors observing in similar wavelength regions (i.e., SPOT HRG and IRS). This was achieved by implementing rigorous geometric, radiometric, atmospheric and topographic correction procedures to give comparability of spectral values from different dates and sensors and greater confidence in the production of derived data such as vegetation indices and end-member fractions. The advantage of the rule-based classification is that rules can be based on spectral information but can also consider topography (slope, aspect) and context (adjacency, enclosure). The rules were developed primarily by using information on the spectral properties of forests, although some topographic (slope and aspect) and context information (adjacent, enclosure) was also considered.

The more detailed classification of forest types around Lake Vyrnwy provided classification accuracies of between 18% (Ash gulleys) and 86% (Mature Spruce), with broadleaved forest types such as Oak and Birch generally showing lower accuracies, compared to conifers such as Spruce and Larch. The classification might be improved by using fuzzy rules, particularly in the scrub classes where

bracken occurred in intricate mosaics with scattered or dense scrub and by refining the segmentation progress.

Using SPOT 5 HRG data classification accuracies of the main forest types, i.e., coniferous, broadleaved woodlands, were lower than expected. Errors were often caused primarily by the segmentation, not the classification. A re-segmentation of broadleaved and coniferous at the sub-level and a subsequent re-classification might have been more successful. This is an important argument for scale-appropriate mapping for different habitat types and the need for well-defined objects. The use of higher spatial resolution data, such as NIR photography for segmentation and subsequent classification using higher spectral resolution data should be considered.

Hyperspectral data could also provide better opportunities for differentiation, both because of better spatial and spectral resolution (Bunting et al., 2006). Problems include limited coverage and problems with bi-directional effects, because of not flying in a north-south direction. Figure 9.1 shows an example of strong bi-directional effects in 2006 CASI data over Lake Vyrnwy, which limit the usefulness of the data severely.
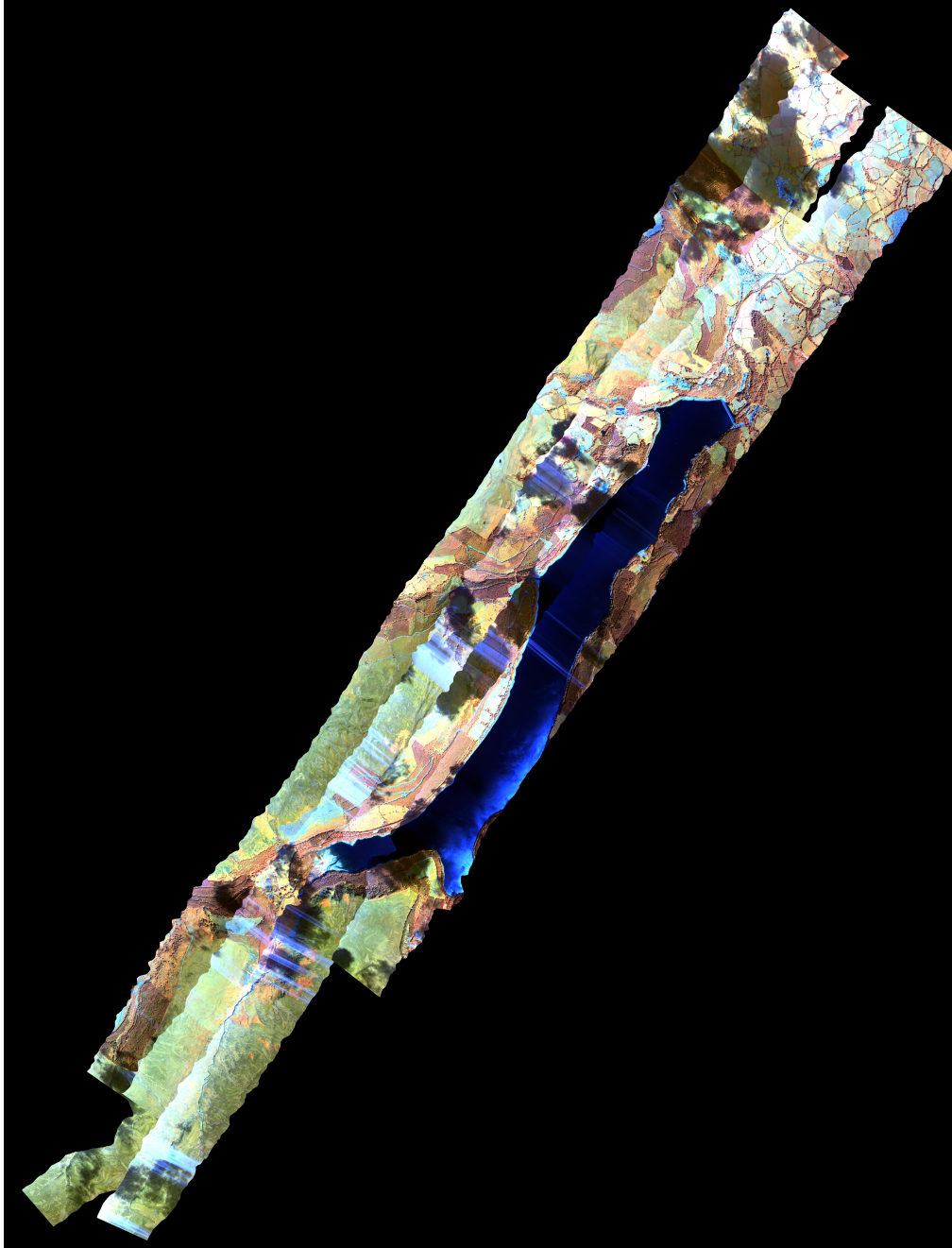
Figure 9.1: August 2006 CASI mosaic over Lake Vyrnwy with strong bi-directional effects

The classification of optical data provides information only on the two dimensional structure of forests, although the three dimensional structure can be inferred. Within a rule-based classification, the inclusion of height would allow discrimination of a greater range of forests, including regrowth stages (particularly in relation to plantations) but also indicate the structural diversity of the forest. The inclusion of canopy openness would facilitate differentiation of open and closed forest and particularly scrub.

9.1.4   Accuracy assessment of remote sensing classifications

1. Accuracy assessment needs to be scale-appropriate. Accuracy assessments assume that a 100% correct classification can be generated. However, this depends on every object fitting the criteria of at least and, at the same time, not more than one class. This is an assumption which in reality is rarely met. Classes would have to be either very broad or, conversely, very detailed. The fewer classes a classification uses, the more accurate it will be, but there is also a greater likelihood that the same classification would have been achieved if classes were randomly assigned to objects. Accuracy, however, can only be tested against classes and objects which have been mapped. If a land cover type is excluded from the classification, accuracy can therefore not be tested subsequently and such areas should be left blank on any map created (Foody, 2008).

2. In the natural environment, habitat areas are rarely clearly delineated by type (e.g., as a woodland and an adjacent grassland would be). In the majority of cases, these form extensive overlapping areas or ecotones, which are

mosaics consisting of vegetation cover typical to two or even more habitats. It can therefore be expected that accuracy is lower in ecotone regions.

3. A further large source of error is the scale of the classification. Different land cover types exist at different scales and should be mapped accordingly, using image objects of varying dimensions. However, this would require a classification prior to the main segmentation into areas of different size, which in turn would need to be assigned prior to this (Powell et al., 2004).

   The smallest achievable scale further depends on the base data used for classification, in this case 10m SPOT data. Many classes of interest in this study, (e.g; isolated trees, hedges and *Juncus spp.* dominated flushes), can occur as objects smaller in area or narrower than the minimum mappable unit (MMU) of 25m^2 and it is therefore assumed that their accuracy is lower than that of habitats covering large areas, such as forests. Accuracy is therefore scale-dependent and so is the utility of the map.

   Useful statements, regarding for example patch fragmentation, using this map can be made on a 1:10000 scale, but become misleading on a smaller scale.

4. Another scale consideration concerns the size of the area to be classified in relation to the training area used to create the rule-base. The further away an object is from the training area, the lower the likelihood that it has been classified accurately due to natural variations in vegetation caused by differences in climate, aspect, elevation or underlying soil type.

A number of methods of assessing accuracy vary according to the area classified (Liu et al., 2007).

The assessment method for accuracy should be suited to the classification ap-

proach. For example, a point checking method is unsuitable in this case, where image objects were classified. Points are at a much smaller scale, which was never intended to be mapped. In this case a suitable number of randomly selected objects should be tested for accuracy (Radoux et al., 2008).

9.2 Forest structure attributes

A disadvantage of using optical remote sensing data for classifying forests is that only limited information on their three-dimensional structure can be obtained. Knowledge of vertical structure is needed, however, to support assessments of biodiversity as many organisms use different areas of the volume space and vegetation structure in itself is an indication of diversity (Boncina, 2000; Qiaoying et al., 2006), while forest vegetation communities alone have been found to be insufficient for the interpolation of species diversity (Cushman et al., 2008). The requirement is hence for high resolution three-dimensional datasets, such as derived from LiDAR, but relationships might be established with spaceborne sensor data, i.e., multi-spectral optical data or laser sensors (Rosette et al., 2008).

There is also a role for these data to support carbon accounting. This is particularly the case for terrestrial laser scanning where individual tree-based estimates of biomass can be obtained and used to inform algorithms that utilize coarser spatial resolution data or that covering a larger area (e.g., InSAR or airborne LiDAR).

Validation of height estimates from LiDAR has provided difficult because the LIDAR estimates are often more reliable than those obtained from the ground (e.g., using clinometers and other measurement devices). Retrieval of height from air-

borne LiDAR has further been difficult because of uncertainties in retrieving the elevation of the underlying terrain through signal attenuation while passing through the canopy. In this study, however, the ground elevation has been rigorously verified through a GPS based surveying system.

The comparison of height derived from LiDAR and terrestrial laser scanner data is given in Chapter 7 and demonstrates that, in general, reasonable estimates of top height can be obtained, although these are more reliable where the canopy closure (as indicated by LiDAR) is less. Comparison of GPS measures of ground elevation and those obtained using the algorithm utilized in Chapter 7 indicate a close correspondence and allowed the height of the trees to be determined. Ground elevation was also able to be extracted from the terrestrial laser scanner. The analysis indicated that similarities in height were obtained but that the airborne LiDAR was not interacting with all of the elements beneath the upper canopy. Similarly, the TLS was not able to penetrate through to the upper canopy although this depended upon the density of branches and foliage. Similar results have been obtained by Chasmer et al. (2006) for a single-species pine forest, while the results of this study indicate a correlation between canopy density and signal attenuation in forest of varying species composition and maturity.

A particular advantage of LiDAR is that continuum classifications can be generated using relationships established between LiDAR data and biophysical properties such as biomass (van Aardt et al., 2006; Popescu, 2007; Ni-Meister et al., 2010).

Validation of these relationships typically relies on the use of plot-based measurements, but in this case, such information can potentially be retrieved using terrestrial laser scanner data. Comparisons with common measures such as height

are provided in Chapter 7 and show the potential for retrieving other structural attributes, although this is beyond the scope of the study.

A limitation of LiDAR is that the spatial estimates of structural attributes derived are limited to only a small area. For this reason, other approaches such as the use of SAR interferometry should be considered, as wider coverage is provided (Hyde et al., 2006a; Balzter et al., 2007). LiDAR or TLS derived estimates of biomass and structural attributes can provide a basis for supporting the development of SAR-based retrieval algorithms, particularly as field-based measurements are often limited in amount and spatial distribution. Data integration with optical sensors also offer a possibility for larger scale forest modeling (Lefsky et al., 2005).

Nevertheless, LiDAR data can play a key role in the verification of retrieved profiles (Slatton et al., 2001), thereby leading to fine-tuning of algorithms and aiding the scaling up between the local and the regional scale (Zimble et al., 2003). LiDAR can also provide a yardstick for assessing the retrieval of structural attributes from other sensors. For example, several studies have demonstrated differences of only a few metres in the errors associated with height retrieval from InSAR and LiDAR (e.g., Balzter et al., 2007; Breidenbach et al., 2008). Hyde et al. (2006a) also suggested that InSAR was best suited for structurally homogeneous forests and that LiDAR provided better estimates of the height of larger trees.

9.3 Bird diversity

A large number of studies have established links between forest structural attributes and bird diversity, either through direct relationships with height (Helle and Fuller, 1988; Hinsley et al., 2002; Hill et al., 2004) or other measures (Boulinier

et al., 2001; Bradbury et al., 2005; Goetz et al., 2007; Hinsley et al., 2006; Clawges et al., 2008).

This study has shown that vertical profiles of laser strikes as a function of height can be related to the known distribution and preferences of bird species. As examples, pied flycatchers favour open woodlands with a relatively spare understory whilst wood warblers prefer a taller woodland (typically beech or oak dominated) with a relatively sparse understory. These preferences are reflected in the different vertical profiles illustrated in Chapter 8.

The results suggest that remote measurement of bird diversity requires both broad species and structural information. For example, some bird species (e.g., Firecrest) are confined largely to coniferous forests whereas others (e.g., Pied Flycatchers) are particularly common to deciduous forests. Some species are generalist whilst others also have very specific requirement requirements regarding canopy structure and the association with forest structure is naturally greatest for specialist woodland species, such as Willow and Wood Warblers (James and Wamer, 1982).

Birds are commonly used as indicators for biodiversity (Gregory et al., Ornis Hungarica) because they tend to be well observed and recorded and large datasets of a great number of species with very different requirements on their environment are available for combination into composite indices (Fuller et al., 2005b). The need for such focal species is particularly pronounced in fragmented landscapes, such as they are found within the United Kingdom (Eycott et al., 2007).

While the study only observed links between bird species distributions and forest structural information retrieved from LiDAR, further integration of the land cover mapping should be attempted to widen the assessment potential for bird diversity

(Barnett et al., 2004). An integrated approach of vegetation cover mapping and vegetation structural assessment is likely to be most productive with regards to bird diversity assessment (Gil-Tena et al., 2010).

The use of habitat suitability models is one approach to establishing where birds might occur and also to predicting where birds might be found in other regions or under different scenarios of land use or climate change. However, habitat suitability models are entirely dependent on their input data. Davenport et al. (2000) demonstrated the use of a fine-resolution airborne laser scanner for the capture of parameters such as crop height and the improved output gained from utilizing such data during habitat modeling, while Martinuzzi et al. (2009) showed the considerable improvement in the predictive ability of a model after integration of LiDAR derived data on the vertical heterogeneity of forest structure.

Whilst habitat suitability models provide an opportunity for understanding the distribution of bird species across a landscape, identifying the input to these models is problematic. In particular, a large number of metrics can potentially be retrieved from LiDAR data but establishing which may be best suited for modeling is uncertain.

The assessment of habitat suitability is likely to be best for bird species which maintain their territories entirely within the volume of the forest. As an example, species such as pied flycatchers, wood warblers and firecrests tend to remain within the confines of the forest whilst others (e.g., blue tits and blackbirds) are common to a wider range of environments and exploit a wider range of niches.

Habitat suitability models are very useful, especially when using LiDAR as an input, but they can never consider all factors contributing to the niche requirements of a particular species, particularly in complex landscapes (e.g., hedgerows).

Considering the value of birds as biodiversity indicators, however, it is suggested that a rule-based approach to bird habitat mapping from both two-dimensional land cover maps and vertical landscape structure data combined breeding bird surveys (Fearer et al., 2007) would be worth further research.

9.4 Biodiversity

The study has indicated the greater potential for mapping and prediction of vegetation land cover across Wales and this is assisted in particular by the greater level of detail provided by the Definiens classification (e.g., in terms of hedgerows and scrub classes). Landscape heterogeneity and structure are in itself indicators of biodiversity (Dauber et al., 2003) and regional land cover mapping hence supports the assessment of biodiversity within Wales.

This study has led to improvements in the assessments of biodiversity by improving

1. information on the distribution of grasslands

2. information on forest structure and distribution of tree species

3. better mapping of landscape structure (e.g., hedgerows)

4. link between forest structure derived from LiDAR and bird distribution

The greater value derived from examining these four research areas as part of a framework for biodiversity assessment, however, consists of an ability to target the employment of various remote sensing methods for the evaluation of specific aspects of biodiversity. Integration of different remote sensing data types to exploit

information synergies such created is another important technique for the assessment of biodiversity (Dalponte et al., 2008; Anderson et al., 2008). Biodiversity consists of many different components it is crucial to be able to perform such integrated analyses of its various elements. However, only a combined approach towards the utilization of remote sensing, as demonstrated in this study, is likely to gain the necessary information.

9.5   Future change and monitoring

Sala et al. (2000) identified the expected main drivers of biodiversity change on a global scale in the future. These are, in order of predicted magnitude:

1. Changes in human landuse

2. Atmospheric CO_2 concentration

3. Nitrogen deposition and acid rain

4. Climate

5. Deliberate or accidental biotic exchanges

The pattern of biotic exchanges influencing biodiversity changes closely mirrors patterns of human activity. In Britain this effect is especially pronounced due to the long history of intensive landuse through agri- and silviculture. Rodwell (1991) points out that few plant communities in the British Isles are unaffected by human activity, despite public perception of untouched wilderness (e.g., in the upland regions).

Future climatic change, for example, is likely to lead to changes in the species

composition and the productivity of most habitats. Climate change is not only defined by increases or decreases in mean values of temperature and precipitation, but also by increased variability in these parameters. Climate variability can help maintain diversity in plant communities by regulating the coexistence of competing species (Adler et al., 2004). Permanent changes resulting from a distinct alteration of climate could thus be offset by this mechanism. This depends though on the time scales involved and on the impacts and frequency of extreme events. Climate variability should therefore be taken into account when predicting future diversity.

The following changes in vegetation might be expected to occur as a consequence of climate change and are addressed in this study as having the greatest potential to be monitored effectively using remote sensing techniques:

1. geographical shifts in the distribution of communities,

2. increased standing biomass through an extended growing season,

3. structural changes within vegetation canopies throughout the seasons.

Considering the likely magnitude of future biodiversity change driven by factors such as the above, reliable methods for change detection and monitoring are essential and efforts to utilize remote sensing data are well developed (Alimohammadi et al., 2004; Hegarat-Mascle et al., 2006).

The results from this study have suggested that hyperspectral remote sensing data, for example, might potentially be used to monitor grasslands such that such subtle changes can be identified as they take place. The data demonstrates that the red-edge wavelength region provides information on the biomass, productivity and improvement level of grasslands.

However, to achieve effective change detection, a long term monitoring strategy based on remote sensing data and further research into the information able to be retrieved from spectral data would have to be put in place. Historic remote sensing data could be utilized to establish a baseline against which change could be estimated.

The land cover mapping undertaken in this study has the potential to provide a baseline from which to assess the impacts of future biodiversity change. If it were possible to survey a selection of change sensitive regions and communities by remote sensing on a regular basis, then this would form a non-biased monitoring scheme through which change could be registered, demonstrated and reliably recorded.

9.6 Summary and conclusions

The study has indicated that more detailed mapping of habitats can be undertaken using finer spatial resolution SPOT HRG data to segment the landscape into recognizable units and by using time-series of other spaceborne optical data to differentiate habitat types. Simply by virtue of the greater detail provided, the classifications give greater opportunity for linking habitats to the distribution of flora and fauna across the landscape. Whilst a number of species can be classified because they form the dominant vegetation cover and occur across large areas (e.g., bracken, *Molinia*, gorse), many species are unable to be mapped individually for reasons of scale and data resolution and diversity can only be inferred. For grasslands, for example, higher diversity is indicated through association with areas that are unimproved. Lowest diversity is linked to improved grasslands and

mono-dominant grasslands (e.g., *Molinia* in the uplands).

For forests, differentiation of tree species is difficult in multi-layered canopies and without the use of high resolution optical sensor data. Where tree species form relatively uniform stands (e.g., birch, oak), some discrimination is possible but the majority of forests in Wales are of mixed species composition. Therefore, from spaceborne data, only broad forest types can be reliably classified.

In terms of assessing the diversity of fauna (including mammals and bats as well as birds), knowledge of the three-dimensional structure of forests is essential. NextMap Britain could potentially provide information on the top height of the canopy but is very limited by the lack of an accurate DTM at a national level. The use of a DEM generated independently from LiDAR may be a viable option, particularly as once obtained, height (and changes in height) can be assessed from subsequent overflights of interferometric SAR.

LiDAR profiles can be reliably extracted which can then in turn be related to the distribution of foliage and branches within the forest volume, with this providing an indication of the likely distribution of bird and other faunal species. Habitat suitability models should exploit the structural information derived from LiDAR data but great care needs to be taken in their parameterization.

This chapter has discussed the outcomes of research in the context of

1. regional mapping of semi-natural habitats from spaceborne data

2. differentiation of grassland improvement levels

3. detailed characterization of forests in two and three dimensions

4. The implications for biodiversity assessment

Whilst this study has not contributed to assessment of all biodiversity, it has

contributed components, which ought to be used in a continuous monitoring and assessment system.

Key benefits of the research include:

1. Differentiation of grassland improvement levels from hyperspectral image data

2. Detailed mapping of vegetation land cover types from multispectral satellite data at the landscape scale

3. Integration of ecological knowledge and remote sensing data for land cover mapping

4. The mapping methods are re-producable and are easily understood

5. There is capacity to implement a monitoring system through regular updates of the map as and when satellite sensor data are acquired

6. Opportunities to bring in other forms of remotely sensed data include higher resolution NIR aerial photography to achieve a better segmentation

7. Airborne LiDAR and terrestrial laser scanner data correlate well and can supply forest structural information

8. Specialist woodland bird species are found to have strong habitat preferences with regard to the forest vertical profile

Modern ecology's emphasis on the variability in structure and function at all spatial and temporal scales can be mirrored by studying these phenomena in remote sensing data of corresponding variability. This study has shown that a wide variety of airborne and spaceborne, optical and laser remote sensing data can be utilized

to assess biodiversity at different scales and in different habitats.

9.6.1 Benefits

This study benefits the scientific community and also conservation organizations, particularly in terms of laser scanner research and biodiversity assessment. A better understanding of the use of remote sensing data for forest structure and tree species mapping in the UK from the local to the landscape level is of particular use to forestry organizations (e.g., the Forestry Commission, Woodland Trust).

The results of the study further support the aims stated in Chapter 1.

Bibliography

, 2005. Riegl laser measurements systems gmbh, company homepage, http://www.riegl.com, accessed October 2007.

Abrams, M., 1999. The advanced spaceborne thermal emission and reflection radiometer (aster): Data products for the high spatial resolution imager on nasa's eos-am1 platform. International Journal of Remote Sensing 1, 1–13.

Adams, J., Sabol, D., Kapos, V., Filho, R., Roberts, D., Smith, M., Gillespie, A., 1995. Classification of multispectral images based on fractions of endmembers: Application to land-cover change in the brazilian amazon. Remote Sensing of the Environment 52, 137–154.

Adler, P. B., Armitage, R. P., Kent, M., Weaver, R. E., 2004. Identification of the spectral characteristics of british semi-natural upland vegetation using direct ordination: a case study from dartmoor, uk. Proceedings of the National Academy of Sciences of the United States 25 (17), 3369–3388.

Alimohammadi, A., Rabiei, H., Firouzabadi, P., June 2004. A new approach for modeling uncertainty in remote sensing change detection process. In: Proceedings of the 12th International ConferenCe on GeoInformatics - GeoSpatial Information Research: Bridging the Pacific and Atlantic. University of Gaevle, Sweden.

Andersen, H., McGaughey, R., Reutebuch, S., 2005. Estimating forest canopy fuel parameters using lidar data. Remote Sensing of Environment 94 (4), 441–449.

Anderson, J., Plourde, J., Martin, M., BrasWell, B., Smith, M., Dubayah, R., Hofton, M., BlAir, J., 2008. Integrating waveform lidar with hyperspectral im-

agery for inventory of a northern temperate forest. Remote Sensing of Environment 112 (4), 1856–1870.

Antonarakis, A., Richards, K., Brasington, J., 2008. Object-based land cover classification using airborne lidar. Remote Sensing of Environment 112 (6), 2988–2998.

Asner, G., Knapp, D., Kennedy-Bowdoin, T., 2008. Invasive species detection in hawaiian rainforests using airborne imaging spectroscopy and lidar. Remote Sensing of Environment 112 (5), 1942–1955.

Asner, G. P., 1998. Biophysical and biochemical sources of variability in canopy reflectance. Remote Sensing of Environment 64 (3), 234–253.

Avery, M., 2008. Spotlight on climate change. Birds 22 (2), 82.

Balzter, H., Luckman, A., Skinner, L., RowLand, C., Dawson, T., 2007. Observations of forest stand top height and mean height from interferometric sar and lidar over a conifer plantation at thetford forest, uk. International Journal of Remote Sensing 28 (6), 1173–1197.

Barbeito, I., Caellas, I., Montes, F., 2009. Evaluating the behaviour of vertical structure indices in scots pine forests. Annals of Forest Science 66 (6), 710–720.

Barnett, P. R., Whittingham, M. J., R.B., B., Wilson, J. D., 2004. Use of unimproved and improved lowland grassland by wintering birds in the uk. Agriculture, Ecosystems and Environment 102 (1), 49–60, no copy.

Bateson, C. A., Asner, G. P., Wessman, C. A., 2000. Endmember bundles: A new approach to incorporating endmember variability into spectral mixture analysis. IEEE Transactions in Geoscience and Remote Sensing 38 (2), 1083–1094.

Baudry, J., Poggio, S., 2007. Landscape ecology and agriculture. In: BunCe, R., Jongman, R., Hojas, L., Weel, S. (Eds.), 25 Years of Landscape Ecology: Scientific Principles in Practice, Proceedings of the 7th IALE World Congress - Part 1. IALE, Wageningen, The NetherLands, pp. 23–24.

Bendelow, V. C., Hartnup, R., 1980. Climatic classification of england and wales. Tech. rep., Soil Survey Technical Monograph No. 15, Harpenden, UK.

Benz, U. C., Hofmann, P., Wilhauck, G., Lingenfelder, I., Heynen, M., 2003. Multi-resolution, object-orientated fuzzy analysis of remote sensing data for gis-ready information. ISPRS Journal of Photogrammetry and Remote Sensing 58, 239–258.

Blair, J. B., Rabine, D. L., Hofton, M. A., 1999. The laser vegetation imaging sensor: a medium-altitude, digitisation-only, airborne laser altimeter for mapping vegetation and topography. ISPRS Journal of Photogrammetry and Remote Sensing 54, 115–122.

Bock, M., Xofis, P., Mitchley, J., Rossner, G., Wissen, M., 2005. Object-oriented methods for habitat mapping at multiple scales - case studies from northern germany and wye downs, uk. Journal for Nature Conservation 131, 75–89.

Boncina, A., 2000. Comparison of structure and biodiversity in the rajhenav virgin forest remnant and managed forest in the dinaric region of slovenia. Global Ecology and Biogeography 9, 201–211.

Bork, E. W., Su, J. G., 2007. Integrating lidar data and multispectral imagery for enhanced classification of rangeland vegetation: A meta analysis. Remote Sensing of Environment 111 (1), 11–24.

Botkin, D., Estes, J., MacDonald, R., Wilson, M., 1984. Studying the earth's vegetation from space. BioScience.

Boulinier, T., Nichols, J. D., Hines, J. E., Sauer, J. R., Flather, C. H., Pollock, K. H., 2001. Forest fragmentation and bird community dynamics: Inference at regional scales. Ecology 82 (4), 1159–1169.

Boutten, T. W., Tieszen, L. L., 1983. Estimation of plant biomass by spectral reflectance in an east african grassland. Journal of Range Management 36 (2), 213–216.

Bradbury, R. B., Hill, R. A., Mason, D. C., Hinsley, S. A., Wilson, J. D., Balzter, H., Anderson, G. Q. A., Whittingham, M. J., Davenport, I. J., Bellamy, P. E., 2005. Modeling relationships between birds and vegetation structure using airborne lidar data: a review with case studies from agricultural and woodland environments. Ibis 147, 443–452.

Brandtberg, T., 2007. Classifying individual tree species under leaf-off and leaf-on conditions using airborne lidar. ISPRS Journal of Photogrammetry and Remote Sensing 61 (5), 325–340.

Breidenbach, J., Koch, B., Kandler, G., 2008. Quantifying the influence of slope, aspect, crown shape and stem density on the estimation of tree height at plot level using lidar and insar data. International Journal of Remote Sensing 29 (5), 1511–1536.

Breyer, J. F., Medcalf, K., 2006. Monitoring and evaluating climate change effects in grassland communities, using remote sensing techniques. IEEM, Cardiff, UK.

Bunting, P., 2009. The sorted point format (spd): An efficient storage format for 3-dimensional point data. Tech. rep., Institute of Geography and Earth Sciences, Aberystwyth University, UK; http://www.spdlib.org.

Bunting, P., Clewley, D., 2009. The remote sensing and gis software library (rsgislib). Tech. rep., Institute of Geography and Earth Sciences, Aberystwyth University, UK; http://www.rsgislib.org.

Bunting, P. J., Lucas, R. M., 2006. The delineation of tree crowns in australian mixed forests using hyperspectral compact airborne spectrographic imager (casi) data. Remote Sensing of Environment 101, 230–248.

Bunting, P. J., Paterson, M., Lucas, R. M., 2006. Discrimination of tree species in australian woodlands using hyperspectral casi data. In: Workshop on 3D Remote Sensing in Forestry. Vienna, Austria.

Chander, G., Markham, B. L., Helder, D., 2009. Summary of current radiometric calibration coefficients for landsat mss, tm, etm+, and eo-1 ali sensors. Remote Sensing of Environment 113, 893–903.

Chapin III, F. S., Zavaleta, E. S., Eviner, V. T., Naylor, R. L., VitoUsek, P. M., Reynolds, H. L., Hooper, D. U., 2000. Consequences of changing biodiversity. Nature 405, 234–242.

Chasmer, L., Hopkinson, C., Treitz, P., 2006. Investigating laser pulse penetration through a conifer canopy by integrating airborne and terrestrial lidar. Canadian Journal of Remote Sensing 32 (2), 116–125.

Chen, J., Gu, S., Shen, M., Tang, Y., Matsushita, B., 2009. Estimating above-ground biomass of grassland having a high canopy cover: an exploratory analysis of in situ hyperspectral data. International Journal of Remote Sensing 30 (24), 6497–6517.

Chen, Q., Gong, P., Baldocchi, D., Tian, Y., 2007a. Estimating basal area and stem volume for individual trees from lidar data. Photogrammetric Engineering and Remote Sensing 73 (12), 1355–1365.

Chen, Q., Gong, P., Baldocchi, D., Tian, Y. Q., 2007b. Estimating Basal Area and Stem Volume for Individual Trees from LiDAR Data. Photogrammetric Engineering and Remote Sensing 73 (12), 1355–1365.

Chen, X., Vierling, L., RoWell, E., De FeliCe, T., 2005. Using lidar and effective lai data to evaluate ikonos and landsat 7 etm+ vegetation cover estimates in a ponderosa pine forest. Remote Sensing of Environment 91, 14–26.

Cherrill, A., McClean, C., 1999. Between-observer variation in the application of a standard method of habitat mapping by environmental consultants in the uk. The Journal of Applied Ecology 36, 989–1008.

Cho, M. A., Skidmore, A., Corsi, F., van Wieren, S. E., Sobhan, I., 2007. Estimation of green grass/herb biomass from airborne hyperspectral imagery using spectral indices and partial least squares regression. International Journal of Applied Earth Observation and GeoInformation 9 (4), 414–424.

Clawges, R., Vierling, K., Vierling, L., RoWell, E., 2008. The use of airborne lidar to assess avian species diversity, density, and occurrence in a pine/aspen forest. Remote Sensing of Environment 112 (5), 2064–2073, print-out in folder.

Congalton, R., 1991. A review of assessing the accuracy of classifications of remotely sensed data. Remote Sensing of Environment 37, 35–46, don't have a copy.

Congalton, R., Green, K., 1993. A practical look at the sources of confusion in error matrix generation. Photogrammetric Engineering & Remote Sensing 59 (5), 641–644, only paper copy.

Coops, N., Hilker, T., Wulder, M., St-Onge, B., 2007. Estimating Canopy Struc-

ture of Douglas-Fir Forest Stands from Discrete-Return LiDAR. Trees-Structure and Function 21, 295–310.

Cushman, S. A., McKelvey, K. S., Flather, C. H., McGarigal, K., 2008. Do forest community types provide a sufficient basis to evaluate biological diversity? Frontiers in Ecology 6 (1), 13–17.

Czaplewski, R., Patterson, P., 2003. Classification accuracy for stratification with remotely sensed data. Forest Science 49, 402–408.

Dalponte, M., Bruzzone, L., Gianelle, D., 2008. Fusion of hyperspectral and lidar remote sensing data for classification of complex forest areas. IEEE Transactions on Geoscience and Remote Sensing 46 (5), 1416–1427.

Danson, F., Hetherington, D., Morsdorf, F., 2007a. Forest canopy gap fraction from terrestrial laser scanning. IEEE Geoscience and Remote Sensing Letters 4 (1), 157–160.

Danson, F., Hetherington, D., Morsdorf, F., Koetz, B., Allgoewer, B., 2007b. Forest canopy gap fraction from terrestrial laser scanning. IEEE Geoscience and Remote Sensing Letters 4 (1), 157–160, print-out in folder.

Dauber, J., Hirsch, M., Simmering, D., Waldhardt, R., Otte, A., Wolters, V., 2003. Landscape structure as an indicator of biodiversity: matrix effects on species richness. Agriculture, Ecosystems and Environment 98 (2003) 321329 98, 321–329.

Davenport, I. J., Bradbury, R. B., Anderson, G. Q. A., Hayman, G. R. F., Krebs, J. R., Mason, D. C., Wilson, J. D., Veck, N. J., 2000. Improving bird population models using airborne remote sensing. International Journal of Remote Sensing 21 (13&14), 2705–2717, print-out in folder.

Definiens, 2008. Definiens in earth sciences. Tech. rep., http://www.definiens.com.

Drake, J., Dubayah, R. O., Knox, R. G., Clark, D. B., BlAir, J., 2002. Sensitivity of large-footprint lidar to canopy structure and biomass in a neo-tropical rainforest. Remote Sensing of Environment 81 (2-3), 378–292.

Du, Y., Teillet, P. M., Cihlar, J., 2002. Radiometric normalization of multitemporal

high resolution images with quality control for land cover change detection. Remote Sensing of Environment 82, 123–134.

Elachi, C., 1987. Introduction to the Physics and Techniques of Remote Sensing. John Wiley & Sons.

European, Commission, 1994. Corine land cover technical guide. Tech. rep., EUR 12585 EN, OPOCe Luxembourg.

Eycott, A., Watts, K., Moseley, D., Ray, D., 2007. Evaluating biodiversity in fragmented landscapes: the use of focal species. Tech. rep., Forestry Commission Information Note 89. Forestry Commission, Edinburgh.

Fargione, J., Tilman, D., Dybzinski, R., Ris Lambers, J. H., Clark, C., Stanley Harpole, W., Knops, J., Reich, P., Loreau, M., 2007. From selection to complementarity: shifts in the causes of biodiversityproductivity relationships in a long-term biodiversity experiment. Proceedings of the Royal Society of Biological Sciences 274, 871–876.

Fearer, T. M., Prisley, S. P., Stauffer, D. F., Keyser, P. D., 2007. A method for integrating the breeding bird survey and forest inventory and analysis databases to evaluate forest bird-habitat relationships at multiple scales. Forest Ecology and Management 243, 128–143.

Foody, G. M., 2002. Status of land cover classification accuracy assessment. Remote Sensing of the Environment 80, 185–201.

Foody, G. M., 2008. Harshness in image classification accuracy assessment. International Journal of Remote Sensing 29 (11), 3137–3158.

Freeman, S. N., Noble, D. G., Newson, S. E., Bailie, S. R., 2003. Modeling bird population changes using data from the common birds census and the breeding bird survey, research report 303. Tech. rep., BTO, Thetford.

Friedla, M. A., Michaelsen, J., Davis, F. W., Walker, H., Schimel, D. S., 1994. Estimating grassland biomass and leaf area index using ground and satellite data. Internation Journal of Remote Sensing 15 (7), 1401–1420.

Fuller, R., Groom, G., Jones, A. R., 1994. The land-cover map of great-britain -

an automated classification of landsat thematic mapper data. Photogrammetric Engineering and Remote Sensing 60, 553–562.

Fuller, R., Smith, G., DEVEREUX, B., 2003. The characterization and measurement of land cover change through remote sensing: problems in operational applications? International Journal of Applied Earth Observation 4, 243–253.

Fuller, R., Smith, G., Sanderson, J., Hill, R., Thomson, A., 2002. The uk land cover map 2000: Construction of a parcel-based vector map from satellite images. Cartographic Journal 39, 15–25.

Fuller, R. J., H, M. J., A, M. R., 1985. How representative of agricultural practice in britain are common birds census farmland plots? Bird Study 32, 56–70.

Fuller, R. M., Amable, G. S., Devereux, B. J., Gillings, S., Hill, R. A., Smith, G. M., 2006. Development and application of a landscape-scale approach to ecology: the evolving framework of the uk remotely sensed land cover maps. In: Applications & Developments in Commercial Remote Sensing & Photogrammetry, The Annual ConferenCe of the Remote Sensing and Photogrammetry Society. RSPSoc, Cambridge.

Fuller, R. M., Cox, R., Clarke, R. T., Rothery, P., Hill, R. A., Smith, G. M., Thomson, A. G., Brown, N. J., Howard, D. C., Stott, A. P., 2005a. The uk land cover map 2000: Planning, construction and calibration of a remote sensing, user-orientated map of broad habitats. International Journal of Applied Earth Observation and GeoInformation 7, 202–216.

Fuller, R. M., Devereux, B. J., Gillings, S., Amable, G. S., Hill, R. A., 2005b. Indices of bird-habitat prefence from field surveys of birds and remote sensing of land cover: a study of south-eastern england with wider implications for conservation and biodiversity assessment. Global Ecology and Biogeography 14 (3), 223–239.

Gamon, J. A., Field, C. B., Goulden, M L Griffin, K. L., Hartley, A. E., Joel, G., Penuelas, J., Valentini, R., 1995. Relationships between ndvi, canopy structure, and photosynthesis in three californian vegetation types. Ecological Applications 5 (1), 28–41.

Gil-Tena, A., Brotons, L., Saura, S., 2010. Effects of forest landscape change and management on the range expansion of forest bird species in the mediterranean region. Forest Ecology and Management 259, 1338–1346.

Gilbert, G., Gibbons, D., Evans, J., 1998. Bird Monitoring Methods: A Manual of Techniques for Key UK Species. RSPB: Sandy.

Goetz, S., 1997. Multi-sensor analysis of ndvi, surface temperature and biophysical variables at a mixed grassland site. International Journal of Remote Sensing 18 (1), 71–94.

Goetz, S., Steinberg, D., Dubayah, R., BlAir, B. J., 2007. Laser remote sensing of canopy habitat heterogeneity as a predictor of bird species richness in an eastern temperate forest, usa. Remote Sensing of Environment 108, 254–263, print-out in folder.

Gong, P., Pu, R., Biging, G. S., Larrieu, M. R., 2003. Estimation of forest leaf area index using vegetation indices derived from hyperion hyperspectral data. IEEE Transactions in Geoscience and Remote Sensing 41 (6), 1355–1362.

Goodin, D., Henebry, G., 1998. Seasonality of finely resolved spatial structure of ndvi and its component reflectances in tallgrass prairie. International Journal of Remote Sensing 19 (16), 3213–3220.

Goodwin, N., Coops, N., Culvenor, D., 2006a. Assessment of forest structure with airborne lidar and the effects of platform altitude. Remote Sensing of Environment 103 (2), 140–152.

Goodwin, N. R., Coops, N. C., Culvenor, D. S., 2006b. Assessment of Forest Structure with Airborne LiDAR and the Effects of Platform Altitude. Remote Sensing of Environment 103 (2), 140–152.

Gorte, B., Pfeifer, N., 2004. Structuring Laser-Scanned Trees Using 3D Mathematical Morphology. In: XXth ISPRS Congress, Istanbul, TurKey, International Archives of Photogrammetry and Remote Sensing.

Gregory, R. D., Noble, D., Field, R., Marchant, J., Raven, M., Gibbons, D. W., Ornis Hungarica. Using birds as indicators of biodiversity. 2003 12, 11–24.

Grimm, C., Kremer, J., 2005. Digicam and litemapper - versatile tools for in-

dustrial projects. In: Fritsch, D. (Ed.), Photogrammetric Week 05. Wichmann Verlag, Heidelberg.

Guisan, A., Thuiller, W., 2005. Predicting species distribution: Offering more than simple habitat models. Ecology Letters 8 (9), 993–1009.

Guo, Q., 2007. The diversitybiomassproductivity relationships in grassland management and restoration. Basic and Applied Ecology 8 (3), 199–208.

Guo, X., Wilmshurst, J., McCanny, S., Fargey, P., Richard, P., 2004. Measuring spatial and vertical heterogeneity of grasslands using remote sensing techniques. Journal of Environmental Informatics 3, 24–32.

Haack, B., Bechdol, M., 2000. Integrating multisensor data and radar texture measures for land cover mapping. Computers and Geosciences 26 (4), 411–421.

Hanski, I., 1998. Metapopulation dynamics. Nature 396, 41–49.

Harding, D. J., Carabajal, C. C., 2005. Icesat waveform measurements of within-footprint topographic relief and vegetation vertical structure. Geophysical Research Letters 32 (21), L21S10.

Harding, D. J., Lefsky, M., Parker, G., BlAir, J., 2001. Laser altimeter canopy height profiles: Methods and validation for closed-canopy, broadleaf forests. Remote Sensing of Environment 76 (3), 283–297.

Hay, G., Blaschke, T., MarCeau, D. (Eds.), 2008. GeoBIA 2008 - Pixels, Objects, IntelligenCe, Geographic Object Based Image Analysis for the 21st Century. No. XXXVIII, 4/C1 in The International Archives of the Photogrammetry, Remote Sensing and Spatial Information Sciences. International Society for Photogrammetry and Remote Sensing.

Hayes, M. J., Sackville Hamilton, N. R., 2001. The effect of sward management on the restoration of species rich grassland: A re-assessment of iger's lowland grassland restoration experiment, trawscoed. Tech. rep., IGER - Institute of Grassland and Environmental Research.

Hayes, M. J., Sackville Hamilton, N. R., TalLowin, J. R. B., Buse, A., Davies, O., 2000. Methods of enhancing diversity in upland esa swards. Tech. rep.

Hector, A., Schmid, B., Beierkuhnlein, C., Caldeira, M. C., Diemer, M., Dimitrakopoulos, P. G., Finn, J. A., Freitas, H., Giller, P. S., Good, J., Harris, R., Hogberg, P., Huss-Dannell, K., Joshi, J., Jumpponen, A., Korner, C., Leadley, P. W., Loreau, M., Minns, A., Mulder, C. P. H., O'Donovan, G., Otway, S. J., Pereira, J. S., Prinz, A., Read, D. J., Scherer-Lorenzen, M., Schulze, E. D., Siamantziouras, A. S. D., Spehn, E. M., Terry, A. C., Troumbis, A. Y., Woodward, F. I., Yachi, S., Lawton, J. H., 1999. Plant diversity and productivity experiments in european grasslands. Science 286 (5442), 1123–1127.

Hegarat-Mascle, L., Seltz, R., Hubert-Moy, L., Corgne, S., Stach, N., 2006. Performance of change detection using remotely sensed data and evidential fusion: Comparison of three cases of application. International Journal of Remote Sensing 27 (16), 3515–3532.

Helle, P., Fuller, R., 1988. Migrant passerine birds in european forest successions in relation to vegetation height and geographical position. Journal of Animal Ecology 57 (2), 565–579.

Henning, J., Radtke, P., 2006a. Ground-based laser imaging for assessing three-dimensional forest canopy structure. Photogrammetric Engineering and Remote Sensing 72 (12), 1349–1358.

Henning, J. G., Radtke, P. J., 2006b. Ground-based laser imaging for assessing three-dimensional forest canopy structure. Photogrammetric Engineering and Remote Sensing 72 (12), 1349–1358.

Hill, M. J., 2004. Remote Sensing for Natural Resource Management and Environmental Monitoring. Vol. 4. John Wiley & Sons, Inc., Hoboken, New Jersey, Ch. Grazing Agriculture: Managed Pasture, Grassland, and Rangeland, pp. 449–530.

Hill, R. A., Hinsley, S. A., Gaveau, D. L. A., Bellamy, P. E., 2004. Predicting habitat quality for great tits (parus major) with airborne laser scanning data. International Journal of Remote Sensing 25 (22), 4851–4855, print-out in folder.

Hill, R. A., Thompson, A. G., 2005. Mapping woodland species composition and structure using airborne spectral and lidar data. International Journal of Remote Sensing 26 (17), 3763–3779, print-out in folder.

Hinsley, S., Hill, R., Bellamy, P., Balzter, H., 2006. The application of lidar in woodland bird ecology: Climate, canopy structure and habitat quality. Photogrammetric Engineering and Remote Sensing 72 (12), 1399–1406, print-out in folder.

Hinsley, S. A., Hill, R. A., Gaveau, D. L. A., Bellamy, P. E., 2002. Quantifying woodland structures and habitat quality for birds using airborne laser scanning. Functional Ecology 16 (6), 851–857, print-out in folder.

Hirzel, A. H., Braunisch, V., LeLay, G., Hausser, J., Perrin, N., 2008. Biomapper 4.0. Tech. rep., Laboratory of Conservation Biology, Department of Ecology and Evolution, University of Lausanne, Lausanne, SwitzerLand. Available from http://www.unil.ch/BioMapper.

Hirzel, A. H., Helfer, V., Metral, F., 2001. Assessing habitat-suitability models with a virtual species. Ecological Modeling 145, 111–121.

Holden, N. M., Brereton, A. J., 2002. An assessment of the potential impact of climate change on grass yield in ireland over the next 100 years. Irish Journal of Agricultural and Food Research 41 (2), 213–226.

Holmgren, J., Persson, A., Soederman, U., 2008. Species identification of individual trees by combining high resolution lidar data with multi-spectral images. Internationl Journal of Remote Sensing 29 (5), 1537–1552.

Howe, L., Blackstock, T., Burrows, C., Stevens, J., 2005. The habitat survey of wales. British Wildlife 16, 153–162.

Hudak, A., Crookston, N., Evans, J., Hall, D., 2008. Nearest neighbour imputation of species-level, plot-scale forest structure attributes from lidar data. Remote Sensing of Environment 112, 2231–2245.

Hug, C., UllRich, A., Grimm, A., 2004. Litemapper-5600 - a waveform-digitizing lidar terrain and vegetation mapping system. ISPRS XXXVI, Part 8/W2, 24–29.

Hyde, P., 2005. Measuring and mapping forest wildlife habitat characteristics using lidar remote sensing and multi-sensor fusion. Ph.D. thesis, University of MaryLand.

Hyde, P., Dubayah, R., Peterson, B., BlAir, J., Hofton, M., Hunsaker, C., Knox,

R., Walker, W., 2005. Mapping forest structure for wildlife habitat analysis using waveform lidar: Validation of montane ecosystems. Remote Sensing of Environment 96 (3-4), 427–437.

Hyde, P., Dubayah, R., Walker, w., Blair, B. J., Michelle, H., Hunsaker, C., 2006a. Mapping forest structure for wildlife habitat analysis using multi-sensor (lidar, sar/insar, etm+, quickbird) synergy. Remote Sensing of Environment 102, 63–73.

Hyde, P., Dubayah, R., Walker, W., Blair, J., Hofton, M., Hunsaker, C., 2006b. Mapping Forest Structure for Wildlife Habitat Analysis Using Multi-Sensor (Li-DAR, SAR/InSAR, ETM+, QuickBird) Synergy. Remote Sensing of Environment 102, 63–73.

Hyppae, J., Hyppae, H., Leckie, D., GouGeon, F., 2008. Review of methods of small-footprint airborne laser scanning for extracting forest inventory data in boreal forests. International Journal of Remote Sensing 29 (10), 1339–1366.

Hyppae, J., Kelle, O., Lehikoinen, M., Inkinen, M., 2001. A segmentation-based method to retrieve stem volume estimates from 3-d tree height models produced by laser scanners. IEEE Transactions on Geoscience and Remote Sensing 39 (5), 969–975.

Inc, R. S., 2003. (rsi) envi user guide.

Innes, J. L., Koch, B., 1998. Forest biodiversity and its assessment by remote sensing. Global Ecology and Biogeography Letters 7 (6), 397–419.

Iverson, L., Graham, R., Cook, E., 1989. Applications of satellite remote sensing to forested ecosystems. Landscape Ecology.

Jacobsen, A., Nielsen, A. A., Ejrns, R., Groom, G. B., 2000. Spectral identification of plant communities for mapping of semi-natural grasslands. Canadian Journal of Remote Sensing 26 (5), 370–383.

James, F. C., Wamer, N. O., 1982. Relationships between temperate forest bird communities and vegetation structure. Ecology 63 (1), 159–171.

Jang, J.-D., Payan, V., Viau, A., Devost, A., 2008a. The use of airborne lidar for

orchard tree inventory. International Journal of Remote Sensing 29 (6), 1767–1780.

Jang, J. D., Payan, V., Viau, A. A., Devost, A., 2008b. The Use of Airborne LiDAR for Orchard Tree Inventory. International Journal of Remote Sensing 29 (6), 1767–1780.

Jiang, X. L., Zhang, W. G., Wang, G., 2007. Biodiversity effects on biomass production and invasion resistance in annual versus perennial plant communities. Biodiversity and Conservation 16 (6), 1983–1994.

Jing, X., Wang, J., WenJiang, H., Liu, L., Wang, J. D., 2009. Computer and Computing Technologies in Agriculture II, Volume 1. Springer Boston, Ch. Study on Forest Vegetation Classification Based on Multitemporal Remote Sensing Images, pp. 115–123.

JNCC, 2003. Handbook for Phase 1 Habitat Survey - A Technique for Environmental Audit. Joint Nature Conservation Committee.

Jones, M. B., Donnelly, A., 2004. Carbon sequestration in temperate grassland ecosystems and the influence of management, climate and elevated co2. New Phytologist 164, 423–439.

Jupp, D., Culvenor, D., Lovell, J., 2009. Estimating forest lai profiles and structural parameters using a ground-based laser called 'echidna'. Tree Physiology 29 (2), 171–181.

Jupp, D., Culvenor, D., Lovell, J., Newnham, G., 2005. Evaluation and validation of canopy laser radar systems for native and plantation forest inventory. Tech. rep., Australian GOvernment: Forest and Wood Products Research and Development CorpoRation.

Kempeneers, P., Deronde, B., Provoost, S., Houthuys, R., 2009. Synergy of airborne digital camera and lidar data to map coastal dune vegetation. Journal of Coastal Research, 73–82.

Keshava, N., 2003. A survey of spectral unmixing algorithms. Lincoln Laboratory Journal 14 (1), 55–78.

Kimes, D., Ranson, K., G.Sun, Blair, J., 2006. Predicting lidar measured forest

vertical structure from multi-angle spectral data. Remote Sensing of Environment 100 (4), 503–511.

Koetz, B., Morsdorf, F., Sun, G., Ranson, K., Itten, K., 2006. Inversion of a LiDAR Waveform Model for Forest Biophysical Parameter Estimation. IEEE Geoscience and Remote Sensing Letters 3 (1), 49–53.

Krauss, J., Klein, A.-M., Steffan-Dewenter, I., Tscharntke, T., 2004. Effects of habitat area, isolation, and landscape diversity on plant species richness of calcareous grasslands. Biodiversity and Conservation 13, 1427–1439.

Krebs, C. J., 2008. Ecology: The Experimental Analysis of Distribution and Abundance, 6th Edition. Pearson Education.

Laba, M., Gregory, S., Braden, J., Ogurcak, D., Hill, E., Fegraus, E., Fiore, J., Degloria, S., 2002. Conventional and fuzzy accuracy assessment of the new york gap analysis project land cover map. Remote Sensing of Environment 81, 443–455.

Lang, S., Blaschke, T., Schoepfer, E. (Eds.), 2006. Bridging Remote Sensing and GIS - 1st International ConferenCe on Object-Based Image Analysis (OBIA 2006). No. XXXVI, 4/C42 in The International Archives of the Photogrammetry, Remote Sensing and Spatial Information Sciences. International Society for Photogrammetry and Remote Sensing.

Langanke, T., Rossner, G., Vrscaj, B., Lang, S., Mitchley, J., 2005. Selection and application of spatial indicators for nature conservation at different institutional levels. Journal for Nature Conservation 13, 101–114.

Lauver, C. L., 1997. Mapping species diversity patterns in the kansas shortgrass region by integrating remote sensing and vegetation analysis. Journal of Vegetation Science 8 (3), 387–394.

Lee, A., Lucas, R. M., 2007a. A lidar-derived canopy density model for tree stem and crown mapping in australian forests. Remote Sensing of Environment 111, 493–518.

Lee, A., Lucas, R. M., 2007b. A lidar derived canopy density model for tree stem

and crown mapping in australian woodlands. Remote Sensing of Environment 111, 493–518.

Lefsky, M., Cohen, W., Acker, S., 1999a. Lidar remote sensing of the canopy structure and biophysical properties of douglas-fir western hemlock forests. Remote Sensing of Environment 70 (3), 339–361.

Lefsky, M. A., Harding, D., Cohen, W., Parker, G., Shugart, H., 1999b. Surface lidar remote sensing of basal area and biomass in deciduous forests of eastern maryland, usa. Remote Sensing of Environment 67 (1), 83–98.

Lefsky, M. A., Hudak, A. T., Guzy, M., Cohen, W. B., 2005. Combining lidar estimates of biomass and landsat estimates of stand age for spatially extensive validation of modeled forest productivity. Remote Sensing of Environment 95 (4), 549–558.

Lin, Y., Mills, J., Smith-Voysey, S., 2008. Detection of weak and overlapping pulses from waveform airborne laser scanning data. In: SilviLaser 2008, Sept. 17-19. Edinburgh, UK.

Liu, C., Frazier, P., Kumar, L., 2007. Comparative assessment of the measures of thematic classification accuracy. Remote Sensing of Environment 107, 606–616.

Lu, D. S., Moran, E., Batistella, M., 2003. Linear mixture model applied to amazonian vegetation classification. Remote Sensingof Environment 87 (4), 456–469.

Lucas, R., Cronin, N., Lee, A., Moghaddam, M., Witte, C., Tickle, P., 2006a. Empirical relationships between airsar backscatter and lidar-derived forest biomass, queensland, australia. Remote Sensing of Environment 100, 407–425.

Lucas, R., Medcalf, K., Brown, A., Bunting, P., Breyer, J., Clewley, D., BlackMore, P., in press. Updating the phase 1 habitat map of wales, uk, using satellite sensor data. International Journal of Remote Sensing and Photogrammetry.

Lucas, R. M., Brown, A., Breyer, J. F., Keyworth, S., Medcalf, K., Bunting, P. J., 2006b. Multi-temporal and multi-sensor classification of habitats and agricultural land in wales. In: Lafortezza, R., Sanesi, G. (Eds.), Patterns and Processes in Forest Landscapes: Consequences of human Management. Academia Italiana di Scienze Forestali, Locorotondo, Italy.

Lucas, R. M., Lee, A., Bunting, P., 2008. Retrieving forest biomass through integration of casi and lidar data. International Journal of Remote Sensing 29 (5), 1553–1577.

Lucas, R. M., Maghaddam, M., Cornin, N., 2004. Microwave scattering from mixed species woodlands, central queensland, australia. IEEE Transactions on Geoscience and Remote Sensing 42 (10), 2142–2159.

Lucas, R. M., RowLands, A., Brown, A., Keyworth, S., Bunting, P. J., 2007. Rulebased classification of multi-temporal and satellite imagery for habitat and agricultural land cover mapping. ISPRS Journal of Photogrammetry and Remote Sensing 62 (3), 165–185.

Maas, H., Bienert, A., Scheller, S., Keane, E., 2008a. Automatic forest inventory parameter determination from terrestrial laser scanner data. International Journal of Remote Sensing 29 (5), 1579–1593, print-out in folder.

Maas, H. G., Bienert, A., Scheller, S., Keane, E., 2008b. Automatic forest inventory parameter determination from terrestrial laser scanner data. International Journal of Remote Sensing 29 (5), 1579–1593.

Maddock, A. (Ed.), 2008. UK Biodiversity Action Plan - Priority Habitat Descriptions. UK Biodiversity Reporting and Information Group (BRIG).

Mallet, C., Bretar, F., 2009. Full-waveform topographic lidar: State-of-the-art. ISPRS Journal of Photogrammetry and Remote Sensing 64 (1), 1–16.

Marchant, J. H., Hudson, R., Carter, S. P., Whittington, P. A., 1990. Population trends in british breeding birds. BTO, Tring.

Martin, M., Newman, S., Aber, J., Congalton, R., 1998. Determining forest species composition using high spectral resolution remote sensing data. Remote Sensing of Environment 65, 249–254.

Martinuzzi, S., Vierling, L., Gould, W., Falkowski, M., Evans, J., Hudak, A., Vierling, K., 2009. Mapping snags and understory shrubs for a lidar-based assessment of wildlife habitat suitability. Remote Sensing of Environment 113 (12), 2533–2546.

Matthew, M., Adler-Golden, S., Berk, A., Richtsmeier, S., Levine, R., Bernstein,

L., Acharya, P., Anderson, G., Felde, G., Hoke, M., Ratkowski, A., Burke, H., Kaiser, R., Miller, D., 2000. Status of atmospheric correction using a modtran4-based algorithm. In: SPIE Proceedings: Algorithms for Multispectral, Hyperspectral, and UltraSpectral Imagery VI. pp. 199–207.

McGarigal, K., Marks, B. J., 2002. Fragstats: Spatial pattern analysis program for quantifying landscape structure. Tech. rep., University of MAssachUSetts Amherst, Available from http://www.umAss.edu/LandEco/Research/Fragstats/Fragstats.html.

Means, J., Acker, S., Harding, D., BlAir, J. B., Lefsky, M., Cohen, W., Harmon, M., Mckee, W., 1999. Use of airborne lidar to estimate forest stand characteristics in the western cascades of oregon. Remote Sensing of Environment 67 (3), 298–308.

Moffiet, T., Mengersen, K., Witte, C., King, R., Denham, R., 2005. Airborne laser scanning: Exploratory data analysis indicates potential variables for classification of individual trees or forest stands according to species. ISPRS Journal of Photogrammetry and Remote Sensing 59 (5), 289–309.

Moghaddam, M., Lucas, R., 2003. Quantifying the biomass of australian subtropical woodlands using SAR inversion models. 2003 IEEE International Geoscience and Remote Sensing Symposium, 2003. IGARSS'03. Proceedings 3.

Mutanga, O., Skidmore, A. K., 2004. Narrow band vegetation indices overcome the saturation problem in biomass estimation. International Journal of Remote Sensing 25 (19), 3999–4014.

Naesset, E., 1997. Determination of mean tree height of forest stands using airborne laser scanner data. ISPRS Journal of Photogrammetry and Remote Sensing 52 (2), 49–56.

Naesset, E., Gobakken, T., 2008. Estimation of above- and below-ground biomass across regions of the boreal forest zone using airborne laser. Remote Sensing of Environment 112 (6), 3079–3090.

Nagendra, H., 2001. Using remote sensing to assess biodiversity. International Journal of Remote Sensing 22 (12), 2377–2400.

Nelson, R., Hyde, P., Johnson, P., Emessiene, B., Imhoff, M., Campbell, R., Edwards, W., 2007. Investigating radar-lidar synergy in a north carolina pine forest. Remote Sensing of Environment 110 (1), 98–108.

Ni-Meister, W. S., Lee, A. H., Strahler, C. E., C., W., Schaaf, T., Yao, K. J.and Ranson, G. S., Blair, J. B., 2010. Assessing general relationships between aboveground biomass and vegetation structure parameters for improved carbon estimate from lidar remote sensing. Journal of Geophysical Research 115, 1–12.

O'Connor, R. J., Marchant, J. H., 1990. A field validation of some common birds census techniques. research report 4. BTO, Tring.

Perkins, D. F., 1968. The ecology of nardus stricta. Journal of Ecology 56, 633–640.

Pimm, S. L., Russell, G. J., Gittlerman, J. L., Brooks, T. M., 1995. The future of biodiversity. Science 269, 347–350.

Pinar, A., Curran, P. J., 1996. Grass chlorophyll and the reflectance red edge. International Journal of Remote Sensing 17 (2), 351–357.

Popescu, S., Zhao, K., 2008. A voxel-based lidar method for estimating crown base height for deciduous and pine trees. Remote Sensing of Environment 112 (3), 767–781.

Popescu, S. C., 2007. Estimating biomass of individual pine trees using airborne lidar. Biomass and Bioenergy 31 (9), 646–655.

Powell, R. L., Matzke, N., de Souza Jr., C., Clark, M., Numata, I., Hess, L. L., Roberts, D. A., 2004. Sources of error in accuracy assessment of thematic landcover maps in the brazilian amazon. Remote Sensing of Environment 90, 221–234.

Psomas, A., Kneubuehler, M., Itten, K., Zimmermann, N. E., 2007. Hyperspectral remote sensing for seasonal estimation of above-ground biomass in grassland habitats. ISPRS Working group.

Qiaoying, Z., Yunchun, Z., Yirdaw, E., Peng, L., Shaoliang, Y., Ning, W., 2006. Species diversity based on vertical structure as indicators of artificial restoration for coniferous forests in southwest china. Wuhan University Journal of Natural Sciences 11, 1003–1008.

Radoux, J., Defourny, P., Bogaert, P., 2008. Comparison of pixel- and object-based sampling strategies for thematic accuracy assessment. In: Hay, G., Blaschke, T., MarCeau, D. (Eds.), GeoBIA 2008 Pixels, Objects, IntelligenCe. Geographic Object Based Image Analysis for the 21st Century, ISPRS Vol. No. XXXVIII-4/C1. University of Calgary, Calgary Alberta, Canada.

Reichholf, J. H., 2005. Die Zukunft der Arten (The Future of Species). Beck Verlag, Munich.

Reitberger, J., Krzystek, P., Stilla, U., 2008. Analysis of Full Waveform LiDAR Data for the Classification of Deciduous and Coniferous Trees. International Journal of Remote Sensing 29 (5), 1407–1431.

Richter, R., 2009. Atmospheric / topographic correction for satellite imagery. Tech. Rep. DLR-IB 565-01/09, Deutsches Zentrum fuer Luft- und Raumfahrt (DLR), Wessling, Germany.

Richter, R., Mueller, A., 2005. De-shadowing of satellite/airborne imagery. International Journal of Remote Sensing 26 (13), 3137–3148.

Robertson, T. R., 2010. Precipitation magnitude and timing differentially affect species richness and plant density in the sotol grassland of the chihuahuan desert. OEcoLOGICA 162, 185–197.

Rock, B., Vogelmann, J., Williams, D., Vogelmann, A., Jan 1986. Remote detection of forest damage. BioScience.

Rodwell, J., 1991. Where the wild plants are. New Scientist 130 (1770), 33–36.

Rosette, J., North, P., Suarez, J., 2008. Vegetation height estimates for a mixed temperate forest using satellite laser altimetry. International Journal of Remote Sensing 29 (5), 1475–1493, print-out in folder.

Rushton, S., Luff, M., Eyre, M., 1989. Effects of pasture improvement and management on the ground beetle and spider communities of upland grasslands. Journal of Applied Ecology 26, 489–503, no paper or Digital copy.

Sala, O. E., Stuart Chapin III, F., Armesto, J. J., BerLow, E., BloomField, J., Dirzo, R., Huber-Sanwald, E., Huenneke, L., Jackson, R., Kinzig, A., Leemans, R., Lodge, D. M., Mooney, H., Oesterheld, M., LeRoy Poff, N., Sykes, M. T.,

Walker, B. H., Walker, M., Wall, D., 2000. Global biodiversity scenarios for the year 2100. Science 287 (5459), 1770–1774.

Schlaepfer, D., Richter, R., 2002. Geo-atmospheric processing of airborne imaging spectrometry data. part 2: Atmospheric/topographic correction. International Journal of Remote Sensing 23 (13), 2631–2649.

Schmidt, K. S., Skidmore, A. K., 2001. Exploring spectral discrimination of grass species in african rangelands. International Journal of Remote Sensing 22 (17), 3421–3434.

Shepherd, J. D., Dymond, J. R., 2003. Correcting satellite imagery for the variance of reflectance and illumination with topography. International Journal of Remote Sensing 24 (17), 3503–3514.

Shimabukuro, Y. E., Smith, J. A., 1991. The least squares mixing model to generate fraction images from remote sensing multispectral data. IEEE Transactions on Geoscience and Remote Sensing 29, 16–20.

Silleos, N. G., Alexandridis, T. K., Gitas, I. Z., Perakis, K., 2006. Vegetation indices: Advances made in biomass estimation and vegetation monitoring in the last 30 years. Geocarto International 21 (4), 21–28.

Silvertown, J., Dodd, M. E., McConway, K., Potts, J., Crawley, M., 1994. Rainfall, biomass variation and community composition in the park grass experiment. Ecology 75 (8), 2430–2437.

Simard, M., Rivera-Monroy, V., ManCer-Pineda, J., Castaneda-Moya, E., Twilley, R., 2008. A systematic method for 3d mapping of mangrove forests based on shuttle radar topography mission elevation data, icesat/glas waveforms and field data: Application to cinaga grande de santa marta, colombia. Remote Sensing of Environment 112, 2131–2144.

Slater, P. N., Biggar, S. F., 1996. Suggestions for radiometric calibration coefficient generation. Journal of Atmospheric and Oceanic Technology 13 (2), 376–382.

Slatton, K., Crawford, M., Evans, B., 2001. Fusing interferometric radar and laser altimeter data to estimate surface topography and vegetation heights. IEEE Transactions on Geoscience and Remote Sensing 39 (11), 2470–2482.

Smita, H. J., Metzger, M. J., Ewert, F., 2008. Spatial distribution of grassland productivity and land use in europe. Agricultural Systems 98, 208–219.

Smith, G. M., Wyatt, B. K., 2007. Multi-scale survey by sample-based field methods and remote sensing: A comparison of uk experience with european environmental assessments. Landscape and Urban Planning 79, 170–176.

Snow, D. W., 1965. The relationship between census results and the breeding population of birds on farmland. Bird Study 12, 287–304.

St-Onge, B., Vega, C., Fournier, R., Hu, Y., 2008. Mapping canopy height using a combination of digital stereophotogrammetry and lidar. International Journal of Remote Sensing 29 (11), 3343–3364.

Stehman, S., Czaplewski, R., 1998. Design and analysis for thematic map accuracy assessment: Fundamental principles. Remote Sensing of Environment 64, 331–344.

Stevens, C. J., Dise, N. B., Gowing, D. J., Mountford, O. J., 2006. Loss of forb diversity in relation to nitrogen deposition in the uk: Regional trends and potential controls. Global Change Biology 12, 1823–1833.

Stevens, J., Blackstock, T., Howe, E., Stevens, D., 2004. Repeatability of phase 1 habitat survey. Journal of Environmental Management 73, 53–59.

Stockwell, D., Peters, D., 1999. The garp modeling system: Problems and solutions to automated spatial prediction. International Journal of Geographical Information Science 13 (2), 143–158.

Stockwell, D. R. B., 1999. Machine Learning Methods for Ecological Applications. Kluwer Academic Publishers, Ch. Genetic Algorithms II, pp. 123–144, do not have a copy.

Story, M., Congalton, R., 1986. Accuracy assessment: A user's perspective. Photogrammetric Engineering & Remote Sensing 52 (3), 397–399, don't have a copy.

Suarez, J. C., Ontiveros, C., Smith, S., Snape, S., 2005. Use of airborne lidar and aerial photography in the estimation of individual tree heights in forestry. Computers and Geosciences 31, 253–262.

Tallis, J. H., 1969. The blanket bog vegetation of the berwyn mountains, north wales. The Journal of Ecology 57 (3), 765–787.

Tansey, K., Selmes, N., Anstee, A., Tale, N., Denniess, A., Sep 2009. Estimating tree and stand variables in a corsican pine woodland from terrestrial laser scanner data. International Journal of Remote Sensing 30 (19), 5195–5209.

Tateishi, R., Shimazaki, Y., Gunin, P. D., 2004. Spectral and temporal linear mixing model for vegetation classification. International Journal of Remote Sensing 25 (20), 4203–4218.

Tickle, P., Lee, A., Lucas, R., Austin, J., Witte, C., 2006a. Quantifying australian forest and woodland structure and biomass using large scale photography and small footprint lidar. Forest Ecology and Management 223 (1-3), 379–394.

Tickle, P. K., Lee, A., Lucas, R. M., Austin, J., Witte, C., 2006b. Quantifying Australian Forest and Woodland Structure and Biomass Using Large Scale Photography and Small Footprint LiDAR. Forest Ecology and Management 223 (1-3), 379–394.

Tieszen, L., Reed, B., Bliss, N., Wylie, B., DeJong, D., 1997. Ndvi, c3 and c4 production and distributions in great plains grassland cover classes. Ecological Applications 7 (1), 59–78.

Tilman, D., Reich, P., Knops, J., 2006. Biodiversity and ecosystem stability in a decade-long grassland experiment. Nature 441, 629–632.

Todd, K. W., Csillag, F., Atkinson, P. M., 2003. Three-dimensional mapping of light transmittance and foliage distribution using lidar. Canadian Journal of Remote Sensing 29, 544–555.

Trenholm, L. E., SchLossberg, M. J., Lee, G., Parks, W., Geer, S. A., 2000. An evaluation of multi-spectral responses on selected turfgrass species. International Journal of Remote Sensing 21 (4), 709–721.

Troll, C., 1939. Luftbildplan und oekologische bodenforschung. Zeitschrift der Gesellschaft fuer Erdkunde 7/8, 241–298.

Tucker, C. J., 1978. Post senescent grass canopy remote sensing. Remote Sensing of Environment 7 (3), 203–210.

Turner, M. G., Gardner, R. H., O'Neill, R. V., 2001. Landscape Ecology in Theory and Practice, Pattern and Process. Springer-Verlag, New York.

van Aardt, J., Wynne, R., Oderwald, R., 2006. Forest volume and biomass estimation using small-footprint lidar-distributional parameters on a per-segment basis. Forest Science 52 (6), 636–649.

van Oort, P., 2007. Interpreting the change detection error matrix. Remote Sensing of Environment 108, 1–8.

van Ruijven, J., Berendse, F., 2005. Diversityproductivity relationships: Initial effects, long-term patterns, and underlying mechanisms. PNAS 102 (3), 695–700.

Wagner, W., Hollaus, M., Briese, C., Ducic, V., 2008. 3d vegetation mapping using small-footprint full-waveform airborne laser scanners. International Journal of Remote Sensing.

Wagner, W., UllRich, A., Ducic, V., Melzer, T., Studnicka, N., 2006. Gaussian decomposition and calibration of a novel small-footprint full-waveform digitising airborne laser scanner. ISPRS Journal of Photogrammetry and Remote Sensing 60 (2), 100–112.

Wamunyima, S., 2005. Estimating fresh grass biomass at landscape level using hyperspectral remote sensing. Ph.D. thesis, Enschede University, Enschede, NetherLands.

Wang, J., PriCe, K. P., Rich, P. M., 2001. Spatial patterns of ndvi in response to precipitation and temperature in the central great plains. International Journal of Remote Sensing 22 (18), 3827–3844.

Warren, A., Collins, M., 2007. A pixel-based semi-empirical system for predicting vegetation diversity in boreal forest. International Journal of Remote Sensing 28 (1), 83–105.

Watt, P., Donoghue, D., 2005a. Measuring forest structure with terrestrial laser scanning. International Journal of Remote Sensing 26 (7), 1437–1446.

Watt, P., Donoghue, D., 2005b. Measuring forest structure with terrestrial laser

scanning. International Journal of Remote Sensing 26 (7), 1437–1446, print-out in folder.

Weiss, E., Marsh, S. E., Pfirman, E. S., 2001. Application of noaa-avhrr ndvi time-series data to assess changes in saudi arabia's rangelands. International Journal of Remote Sensing 22 (6), 1005–1027.

Whittaker, R. H., 1972. Evolution and measurement of species diversity. Taxon 21, 213–251.

Wilcox, B. A., 1984. In situ conservation of genetic resources: Determinants of minimum area requirements. In: McNeely, J. A., Miller, K. R. (Eds.), National Parks, Conservation and Development: Proceedings of the World Congress on National Parks. pp. 18–30.

Wright, W., Liu, P., Slatton, K., Shrestha, R., Carter, W., Lee, H., 2008. Predicting l-band microwave attenuation through forest canopy using directional structuring elements and airborne lidar. In: Geoscience and Remote Sensing Symposium, 2008. IGARSS 2008. IEEE International.

Wulder, M., Franklin, S., White, J., Linke, J., Magnussen, S., 2006. An accuracy assessment framework for large-area land cover classification products derived from medium-resolution satellite data. International Journal of Remote Sensing 27 (4), 663–683.

Wulder, M., Han, T., White, J., Sweda, T., Tsuzuki, H., 2007a. Integrating profiling lidar with landsat data for regional boreal forest canopy attribute estimation and change characterization. Remote Sensing of Environment 110 (1), 123–137.

Wulder, M., Niemann, K. O., Goodenough, D. G., 2000. Local maximum filtering for the extraction of tree locations and basal area for high spatial resolution imagery. Remote Sensing of Environment 73, 103–114.

Wulder, M. A., Han, T., White, J. C., Sweda, T., Tsuzuki, H., 2007b. Integrating Profiling LiDAR with Landsat Data for Regional Boreal Forest Canopy Attribute Estimation and Change Characterization. Remote Sensing of Environment 110 (1), 123–137.

Wyatt, G., 1991. A Review of Phase 1 Habitat Survey in England. Nature Conservancy Council, Peterborough.

Yamano, H., Chen, J., Tamura, M., 2003. Hyperspectral identification of grassland vegetation in xilinhot, inner mongolia, china. International Journal of Remote Sensing 24 (15), 3171–3178.

Yamanoa, H., Chena, J., Tamuraa, M., 2003. Hyperspectral identification of grassland vegetation in xilinhot, inner mongolia, china. International Journal of Remote Sensing 24 (15), 3171–3178.

Yeo, M., Blackstock, T., 2002. A vegetation analysis of the pastoral landscapes of upland wales, uk. Journal of Vegetation Science 13, 803–816.

Yu, X., Hyppä, J., Hyppä, H., Maltamo, M., 2004. Effects of flight altitude on tree height estimation using airborne laser scanning. In: International ConferenCe NATScan 'Laser-Scanners for Forest and Landscape Assessment – Instruments, Processing Methods and Applications', 3–6 October 2004, Freiburg, Germany. In International Archives of Photogrammetry, Remote Sensing and Spatial Information Sciences, XXXVI, 8/W2. pp. 96–101.

Zha, Y., Gao, J., Zhang, Y., 2005. Grassland productivity in an alpine environment in response to climate change. Area 37 (3), 332–340.

Zimble, D. A., Evans, D. L., Carlson, G. C., Parker, R. C., Grado, S. C., Gerard, P. D., 2003. Characterizing vertical forest structure using small-footprint airborne lidar. Remote Sensing of Environment 87, 171–182.

Appendix A

Appendices

A.1 Appendix I - Abbreviations

AGI - Association for Geographic Information

ALOS - Advanced Land Observing Satellite

ARSF - Airborne Remote Sensing Facility

ASTER - Advanced Spaceborne Thermal Emissions and Reflection Radiometer

ATCOR - Atmospheric/Topographic Correction software

AU - Aberystwyth University

AVHRR - Advanced Very High Resolution Radiometer

AVIRIS - Advanced Visible/Infrared Imaging Spectrometer

BAP - Biodiversity Action Plan

BNSC - British National Space Centre

BRDF - bidirectional reflectance distribution function

BTO - British Trust for Ornithology

CASI - Compact Airborne Spectrographic Imager

CCW - Countryside Council for Wales

CBC - Common Bird Census

DEFRA - Department for Environment, Food and Rural Affairs

DEM - Digital Elevation Model

DESDyni - Deformation, Ecosystem Structure and Dynamics of Ice

dGPS - differential Global Positioning System

DLR - Deutsches Zentrum fuer Luft- und Raumfahrt (German Aerospace Center)

DN - Digital Number

DSM - Digital Surface Model

DTM - Digital Terrain Model

EO - Earth Observation

ESA - Environmentally Sensitive Area (farming support scheme)

ESA - European Space Agency

ETM+ - Enhanced Thematic Mapper Plus

FLAASH - Fast Line-of-sight Atmospheric Analysis of Spectral Hypercubes

FOV - Field of View

FP - Framework Project

fPAR - fraction Photosynthetically Active Radiation

GARP - Genetic Algorithm for Rule-set Production

GCP - Ground Control Point

GeoTIFF - Geographic Tagged Image File Format

GLAS - Geoscience Laser Altimeter System

GIFTSS - Government Information from the Space Sector

GIS - Geographic Information System

GPS - Global Positioning System

GRN - Global Restoration Network

HDF - Hierarchical Data Format

HRG - High Resolution Geometric (sensor)

HRS - High Resolution Stereoscopic (sensor / imaging instrument)

HRV - High Resolution Visible (sensor)

HRVIR - High Resolution Visible and Infrared

HSCOI - Height Scaled Crown Openness Index

IALE - International Association of Landscape Ecology

ICESat - Ice, Cloud, and land Elevation Satellite

IEEE - Institute of Electrical and Electronics Engineers

IGER - Institute of Grassland and Environmental Research

IGES - Institute of Geography and Earth Sciences

IPCC - Intergovernmental Panel on Climate Change

IRS - Indian Remote Sensing Satellite

ISPRS - International Society for Photogrammetry and Remote Sensing

IUCN - International Union for the Conservation of Nature and Natural Resources

IUFRO - International Union of Forest Research Organizations

JERS - Japanese Earth Resources Satellite

LAD - Leaf Angle Distribution

LAI - Leaf Area Index

Laser - Light Amplification by Stimulated Emission of Radiation

LCM - Land Cover Map

LiDAR - Light Detection and Ranging Aperture Radar

LISS - Linear Imaging Self Scanning System

LPIS - Land Parcel Information System

LSUM - Linear Spectral Unmixing

LVIS - Laser Vegetation Imaging Sensor

MAFF - Ministry of Agriculture, Forestry and Fisheries

MISR - Multi-angle Imaging Spectroradiometer

MODIS - Moderate Resolution Imaging Spectrometer

NERC - Natural Environment Research Council

NIR - Near Infrared part of the solar spectrum (0.7-1.3mum)

NIWT - National Inventory of Woodland and Trees

NDVI - Normalized Difference Vegetation Index

NNR - National Nature Reserve

NOAA - National Oceanic Atmospheric Administration

NPP - Net Primary Productivity

NPV - Non-Photosynthetic Vegetation

PALSAR - Phased Array type L-band Synthetic Aperture Radar

PAR - Photosynthetically Active Radiation

PIMHAI - Plate-forme d'Imagerie Multi et Hyperspectrale de l'Acquisition l'Interprtation pour l'expertise et l'aide la dcision en gestion de l'environnement / Platform for Analysis of Multispectral and Hyperspectral Images from Acquisition to Interpretation for Environmental Monitoring and Decision Making

POS - position and orientation data

PV - Photosynthetic Vegetation

Radar - Radio Detection and Ranging

RSPB - Royal Society for the Protection of Birds

SAC - Special Area of Conservation

SAIL - Scattering by Arbitrarily Inclined Leaves (canopy reflectance model)

SAR - Synthetic Aperture Radar

SDF - Sample Data File

SeaWiFs - Sea-viewing Wider Field-of-View Sensor SER International - Society for Ecological Restoration International

SLICER - Scanning LiDAR Imager of Canopies by Echo Retrieval

SOCS - Scanner's own coordinate system

SPA - Special Protection Area

SPIN - Spatial Indicators for Nature Conservation

SPOT - Satellite Pour l'Observation de la Terre, French satellite supporting the HRG sensor

SQL - Structured Query Language

SRTM - Shuttle Radar Topography Mission

SSSI - Site of Special Scientific Interest

SWIR - Short Wave Infrared part of the solar spectrum (0.7-2.5μm)

TIFF - Tagged Image File Format

TIR - Thermal Infrared part of the solar spectrum (8.4-11.6μm) TM - Thematic Mapper

UTM - Universal Transverse Mercator

VIS - VISible part of the solar spectrum (0.3-07 μm)

VNIR - Visible and Near-Infrared part of the solar spectrum (0.3-1.3μm)

WAG - Welsh Assembly Government

WiFS - Wide Field-of-View Sensor

WGS 84 - World Geodetic System 1984

A.2 Appendix II - Sensor specifications

A.2.1 Vexcel Aerial Photography

The aerial photography used in this study was captured in 2006 by GeoPerspectives, a joint venture between Infoterra Ltd. and BlueSky Ltd., in partnership with aerial surveying company COWI. The survey was originally undertaken as the result of a contract awarded by the Welsh Assembly Government to create a map-accurate image layer for the whole of Wales for projects including the administration of land management, agricultural and environmental monitoring and control.

The full colour photography covers approximately 20,000 square kilometres at 40cm ground resolution in around 7000 individual image tiles. It was captured using the Vexcel UltraCamD photogrammetric aerial survey camera and colour infrared imagery (CIR) for the whole of Wales was acquired simultaneously. The data were converted subsequently to orthophotos of very high positional accuracy with NextMap radar scanning data as input for a digital terrain model.

For ease of use in this study, the image tiles were combined into a Wales wide ECW mosaic using Global Mapper software.

A.2.2 Satellite Sensors

a.) Terra 1

The sensor onboard NASA's Terra-1 is the Advanced Spaceborne Thermal Emission and Reflection Radiometer (ASTER) which is an advanced multispectral imager.

ASTER can acquire data over the entire globe with an average duty cycle of 8% per orbit. This translates to acquisition of about 650 scenes per day that are processed to Level 1A; of these about 150 are processed to Level 1B.

ASTER Level 1A data are formally defined as reconstructed, unprocessed instrument data at full resolution. They consist of the image data, radiometric coefficients, the geometric coefficients and other auxillary data without applying the coefficients to the image data, thus maintaining original data values. This is the preferred data processing level for this project. The L1B data are generated by applying these coefficients for radiometric calibration and geometric resampling.

All 1A and 1B scenes are transferred to the EOSDIS archive at the EROS data centre's (EDC) Land Processes Distributed Active Archive Centre (LP-DAAC), for storage, distribution, and processing to higher level data products. All ASTER data products are stored in a specific implementation of Hierarchical Data Format called HDF-EOS.

The ASTER instrument consists of three separate instrument subsystems:

- Visible and Near-infrared (VNIR) - 3 bands with an additional backward telescope for stereo

- Shortwave Infrared (SWIR) - 6 bands

- Thermal Infrared (TIR) - 5 bands

Each subsystem operates in a different spectral region, with its own telescope(s). The Terra spacecraft is flying in a circular, near-polar orbit at an altitude of 705km. The orbit is sun-synchronous so that solar illumination conditions vary as little as possible, with equatorial crossing at a local time of 10.30 a.m., returning to the same orbit every 16 days. The orbit parameters are the same as those of Landsat 7, except for the local equatorial crossing time.

Table A.1: Terra-1 ASTER specifications

Bands		Spectral Resolution (μm)	Spatial Resolution (m)
Band 1 - Nadir looking	VNIR	0.52-0.60	15
Band 2 - Nadir looking	VNIR	0.63-0.69	15
Band 3 - Nadir looking	VNIR	0.76-0.86	15
Band 3 - Backward looking	VNIR	0.76-0.86	15
Band 4	SWIR	1.6-1.7	30
Band 5	SWIR	2.155-2.185	30
Band 6	SWIR	2.195-2.225	30
Band 7	SWIR	2.235-2.285	30
Band 8	SWIR	2.295-2.385	30
Band 9	SWIR	2.380-2.430	30
Band 10	TIR	8.125-8.475	90
Band 11	TIR	8.475-8.825	90
Band 12	TIR	8.925-9.275	90
Band 13	TIR	10.25-10.95	90
Band 14	TIR	10.95-11.65	90

b.) Satellite Pour l'Observation de la Terre 5 (SPOT)

The sensors onboard SPOT 5 are two High Resolution Geometric (HRG) instruments from the HRVIR instruments on SPOT 4 and one High Resolution Stereo-

scopic (HRS) imaging instrument able to acquire stereo pair images almost simultaneously for optimized production of digital elevation models (DEM). SPOT 5 is also carrying the recurring VEGETATION 2 instrument and the Doppler Orbitography and Radiopositioning Integrated by Satellite (DORIS) instrument. The objective of the DORIS instrument is to meet new requirements for precise satellite orbit determination and ground beacon location.

The HRG imaging instruments have a field of view of 45°, it can therefore observe a 60 kilometer wide swath on the ground and can be pointed 270° either side of the nadir for oblique viewing. The oblique viewing capability of the SPOT imaging instruments enable them to acquire imagery of any point on the globe within less then 5 days along the equator and in less then 3 days at temperate latitudes (above 45°). Users are therefore able to task specific scene acquisition.

Only SPOT HRG data were used in this project and they were purchased at the processing Level 1A, which indicates that the only difference to the raw data is a radiometric correction of distortions due to differences in sensitivity of the elementary detectors of the viewing instrument, because further processing, as outlined in section 4.1.1, was undertaken in-house to retain full control over the quality of the data products.

The data were made available in Digital Image Map (DIMAP) format which consists of two parts, image and metadata. The image is described in GeoTIFF (Geographic Tagged Image File Format) format whereas the metadata is written in XML. The metadata contains the necessary information for the pre-processing of the images, such as the date and time of capture, exact image size as well as the gain and offset values.

The SPOT 5 satellite orbits the earth at an altitude of 822 kilometers at the

Equator.

The orbit is near polar, circular and sun-synchronous with equatorial crossing at a local time of 10.30 a.m. The orbit is phased so that a satellite passes over the same point every 26 days.

Table A.2: SPOT 5 HRG specifications

	Bands	Spectral Resolution (μm)	Spatial Resolution (m)
Band 1	NIR	0.79-0.89	10
Band 2	Green	0.50-0.59	10
Band 3	Red	0.61-0.68	10
Band 4	SWIR	1.58-1.75	20
Band 5	Pan (or Supermode)[a]	0.51-0.73	5 (or 2.5)

[a]Supermode is a unique sampling concept, which yields a 2.5m resolution image from two 5m resolution images. Not all imagery is supplied with this.

c.) Indian Remote Sensing Satellite 1C, 1D & P6 (IRS)

Table A.3 shows the four generations of India's Earth observation program beginning in March 1988. IRS satellites operate in a circular, sun-synchronous, near polar orbit with an inclination of 98.69° at an altitude of 817 km. The orbit is phased so that a satellite passes over the same point every 24 days and crosses the equator in descending mode at 10.30 a.m. local time.

The LISS-III sensor was improved slightly on each satellite (see table A.4). The most important improvement is an increase in spatial resolution in the SWIR band from 70m to 23.5m between the older satellites and IRS-P6.

IRS standard data products are offered with two processing levels - radiometrically corrected and system corrected. System corrected is the higher level, which includes the radiometric and geometric correction of the data. The data for this project were provided in two different formats, EOSat /Euromap Fast Format

Table A.3: IRS satellite generations and their sensors

Satellite name	Sensors	Year launched
IRS-1A		1988
IRS-1C	Pan	1995 (defunct by 2006)
	WiFs	
	LISS^a-III	
IRS-1D	Pan	1997 (defunct by 2006)
	WiFs	
	LISS-III	
IRS-P6	AWiFs	2003
(Resourcesat-1)	LISS-III	
	LISS-IV	

^{a}Linear Self Imaging Scanning System

Table A.4: Linear Self Imaging Scanning System specifications on IRS satellites

Satellite	Band	Spectral Resolution (μm)	Spatial Resolution (m)
1C (1995) & 1D (1997)	Green	0.52-0.60	23
	Red	0.62-0.68	23
	NIR	0.77-0.86	23
	SWIR	1.55-1.70	70
P6 (2003)	Green	0.52-0.59	23.5
	Red	0.62-0.68	23.5
	NIR	0.77-0.86	23.5
	SWIR	1.55-1.70	23.5

and Super Structure Format and only radiometrically corrected, so all further pre-processing was carried out in-house.

Fast Format consist of one ASCII header file and one simple binary image file for each band. The ASCII header includes the image size (number of pixels per line and number of lines), image location (4 corner co-ordinates and one centre co-ordinate, path, row), acquisition parameters (date, sun elevation, sun azimuth, gain settings) and some technical parameters related to the processing (product code, etc.).

Super Structure Format has a much more complex structure than the Fast Format. A typical dataset consists of a 'volume directory file' (which includes a short description of the data product and a number of pointers and corresponding descriptors), one 'leader file', one or several 'image data files', one 'trailer file' and one concluding 'null file'. Other than the Fast Format, the Super Structure Format contains information related to ephemeris and spacecraft attitude.

Landsat

Landsat data were available for the whole of Wales and therefore all study sites, but were not used because of the timing of the available scenes and the relative coarseness of the spatial resolution. Furthermore, all image data acquired by the Landsat 7 ETM+ from 14th July 2003 to present have been collected in Scan Line Corrector (SLC)-off mode due to an instrument malfunction. The problem was caused by failure of the Scan Line Corrector (SLC), which compensates for the forward motion of the satellite. Without an operating SLC, the Enhanced Thematic Mapper Plus (ETM+) line of sight now traces a zig-zag pattern along

the satellite ground track (see figure A.1) with a resulting depletion of imaged area that increases towards the scene edge.
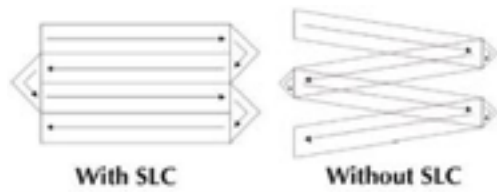
Figure A.1: Illustration of the SLC failure effect

A.3 Appendix III - Phase I Habitat Classes

A.4 Appendix IV - BTO Species Codes

Table A.5: BTO Species Codes

Code	Common Name	Scientific Name
AX	Alexandrine Parakeet	*Psittacula eupatria*
AC	Arctic Skua	*Stercorarius parasiticus*
AE	Arctic Tern	*Sterna paradisaea*
AV	Avocet	*Recurvirostra avosetta*
HD	Bar-headed Goose	*Anser indicus*
BO	Barn Owl	*Tyto alba*
BY	Barnacle Goose	*Branta leucopsis*
BA	Bar-tailed Godwit	*Limosa lapponica*
BE	Bean Goose	*Anser fabalis*

Code	Common Name	Scientific Name
BR	Bearded Tit	*Panurus biarmicus*
MZ	Bee-Eater	*Merops apiaster*
BS	Bewick's Swan	*Cygnus columbianus*
BI	Bittern	*Botaurus stellaris*
BK	Black Grouse	*Tetrao tetrix*
TY	Black Guillemot	*Cepphus grylle*
KB	Black Kite	*Milvus migrans*
BX	Black Redstart	*Phoenicurus ochruros*
OS	Black Stork	*Ciconia nigra*
AS	Black Swan	*Cygnus atratus*
BJ	Black Tern	*Chlidonias niger*
B.	Blackbird	*Turdus merula*
BC	Blackcap	*Sylvia atricapilla*
BH	Black-headed Gull	*Larus ridibundus*
BN	Black-necked Grebe	*Podiceps nigricollis*
BW	Black-tailed Godwit	*Limosa limosa*
BV	Black-throated Diver	*Gavia arctica*
BT	Blue Tit	*Parus caeruleus*
BU	Bluethroat	*Luscinia svecica*
OQ	Bobwhite	*Colinus virginianus*
BL	Brambling	*Fringilla montifringilla*
BG	Brent Goose	*Branta bernicla*

Code	Common Name	Scientific Name
UG	Budgerigar	*Melopsittacus undulatus*
BF	Bullfinch	*Pyrrhula pyrrhula*
BZ	Buzzard	*Buteo buteo*
CG	Canada Goose	*Branta canadensis*
CP	Capercaillie	*Tetrao urogallus*
C.	Carrion Crow	*Corvus corone corone*
CW	Cetti's Warbler	*Cettia cetti*
CH	Chaffinch	*Fringilla coelebs*
CC	Chiffchaff	*Phylloscopus collybita*
HL	Chiloe Wigeon	*Anas sibilatrix*
CF	Chough	*Pyrrhocorax pyrrhocorax*
KR	Chukar	*Alectoris chukar*
CL	Cirl Bunting	*Emberiza cirlus*
CT	Coal Tit	*Parus ater*
QL	Cockatiel	*Nymphicus hollandicus*
CD	Collared Dove	*Streptopelia decaocto*
CM	Common Gull	*Larus canus*
SQ	Common Rosefinch	*Carpodacus erythrinus*
CS	Common Sandpiper	*Actitis hypoleucos*
CX	Common Scoter	*Melanitta nigra*
CN	Common Tern	*Sterna hirundo*
CO	Coot	*Fulica atra*

Code	Common Name	Scientific Name
CA	Cormorant	*Phalacrocorax carbo*
CB	Corn Bunting	*Miliaria calandra*
CE	Corncrake	*Crex crex*
CQ	Cory's Shearwater	*Calonectris diomedea*
AN	Crane	*Grus grus*
CI	Crested Tit	*Parus cristatus*
CR	Crossbill	*Loxia curvirostra*
CK	Cuckoo	*Cuculus canorus*
CU	Curlew	*Numenius arquata*
CV	Curlew Sandpiper	*Calidris ferruginea*
DW	Dartford Warbler	*Sylvia undata*
DI	Dipper	*Cinclus cinclus*
DO	Dotterel	*Charadrius morinellus*
DN	Dunlin	*Calidris alpina*
D.	Dunnock	*Prunella modularis*
EG	Egyptian Goose	*Alopochen aegyptiacus*
E.	Eider	*Somateria mollissima*
EM	Emperor Goose	*Anser canagica*
FP	Feral Pigeon	*Columba livia*
ZL	Feral/hybrid Goose	*Anser sp*
ZF	Feral/hybrid mallard type	
FD	Ferruginous Duck	*Aythya nyroca*

Code	Common Name	Scientific Name
FF	Fieldfare	*Turdus pilaris*
FC	Firecrest	*Regulus ignicapillus*
F.	Fulmar	*Fulmarus glacialis*
GA	Gadwall	*Anas strepera*
GX	Gannet	*Morus bassanus*
GW	Garden Warbler	*Sylvia borin*
GY	Garganey	*Anas querquedula*
GZ	Glaucous Gull	*Larus hyperboreus*
GC	Goldcrest	*Regulus regulus*
EA	Golden Eagle	*Aquila chrysaetos*
OL	Golden Oriole	*Oriolus oriolus*
GF	Golden Pheasant	*Chrysolophus pictus*
GP	Golden Plover	*Pluvialis apricaria*
GN	Goldeneye	*Bucephala clangula*
GO	Goldfinch	*Carduelis carduelis*
GD	Goosander	*Mergus merganser*
GI	Goshawk	*Accipiter gentilis*
GH	Grasshopper Warbler	*Locustella naevia*
GB	Great Black-backed Gull	*Larus marinus*
GG	Great Crested Grebe	*Podiceps cristatus*
SR	Great Grey Shrike	*Lanius excubitor*
ND	Great Northern Diver	*Gavia immer*

Code	Common Name	Scientific Name
QW	Great Reed Warbler	*Acrocephalus arundinaceus*
GQ	Great Shearwater	*Puffinus gravis*
NX	Great Skua	*Stercorarius skua*
GS	Great Spotted Woodpecker	*Dendrocopos major*
GT	Great Tit	*Parus major*
GE	Green Sandpiper	*Tringa ochropus*
G.	Green Woodpecker	*Picus viridis*
GR	Greenfinch	*Carduelis chloris*
GK	Greenshank	*Tringa nebularia*
H.	Grey Heron	*Ardea cinerea*
P.	Grey Partridge	*Perdix perdix*
PL	Grey Phalarope	*Phalaropus fulicarius*
GV	Grey Plover	*Pluvialis squatarola*
GL	Grey Wagtail	*Motacilla cinerea*
GJ	Greylag Goose	*Anser anser*
GU	Guillemot	*Uria aalge*
HA	Harris Hawk	*Parabuteo unicinctus*
HF	Hawfinch	*Coccothraustes coccothraustes*
FW	Helmetted Guineafowl	*Numidia meleagris*
HH	Hen Harrier	*Circus cyaneus*
HG	Herring Gull	*Larus argentatus*
HY	Hobby	*Falco subbuteo*

Code	Common Name	Scientific Name
HZ	Honey Buzzard	*Pernis apivorus*
HC	Hooded Crow	*Corvus corone cornix*
HP	Hoopoe	*Upupa epops*
HM	House Martin	*Delichon urbica*
HS	House Sparrow	*Passer domesticus*
IG	Iceland Gull	*Larus glaucoides*
IC	Icterine Warbler	*Hippolais icterina*
JS	Jack Snipe	*Lymnocryptes minimus*
JD	Jackdaw	*Corvus monedula*
J.	Jay	*Garrulus glandarius*
KP	Kentish Plover	*Charadrius alexandrinus*
K.	Kestrel	*Falco tinnunculus*
KF	Kingfisher	*Alcedo atthis*
KI	Kittiwake	*Rissa tridactyla*
KN	Knot	*Calidris canutus*
LM	Lady Amherst's Pheasant	*Chrysolophus amherstiae*
FB	Lanner Falcon	*Falco biarmicus*
LA	Lapland Bunting	*Calcarius lapponicus*
L.	Lapwing	*Vanellus vanellus*
TL	Leach's Petrel	*Oceanodroma leucorhoa*
LB	Lesser Black-backed Gull	*Larus fuscus*
LR	Lesser Redpoll	*Carduelis cabaret*

Code	Common Name	Scientific Name
LS	Lesser Spotted Woodpecker	*Dendrocopos minor*
LW	Lesser Whitethroat	*Sylvia curruca*
LI	Linnet	*Carduelis cannabina*
LK	Little Auk	*Alle alle*
ET	Little Egret	*Egretta garzetta*
LG	Little Grebe	*Tachybaptus ruficollis*
LU	Little Gull	*Larus minutus*
LO	Little Owl	*Athene noctua*
LP	Little Ringed Plover	*Charadrius dubius*
LX	Little Stint	*Calidris minuta*
AF	Little Tern	*Sterna albifrons*
LE	Long-eared Owl	*Asio otus*
LN	Long-tailed Duck	*Clangula hyemalis*
OG	Long-tailed Skua	*Stercorarius longicaudus*
LT	Long-tailed Tit	*Aegithalos caudatus*
MG	Magpie	*Pica pica*
MA	Mallard	*Anas platyrhynchos*
MN	Mandarin	*Aix galericulata*
MX	Manx Shearwater	*Puffinus puffinus*
MR	Marsh Harrier	*Circus aeruginosus*
MT	Marsh Tit	*Parus palustris*
MW	Marsh Warbler	*Acrocephalus palustris*

Code	Common Name	Scientific Name
MP	Meadow Pipit	*Anthus pratensis*
FR	Mealy Redpoll	*Carduelis flammea*
MU	Mediterranean Gull	*Larus melanocephalus*
ML	Merlin	*Falco columbarius*
M.	Mistle Thrush	*Turdus viscivorus*
MO	Montagu's Harrier	*Circus pygargus*
MH	Moorhen	*Gallinula chloropus*
MY	Muscovy Duck	*Cairina moschata*
MS	Mute Swan	*Cygnus olor*
NT	Night Heron	*Nycticorax nycticorax*
N.	Nightingale	*Luscinia megarhynchos*
NJ	Nightjar	*Caprimulgus europaeus*
NH	Nuthatch	*Sitta europaea*
OP	Osprey	*Pandion haliaetus*
X.	Other cage bird species	
OC	Oystercatcher	*Haematopus ostralegus*
PC	Parrot Crossbill	*Loxia pytyopsittacus*
PX	Peacock	*Parvo cristatus*
PP	Pectoral Sandpiper	*Calidris melanotos*
PE	Peregrine	*Falco peregrinus*
PH	Pheasant	*Phasianus colchicus*
PF	Pied Flycatcher	*Ficedula hypoleuca*

Code	Common Name	Scientific Name
PW	Pied Wagtail	*Motacilla alba*
PG	Pink-footed Goose	*Anser brachyrhynchus*
PT	Pintail	*Anas acuta*
PO	Pochard	*Aythya ferina*
PK	Pomarine Skua	*Stercorarius pomarinus*
PM	Ptarmigan	*Lagopus mutus*
PU	Puffin	*Fratercula arctica*
UR	Purple Heron	*Ardea purpurea*
PS	Purple Sandpiper	*Calidris maritima*
Q.	Quail	*Coturnix coturnix*
RN	Raven	*Corvus corax*
RA	Razorbill	*Alca torda*
RG	Red Grouse	*Lagopus lagopus*
KT	Red Kite	*Milvus milvus*
ED	Red-backed Shrike	*Lanius collurio*
EB	Red-breasted Goose	*Branta ruficollis*
RM	Red-breasted Merganser	*Mergus serrator*
RQ	Red-crested Pochard	*Marmaronetta angustirostris*
RL	Red-legged Partridge	*Alectoris rufa*
RX	Red-necked Grebe	*Podiceps grisegena*
NK	Red-necked Phalarope	*Phalaropus lobatus*
RK	Redshank	*Tringa totanus*

Code	Common Name	Scientific Name
RT	Redstart	*Phoenicurus phoenicurus*
RH	Red-throated Diver	*Gavia stellata*
RE	Redwing	*Turdus iliacus*
RB	Reed Bunting	*Emberiza schoeniclus*
RW	Reed Warbler	*Acrocephalus scirpaceus*
RV	Reeve's Pheasant	*Syrmaticus reevesi*
RZ	Ring Ouzel	*Turdus torquatus*
IN	Ring-billed Gull	*Larus delawarensis*
RP	Ringed Plover	*Charadrius hiaticula*
RI	Ring-necked Parakeet	*Psittacula krameri*
R.	Robin	*Erithacus rubecula*
DV	Rock Dove	*Columba livia*
RC	Rock Pipit	*Anthus petrosus petrosus*
RO	Rook	*Corvus frugilegus*
RS	Roseate Tern	*Sterna dougallii*
RF	Rough-legged Buzzard	*Buteo lagopus*
RY	Ruddy Duck	*Oxyura jamaicensis*
UD	Ruddy Shelduck	*Tadorna ferruginea*
RU	Ruff	*Philomachus pugnax*
JF	Saker	*Falco cherrug*
SM	Sand Martin	*Riparia riparia*
SS	Sanderling	*Calidris alba*

Code	Common Name	Scientific Name
TE	Sandwich Tern	*Sterna sandvicensis*
VI	Savi's Warbler	*Locustella luscinioides*
SP	Scaup	*Aythya marila*
CY	Scottish Crossbill	*Loxia scotica*
SW	Sedge Warbler	*Acrocephalus schoenobaenus*
NS	Serin	*Serinus serinus*
SA	Shag	*Phalacrocorax aristotelis*
SU	Shelduck	*Tadorna tadorna*
SX	Shorelark	*Eremophila alpestris*
SE	Short-eared Owl	*Asio flammeus*
TH	Short-toed Treecreeper	*Certhia brachydactyla*
SV	Shoveler	*Anas clypeata*
PV	Silver Pheasant	*Lophura nycthemera*
SK	Siskin	*Carduelis spinus*
S.	Skylark	*Alauda arvensis*
SZ	Slavonian Grebe	*Podiceps auritus*
SY	Smew	*Mergus albellus*
SN	Snipe	*Gallinago gallinago*
SB	Snow Bunting	*Plectrophenax nivalis*
SJ	Snow Goose	*Anser caerulescens*
ST	Song Thrush	*Turdus philomelos*
OT	Sooty Shearwater	*Puffinus griseus*

Code	Common Name	Scientific Name
SH	Sparrowhawk	*Accipiter nisus*
NB	Spoonbill	*Platalea leucorodia*
AK	Spotted Crake	*Porzana porzana*
SF	Spotted Flycatcher	*Muscicapa striata*
DR	Spotted Redshank	*Tringa erythropus*
SG	Starling	*Sturnus vulgaris*
SD	Stock Dove	*Columba oenas*
SC	Stonechat	*Saxicola torquata*
TN	Stone-curlew	*Burhinus oedicnemus*
TM	Storm Petrel	*Hydrobates pelagicus*
SL	Swallow	*Hirundo rustica*
SI	Swift	*Apus apus*
TO	Tawny Owl	*Strix aluco*
T.	Teal	*Anas crecca*
TK	Temminck's Stint	*Calidris temminckii*
TP	Tree Pipit	*Anthus trivialis*
TS	Tree Sparrow	*Passer montanus*
TC	Treecreeper	*Certhia familiaris*
TU	Tufted Duck	*Aythya fuligula*
TT	Turnstone	*Arenaria interpres*
TD	Turtle Dove	*Streptopelia turtur*
TW	Twite	*Carduelis flavirostris*

Code	Common Name	Scientific Name
VS	Velvet Scoter	*Melanitta fusca*
WI	Water Pipit	*Anthus petrosus spinoletta*
WA	Water Rail	*Rallus aquaticus*
WX	Waxwing	*Bombycilla garrulus*
W.	Wheatear	*Oenanthe oenanthe*
WM	Whimbrel	*Numenius phaeopus*
WC	Whinchat	*Saxicola rubetra*
OR	White Stork	*Ciconia ciconia*
WG	White-fronted Goose	*Anser albifrons*
WE	White-tailed Eagle	*Haliaeetus albicilla*
WH	Whitethroat	*Sylvia communis*
WS	Whooper Swan	*Cygnus Cygnus*
WN	Wigeon	*Anas penelope*
WT	Willow Tit	*Parus montanus*
WW	Willow Warbler	*Phylloscopus trochilus*
DC	Wood Duck	*Aix sponsa*
WP	Wood Pigeon	*Columba palumbus*
OD	Wood Sandpiper	*Tringa glareola*
WO	Wood Warbler	*Phylloscopus sibilatrix*
WK	Woodcock	*Scolopax rusticola*
WL	Woodlark	*Lullula arborea*
WR	Wren	*Troglodytes troglodytes*

Code	Common Name	Scientific Name
WY	Wryneck	*Jynx torquilla*
YW	Yellow Wagtail	*Motacilla flava*
Y.	Yellowhammer	*Emberiza citrinella*
YG	Yellow-legged Gull	*Larus arg. michahellis*
FI	Zebra Finch	*Taeniopygia guttata*

A.5 Phase 1 habitat classes

Woodland and scrub		Heathland		Coastland		Rock exposure and waste	
A1.1.1	semi-natural broadleaved woodland	D1.1	dry acid heath	H1.1	intertidal mud/sand	I2.2	spoil
A1.1.2	planted broadleaved woodland	D1.2	dry basic heath	H1.2	intertidal cobbles/shingle	I2.3	mine
A1.2.1	semi-natural coniferous woodland	D1.3	scattered dry heath	H1.3	intertidal rocks/boulders	I2.4	refuse-tip
A1.2.2	planted coniferous woodland	D2	wet heath	H2.4	scattered salt marsh plants		
A1.3.1	semi-natural mixed woodland	D3	lichen/bryophyte heath	H2.6	salt marsh	Miscellaneous	
A1.3.2	planted mixed woodland	D5	dry heath/acid grassland mosaic	H3.1	mud/sand above mlw	J1.1	arable
A2.1	dense scrub	D6	wet heath/acid grassland mosaic	H3.2	shingle/gravel above mhw	J1.2	amenity grassland
A2.2	scattered scrub	D7	basic dry heath/calcareous grassland mosaic	H4	rocks/boulders above mlw	J1.3	ephemeral/short perennial
A3.1	scattered broadleaved trees	Mire		H6.4	dune slack	J1.4	introduced scrub
A3.2	scattered coniferous trees	E1.6.1	blanket bog	H6.5	dune grassland	J1.5	gardens
A3.3	scattered mixed trees	E1.6.2	raised bog	H6.6	dune heath	J3.4	caravan site
A4.1	felled broadleaved woodland	E1.7	wet modified bog	H6.7	dune scrub	J3.5	sea-wall
A4.2	felled coniferous woodland	E1.8	dry modified bog	H6.8	open dune	J3.6	buildings
A4.3	felled mixed woodland	E2	flush and spring	H8.1	hard cliff	J3.7	tracks (not comprehensively digitised)
Grassland and marsh		E2.1	acid/neutral flush	H8.2	soft cliff	J4	bare ground
B1	acid grassland	E2.2	basic flush	H8.4	coastal grassland	NA	not accessed land
B1.1	unimproved acid grassland	E2.3	bryophyte-dominated spring	H8.5	coastal heath		
B1.2	semi-improved acid grassland	E3	fen	H8.6	coastal heath/coastal grassland mosaic		
B2.1	unimproved neutral grassland	E3.1	valley mire	Rock exposure and waste			
B2.2	semi-improved neutral grassland	E3.1.1	modified valley mire	I1	natural rock exposure		
B3.1	unimproved calcareous grassland	E3.2	basin mire	I1.1	inland cliff		
B3.2	semi-improved calcareous grassland	E3.2.1	modified basin mire	I1.1.1	acid/neutral cliff		
B4	improved grassland	E3.3	flood-plain mire	I1.1.2	basic cliff		
B5	marshy grassland	E3.3.1	modified flood plain mire	I1.2	scree		
B5.1	marshy grassland Juncus dominated	E4	bare peat	I1.2.1	acid/neutral scree		
B5.2	marshy grassland Molinia dominated	Swamp, marginal and inundation		I1.2.2	basic scree		
Tall herb and fern		F1	swamp	I1.3	limestone pavement		
C1.1	bracken	F1.1	scattered swamp	I1.4	other rock exposure		
C1.2	scattered bracken	F2.1	inundation vegetation	I1.4.1	acid/neutral rock		
C2	upland species rich ledges	Open water		I1.4.2	basic rock		
C3.1	tall ruderal herb	G1	standing water	I1.5	cave		
C3.2	non-ruderal herb and fern	G2	running water	I2.1	quarry		

Figure A.2: Phase1 Habitat classes (JNCC, 2003)

A.6 Individual Grassland Plots

Figure A.3: B1 v Biomass

Figure A.4: B2 v Biomass

(a) T1a

(b) T1b

(c) T1c

(d) T2a

(e) T2b

(f) T2c

(g) T3a

(h) T3b

(i) T3c

(j) T4a

(k) T4b

(l) T4c
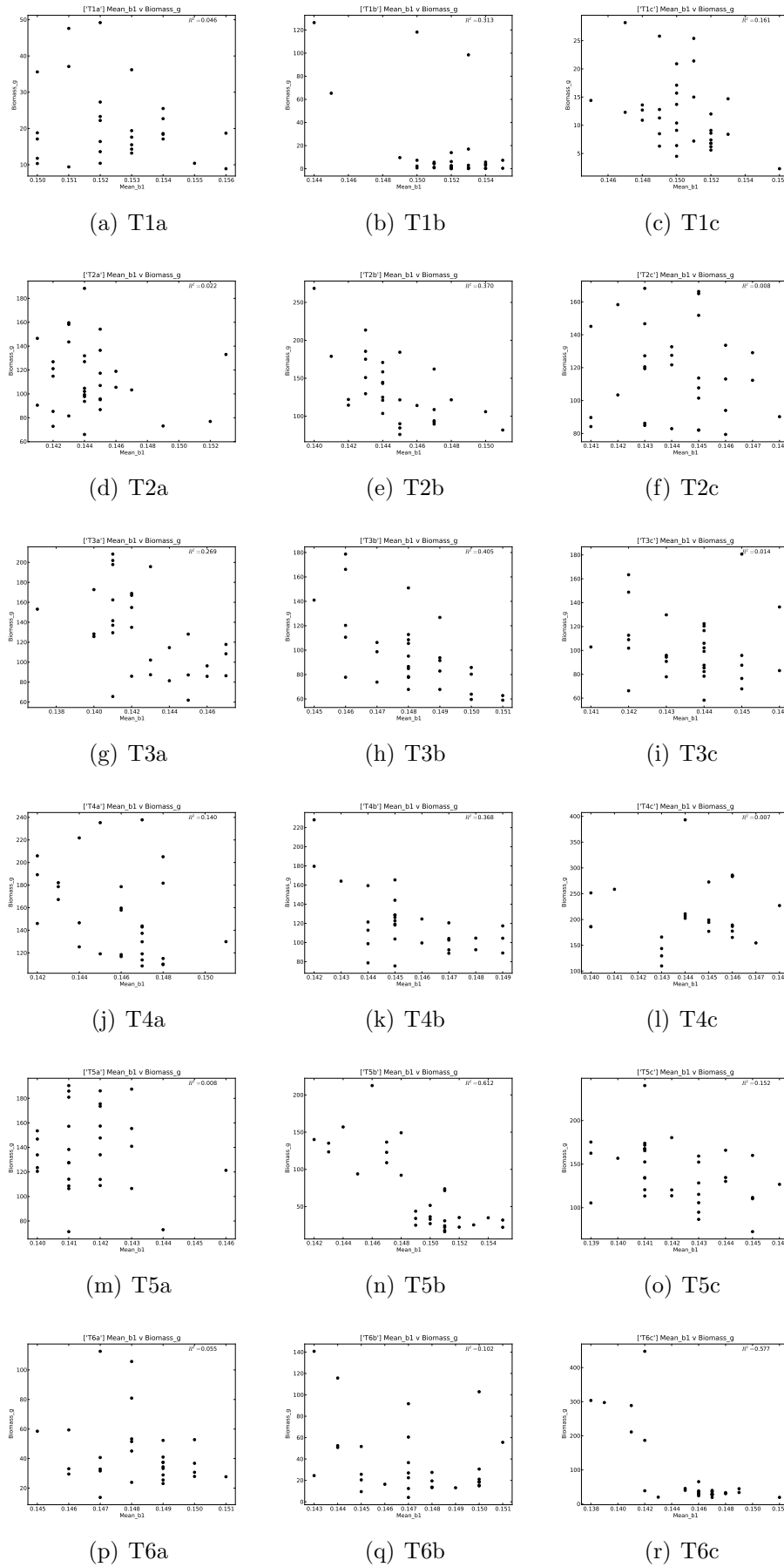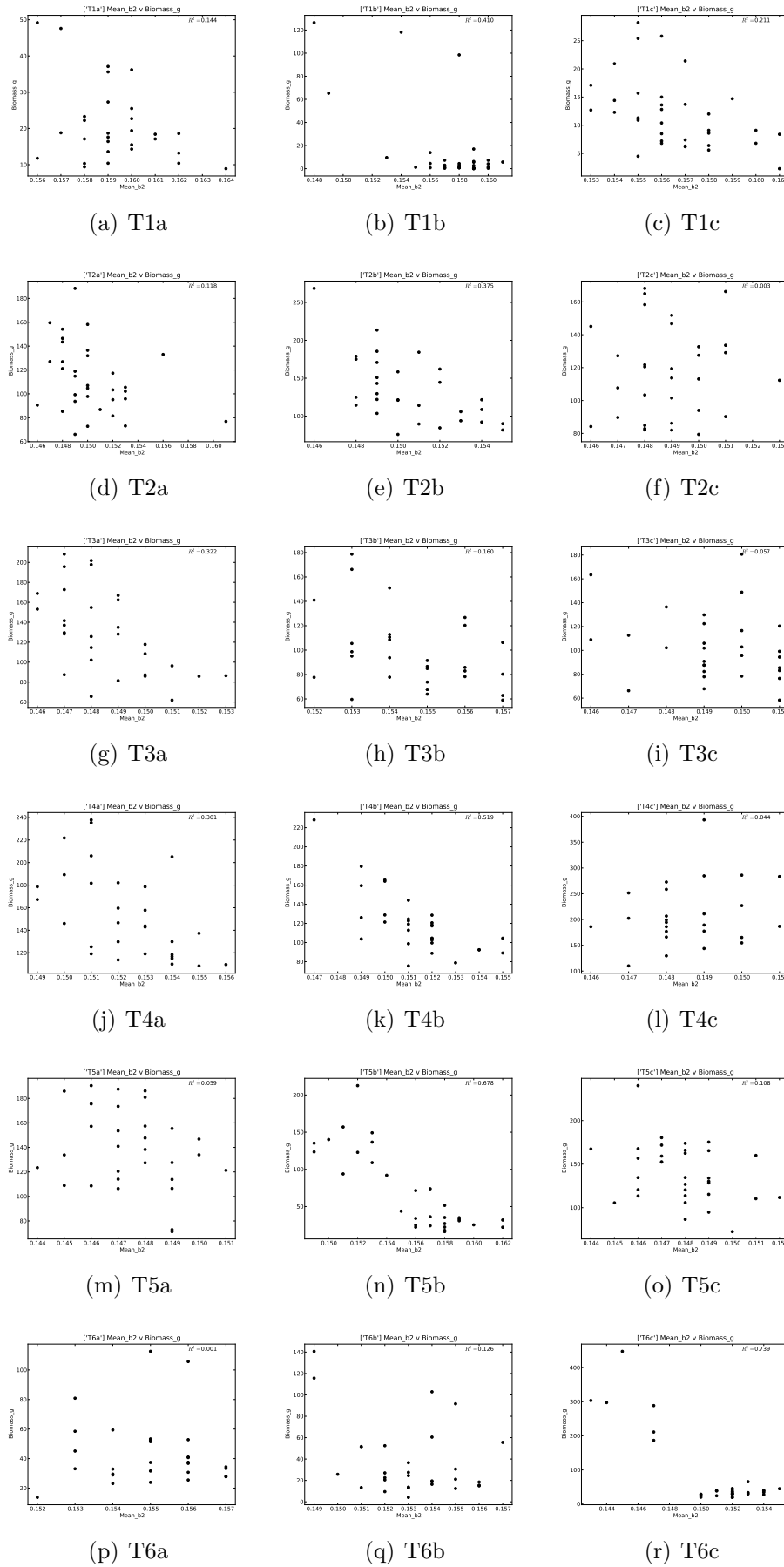
(m) T5a

(n) T5b

(o) T5c
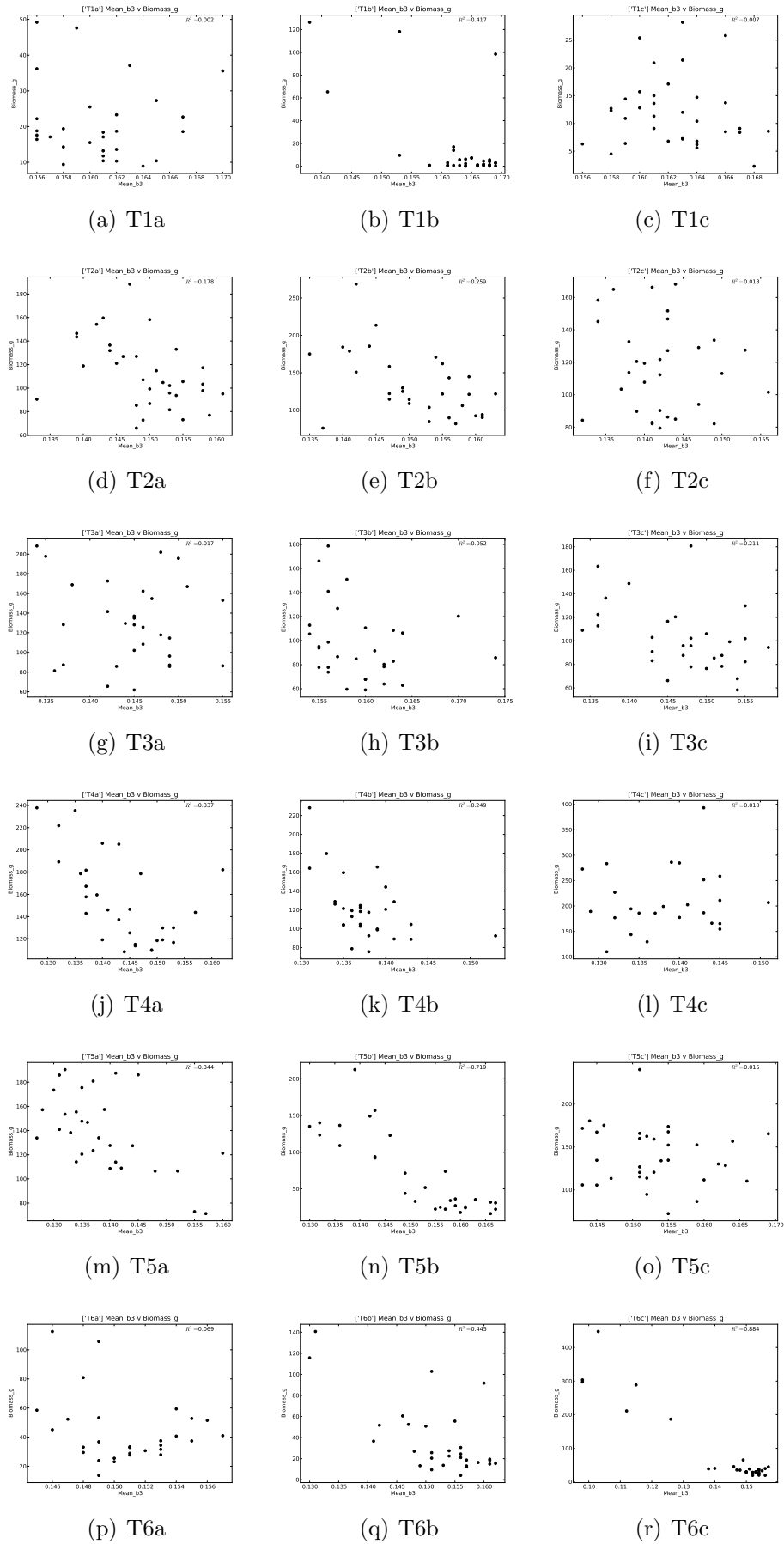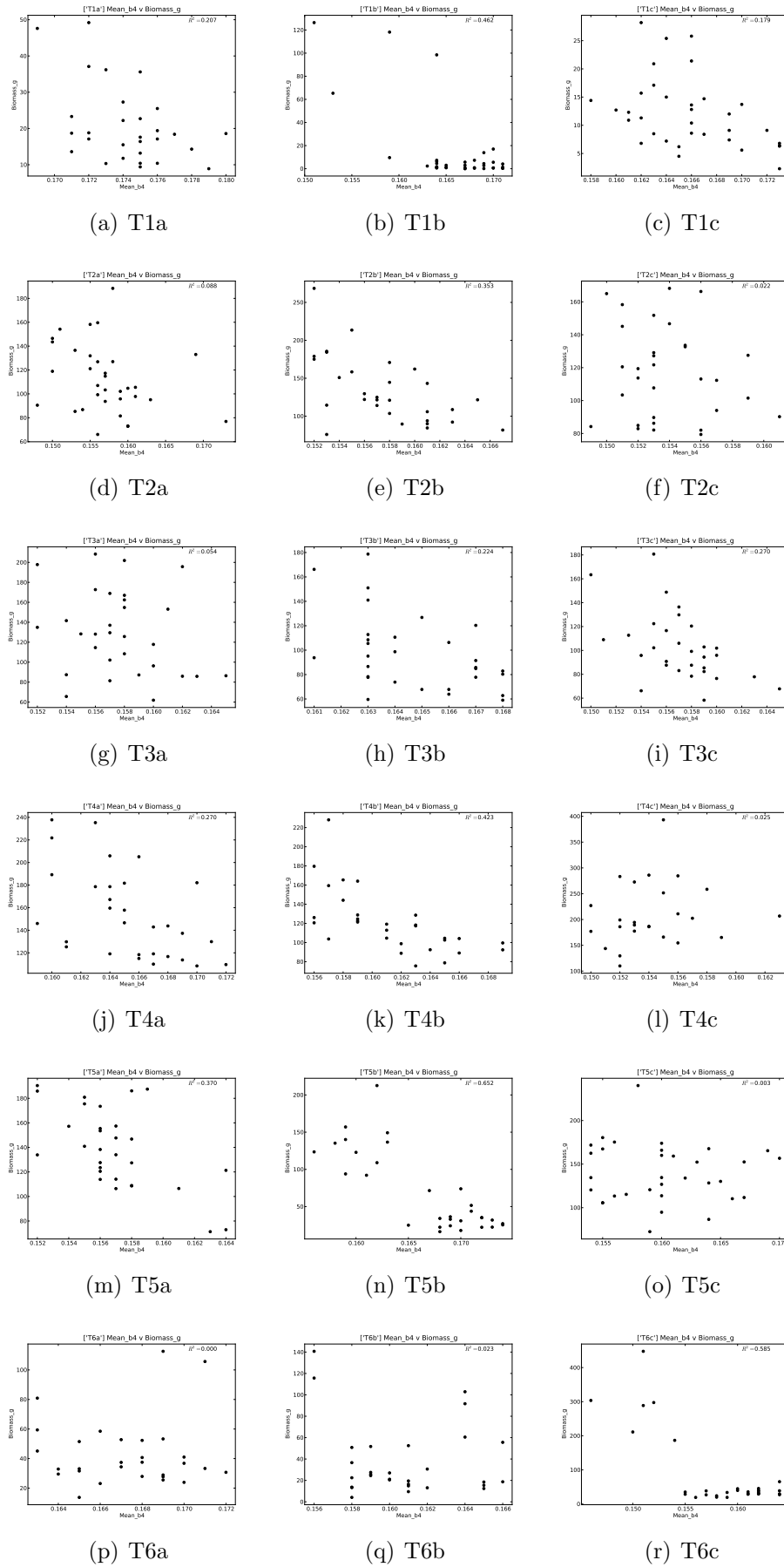
(p) T6a

(q) T6b

(r) T6c

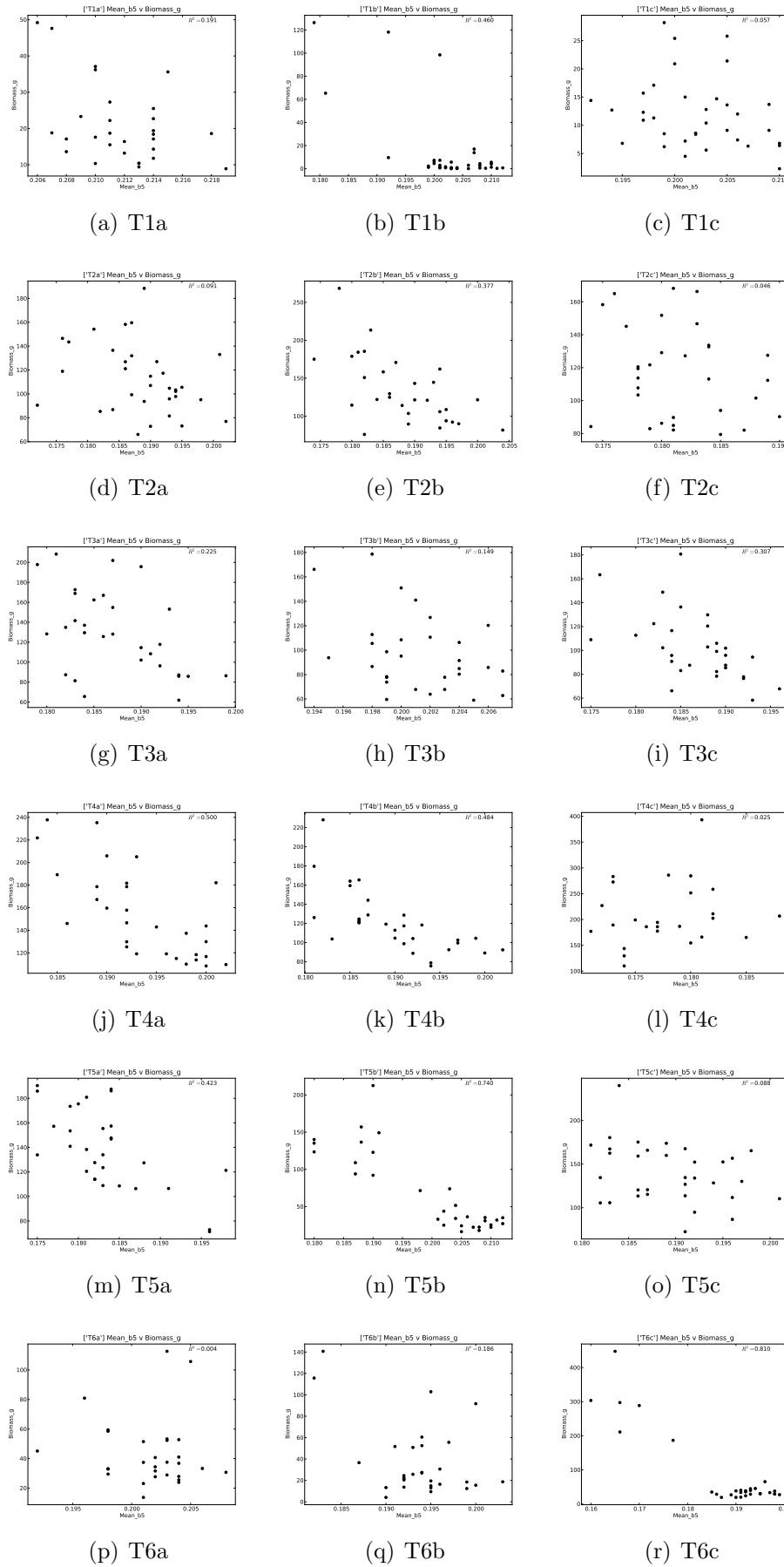Figure A.5: B3 v Biomass

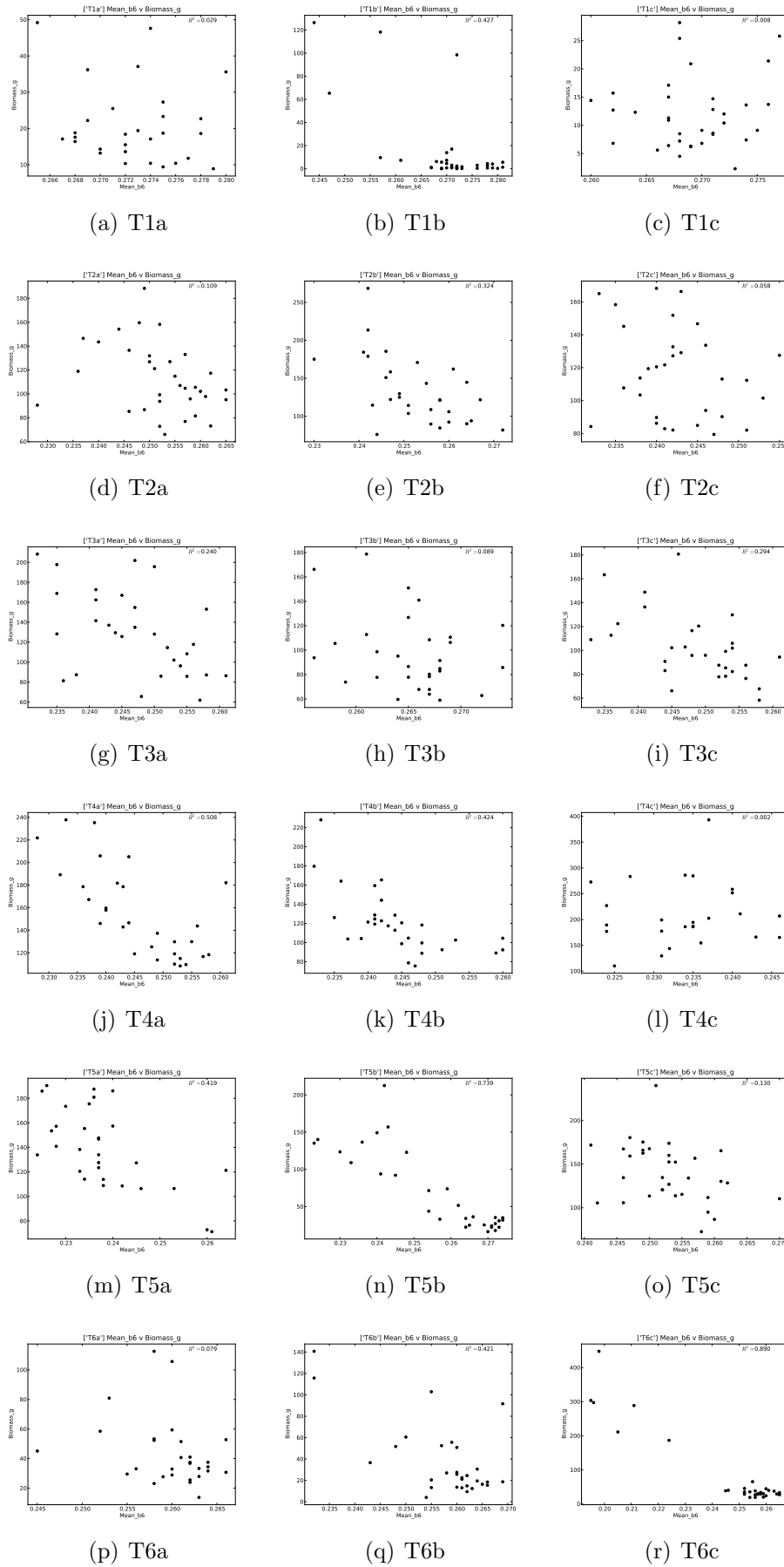Figure A.6: B4 v Biomass

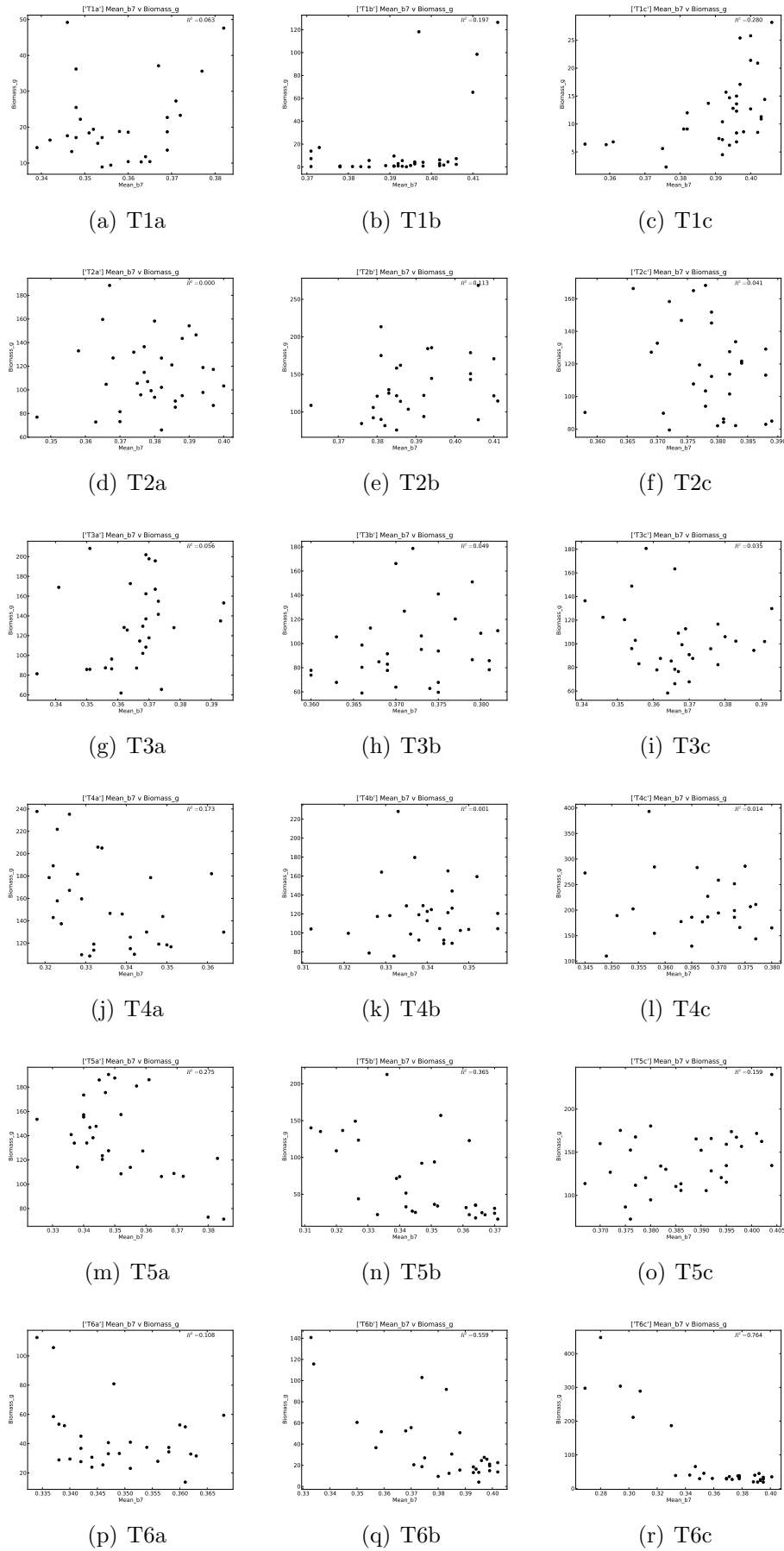Figure A.7: B5 v Biomass
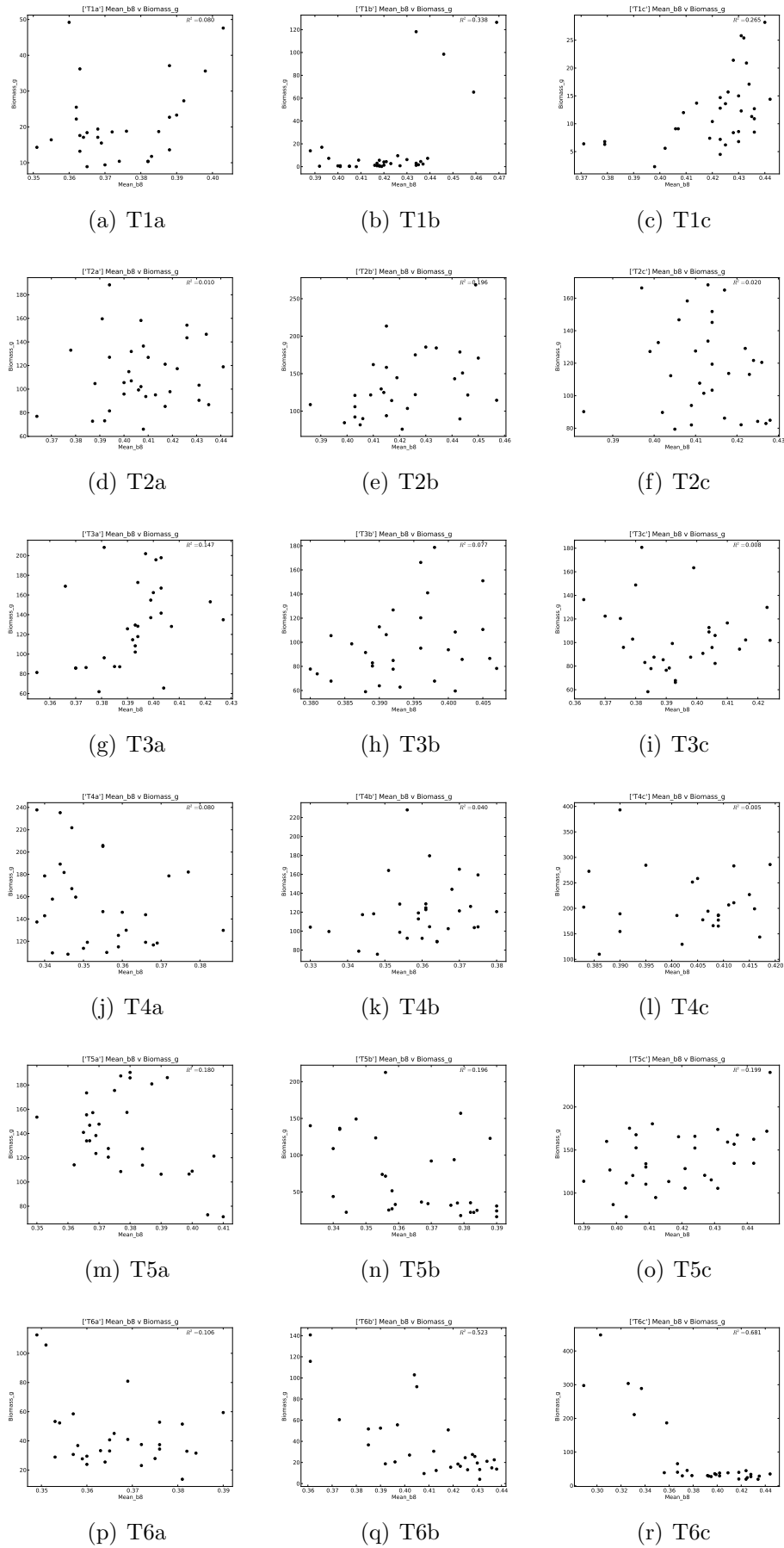
Figure A.8: B6 v Biomass

Figure A.9: B7 v Biomass
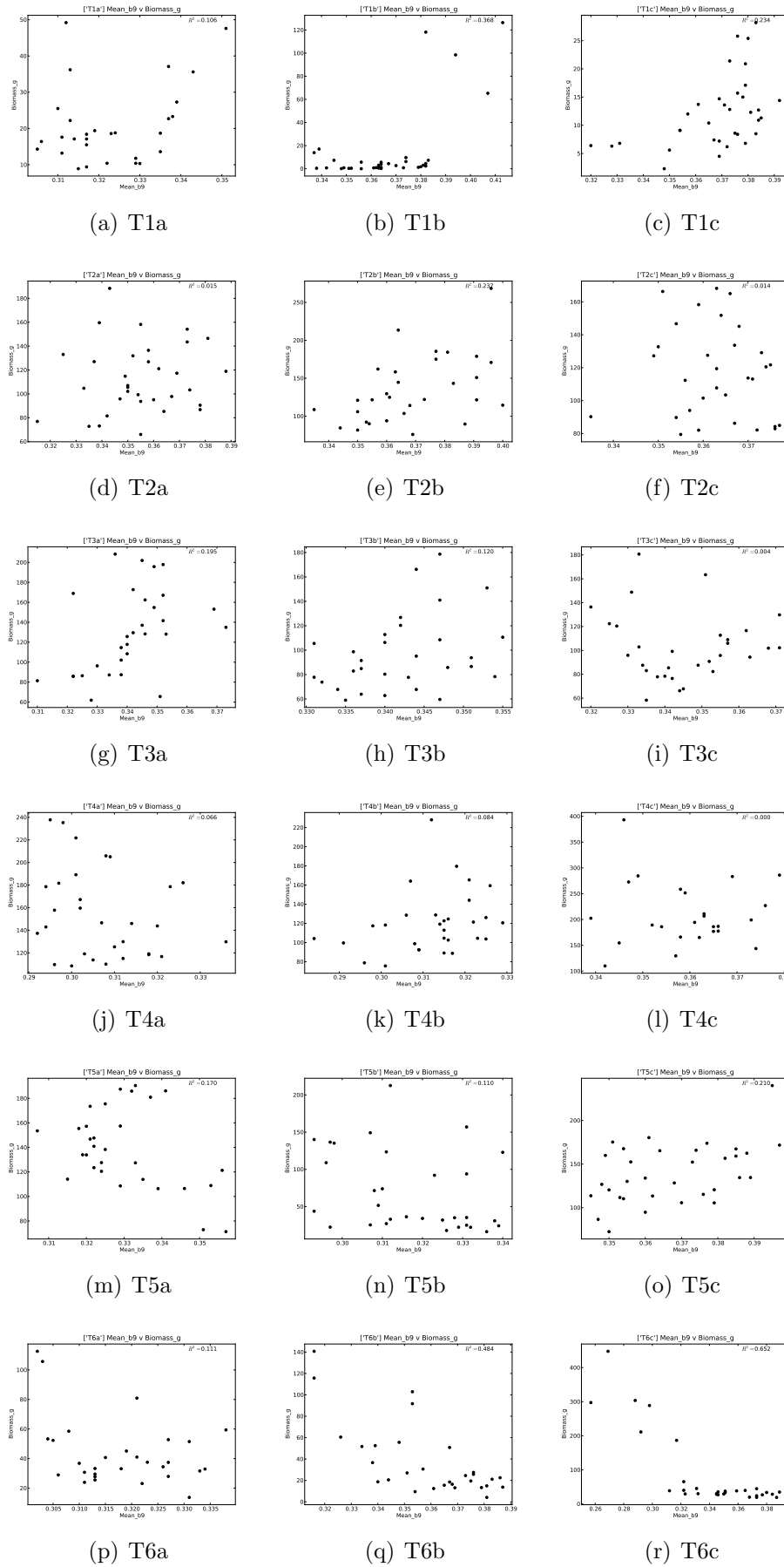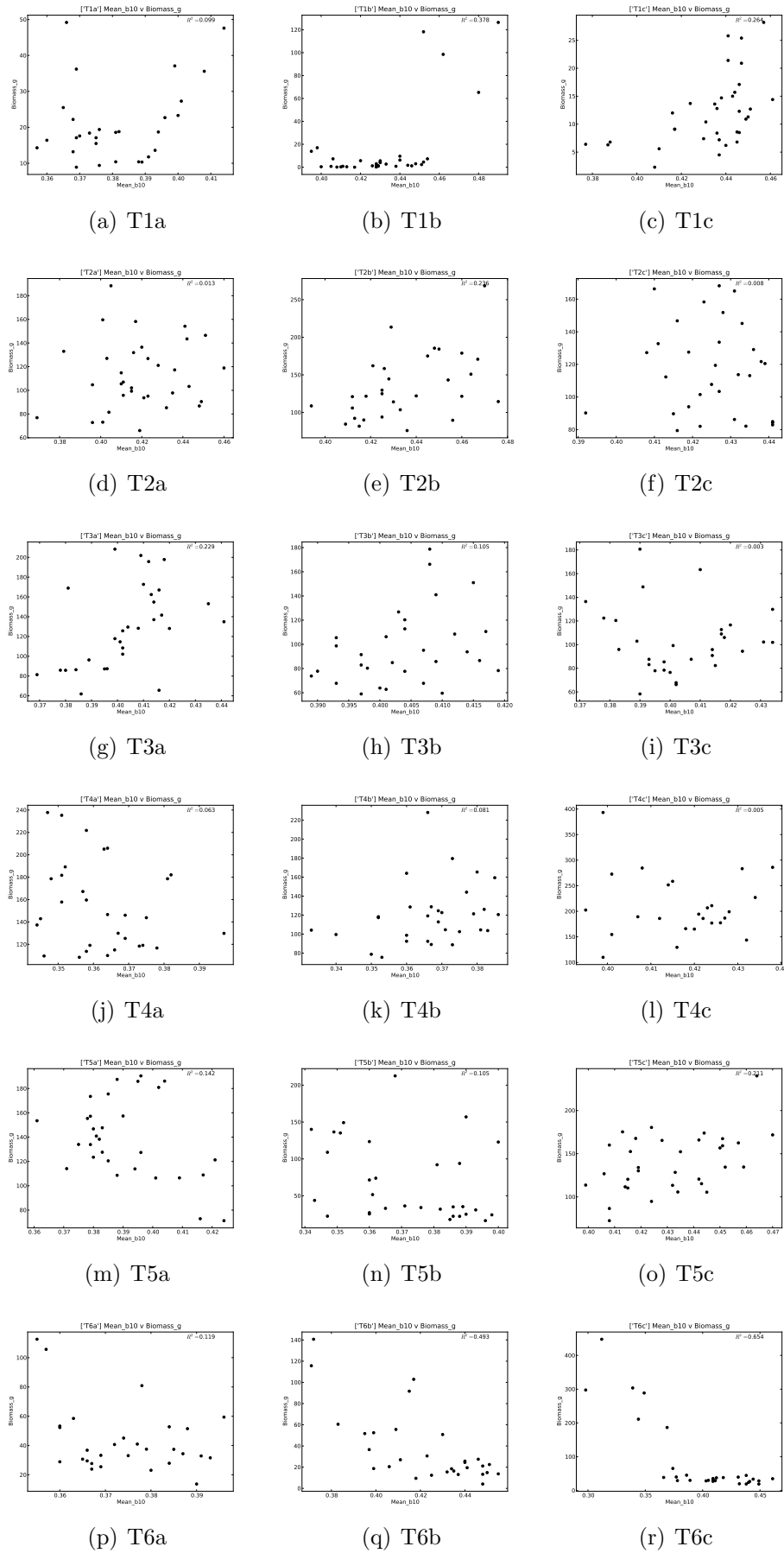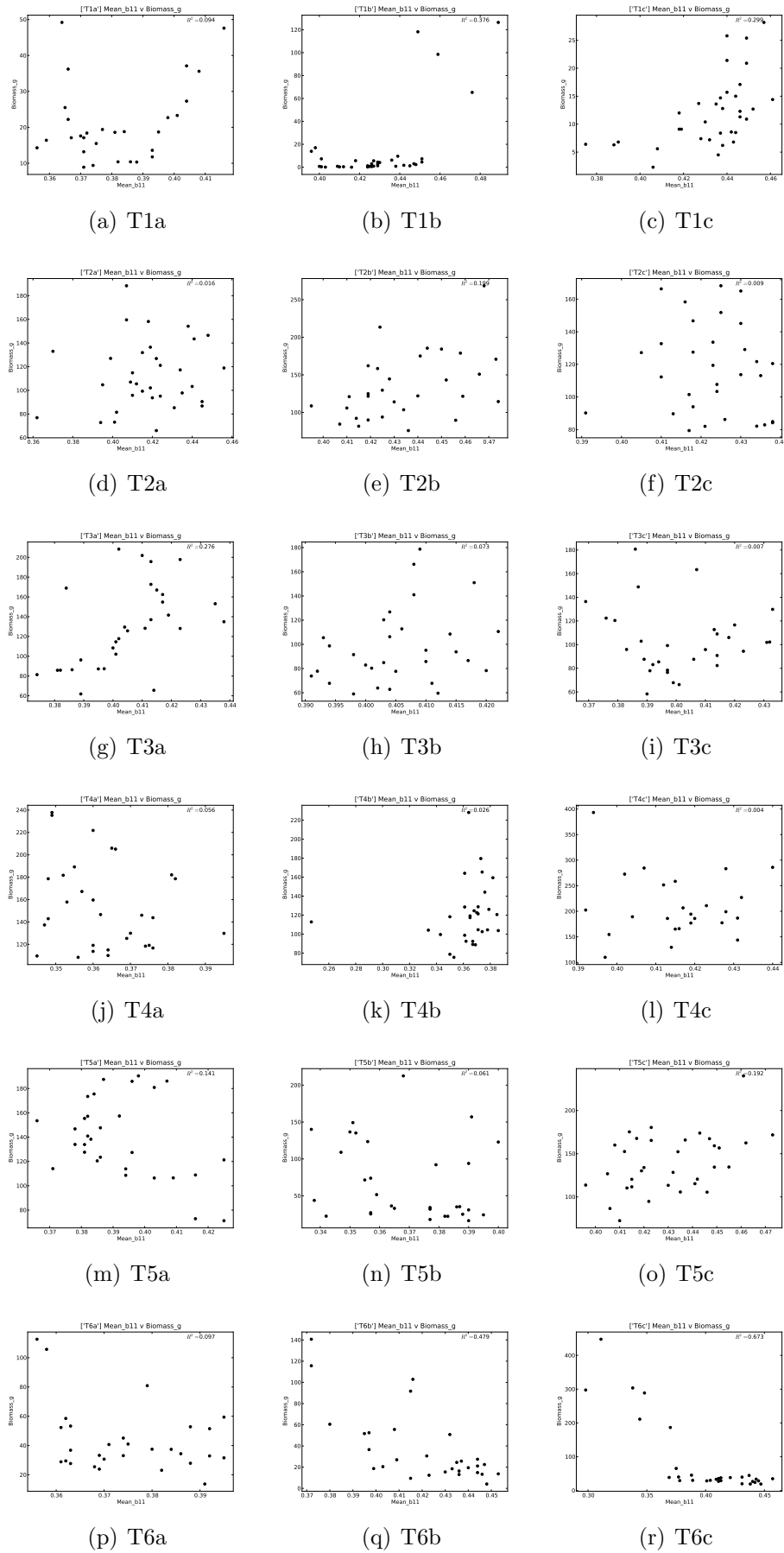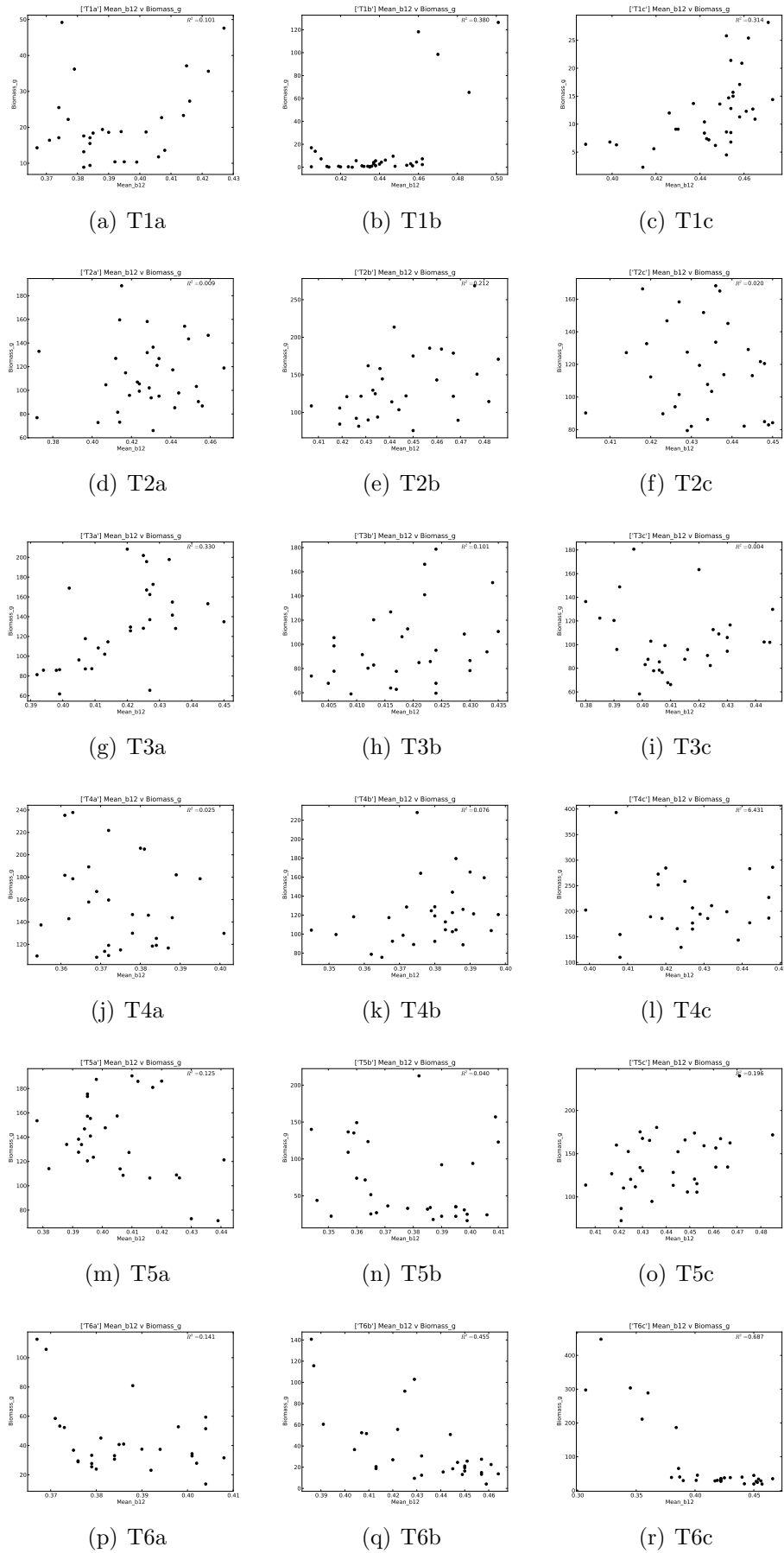
Figure A.10: B8 v Biomass

Figure A.11: B9 v Biomass

Figure A.12: B10 v Biomass

Figure A.13: B11 v Biomass

Figure A.14: B12 v Biomass